Development of an Algorithm for Physical Layer Impairment Aware Routing in WDM Network

Thesis submitted in fulfillment of requirements for the award of degree of

DOCTOR OF PHILOSOPHY

Submitted by

Karamjit Kaur Sekhon

Regn. No.: 950904006

Supervisor

Dr. Hardeep Singh

Assistant Professor (ECED)

Department of Electrical and Instrumentation Engineering

Thapar University, Patiala-147001, INDIA

August 2016

Certificate

I hereby certify that work which is presented in this thesis entitled "**Development of an Algorithm for Physical Layer Impairment Aware Routing in WDM Network**" being submitted to the Department of Electrical and Instrumentation Engineering, Thapar University, Patiala, Punjab for the award of degree of Doctor of Philosophy in Electrical and Instrumentation Engineering, is an authentic record of my own work carried out under the supervision and guidance of **Dr. Hardeep Singh, Assistant Professor, ECED**.

The content in this thesis have not been in part or full submitted to any other University for the award of any degree or diploma.

(Karamjit Kaur Sekhon)
Regn No-950904006

This is to certify that the above statement made by the candidate is correct and true to the best of my knowledge.

Dr. Hardeep Singh
Assistant Professor (ECED)
Thapar University, Patiala
Punjab, India

ABSTRACT

A communication system is an entity involving the set of physical equipments meant for information transfer from one place to another. Till 1980s, most of the communication systems implemented electrical transmission technology via copper cables, radio frequency, microwave and satellite links. The invent of lasers stirred focus of research towards implementing optical region of electromagnetic spectrum instead of High Frequency (HF) or Ultra High Frequencies (UHF) as carrier wave. The advantages like long transmission distance, large information carrying capacity, small size, immunity to electrical interference and signal security played a vital role in replacement of copper cable as communication medium. An important breakthrough came with invent of Wavelength Division Multiplexed (WDM) networks further supported by introduction of Erbium Doped Fiber Amplifiers (EDFA). The popularity of computer usage and internet applications resulted in exponential increase in data traffic transferred using optical networks. Recent trend in growth of internet traffic shows that voice traffic being transferred increase approximately 7% per year, while data traffic has been growing at rate much higher. To achieve these higher capacities, many new technological developments were done in the construction of lasers and fibers, installation procedures, network test and monitoring equipments. Implementation of WDM networks having dynamic network provisioning capabilities is sought as one of the possible solutions.

WDM network involves modulation and multiplexing of optical carriers of different wavelengths into a fiber for transmission over long distances and has enormously increased the data carrying ability of the network. Theoretically, if the full transmission capacity of WDM be explored, bandwidth of tens of terahertz may be easily achieved. As the infrastructure of present system may easily handle 160 channels over the same fiber, a simple 10 Gbps signal may easily be expanded up to 1.6 Tbps. In the subsequent years, a lot of developments have taken place in optical networks to develop and deploy sophisticated and reliable communication system with focus on improving transmission fidelity, increased data rate or carrying capacity of the network, increased transmission distance between inline repeater or amplifiers. The deployment of optical components like Optical Add Drop Multiplexers (OADM), Optical Cross Connects (OXCs,) wavelength convertor switches etc on network nodes has begun the phase of transition in optical networks where requirement of Optical to

Electrical (O-E) signal transfer during the data transmission from a source to destination point is minimized. Based on O-E conversions taking place in the optical links, WDM networks may be broadly categorized as opaque, translucent and transparent networks. A single optical hop of lightpath never cross more than one physical fiber link in opaque network, could cross one or more fiber links in translucent networks and cross the entire source-destination route in translucent networks. Although opaque networks makes the process of design, control and management easier, but are not the practical solution to increased traffic growth as there is a huge potential for reducing power consumption and cost by eradicating unnecessary opto-electronic (OE) transformations on a signal path in a core optical network. *Transparent networks* have advantages like data format and bit rate transparency, significant footprint and power savings, reduced network costs. A complete transition of backbone networks from opaque to transparent is a far off dream till date due to limitations like absence of wavelength conversions, lack of signal quality enhancement at each node, routing and restoration issues, interoperability among the multiple service providers etc. The networks where an O-E-O operation is performed at certain nodes, in accordance with the optical components used, are called *translucent networks*.

The current generation point to point network architectures are evolving from traditional opaque networks towards translucent and transparent networks and is attracting the focus of research community for technological advancements. The dominating issues that need to be addressed while planning and operation of transparent and translucent networks include connection provisioning with focus on minimizing the network cost and improve the resource utilization efficiency and addressed in the present research work.

The process of connection provision involves setting up lightpath for individual call requests and assigning wavelength to each connection and is known as routing and wavelength assignment (RWA). For each connection request, once the route is calculated considering various constraints of network topology, the lightpath is set-up by allocating specific wavelength to the signal. The quality of signal received at the destination node must satisfy the conditions laid by Service Level Agreements (SLAs) for different class of users. Most of the routing algorithms consider the optical layer to be the ideal one, thus making all the outcomes of routing algorithms valid and feasible. Practically, some of the calculated lightpath may not be satisfying the SLAs as the quality of signal transmission is influenced by the physical properties and operating conditions of optical fiber. Lack of O-E conversions taking place, plenty of network components involved, additive nature of Physical Layer Impairments (PLIs) and dynamic configuration of network further contribute towards the signal degradation. Accordingly, it is important for network designers and operators to know various important factors influencing the signal quality, techniques to monitor, model and mitigate their effects, various techniques to communicate the information regarding these disparaging effects to network layer and control plane protocols; and finally, how to use all these techniques in conjunction with control and management plane protocols to dynamically set up and manage optically feasible lightpath.

In the present research work an effort has been put in to identify the different parameters affecting the signal quality which necessarily need to be monitored and controlled to meet the requirements of Quality of Service (QoS) and Service Level Agreement (SLA). A novel algorithm is developed for routing of optical networks considering the degradation effect posed by physical layer impairments. The regenerator placement and utilization is considered for optimum utilization of network resources and minimizing the blocking probability. The focus of algorithms is on comprehensiveness, transparency, fault localization capability and scalability of the system. The analysis and evaluation of the physical layer parameters affecting the signal quality is done using network simulations. The result of performance monitoring is used for the routing. The signal measurements done are used for network management with routing capabilities, where priority traffic that requires high performance can be dynamically tuned to the appropriate channels. The proposed system is cost effective with sufficiently high update speed and reduced processing time.

In this work, different optical impairments responsible for signal degradation and their mathematical models, including higher order impairments, are studied. The different physical layer impairments are broadly classified as linear (Dispersion, attenuation) and non-linear impairments (Self Phase Modulation (SPM), Cross Phase Modulation (XPM), Four Wave Mixing (FWM)). The influence of these impairments on system performance in form of BER and Q-factor, influence of variations in system parameters like wavelength, length of fiber and interaction between different impairments is studied. The different techniques that may be implemented for monitoring are broadly categorized as digital and analog techniques [35]. The digital monitoring involves BER, Q-factor monitoring by studying the sequence of bits being transferred. The analog techniques involves polarization domain analysis using polarization nulling, or degree of polarization including [37-42], time domain analysis using eye diagrams, delay tap plots, constellation diagrams, histograms etc [43-61] and frequency domain analysis using optical or RF spectrum [62-68]. Digital techniques focus on digital bits being transferred through the fiber while analog techniques analyze the signals at the output to extract the information about network stage, the identification, location and measurement of different impairments being present. In the present work, the individual impairments are diagnosed through eye diagrams and optical spectrum, while the overall status of the network in presence of all the impairments is presented through BER and Q-factor. BER is used in Q-matrix of routing algorithm. Q-value is also measured to ensure the signal satifying the threshold conditions as per SLAs. The Q-value for signal propagating in the fiber link decreases with increased length of fiber due to higher accumulation of impairments in the fiber. The corresponding value of BER is increased. This is the reason making uniform placement of regenerators a neccesasity in optical fiber links. The quality of link is also influenced by the number of wavelengths propagating inside the optical fiber.

The numerous heuristic algorithms are presented in the literature on finding the optimal solutions to RWA considering the role of physical layer on transmission. The impact may be inculcated either by considering impairments as one of the constraints to route calculations, known as Impairment Constraint Based Routing (ICBR), or by setting some threshold for quality factor of link and calculating route considering the links satisfying the minimum threshold, known as Physical Layer Impairment Aware Routing (PLIAR). These routing algorithms present either single impairment, multiple impairments (i.e. combination of few e.g. PMD, XPM or PMD, ASE, XPM, FWM) quantized in the form of either of BER, Q-factor, OSNR or aggregate power flowing in the links [71-88]. Most of the studies are based on assumption that the PLIs are of static nature therefore may be estimated analytically. But impairments like crosstalk, SPM, XPM, FWM depends upon the network state. Their values may vary by bare minimum variations in properties of signal being transmitted in channel e.g. power, bit rate or by the state of signal flowing in adjacent channels. In dynamically reconfigurable networks, there is a need to monitor them online and broadcast the information into the control plane through centralized or distributed architectures. In the reports demonstrating online monitoring of PLIs, only one or two impairments are considered. For accurate estimation of optical reach in links, it is necessary that not only all the impairments (both linear and non-linear) must be monitored, but the impact of mutual interaction of specific impairment must also be considered during RWA. In the present work, a routing algorithm is presented which take into account the impact of impairments on the quality of signal flowing in the links.

The routing algorithm assume homogeneous and single granularity network i.e. all the links carry same number of wavelengths and all wavelengths support same bit rate. The parameter used for performance evaluation is blocking rate which is defined as the ratio of number of blocked lightpath requests over the total number of requested lightpath. The performance of proposed algorithm is evaluated, tested and validated for certain set of path set up demands. In order to implement the algorithm, a network of nine nodes is used. The designed algorithm implements sequential approach for path computation. Three different variations for path selection are designed namely First Fit (FF), Best Fit (BF) and Shortest Path (SP).

The validation of algorithm is done by testing the performance of algorithm over Internet2 network and European Optical Network (EON) and comparing with existing techniques. The results obtained by presented algorithm are compared. It has been found that the response of presented algorithm is better than Simplified Lightpath Establishment and Regenerator Placement (sLERPS) due to less blocking rate being offered and comparable with Shortest Path First (SPF) and Longest Path First (LPF) algorithm. All the algorithms (BF, FF and SP) outperform than LPF as LPF consider longest path first. The increased path length will increase the impairment level of Q-matrix, thereby increasing the blocking probability of network. Moreover a signal which transverse more distance in the network will influence more number of already established lightpaths, resulting in call drops. The number of paths acting as potential candidates for lightpath setup through routing matrix plays an important role. The SPF algorithms use 10-shortest path search for lightpath set up, while the designed algorithm has no limit on number of potential paths for lightpath setup. This help in finding more optimum paths for specified connection request. Moreover, the performance of network changes with the network topology, number of nodes involved. The algorithm is implemented on a portion of EON network (only 9 nodes), while referred author used 15 nodes. The blocking probability for EON is high because the presented algorithm uses few nodes of EON (9 out of 15) so the number of available paths between source to destination is less, making it difficult to find path for high traffic load. The increased number of nodes might have increased the blocking rate of the network. The reason for difference in behavior of FF, BF and SP is same as already stated. The performance of SP is most reliable than all other algorithms.

To further improve the system performance it is mandatory to improve the quality of link for signal transfer. The optimum placement of regenerators is one of the solutions for the same, where signal regeneration may takes place at certain pre-specified nodes. The existing strategies for regenerator placement are broadly classified as sparse regenerator placement and generation of transparent islands. [90] The sparse placement of regenerators seems to be a more economical solution since it distributes the regenerators throughout the network and probability of signal successfully reaching at destination node is more as it helps the signal maintaining its quality requirements. The nodes where regenerator must be placed may be calculated either by using an approximation algorithm [91] [92] [93] [94] or a heuristic algorithm [95] [96] [97] [98] [99] [100] [101] where the incremental traffic [102] [103] [104] and static traffic scenario [105] [106] [107] [108] [109] are considered. In the present work, sparse placement of regenerators is considered for dynamic traffic scenario. Three different algorithms are presented using information of network topology, history of traffic flow in the network and presence of PLIs. The advantage of presented algorithms includes the simplicity in implementation and better network performance for the load distribution used during the optimization process. The algorithms include Maximum Utilized Node First, Traffic based regenerator placement and PLI constraint based regenerator placement. Three different cases of regenerator placement are considered i.e. when no regenerator is placed at all, when 40% of the available nodes are equipped with regeneration capability and when all the nodes have regeneration capability. The blocking rate of all the three cases is studied for a link supporting maximum of 15 wavelengths. Among the different routing algorithms SP algorithm responds best to all the three regenerator based strategies. Among the different regenerator based strategies, PLI based regenerator placement has maximum effect on reducing the blocking rate of the network. The performance of regenerator placement algorithms is compared with existing techniques. Although the performance of algorithm is comparable with existing results, but there is great scope in improvement due to numerous assumptions and network states considered by the author. The foremost reason is that referred work put limitation on the maximum number of wavelengths being transferred through the fiber. The number of impairments considered also influences the signal quality and overall call acceptance probability. The more complex, multigranuality networks may be explored in the future for further improvement in the field.

Page Left Blank Intentionally

LIST OF PUBLICATIONS

1. Karamjit Kaur, Hardeep Singh, "*A Unified Approach for Calculating Error Rates of 10Gbps WDM Network in Presence of Higher Order Dispersion"* Journal of Optical Communications, DOI: 10.1515/joc-2016-0101, Sept. 2016 (**In Press**).

2. Karamjit Kaur, Hardeep Singh, "*Analysis of Single-Mode Fiber Link Performance for Attenuation in Long-Haul Optical Networks*" Journal of Optical Communications, DOI: 10.1515/joc-2016-0027, May 2016 (**In Press**).

3. Karamjit Kaur, Hardeep Singh, "*An algorithm of impairment aware routing for wavelength division multiplexed optical networks*" Microwave and Optical Technology Letters, Volume 57, Issue 7, July 2015, pp. 1632–1636.

4. Karamjit Kaur, Hardeep Singh, "*Neural Network based Optical performance monitoring"* Proceedings of International Conference on Future Challenges in Wireless Communications, Optical Communications and Networks, held on 27-29 Nov, 2010 organized by Institution of Engineers India, paper ID-IC05, pp-21-26.

5. Karamjit Kaur, Hardeep Singh, "*Impact of Higher Order Impairments on QoS Aware Connection Provisioning in 10 Gbps NRZ Optical Networks"* communicated to International Journal of System Assurance Engineering and Management.

6. Karamjit Kaur, Hardeep Singh, "*Impact of Physical Layer Impairment Aware Routing for WDM Optical Networks"* communicated to Photonic Network Communications.

7. Karamjit Kaur, Hardeep Singh, "*Performance Improvement for WDM Optical Networks using Optimal Regenerator Placement Strategy"* communicated to Microwave and Optical Technology Letters.

Page Left Blank Intentionally

Acknowledgment

First and foremost, praises and thanks to the God, the Almighty, for His showers of blessings throughout my research work to complete the research successfully. You have given me the power to believe in myself and pursue my dreams. I could never have done this without the faith I have in you, the Almighty.

In all these years, being a PhD student at Thapar University was a wonderful experience for me. During my entire course, many people were involved directly or indirectly in shaping up my academic career. It was hardly possible for me to complete my doctoral work without the precious support of several persons whom I would like to thank sincerely.

First of all, I would like to express my gratitude to my supervisor, Dr. Hardeep Singh for his guidance and consistent support that enabled me to achieve all goals to complete this research. It was only due to his valuable guidance, enthusiasm and friendly nature that I was able to complete my research work. I am indebted to him for his valuable guidance and encouragement.

Besides my supervisor, I would like to thank Dr. Ravinder Aggarwal, Head of the Department, EIED, and Dr. Sanjay Jain, PhD Coordinator for their encouragement, support and providing the facilities for the completion of my research work. I am also thankful to my thesis committee members Dr. R.S. Kaler, Dr. Mandeep Singh and Dr. Sunil Singla for their continuous encouragement which incented me to widen my research from various perspectives.

I would like to convey my deep regards to my colleagues, Dr. Priti Singh and Mr. Anil Kumar for allowing their precious time to read my manuscripts and reports and providing their valuable suggestions. I am thankful to Amity University for providing me enough time and facilities to carry out my research and helping me out in all aspects during my work.

Last but not the least, I would like to thank my parents and family members for supporting me spiritually throughout writing this thesis and my life in general. I would also like to thank all of my friends who supported me in writing, and incented me to strive towards my goal.

(Karamjit Kaur Sekhon)

Page Left Blank Intentionally

TABLE OF CONTENTS

LIST OF ACRONYMS

ALD	Ad-Hoc Lightpath Demand
AM	Amplitude Modulation
ASK	Amplitude Shift Keying
ASON	Automatic Switched Optical Network
ATM	Automated Teller Machine
BER	Bit Error Rate
BF	Best Fit
BILP	Binary Integer Linear Programming
CAPEX	Capital Expenditure
CD	Chromatic Dispersion
CR-LDP	Constraint-Based Routing-Label Distribution Protocol
CW	Continuous Wave
CWDM	Course Wavelength Division Multiplexing
DGD	Differential Group Delay
DWDM	Dense Wavelength Division Multiplexing
EDFA	Erbium Doped Fiber Amplifier
EON	European Optical Network
FF	First Fit
FM	Frequency Modulation
FSC	Fiber Switch Capable
FSK	Frequency Shift Keying
FWHM	Full Width at Half Maximum
FWM	Four Wave Mixing
GMPLS	Generalized Multi-Protocol Label Switching
GUI	Graphical User Interface
GVD	Group Velocity Dispersion
HF	High Frequency
ICBR	Impairment Constraint Based Routing
IETF	Internet Engineering Task Force
IP	Internet Protocols
IS-IS	Intermediate System-to-Intermediate System

ITU-T	International Telecommunications Union-Telecommunication Standardization Sector
LAN	Local Area Network
LMP	Link Management Protocol
LPF	Longest Path First
LSC	Lambda Switch Capable
LSP	Label Switch Path
MPLS	Multi-Protocol Label Switching
MZM	Mach Zehnder Modulator
NE	Network Element
NRZ	Non Return to Zero
OADM	Optical Add Drop Multiplexer
O-E	Optical-Electrical
O-E-O	Optical-Electrical-Optical
OIF	Optical Internetworking Forum
OOK	On Off Keying
OPEX	Operation Expenditure
OPM	Optical Performance Monitoring
OSNR	Optical Signal to Noise Ratio
OSPF-IE	Open Shortest Path First with Traffic Engineering Extensions
OXC	Optical Cross Connect
PCE	Path Computation Element
PDF	Probability Density Function
PLIAR	Physical Layer Impairment Aware Routing
PM	Phase Modulation
PMD	Polarized Mode Dispersion
PSK	Phase Shift Keying
QoS	Quality of Service
RF	Radio Frequency
ROADMS	Reconfigurable Optical Add Drop Multiplexers
RSVP-TE	Resource Reservation Protocol with Traffic Engineering extensions
RWA	Routing and Wavelength Assignment
SBS	Stimulated Brillouin Scattering

SDH	Synchronous Digital Hierarchy
SLA	Service Level Agreement
SLD	Scheduled Lightpath Demand
SLERP	Simplified Ligthpath Establishment and Regenerator Placement
SONET	Synchronous Optical Network
SP	Shortest Path
SPF	Shortest Path First
SPM	Self Phase Modulation
SRS	Stimulated Raman Scattering
TDM	Time Division Multiplexing
TED	Traffic Engineering Database
UHF	Ultra High Frequency
UNI	User Network Interface
WADM	Wavelength Add Drop Multiplexer
WDM	Wavelength Division Multiplexing
XPM	Cross Phase Modulation

LIST OF SYMBOLS

E	Electric field vector
H	Magnetic field vector
ϕ_d	Flux density
P	Induced electrical polarization
M	Induced magnetic polarization
μ_o	Permeability of free space
ε_o	Permittivity of free space
χ	Linear susceptibility
c	Speed of light
μ	Permeability of the medium
ε	Permittivity of the medium
v_p	Phase velocity
k_0	Wave number
λ	Vacuum wavelength
β	Propagation constant
$\Delta\tau$	Differential group delay
ω	Angular frequency
L	Length of fiber
n	Refractive index
V	Normalized frequency
σ	Spectral width
β_2	Chromatic dispersion
D	Dispersion parameter
S	Dispersion slope parameter
τ_g	Group delay
v_g	Group velocity
α	Attenuation coefficient
P	Optical power
K_B	Boltzmann's constant
β_T	Isothermal compressibility of material
T_f	Temperature at which density fluctuations are frozen
$\Delta\Phi$	Phase shift

η	Efficiency
x	degeneracy factor
σ^2	Variance of noise
μ	Mean

LIST OF TABLES

Table No. Description Page No.

Page Left Blank Intentionally

LIST OF FIGURES

Figure No. Description Page No.

Chapter 1

Introduction

This chapter gives brief introduction to optical communication networks. The different issues involved with to-date optical networks are discussed and gaps are identified. Based on these, the objectives set and major contributions by the research work are discussed.

CHAPTER 1: INTRODUCTION

A communication system is an entity involving the set of physical equipments meant for information transfer from one place to another. Till 1980s, most of the communication systems implemented electrical transmission technology via copper cables, radio frequency, microwave and satellite links. The invent of lasers stirred focus of research towards implementing optical region of electromagnetic spectrum instead of High Frequency (HF) or Ultra High Frequencies (UHF) as carrier wave. The breakthrough for optical fiber communication started when researchers demonstrated feasibility of producing a glass fiber with attenuation loss of order 20 dB/km. This loss was considered low enough to implement fibers for practical communication systems. The advantages like long transmission distance, large information carrying capacity, small size, immunity to electrical interference and signal security played a vital role in replacement of copper cable as communication medium. The significant advances embarked on with invent of first ultrapure fiber in early 1970s leading to launch of optical communication systems worldwide. With progression of sophisticated research and development in this field, data carrying capability of system increased from 6 Mb/s over the distance of 10 Km to beyond terabits per seconds over the distance of hundreds of kilometers. The First generation optical networks were implemented using GaAs semiconductor lasers operating at 850nm. Due to influence of intermodal dispersion and fiber attenuation losses, the repeater spacing was just 10-15 Km. Second generation optical networks implemented single mode fibers, InGaAs semiconductor laser and transmission wavelength of 1300 nm. This increased the repeater spacing to 50 Km. Third generation networks offered lower attenuation losses of the order of 0.2 dB/km as they operated on 1550 nm wavelength at 2-10 Gbps over 100 Km without repeaters. In fourth generation networks, concept of optical amplifiers was introduced to reduce the need for repeaters and increase the transmission capacity.

The popularity of computer usage and internet applications resulted in exponential increase in data traffic transferred using optical networks. The high data carrying capacity requirements are further fueled by bandwidth striving applications of internet such as high definition video transfers, conference calls, online gaming applications, large scale database queries, extensive choice of remotely accessible programs etc. Recent trend in growth of internet traffic shows that voice traffic being transferred increase roughly 7% per annum, while data traffic has been growing at much higher rate. To achieve these higher capacities, many new technological developments were done in the construction of lasers and fibers, installation procedures, network test and monitoring equipments. An important breakthrough came with invent of Erbium Doped Fiber Amplifiers (EDFA) further supported by introduction of Wavelength Division Multiplexed (WDM) networks. EDFA has large gain bandwidth, typically tens of nanometers and helps in amplification of high data rate channels of different wavelengths without introducing any effects of gain narrowing [1]. These amplifiers are typically used in 1530-1560 nm region owing to maximum gain achieved in this spectrum. Before the invent of EDFAs, all data channels were required to be separated, transformed to electrical form, amplified and resubmitted back on the link in the optical form after multiplexing. The major advantages of EDFA include high gain, low noise figure, increased transparency, invulnerability to crosstalk, reduced the computational complexity and cost of network.

WDM network involves modulation and multiplexing of optical carriers of different wavelengths into a fiber for transmission over long distances. The implementation of WDM networks has enormously increased the data carrying ability of the network. Theoretically, if the full transmission capacity of WDM be explored, bandwidth of tens of terahertz may be easily achieved. As the infrastructure of present system may easily handle 160 channels over the same fiber, a simple 10 Gbps signal may easily be expanded up to 1.6 Tbps. The channel spacing between the wavelength channels may vary from 20 nm to even less than 1.6 nm. The networks implementing 20 nm spacing between the different wavelength sources are often referred as Course Wavelength Division Multiplexed (CWDM) networks and networks using 1.6 nm or even less are called Dense Wavelength Division Multiplexed (DWDM) networks. CWDM networks can support maximum of 18 channels of different wavelengths and are typically used for small distance communications. On the other hand, DWDM networks may support hundreds of channels and are used in long haul networks. A four channel WDM link is shown in Figure 1.1.

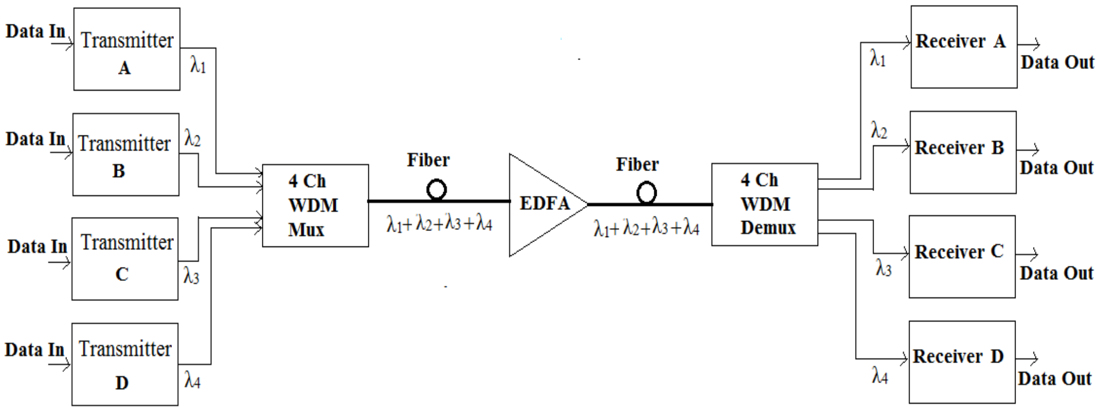

Figure 1.1: A Four channel WDM link

The transmitter of WDM network consists of an optical source (usually laser) and modulator. Another important component required for tuning purposes is optical filter. The number of wavelengths required for signals are obtained either by using array of fixed wavelength lasers or through tunable lasers. The lasers may be tuned either mechanically or by using external filters, gratings etc. While selecting a particular laser for optical network, tuning range, time and technique (continuous or discrete tunable) are taken into account. The modulation may be implemented through analog or digital techniques. Frequency, Amplitude and Phase Modulation (FM, AM, PM) are analog techniques and Phase, Frequency and Amplitude Shift Keying (PSK, FSK, ASK) are digital techniques. Among the different modulation formats available, ASK also called On–Off Keying (OOK) is preferred owing to its simplicity. In order to decrease chirp factor, external modulators like Mach–Zehnder Interferometer (MZI) is used. Several independent information streams of different transmission formats and bit rates from modulator are coupled into fiber using a multiplexer. The spectral region of operation of optical fibers may range from 1260-1675 nm for full spectrum fibers. EDFA’s are used for increasing the transmitter power, quality of signal propagating in the fiber or before receiver to reduce the noise of link. Additional components used in transmission involve tunable or direct filters, switching elements like optical cross connects wavelength convertors etc. At the intermediate nodes, signal may be dropped or added using Optical Add Drop Multiplexers (OADMs). For interconnected nodes or mesh topologies, Optical Cross Connects (OXC’s) are used for lightpath set up in either a wavelength-continuous mode or non-wavelength-continuous modes. In wavelength continuous lightpath, wavelength assigned at the source node is maintained till signal reaches its destination node i.e. no wavelength conversion takes place over the entire lightpath. In non-wavelength continuous lightpath, wavelength convertor switches are utilized for wavelength conversion. Here, setting up the lightpath involves best route calculations as well as decision regarding the wavelengths to be used in the selected route. Due to possibility to implement multiple wavelengths in path set up, blocking probability of network is reduced and performance of network is improved [2]. At the receiver end, either direct detection through photodiodes or coherent detection technique using laser source as an oscillator may be implemented. Although more elaborative but practical implementation of coherent detection technique is limited by excessive phase fluctuations in the signal detected as compared to direct detection technique [3]. With the advent of high quality optical laser sources, many independent wavelength channels spaced less than a nanometer apart could be placed on the same fiber, thereby dramatically increasing the information carrying capacity of original networks.

The practical application of WDM networks involves full spectrum of transport networks from core backbone (long haul networks spanning between 100's and 1000's of Km) and metropolitan (covering 10-100km) down to the access network (spanning about 1-10 Km) domains.

i) Access network serves as last mile of information flow as it connects the end users of internet i.e. domestic and commercial users as per Service Level Agreements (SLAs). These networks may be implemented through a star, bus or ring topologies. Optical technology is a prospective contender to accommodate the ever increasing data traffic by facilitating 10 to 100 times more bandwidth with minimal investment over the existing infrastructure.

ii) Metropolitan Networks integrate access networks to service providers by serving geographical areas across several hundred kilometers, especially metropolitan areas. The present optical networks used Synchronous Digital Hierarchy (SDH) or Synchronous Optical Networks (SONET) protocols implementing Time Division Multiplexing (TDM). As WDM technology has surfaced, the system is being upgraded from single channel SONET to multichannel WDM/SONET rings. Traffic grooming is done for minimizing the resource utilization via high speed traffic streams generated after grouping different low speed traffic streams. This is achieved by introducing new technology equipments like Wavelength Add Drop Multiplexers (WADM), OXC, utilizing minimum wavelengths for data traffic at each node. The future metro networks implement mesh topologies to achieve architecture that is scalable, flexible, and efficient with maximum utilization of available bandwidth.

iii) Backbone networks are the core of communication networks from where the whole network tree expands. It interconnects all the metropolitan networks for long distance communication. These networks utilize WDM networks connected through mesh topology to carry high bandwidth data over different wavelength channels from one end to the other [4] [3]. These networks are normally classified as serial (devices are linked in series), parallel (multiple connection between high level routers and network segments), collapsed (central connection point for multiple sub networks) and distributed (implementing hierarchical design) backbone networks. For long haul networks, distributed networks are implemented owing to advantage of easy management, easy expansion and minimum capital investment required for growth.

The hierarchy of such networks is shown in Figure 1.2. The access networks are close to the users and the technology used for their design plays an integral role in design of backbone networks. This access network layer is connected together by implementing gateways through distribution layer. The core layer connects backbone network to distribution layer and different backbone networks together. The architecture of these networks involves combination of routers, switches or virtual LANs moving packets depending upon the networks layers address. The uniqueness of each network type is important for selecting an appropriate method of transmission. The long haul backbone network requires a high capacity communication system over long distances, while the same may not be suitable and cost effective in an access network. The implementation of same technology may also differ across the different networks. For example, WDM technology when implemented for long haul backbone networks requires 80 to 160 wavelengths per fiber. The same technology, when implemented for metro networks, will be implemented using a fiber supporting maximum of 40 wavelengths and usually no more than 8 wavelengths in access networks [5].

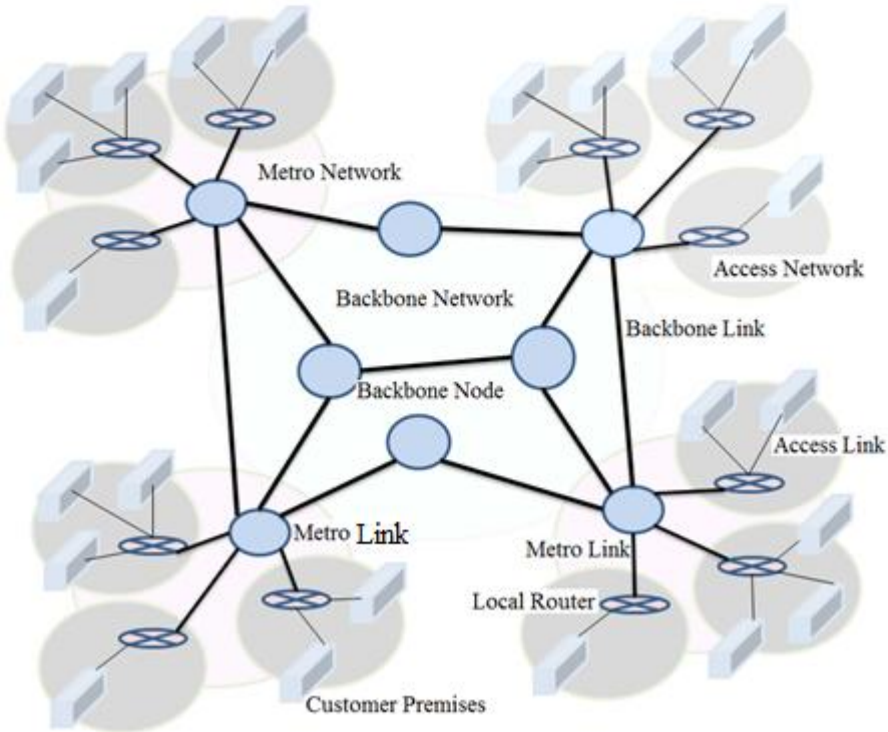

Figure 1.2: Optical Network Overview

In the subsequent years, a lot of developments have taken place in optical networks to develop and deploy sophisticated and reliable communication system with focus on improving transmission fidelity, increased data rate or carrying capacity of the network, increased transmission distance between inline repeater and amplifiers. The deployment of optical components like OADM, OXCs, wavelength convertor switches etc on network nodes has begun the phase of transition in optical networks where requirement of Optical to Electrical (O-E) signal transfer during the data transmission from a source to destination point is minimized. Based on O-E conversions taking place in the optical links, WDM networks may be broadly categorized as opaque, translucent and transparent networks. A single optical hop of lightpath never cross more than one physical fiber link in opaque network, could cross one or more fiber links in translucent networks and cross the entire source-destination route in translucent networks.

In an *opaque network* Optical-Electrical-Optical (O-E-O) transformation takes place at every node mainly due to all electronic switching components involved. Using this approach physical layer becomes completely autonomous entity making design, control and management simpler. Optical switch architecture is shown in

Figure 1.3. The major advantage of opaque networks is the superior quality of signal owing to regeneration of signal at almost every node. It is possible to have longer lightpath and large sized networks without compromising signal quality. Interoperability, traffic grooming, network sharing and restoration offer additional cost savings. However, the opaque network components may not be the practical solution to increased traffic growth as it requires a huge number of O-E-O conversions thereby increasing the unnecessary data processing and delays. Also, with increasing traffic load, more number of devices installation will be required, increasing the total network cost and power consumption. The research community has agreed upon the fact that there is a huge potential for reducing power consumption and cost by eradicating unnecessary opto-electronic (OE) transformations on a signal path in a core optical network.

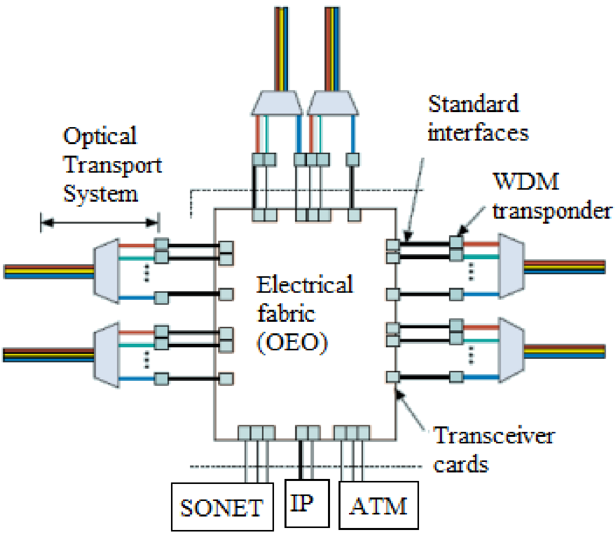

Figure 1.3: Opaque switch architecture **[6]**

In *transparent networks*, no O-E-O conversion takes place at all and the signal transverse throughout the fiber in optical domain only. A signal from source network element like router is either transmitted using a specific wavelength throughout without undergoing any wavelength conversion or may implement wavelength selective switches, tunable lasers etc for multiple wavelength architectures. The transparent switch architecture is shown in Figure 1.4. These networks have advantages data format and bit rate transparency, significant footprint and power savings, reduced network costs. By introducing transparent switch architecture in to opaque networks, the independence of physical layer from logical layer vanishes.

Thus, network design and operation becomes cross-layer problem. A complete transition of backbone networks from opaque to transparent is a far off dream till date due to limitations like absence of wavelength conversions, lack of signal quality enhancement at each node, routing and restoration issues, interoperability among the multiple service providers etc [6] [7] [8].

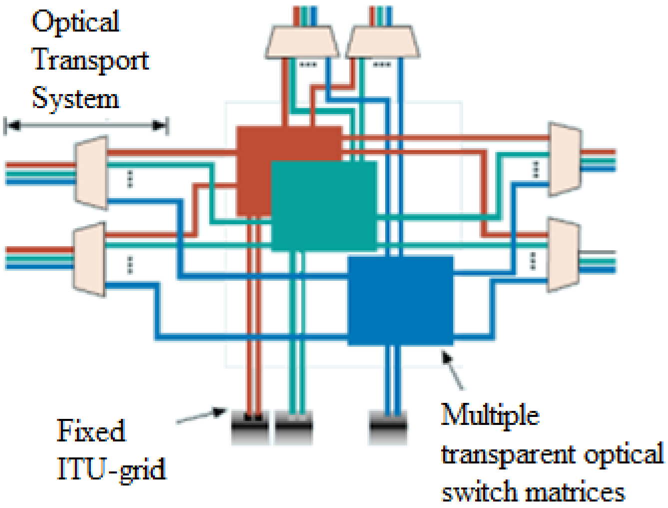

Figure 1.4: Transparent switch architecture **[6]**

A significant factor that hinders the implementation of transparent networks is analog nature of most of the existing optical technologies. There exists maximum transmission distance for the signals in optical domain, beyond which signal regeneration is required in order to amplify, reform and retime the optical signals. Although the regeneration may be done either using O-E-O conversions or in the optical domain only, but with the existing technologies, it is more economical and reliable to implement O-E-O conversions rather than going for all-optical components. Thus, instead of large scale deployment of transparent networks, deliberate use of transparent switches and 2R or 3R regenerators results in a network which seems to be a good compromise between purely optical and purely electrical networks demonstrating good balance between network design cost and performance.

In this configuration of optical networks, components performing O-E conversion are not available at all nodes, but strategically placed at certain nodes making them regeneration capable. These networks are called *translucent networks* [9]. These networks may be realized by combination of different transparent islands, by sparsely placed opaque nodes or by using translucent nodes. Term transparent island refers to domain of network with optical transparency, while nodes connecting different islands possess O-E-O conversion capability (shown in Figure 1.5). In second possible configuration, nodes with regeneration and wavelength conversion capability may be strategically placed in the network such that it may be used while lightpath setup whenever the need arises (shown in Figure 1.6). The third configuration implements switches having both optical and electronic switching core and OE conversion may be applied if necessary.

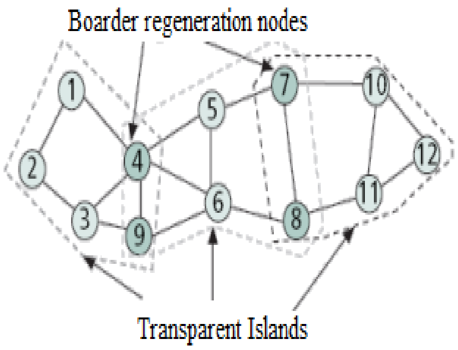

Figure 1.5: Translucent network with transparent island

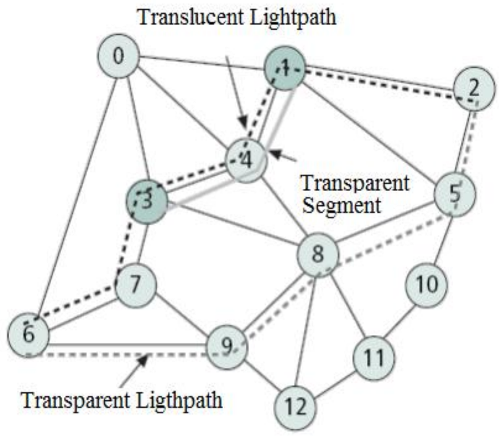

Figure 1.6: Translucent network with sparsely placed opaque nodes

The practical implementation of these optical networks requires design of three planes namely transport plane, control plane, management plane and their proper coordination. The transport plane includes network equipments (e.g. interface cards, fiber plants, switch etc) carrying the user data (e.g. voice, video, databases etc). Management plane handles operations, administration, maintenance, and provisioning security of the network. The control plane implements Network Elements (NEs) with access to network topology, resource information and accordingly plan, establish and maintain user services. The standard architecture for design of optical networks is specified by bodies like Optical Internetworking Forum (OIF), Internet Engineering Task Force (IETF) and International Telecommunications Union-Telecommunication Standardization Sector (ITU-T). The standard architecture called Automatic Switched Optical Network (ASON) is defined by ITU-T and various requirements of control plane design have been laid out. The focus of OIF is to provide standards that are interoperable for enabling multiple service providers to work collectively [10].The different standards laid for control plane are summarized in Table 1.1 [11].

Table 1.1: Different standards for control plane

Standards / Parameters	ITU-T	IETF	OIF
Requirements and Architecture	G.8080	RFC 3495	-
Auto Discovery	G.7714, G.7714.1	RFC 4204, RFC 4207	-
Signaling	G.7713, G.7713.2	RFC 3473, RFC 3474, RFC 3946, RFC 4208	ENNI 1.0, ENNI 2.0, UNI 1.0, UNI 2.0
Routing	G.7715, G.7715.1, G.7715.2	RFC 4202	ENNI OSPF 1.0
Management	G.7718, G.7718.1	GMPLS MIB RFCs	-

As per ASON architecture, the end user initializes the request through User Network Interface (UNI) which is established by the network. The connection requests may be permanent connections established directly by management layer, switched connections triggered by user equipments and set up using control plane, soft permanent connection, often called hybrid connections as involves both control and management plane. ITU focused on architecture of ASON unambiguously avoiding the development of new protocols, while IETF emphasized on development of new protocols as per requirements of general industry. They introduced GMPLS protocol which leads to introduction of technologies like Time Division Multiplexing (TDM), wavelength and wave band based switching often referred as Fiber Switch Capable (FSC) and Lambda Switch Capable (LSC) technologies with a focus on control plane implementation to IP routers, ATM switches, OXCs etc [12] .

The process of standardization mainly focused on the usage of network topology, routing and signaling applications like broadcasting, path computation, link management etc. The different standard protocols are implemented through bottom up approach for architecture and top-down functionality analysis. Traffic engineering extensions of Open Shortest Path First (OSPF-TE) is used as standard routing protocol where as Resource Reservation Protocol (RSVP-TE) is used as signaling protocols by GMPLS. The tracking of network topology and source discovery is controlled by Intermediate System to Intermediate System (IS-IS) protocol. The connection provisioning and maintenance is guided by Link Management Protocol (LMP) and Constraint-Based Routing-Label Distribution Protocol (CR-LDP). The additional features like link bundling for traffic engineering reduce the information distribution, improves routing scalability. An example of GMPLS architecture is shown in Figure 1.7 [13].

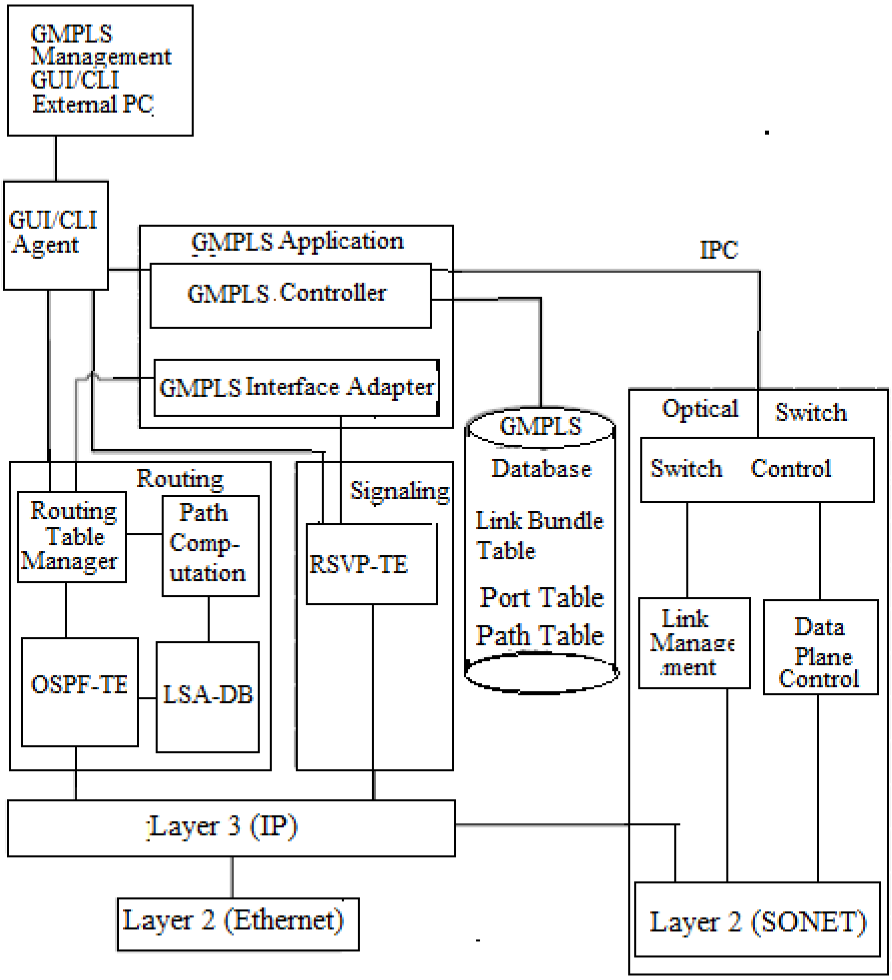

Figure 1.7: GMPLS control plane architecture **[13]**

In this architecture, client and network management plane interact through Graphical User Interface (GUI). The distributed plane is responsible for interaction of control and data planes. The function of routing, signaling and link management is performed by GMPLS manager. On start up, it initialize and create data structure required for signaling and routing. The GMPLS manager has two sub-components namely

GMPLS controller for control functions and GMPLS adapter for routing and signaling applications. On the arrival of connection request, admission control is performed by access node. The route calculation is done through path computation module with the help of routing table manager. The path to be set up is decided and its setup is initiated using signaling component. The routing tables are updates accordingly. Other functions of signaling unit includes setup and end the connection request, admission control and resource utilization at the nodes.

With the help of automatic configuration of networks using protocols like GMPLS, the need to support rapid establishment of dynamic services like large scale distributed computing, high bandwidth transmission has surfaced. Proper design, planning and operation of the network involves selecting network nodes, topology to interconnect these nodes, required switching and transmission system, methodology to accommodate the traffic through routing, protection and grooming. Owing to bandwidth hungry multimedia applications of internet, there have been great concern for designing a system with lower cost, higher data transfer capacity, minimum energy consumption without requiring much change in existing physical infrastructure. These applications resulted in networking trends like implementation of large number of wavelengths e.g. more than 150 wavelengths per fiber, high line rates, coarser granularities at switching level, thereby providing a cost-effective reconfigurable and dynamic optical network.

The current generation point to point network architectures are developing from traditional opaque networks towards transparent networks and are attracting the focus of research community for technological advancements. The major concerns for planning of these networks is connection provisioning with focus on minimizing the network cost and improve the resource utilization efficiency and will be addressed in the present research work.

The process of connection provision is also known as routing and wavelength assignment (RWA) and it involves setting up lightpath for individual call requests and assigning a particular wavelength to each connection request. In order to reduce the computational complexity, RWA can be studied as set of two problems (i) routing and (ii) wavelength assignment. Routing involves the lightpath setup between specific source and destination nodes as required by traffic demand matrix. For any network, the call requests for light path set up may be static or dynamic. With static RWA, traffic load on network is known well in advance and the process of path computation between all the possible combination of source and destination node is calculated beforehand and implemented accordingly. The main focus of static RWA is to establish lightpath with minimum resource utilization. In dynamic RWA also known as dynamic lightpath establishment, the arrival time and life time of dynamic load demands may or may not be known. Based on the lifetime of call requests, the path requests may be categorized as scheduled demands and adhoc demands. In scheduled lightpath demands (SLDs), lifetime of these demands is known in advance while adhoc lightpath demands (ALDs) are not known proiri. The call requests arrive randomly and utilize the network for quite long time. The lightpath is set up based on the available resources and links at the time of call request only. The dynamic RWA focuses on lightpath setup by minimizing the blocking probability of the network over a period of time.

For each connection request, once the route is calculated considering various constraints of network topology, the light path is set-up by allocating specific wavelength to the signal. If the wavelength remains same throughout as the signal transverse from source to destination node, it is bound by wavelength continuity constraint. This is the constraint for connection provision where wavelength conversion is not possible either because of network topology, route to be followed, and components installed etc. But if wavelength conversion capability is possible in the given route, distinct wavelengths may be assigned to each route to avoid interference. Thus, if the wavelength is available for the signal, all the possible solutions to the routing algorithms are assumed as feasible.

The minimum quality of transmission is usually defined by SLA signed between service providers and the clients. As per SLAs, the connection requirements are normally classified into four types namely premium, gold, silver and bronze. The class based differentiation in services has been initiated by service providers to accommodate the different requirements of users in a unified network and to sell high value added services at higher rates. Moreover, in dynamic networks, the route calculation is done spontaneously on the arrival of path requests based on the available resources at that instant. So, the priority for entertaining the path request may be set up according to class of the user maintaining the minimum agreed quality of transmission as per SLAs. Service level specifications as found in literature are summed up in Table 1.2 [14].

Table 1.2: SLA for class based routing

Parameters	Premium	Gold	Silver	Bronze
Out of Service Criterion	Degraded BER=10^{-4}	Degraded BER=10^{-3}	Fault	Fault
Recovery Time with Degraded SLA	Not specified	50 ms	500 ms	5 s
Full Recovery Time	50 ms	300 ms	5 s	5 min
Route Differentiation	Fully Supported (link, node, SRLG)	Partially Supported (link, node)	Partially Supported (link)	Not Supported
Maximum Delay	35 ms	100 ms	500 ms	5 s
Jitter	3 ms	10 ms	50 ms	1 s
Packet Loss	10^{-9}	10^{-6}	10^{-4}	10^{-2}

Most of the routing algorithms consider the optical layer to be the ideal one, thus making all the outcomes of routing algorithms valid and feasible. Practically, some of the calculated lightpath may not be satisfying the SLAs as the quality of signal transmission is influenced by the physical properties and operating conditions of optical fiber. Hence, it becomes necessary to monitor the quality of signal while it transverse from set of nodes to reach its destination, figure out important factors influencing the signal quality, techniques to monitor, model and mitigate their effects, communicate the information regarding these disparaging effects to network layer and control plane protocols for network management.

The networks capable of periodic OEO conversion offers an advantage of high signal quality maintained through 3R functions (reshaping, retiming, and regeneration). But in transparent networks all the components used are optical switches so as to eliminate the need for OEO conversions and make systems more flexible. In these networks, the signal has to transverse through the plenty of network elements including different type of fibers, amplifiers, optical add/drop multiplexers, cross-connects etc. This increasing complexity of networks makes the data transmission vulnerable to disparaging effect of signal impairments. As most of the physical impairments are additive in nature, they tend to accumulate along the lightpath and it may be possible that signal quality at the destination end is totally degraded. For this reason, future networks must consider the various impairments responsible for degrading the signal quality along with minimizing the blocking probability when selecting a route

Also, the lightpath is set up through the combination of different independent fiber links having different physical characteristics. In dynamic networks, the paths are set up and torn off dynamically. Each path will have different influence on signal quality depending on the number of links involved in setting the end to end connection. Moreover, non-linear fiber impairments on the lightpath are also influenced by the network state, number of co-propagating signals, power of individual signal and the channel wavelength under consideration. Thus it is becoming a necessity to measure the signal quality on per-channel basis in all-optical networks, rather than monitoring a single channel only.

It is quite evident that new forms of physical layer functionalities strongly influence the quality of transmission of signal and thus demand sophisticated techniques to monitor the quality of the optical signal throughout the network. The quality of signal once monitored, must be effectively implemented for routing applications in order to achieve optimum system performance. Another potential applications of performance monitoring includes activation of impairment reduction/compensation device; fault detection, path protection when monitoring a link failure; signal quality characterization for Quality assurance etc. In the present work, its application in path provisioning and traffic routing is taken into account.

Due to degradation of signal quality during transmission, the optical reach of signals being transmitted is limited. The one of the possible method to improve the optical reach is to place regenerators at some nodes in the network. In transparent and translucent networks placement and utilization of regenerators is important as high bit rate devices implemented in backbone networks and decreased wavelength spacing due to usage of multiple wavelength channels adversely affect the system performance. Also, in these optical networks, proper placement and utilization of regenerators helps in improved wavelength utilization, resource utilization, optical reach and call acceptance ratio. Although regenerators available to date may use all-optical signals or implement OEO conversions, but later one are cost effective and easy to install, hence are preferred by network providers till date. In order to trim down the capital expenses of the network, these regenerators must be carefully placed in the network without compromising with the performance expectations of the network. Even when they do exist in the lightpath set up, optimum utilization must be done in order to reduce computational complexity, avoid unnecessary signal processing and improve the delays for connection set up.

In the present research work an effort has been put in to develop novel algorithms for routing of optical networks considering the degradation effect posed by physical layer impairments. The regenerator placement and utilization is considered for optimum performance of network and minimum blocking probability. The focus of algorithms is on comprehensiveness, transparency, fault localization capability and scalability of the system. The analysis and evaluation of the physical layer parameters affecting the signal quality is done using network simulations. The result of performance monitoring is used for improving the routing capability of network. The proposed system is cost effective with sufficiently high update speed and reduced processing time. The upcoming sections of this chapter will discuss the major objectives laid out, significant contributions and organization of thesis.

CONTRIBUTION OF THESIS

Based on the initial studies and identified gaps, the major contribution of present research work is to design a routing algorithm taking in to consideration various physical layer impairments for WDM optical networks. This is successfully achieved through the following:

1. The different parameters affecting the signal quality which essentially need to be monitored so as to satisfy various SLAs are identified.

2. The influence of above identified parameters on signal quality is studied. It includes the impact of individual signals as well as overall impact on quality of the signal.

3. The overall impact of identified impairments is quantified and further implemented for connection provisioning and management of dynamically reconfigurable optical networks.

4. Implementing the developed algorithm in dynamically reconfigurable optical network for connection provisioning and network management

5. Efficiently place and utilize regenerators and monitors for increasing the optical reach and average call acceptance ratio at minimum cost.

OUTLINE OF THESIS

Considering the objectives achieved in the present research work, the thesis is organized in six chapters. The developments in optical communication systems from invent of fiber to the implementation of WDM for practical systems, hierarchy of optical networks and various standard protocols involved are presented in chapter 1. The different types of networks, including opaque, transparent and translucent networks, are specified and the different issues involved with the present networks are discussed. From these gaps are identified, objectives are laid out and discussed in subsequent chapters.

Chapter 2 discusses the various disparaging effects seriously influencing the signal quality. The mathematical model for the outlined effects is presented and demonstrated using certain simulations.

Chapter 3 discusses the need to monitor these impairments, various issues and challenges involved in their measurement. The system response for these impairments is studied for varying system parameters like wavelengths travelling, interaction of different impairments and their influence on system BER and Q-value. The technique used for signal quality estimation is discussed and general output of performance monitoring technique is presented.

Chapter 4 discusses the routing algorithm designed and its implementation on various standard networks. For testing purpose, a nine node network is assumed and route computation is done using three algorithms namely First Fit, Best Fit and Shortest Path algorithm. In order to validate the techniques presented, the algorithm is implemented over Internet2 and European Optical Network (EON) and the results obtained are compared with the different algorithms already existing in literature.

Chapter 5 discusses the different strategies of regenerator placement in translucent or transparent network. Three different variations are presented namely regenerator placement according to nodes most utilized among all the possible paths, regenerator placement as per maximum path utilization by the current traffic matrix and placement according to influence of impairments present in different links. The effect of these techniques on routing algorithms of chapter 4 is presented.

Chapter 6 summarizes the different results obtained with their practical applications, future prospective of the present work.

Chapter 2

Physical layer impairments

This chapter discusses the various disparaging effects seriously influencing the signal quality. The mathematical model for the outlined effects is presented and demonstrated using certain simulations.

CHAPTER 2: PHYSICAL LAYER IMPAIRMENTS

In the past decade, implementation of WDM networks has completely revolutionized the telecommunication system by providing larger bandwidth for high data rate transmission. The handling of increased data traffic in the network is a potential challenge for the service providers. Even a small error in any parameter may result in the network failure causing enormous data loss. For efficient operation, today's network must be reconfigurable, secure, robust and flexible enough for optimum utilization of network resources. To achieve that, it is essential to continuously monitor the substantial condition of network, quality of signal being transmitted, identify various security risks and formulate back up plans for preventing data loss and network failure. It is quite challenging due to presence of large number of degrading factors across the links, different data formats used, multiple data rates existing over the same network. Sometimes, the degradation will be such that it is difficult to identify the signal at destination. The class based routing, need for satisfied SLAs, accumulation of impairments along the lightpath further fuel the need of continuous monitoring of fiber links. In order to inculcate performance monitoring system for network design and planning, it is vital to study the different factors responsible for degrading quality of link. The key contribution of this chapter is to study the disparaging effects of physical layer and make out different parameter disturbing the signal quality. These parameters are essential to monitor in order to maintain the standards agreed upon in different SLA. The different approaches available for their monitoring are reported and strategy to monitor them is outlined.

The different parameters include physical layer impairments and are categorized as non-linear and linear impairments. Linear impairments account for losses taking place inside the fiber due to varying physical properties of fiber like refractive index, temperature, presence of impurities etc, but are independent of signal intensity or co-propagating channels. They are static in nature and can be easily pre-estimated for any network. The examples of linear impairments include Attenuation, Dispersion, Linear Crosstalk, Amplified Spontaneous Emission (ASE) noise. The degradation effects varying with optical intensity existing within the fiber link are called non-linear effects. The variation in optical intensity of fiber link results in inelastic scattering and uneven refractive index giving birth to non-linear impairments. Different non-linear impairments include Four Wave Mixing (FWM), Self Phase Modulation (SPM) and Cross Phase Modulation (XPM) etc. In this chapter, different optical impairments responsible for signal degradation are studied. This chapter thrashes out various linear and non-linear impairments responsible for signal degradation in fiber link. It includes dispersion, attenuation, SPM, XPM and FWM. The mathematical model for higher order dispersion is obtained and their impact on system performance is studied. Analytical modeling of non-linear impairments SPM, XPM, FWM and their influence on system performance is presented.

2.1 LINEAR IMPAIRMENTS

To account for linear impairments present in the optical fiber, the electromagnetic interactions taking place while the light wave propagates inside the fiber core must be studied. For non-conducting medium, Maxwell's equations as specified in [1] and [15] are used to analyze the system behavior and are reproduced (Eq 2.1-2.20) for better understanding of the concept. The Maxwell's equations for step index fiber of core and cladding index n_1 and n_2 is given by

$$\nabla \times E = -\frac{\partial B}{\partial t}, where\ B = \mu_o H + M, M = 0 \qquad (2.1)$$

$$\nabla \times H = \frac{\partial \phi_d}{\partial t} where\ \phi_d = \epsilon_o E + P, \qquad (2.2\ a)$$

$$P(r,t) = \epsilon_o \int_{-\infty}^{\infty} \chi(r, t - t')E\,(r, t')dt' \qquad (2.2\ b)$$

$$\nabla . \phi_d = 0 \qquad (2.3)$$

$$\nabla . B = 0 \qquad (2.4)$$

In these, E - Electric Field Vector, H - Magnetic Field Vector, ϕ_d- flux density because of E, B - flux density because of H, P – induced electrical polarization, M is induced magnetic Polarization, μ_o and ε_o are vacuum permeability and permittivity respectively, χ is linear susceptibility. [1] [15]The relation between P and E may be non-linear. Ignoring the non-linear component P and solving the four equations yields the equation of propagation in time domain as

$$\nabla^2 E = \frac{1}{c^2}\frac{\partial^2 E}{\partial t^2} + \mu_o \frac{\partial^2 P}{\partial t^2} \; where \; \frac{1}{c^2} = \mu_o \epsilon_o \; and \; \mu\epsilon = \frac{1}{v_p} \qquad (2.5)$$

Here, c – speed of light, μ, ε are permeability and permittivity of the medium, v_p is phase velocity.

In frequency domain, this equation can be rewritten as

$$\nabla^2 E + k_o^2 \epsilon_{r,\omega} \bar{E} = 0, where \; k_o = \frac{\omega}{c} = \frac{2\pi}{\lambda} \; is \; wave \; number \qquad (2.6)$$

λ is the vacuum wavelength of the optical field oscillating with frequency ω.

In cylindrical coordinates, E has three components E_ρ, E_ϕ, E_z. It is customary to represent equation considering z as independent coordinate. Thus, equation (2.6) can be rewritten as

$$\frac{\partial^2 E_z}{\partial \rho^2} + \frac{1}{\rho}\frac{\partial E_z}{\partial \rho} + \frac{1}{\rho^2}\frac{\partial^2 E_z}{\partial \phi^2} + + n_1^2 k_o^2 E_z = 0 \qquad (2.7)$$

Rewriting equation (2.7) as function of ρ, ϕ, z

$$E_z(\rho, \phi, z) = F(\rho)\Phi(\phi)Z(z) \qquad (2.8)$$

Using ordinary differential equations, Equation (2.7) can be solved through separation of variables, where three ordinary differential equations obtained are

$$\frac{\partial^2 Z}{\partial z^2} + \beta^2 z = 0 \qquad (2.9)$$

$$\frac{\partial^2 \Phi}{\partial \phi^2} + m^2 \phi = 0 \qquad (2.10)$$

$$\frac{\partial^2 F}{\partial \rho^2} + \frac{1}{\rho}\frac{\partial F}{\partial \rho} + \left(n^2 k_o^2 - \beta^2 - \frac{m^2}{\rho^2}\right) F = 0 \qquad (2.11)$$

Solution of (2.9) is

$Z = e^{i\beta z}$, where β is the propagation constant (2.12)

Solution of (2.10) is

$\Phi = e^{im\varphi}$, where m will have integer values only. (2.13)

Solution of (2.11) is obtained using Bessel's function and is given as

$$F(\rho) = \begin{cases} AJ_m(p\rho) + A^{'}Y_m(p\rho); & \rho \leq a \\ CK_m(q\rho) + C^{'}I_m(q\rho); & \rho > a \end{cases} \tag{2.14}$$

Here, A, A', C, C',p,q are constants and J_m, Y_m, K_m, I_m are Bessel Functions.

$$p^2 = n_1^2 k_o^2 - \beta^2 \tag{2.15}$$

$$q^2 = \beta^2 - n_2^2 k_o^2 \tag{2.16}$$

Using boundary conditions:

a) Optical field for guided waves should be finite at ρ=0 and decay at ρ=∞ .
b) $Y_m(p\rho)$ at p=0, and F(0) can be finite iff A'=0
c) F'(ρ) vanishes at infinity iff c'=0.

The solution obtained after implementing these stated conditions is

$$E(z) = \begin{cases} AJ_m(p\rho)\exp(im\phi)\exp(i\beta z); & \rho \leq a \\ CK_m(q\rho)\exp(im\phi)\exp(i\beta z); & \rho > a \end{cases}, \; where\ a\ is\ radius\ of\ fiber \tag{2.17}$$

Assuming tangential components of H and E is continuous at interface of core and cladding; values of A, C can be calculated. Calculating A, C and substituting in above equations yields the Eigen value equation as

$$\left[\frac{J_m^{'}(pa)}{pJ_m(pa)} + \frac{K_m^{'}(qa)}{qK_m(qa)}\right]\left[\frac{J_m^{'}(pa)}{pJ_m(pa)} + \frac{n_2^2 K_m^{'}(qa)}{n_1^2 qK_m(qa)}\right] = \frac{m^2}{a^2}\left(\frac{1}{p^2} + \frac{1}{q^2}\right)\left(\frac{1}{p^2} + \frac{n_2^2}{n_1^2 q^2}\right) \tag{2.18}$$

For given set of k_o, a, n_1, n_2, values of β may be calculated for each value of m using (2.18) and expressed as β_{mn}. Field distribution satisfies all boundary conditions and does not change with propagation except for phase factor. Each value of β_{mn} represents a mode of field propagating inside the fiber spatial distribution given by above said equations. Practically the core of fiber shows considerable variations along fiber length. The resulting non-symmetrical cylindrical geometry disturbs the orthogonally polarized modes introducing birefringence into the fiber. The degree of birefringence is given by

$$B_m = |\bar{n}_x - \bar{n}_y|, where\ \bar{n}_x\ and\ \bar{n}_y\ - mode\ indices\ of\ orthogonal\ modes \tag{2.19}$$

Owing to birefringence, different frequencies of a pulse acquire variable polarization states because of intervallic power exchange between two polarization components. This phenomena leads to degenerating factors in the form of linear impairments along the fiber link and are discussed in detail in this section.

2.1.1 Dispersion

The phenomena of pulse broadening while signal propagates in the fiber of length L is known as Dispersion (shown in Figure 2.1). The effect causes neighboring pulses to overlap and difficult to distinguish. It limits the available bandwidth of optical fibers and lowers the bit rate.

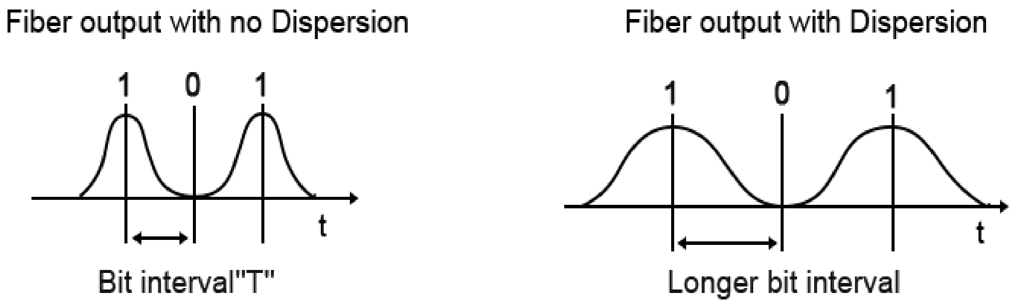

Figure 2.1: Pulse broadening due to Dispersion

Depending on the cause of pulse broadening, the dispersion is classified as Polarized Mode Dispersion (PMD) and Group Velocity Dispersion (GVD). [16] PMD is broadening due to presence of birefringence where linearly polarized light periodically oscillates its shape between linear and elliptical as it propagates inside the fiber. Because of non-uniformity stress of core, it actually reaches stage of arbitrary polarization and two orthogonally polarized modes disperse along the fiber length resulting in pulse broadening. GVD is pulse broadening owing to frequency dependence of group velocities. The different wavelength groups travel with different velocities ensuing delay at the output.

a) Polarized Mode Dispersion

Light energy at given wavelength has two orthogonal polarization states. At start, both are aligned but because of variations in cylindrical geometry along the length of fiber, each one will encounter different refractive index. Each polarization mode will move at different velocity, introducing time variation between transmission of modes will cause pulse spread and is called PMD (shown in Figure 2.2).

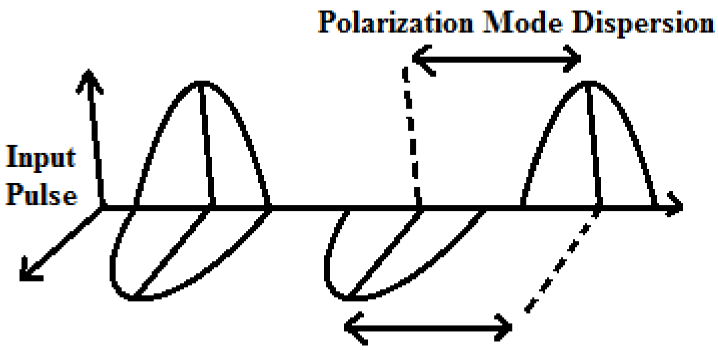

Figure 2.2: The delay in two orthogonal polarizations of a signal due to PMD

PMD of ideal uniform fiber as described by [17] is given by

$$\Delta\tau_{pmd} = L|\beta_{1x} - \beta_{1y}| = L\left|\frac{1}{v_{gx}} - \frac{1}{v_{gy}}\right| = D_{pmd}\sqrt{L}, \qquad (2.20)$$

where β_{1x}, β_{1y} are propagation constants and v_{gx}, v_{gy} are group velocities of polarization component along x and y axis, D_{pmd} is average PMD parameter measured in ps/√km. The maximum tolerable value of τ_{pmd} ranges between 10-20% of a bit duration.

Polarized mode dispersion can also be characterized by PMD vector using Muller Matrix method, Jones Matrix Eigen Analysis or using Poincare sphere. One such representation using Principle State Model is presented in [17]. According to Principle States Model, while studying power of optical signal in long length fibers during time domain analysis, one can find at least two orthogonal polarization states at input of fiber that results in output pulse without causing any distortion up to first order. Similarly, for every frequency there exist atleast two polarization states for which the output remains undistorted for first order. Accordingly, PMD can be characterized by

$$\text{PMD vector in 3} - \text{D Strokes space}, \tau = \Delta\tau\hat{p}, \qquad (2.21)$$

$\Delta\tau$ - Differential Group Delay (DGD)

$\hat{p}$ -unit vector pointing toward slower principle state of polarization [17]

The equations for higher order PMD can be obtained by studying variation of PMD with angular frequency ω, through a Taylor series expansion.

Taylor Series expansion of equation (2.21) is given by

$$T(\omega_o + \Delta\omega) = T(\omega_0) + \Delta\omega \frac{dT}{d\omega} + \frac{(\Delta\omega)^2}{2!}\frac{d^2T}{d\omega^2} + \frac{(\Delta\omega)^3}{3!}\frac{d^3T}{d\omega^3} \ldots\ldots \tag{2.22}$$

As is clear from the equation (2.22), second order PMD is given by second term

$$\Delta\omega \frac{d\tau}{d\omega} = \Delta\omega \left(\frac{d\Delta\tau}{d\omega}\hat{p} + \frac{d\hat{p}}{d\omega}\Delta\tau \right) \tag{2.23}$$

In RHS of equation (2.23), first term represent component of PMD along the T while the second term represents the perpendicular to T as is shown in Figure 2.3.

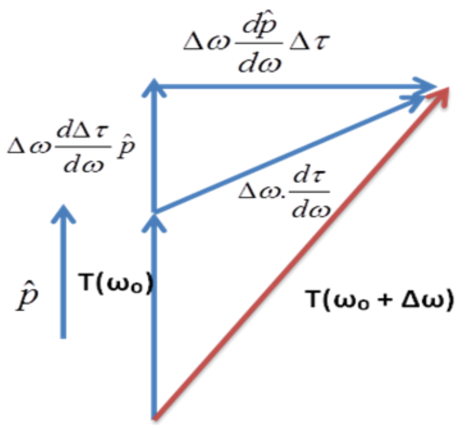

Figure 2.3: Phasor diagram of 2nd order PMD

Third order PMD calculated from equation (2.22) is:

$$\left\{ \frac{1}{2}\left(\Delta\omega^2 \frac{d^2\tau}{d\omega^2} \right) \right\} = \frac{\Delta\omega^2}{2} \frac{d^2(\Delta\tau\hat{p})}{d\omega^2} = \frac{\Delta\omega^2}{2} \frac{d\left\{ \frac{d}{d\omega} \left\{ \frac{d\Delta\tau}{d\omega}\hat{p} + \frac{d\hat{p}}{d\omega}\Delta\tau \right\} \right\}}{d\omega} \tag{2.24}$$

On solving,

$$\left\{ \frac{1}{2}\left(\Delta\omega^2 \frac{d^2\tau}{d\omega^2} \right) \right\} = \frac{\Delta\omega^2}{2} \left\{ \hat{p}\frac{d^2\Delta\tau}{d\omega^2} + 2\frac{d\hat{p}}{d\omega}\frac{d\Delta\tau}{d\omega} + \frac{d^2\hat{p}}{d\omega^2}\Delta\tau \right\} \tag{2.25}$$

Equation for further higher order may be derived in the similar manner using Taylor series expansion.

b) Intermodal Dispersion or Modal Dispersion:

It is degradation effect that appears only in multimode fibers. In this case, the spread of pulse is due to the fact that each mode has different group velocities at same frequency. It may be decreased by using graded index multimode fibers or single mode fibers (shown in Figure 2.4).

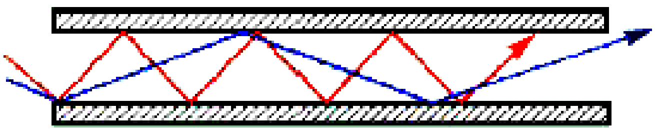

Figure 2.4: Modes travelling at different velocities resulting in intermodal dispersion

For the fiber of length L, core refractive index n_1, broadening of pulse at output is as specified in [1] given by

$$\Delta\tau = \frac{L}{2cn_1}(NA)^2 \tag{2.26}$$

In order for the pulses to be distinguishable, $\Delta\tau<1/B$, B-bit rate

RMS impulse response because of intermodal dispersion as specified in [1] is given by

$$\sigma_s \cong \frac{L(NA)^2}{4\sqrt{3}\, n_1 c} \tag{2.27}$$

c) Intramodal Dispersion or Group Velocity Dispersion:

It occurs in all type of optical fibers where different wavelengths are used (e.g. WDM networks). In this degradation effect, pulse spreading takes place as a result of group velocity as the function of wavelength within the single mode. It may be broadly classified as material and waveguide dispersion. *Material dispersion* (also called Chromatic Dispersion) is because of variation of refractive index of core material as a function of wavelength. Pulse spreading occurs even when different wavelengths follow the same path shown in Figure 2.5.

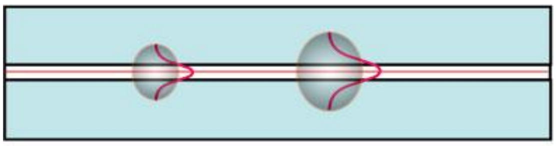

Figure 2.5: Effect of Chromatic dispersion

Time delay resulting from material dispersion is as specified in [1] is given by

$$\tau_{mat} = \frac{L}{c}\left(n - \lambda\frac{dn}{d\lambda}\right) \tag{2.28}$$

Pulse spread for source of spectral width σ_λ as specified in [1] is given by

$$\sigma_{mat} = \frac{\sigma_\lambda L}{c}\left|\lambda \frac{d^2 n}{d\lambda^2}\right| = \sigma_\lambda L |D_{mat}(\lambda)|, \quad (2.29)$$

Where, D_{mat} (λ) is material dispersion

In *waveguide dispersion* pulse spreading takes place because only a part of optical power propagation along the fiber is confined to core while longer one penetrate into the cladding. Practically, only 80% of power is confined to core. As $n_2 < n_1$, fraction of light propagating in cladding travel faster than in core. Also, as refractive index depends on wavelength as well, different spectral components will have different speed. Pulse broadening happens because of difference in core-cladding power distributions and speed variation of wavelengths. The effect is dominant in step index fibers with small effective mode area shown in Figure 2.6. The effect of material dispersion is dominating as compared to waveguide dispersion in fibers with large effective mode areas.

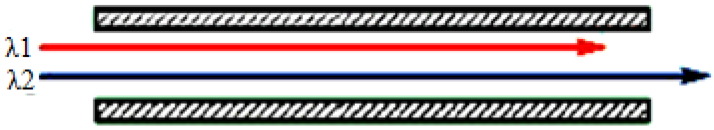

Figure 2.6: Waveguide dispersion in step index fiber

Time delay resulting from waveguide dispersion as specified in [1] is given by

$$\tau_{wg} = \frac{L}{c}\left(n_2 + n_2\Delta\frac{dkb}{dk}\right) = \frac{L}{c}\left(n_2 + n_2\Delta\frac{d(Vb)}{dV}\right) \quad (2.30)$$

Where, Δ is index number given by $\Delta = \frac{n_1 - n_2}{n_1}$, $k = \frac{2\pi}{\lambda}$ and $b \approx \frac{\beta/k - n_2}{n_1 - n_2}$, V-normalized frequency

Pulse spread for source of spectral width σ_λ as specified in [1] is given by

$$\sigma_{wg} = \left|\frac{d\tau_{wg}}{d\lambda}\right|\sigma_\lambda = \frac{V}{\lambda}\left|\frac{d\tau_{wg}}{dV}\right|\sigma_\lambda = \sigma_\lambda L\left|D_{wg}(\lambda)\right| = \frac{\sigma_\lambda L \Delta n_2}{c\lambda} V \frac{d^2(Vb)}{dV^2} \quad (2.31)$$

Where, D_{wg} (λ) is waveguide dispersion

To calculate total group velocity dispersion, variations in wave propagation constant β, as a function of λ or ω are studied. For the same, general expressions Eq. 2.33, 2.34, 2.38 to 2.42 are obtained from [1] and [15] . The higher order β is obtained by its Taylor series expansion about central frequency ω_o yields.

$$\beta(\omega) \approx \beta_o(\omega_o) + \beta_1(\omega_o)(\omega - \omega_o) + \frac{1}{2}\beta_2(\omega_o)(\omega - \omega_o)^2 + \frac{1}{6}\beta_3(\omega_o)(\omega - \omega_o)^3$$

(2.32)

Where, $\beta_m = \left(\frac{\partial^m \beta}{\partial \omega^m}\right)_{\omega=\omega_0}$

Group velocity dispersion parameter (or Chromatic dispersion)

$$\beta_2 = -D\frac{\lambda^2}{(2\pi c)} \quad (2.33)$$

Here, D-dispersion parameter given by

$D = \frac{d(v_g)^{-1}}{d\lambda}$ and is measured in ps/(nm.km) (2.34)

Third order dispersion parameter

$$\beta_3 = \frac{d\beta_2}{d\omega} = \frac{d\beta_2}{d\lambda}\frac{d\lambda}{d\omega} = -\frac{\lambda^2}{(2\pi c)^2}\left(\frac{\partial(\lambda^2 D)}{\partial \lambda}\right) = \frac{\lambda^2}{(2\pi c)^2}(\lambda^2 S + 2\lambda D) \quad (2.35)$$

Where, S-dispersion slope parameter given by $S = \frac{dD}{d\lambda}$,

Fourth order dispersion parameter

$$\beta_4 = \frac{d\beta_3}{d\omega} = -\frac{\lambda^2}{(2\pi c)}\frac{d\beta_3}{d\lambda} = -\frac{\lambda^2}{(2\pi c)}\frac{\lambda^2}{(2\pi c)^2}\frac{d\beta_3}{d\lambda} = -\frac{\lambda^4}{(2\pi c)^3}\left(4\lambda S + \lambda^2\frac{dS}{d\lambda} + 2D\right)$$

(2.36)

Fifth order dispersion parameter

$$\beta_5 = \frac{d\beta_4}{d\omega} = -\frac{\lambda^2}{(2\pi c)}\frac{d\beta_4}{d\lambda} = \frac{\lambda^6}{(2\pi c)^4}\frac{d(4\lambda S + \lambda^2\frac{dS}{d\lambda} + 2D)}{d\lambda} = \frac{\lambda^6}{(2\pi c)^4}\left(6S + 6\lambda\frac{dS}{d\lambda} + \lambda^2\frac{d^2 S}{d\lambda^2}\right)$$

(2.37)

Now, different components of β and z are examined, where z is distance travelled in the fiber and β_{oz} represents phase shift of propagating optical wave.

Group velocity, $v_g = \frac{1}{\beta_1} = c\frac{dk}{d\beta}, \quad where, k = \frac{2\pi}{\lambda}$ (2.38)

Group delay, $\tau_g = L/v_g$ (2.39)

For spectral components that are δλ apart and lie between δλ/2 above and below central wavelength λ_o, total delay difference over a distance L is given by

$$\delta\tau = \frac{d\tau_g}{d\lambda}\delta\lambda = -\frac{L}{2\pi c}\left(2\lambda\frac{d\beta}{d\lambda} + \lambda^2\frac{d^2\beta}{d\lambda^2}\right)\delta\lambda \quad (2.40)$$

In terms of angular frequency,

$$\delta\tau = \frac{d\tau_g}{d\omega}\delta\omega = \frac{d}{d\omega}\left(\frac{L}{v_g}\right)\delta\omega = L\left(\frac{d^2\beta}{d\omega^2}\right)\delta\omega \qquad (2.41)$$

Pulse spread in terms of rms pulse width is given by

$$\sigma_g = \frac{d\tau_g}{d\lambda}\sigma_\lambda = -\frac{L\sigma_\lambda}{2\pi c}\left(2\lambda\frac{d\beta}{d\lambda} + \lambda^2\frac{d^2\beta}{d\lambda^2}\right) \qquad (2.42)$$

Enormous work has been done till date to calculate the dispersion accumulation in the network using time of flight, modulation phase shift and interferometric techniques [18] [19] [20] [21] [22] [23] [24]. Measuring time of flight being the simpler one is implemented to describe the effect of dispersion. To study the effect of dispersion on system performance, a simple source to destination node link as shown in Figure 2.7 is considered. CW Lorentzian laser of 1550 nm wavelength is used as the source of optical signal. 10 Gbps NRZ signal is generated and modulated using dual arm Mach Zehnder Modulator. Standard single mode fiber (Implementing recommendation ITU-T G.652 or TIA 492CAAA / OS1) of 100km length is used to transmit the signal. In order to isolate the effect of dispersion from other impairments, coefficients of degradation factors like attenuation, non-linearity, Raman crosstalk etc are turned off. At the receiver end, PIN diode is used for O-E conversion. The electrical output is filtered using fourth order Bessel filter and the output is analyzed.

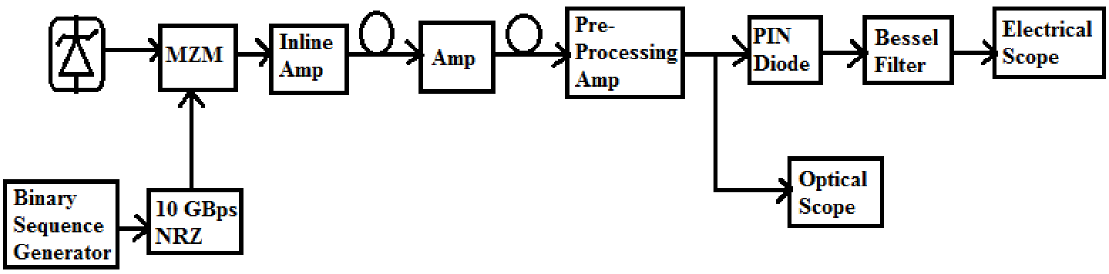

Figure 2.7: A source to destination node link to measure the impact of PLIs

To describe the effect of higher order dispersions in optical networks, the different combinations of β_2, β_3, β_4 and β_5 are simulated and corresponding effects on system performance is studied using eye diagram analysis. As represented in Table 2.1, all possible combinations of higher order are considered with a fixed value to β. The corresponding eye diagrams obtained are shown in Figure 2.8 to Figure 2.15.

Table 2.1: Values of different orders of beta for different runs

Run no.	β_2	β_3	β_4	β_5	**Run no.**	β_2	β_3	β_4	β_5
1	0	0	0	0	9	5	0	0	0
2	0	0	0	5	10	5	0	0	5
3	0	0	5	0	11	5	0	5	0
4	0	0	5	5	12	5	0	5	5
5	0	5	0	0	13	5	5	0	0
6	0	5	0	5	14	5	5	0	5
7	0	5	5	0	15	5	5	5	0
8	0	5	5	5	16	5	5	5	5

Figure 2.8 to Figure 2.11 shows the eye diagram of system with no dispersion being superimposed by eye diagram of system having dispersion of single higher order only. Here, in Figure 2.8 eye diagram of system with fifth order impairment only is superimposed over the system considering no dispersion at all. Similarly, system with fourth order, third order and second order dispersion are superimposed to obtain Figure 2.9 to Figure 2.11 respectively. It can be visualized that among the different orders of impairments present, maximum impact is caused by second order dispersion. Delay introduced by third, fourth and fifth order only is negligible as compared to delay caused by second order dispersion. The impact may also be studied from variation in eye opening, Q-value and the power delivered at the receiver. The value of eye opening (0.71E-4) and power delivered (0.39E-01) is minimum for system with second order dispersion.

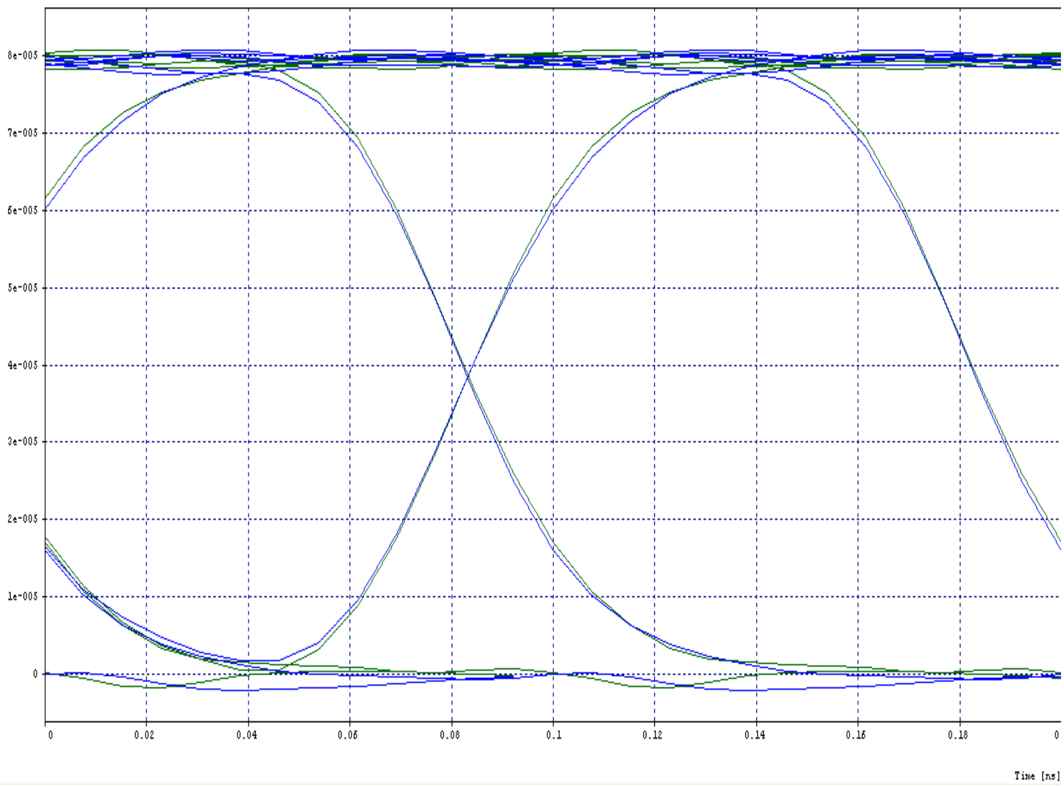

Figure 2.8: Eye diagram of system with no dispersion being superimposed by eye diagram of system having fifth order dispersion only

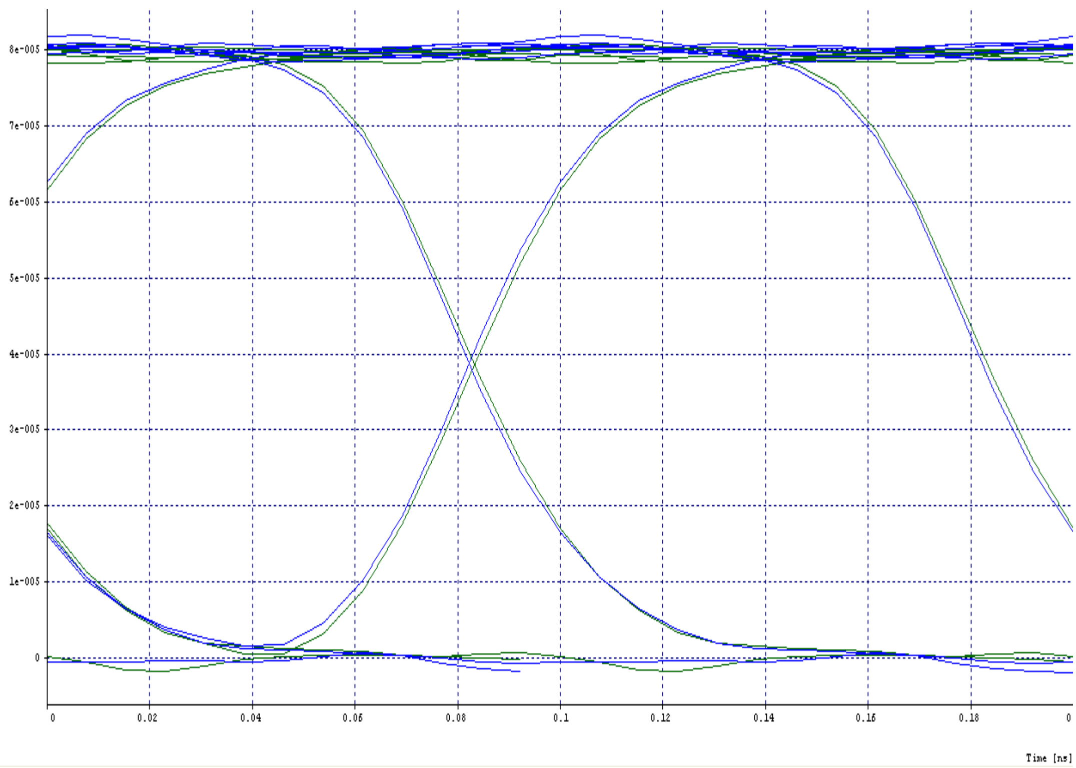

Figure 2.9: Eye diagram of system with no dispersion being superimposed by eye diagram of system having forth order dispersion only

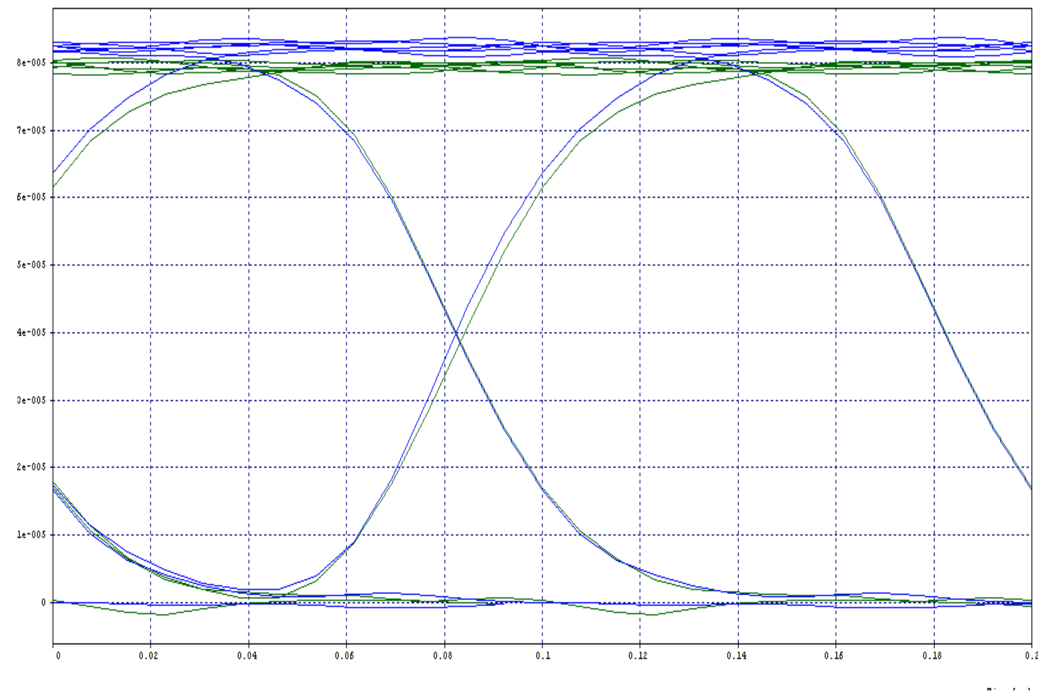

Figure 2.10: Eye diagram of system with no dispersion being superimposed by eye diagram of system having third order dispersion only

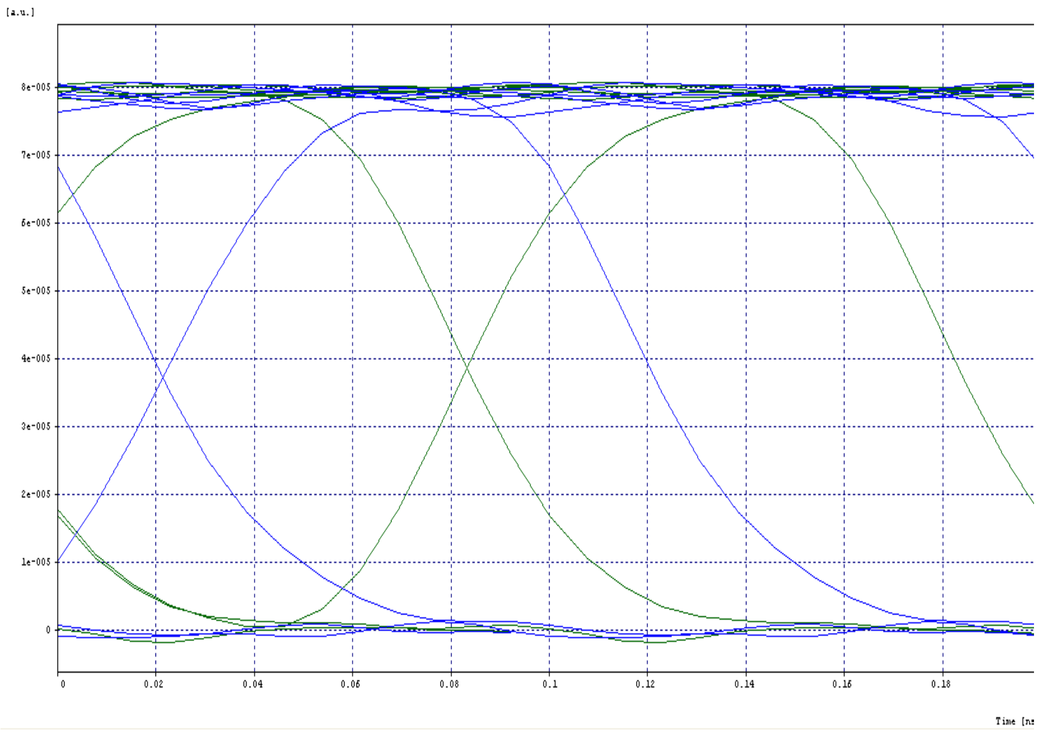

Figure 2.11: Eye diagram of system with no dispersion being superimposed by eye diagram of system having second order dispersion only

Figure 2.12 and Figure 2.13 represents output of system having total dispersion as the combination of odd and even higher order impairments superimposed over the output of system with no dispersion at all respectively. The odd order impairments (third and fifth order) have minimum impact on system performance as the delay induced is even less than 0.0005 ns. The combination of even order dispersion poses a significant delay in propagation of pulses (of the order 0.08ns). With the introduction of fourth order dispersion along with third and fifth order, the delay introduced is increased to 0.06ns as shown in Figure 2.14. The stated facts are backed up by the values of eye opening and power delivered for these combinations. The odd order impairments have average eye opening 0.79E-04 while that of even orders has opening 0.76E-4. The decreased eye opening and delivered power represents decreased efficiency of the system. Figure 2.15 represents the overall delay introduced by the combination of all orders of impairments. The values of Q-factor, eye opening, eye closure optical power delivered at the output for all the 16 possible combinations and are summarized in Table 2.2.

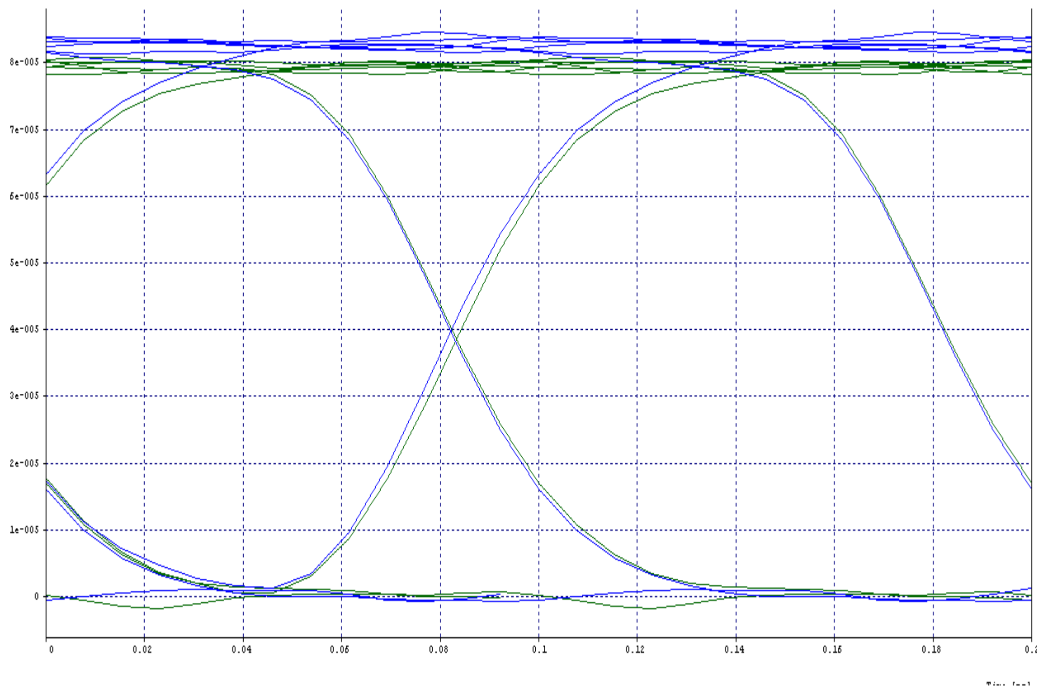

Figure 2.12: Eye diagram of system with no dispersion being superimposed by eye diagram of system having third and fifth order dispersion

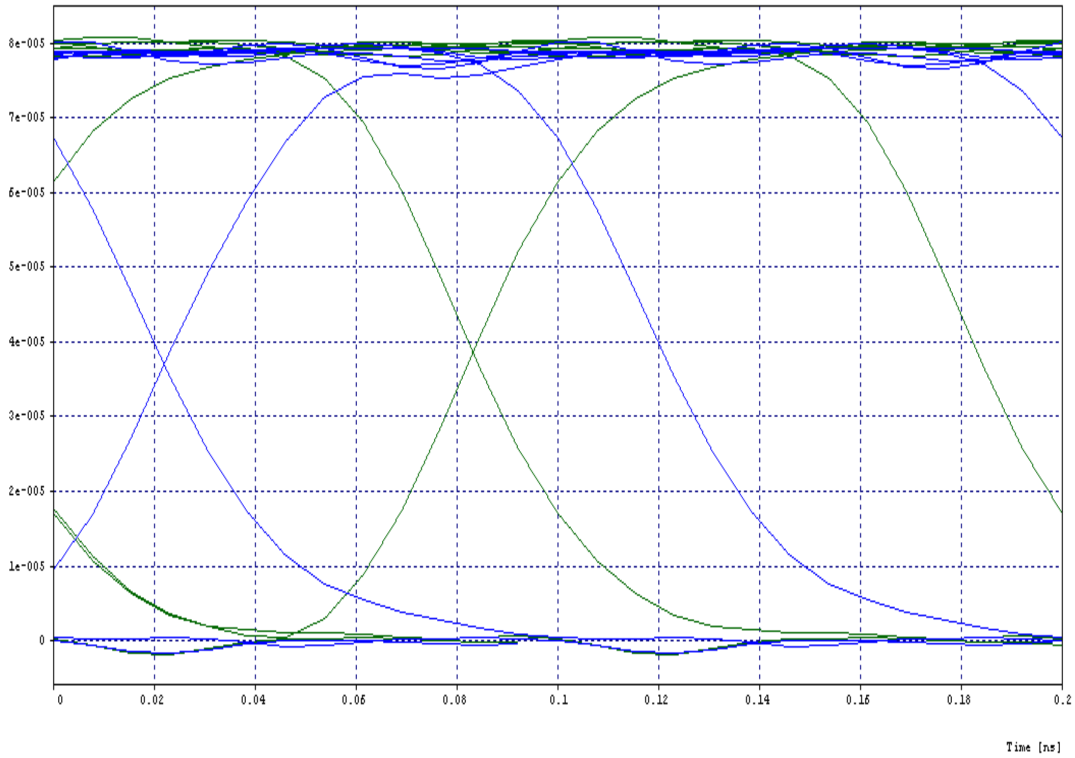

Figure 2.13: Eye diagram of system with no dispersion being superimposed by eye diagram of system having second and forth order dispersion

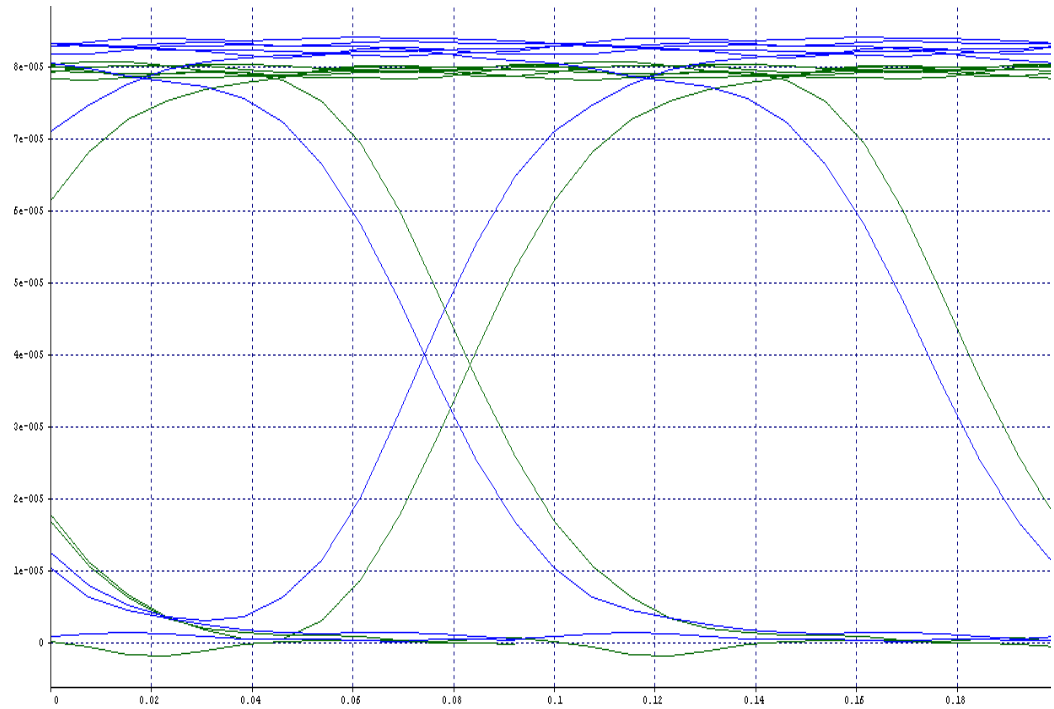

Figure 2.14: Eye diagram of system with no dispersion being superimposed by eye diagram of system having third, forth and fifth order dispersion

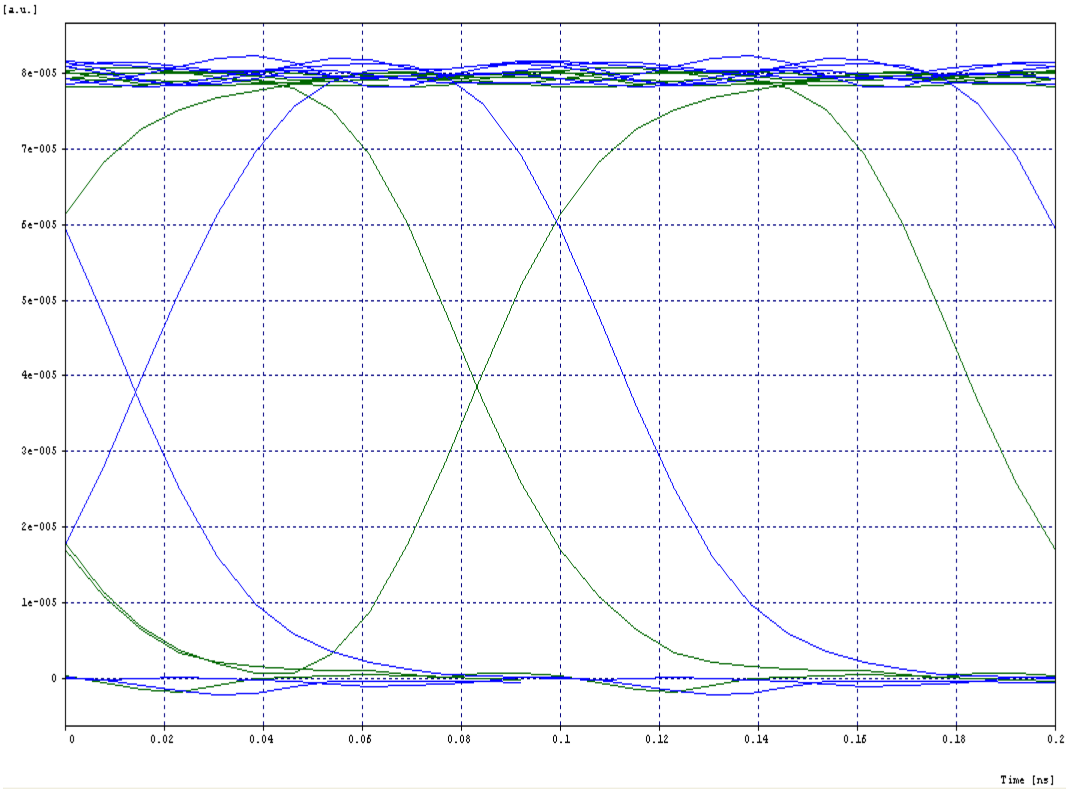

Figure 2.15: Eye diagram of system with no dispersion being superimposed by eye diagram of system having second, third, forth and fifth order dispersion

Table 2.2: Q-factor, eye opening, eye closure optical power delivered at the output

Run	Q-Value (dB)	Q-Value (linear)	Eye Closure (dB)	Eye Opening	Average Eye Opening	Optical Power (dB)	Optical Power (mW)
1	30.8945	35.05303	0.33999	0.72061E-04	0.77929E-04	-13.953	0.402E-01
2	31.1886	36.26017	0.22964	0.73727E-04	0.77731E-04	-13.958	0.402E-01
3	31.5371	37.74461	0.26470	0.73454E-04	0.78070E-04	-13.950	0.403E-01
4	31.3767	37.05423	0.22582	0.73503E-04	0.77426E-04	-13.956	0.402E-01
5	28.0840	25.36310	0.35115	0.73131E-04	0.79290E-04	-13.841	0.413E-01
6	27.8355	24.64755	0.37969	0.72638E-04	0.79275E-04	-13.840	0.413E-01
7	27.4611	23.60783	0.36684	0.72700E-04	0.79108E-04	-13.840	0.413E-01
8	27.9999	25.11871	0.34756	0.73042E-04	0.79127E-04	-13.838	0.413E-01

9	30.4065	33.13806	0.30276	0.71844E-04	0.77031E-04	-14.007	0.397E-01
10	30.5655	33.74998	0.31434	0.71768E-04	0.77155E-04	-14.007	0.398E-01
11	29.8403	31.04668	0.27850	0.71728E-04	0.76479E-04	-14.011	0.397E-01
12	30.1950	32.34059	0.36079	0.70218E-04	0.76300E-04	-14.010	0.397E-01
13	30.1884	32.31602	0.35600	0.71505E-04	0.77613E-04	-13.952	0.403E-01
14	30.2730	32.63247	0.25432	0.73302E-04	0.77723E-04	-13.953	0.402E-01
15	30.04503	31.78716	0.29189	0.72896E-04	0.77964E-04	-13.950	0.403E-01
16	29.72864	30.65012	0.32276	0.72430E-04	0.78018E-04	-13.950	0.403E-01

2.1.2 Attenuation

Attenuation is one of the important phenomena that determines the quantity and position of amplifiers and repeaters in optical networks. The major factors contributing towards attenuation in fibers are absorption (due to fiber constituent), scattering (due to structural imperfections) and radiative losses of optical energy (due to perturbations of fiber geometry).

The decrease in optical power as it propagates along length L of fiber is given by [1]

$$P_{out}=P_{in}e^{-\alpha L} \tag{2.43}$$

Where α is attenuation coefficient given by expression

$$\alpha_o = \frac{1}{L} ln \left[\frac{P_{in}}{P_{out}}\right] \text{km}^{-1} \tag{2.44}$$

Fiber attenuation or fiber loss is given by

$$\alpha = \frac{10}{L} log \left[\frac{P_{in}}{P_{out}}\right] = 4.343\alpha_o \quad \text{dB/km} \tag{2.45}$$

In particular, the loss caused by ultra violet absorption at any wavelength may be expressed as a function of mole fraction x of GeO_2 in fiber material by the expression obtained from [1]

$$\alpha_{uv} = \frac{1.542x}{46.6x+60} \exp\left(\frac{4.63}{\lambda}\right) \tag{2.46}$$

Losses caused by infrared absorption is given by

$$\alpha_{ir} = 7.81 \times 10^{11} \exp\left(\frac{-48.48}{\lambda}\right) \tag{2.47}$$

Scatterings losses (mainly due to Rayleigh scattering) is expressed as

$$\alpha_{scat} = \frac{8\pi^3}{3\lambda^4}(n^2 - 1)^2 k_B T_f \beta_T \tag{2.48}$$

Where n is refractive index, k_B is Boltzmann's constant, β_T is isothermal compressibility of material, T_f is temperature at which density fluctuations are frozen into glass as it solidifies after been drawn into fiber [1].

Practical permissible range for α is 0.16 dB/km for 1.55μm range and 0.5 dB/km for 1.39 μm range. The numerous methodologies have been presented so far for measurement of power losses in the fiber because of attenuation, scattering and dispersive properties of media. These include implementation of optical time domain reflectometer, back scattering, SBS between a counter propagating pulsed pump and continuous probe wave. [25] [26] [27] [28] [15]. Among the different techniques proposed, the simplest is to measure the optical power input into the fiber and that flowing in the circuit through performance monitors and evaluate attenuation of fiber using mathematical expressions stated above. To study the impact of attenuation, the network shown in Figure 2.7 is considered. The system is modeled for different values of attenuation coefficients and the impact of attenuation on eye diagrams and optical spectrum is studied. In order to study the effect of attenuation, system is first simulated with different values of attenuation coefficients shown in Table 2.3.

Table 2.3: Different values of attenuation coefficients used for simulation

Run No.	1	2	3	4	5	6	7	8	9
Attenuation Coefficient	0.01	0.1	0.03	0.04	0.12	0.09	0.07	0.08	0.16

The corresponding optical spectrum and eye diagrams are studied to see the change in patterns. As the value of attenuation coefficient for the optical system increases, the power delivered at the receiver section reduces as presented in Figure 2.16. When the eye diagram is obtained at the receiver end after being filtered by

Bessel filter, it has been found that the eye width remains same while eye height decreases with increase in value of attenuation coefficient as represented in Figure 2.17. Eye formation is so precise as the parameters representing other impairments like dispersion, Raman crosstalk and other nonlinearities are turned off.

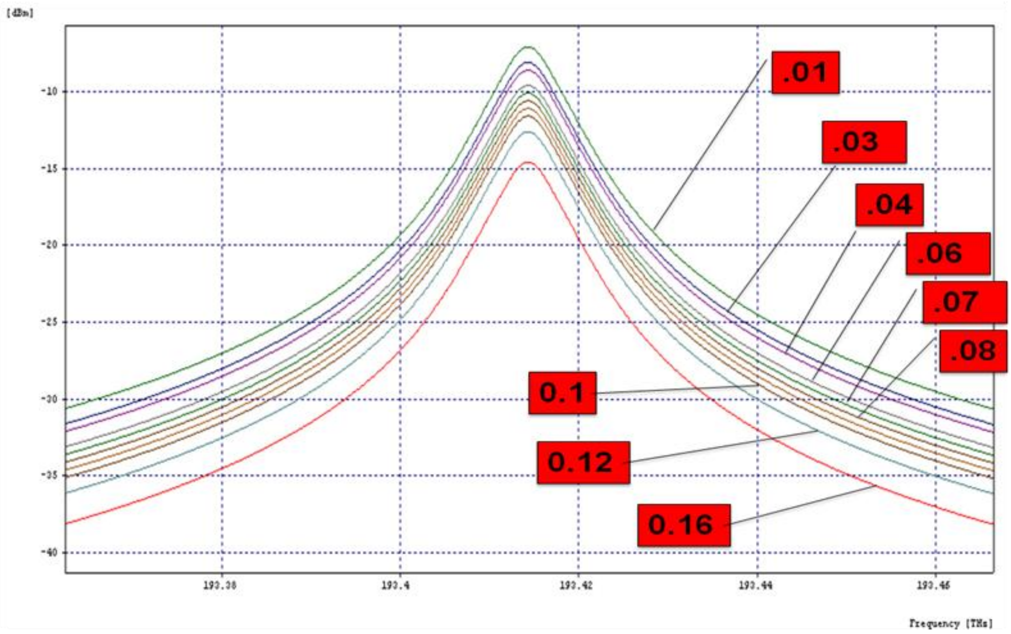

Figure 2.16: Optical Spectrum with variable attenuation coefficient

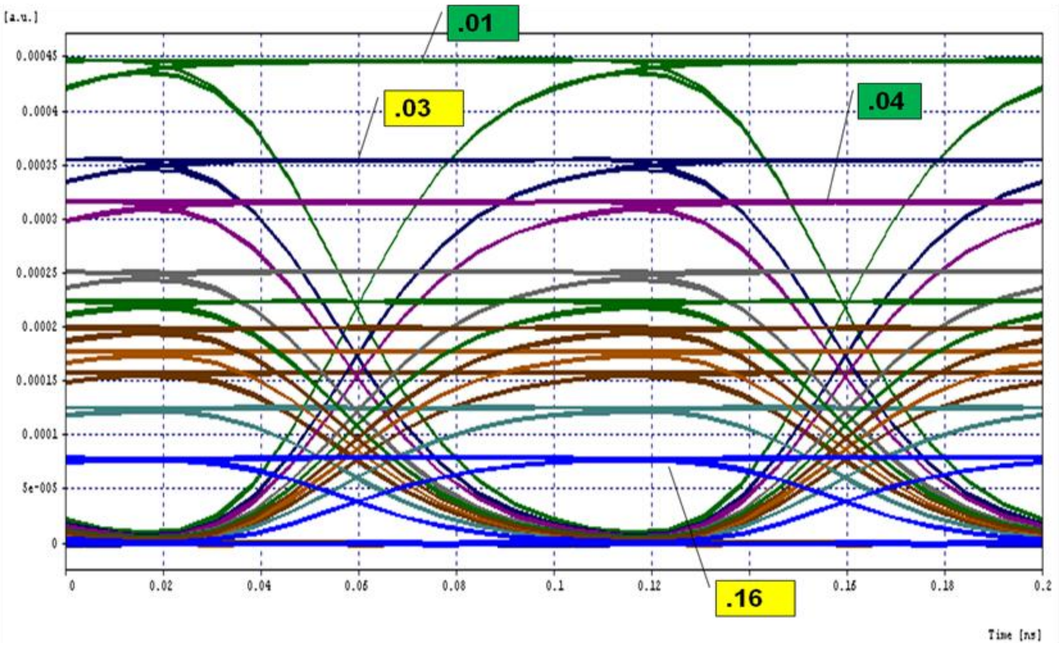

Figure 2.17: Eye diagram with variable attenuation coefficient

2.2 NON-LINEAR IMPAIRMENTS

It is common practice to increase the power levels as much as possible to overcome the power penalty effects and better transmission, but this introduces several non-linear impairments in the link. These impairments arise when several high strength optical fields of different wavelengths interact with molecular vibrations and acoustic waves. The different non-linear impacts include SPM, XPM, FWM and scattering effects like Stimulated Raman Scattering (SRS), Stimulated Brillouin Scattering (SBS). The main cause of these impairments is variation in refractive index of fiber (also called Kerr effect) due to intensity of signal flowing through fiber. In the present work, degradation effect posed by SPM, XPM and FWM are discussed. In several cases, these non-linear effects act as compensation for other degradation factors like dispersion thereby increasing the resultant power being transmitted. SBS, SRS and FWM result in gains or losses in a particular channel by providing gains to some channels while decreasing power from some others. The phase of signals is influenced by SPM and XPM causing chirping of digital signals.

The various non-linear effects arise as the response of optical fiber (which is a dielectric medium) to intense magnetic fields. Actually, applied field disturbs the harmonic motion of bound electrons originating the nonlinearity component. As a result, the total polarization P induced by electric dipoles is given by [29] as:

$$P = \varepsilon_0 \chi_1 E + \varepsilon_0 \chi_2 E^2 + \varepsilon_0 \chi_3 E^3 + \cdots. \qquad (2.49)$$

Where, ε_o is permittivity of vacuum, χ_k (k=1, 2, 3..) is k^{th} order susceptibility. The first order susceptibility χ_1 represents the linear portion of polarization$P_L = \varepsilon_0 \chi_1 E$, while the second and higher order terms represents the non-linear polarization P_{NL}.

For an electric field vector E such that $E = E_o \cos{(\omega t - kz)}$ equation (2.49) may be written as

$$P = \varepsilon_0 \chi_1 E_o \cos(\omega t - kz) + \varepsilon_0 \chi_2 {E_o}^2 (\cos(\omega t - kz))^2 + \varepsilon_0 \chi_3 {E_o}^3 (\cos(\omega t - kz))^3 \qquad (2.50)$$

Since fiber is an isotropic medium, the polarization vector P will always be in the direction of E, so scalar notations may be used. Using basic trigonometric relations, equation (2.50) becomes

$$P = \varepsilon_0 \chi_1 + \frac{1}{2} \varepsilon_0 \chi_2 {E_o}^2 + \frac{1}{2} \varepsilon_0 \chi_2 {E_o}^2 \cos 2(\omega t - kz) + \frac{3}{4} \chi_3 {E_o}^2 E_o \cos(\omega t - kz) + \frac{1}{4} \varepsilon_0 \chi_3 {E_o}^3 \cos 3(\omega t - kz) + \cdots \qquad (2.51)$$

The first term in this equation is constant and gives DC field across the medium so have a little influence. The linear susceptibility of first order has dominating contribution towards P through varying refractive index and attenuation coefficient. The optical fiber is not influenced by second order susceptibility (represented by third term), owing to optical isotropy unless the glass has been poled. It must be noted that defects in the fiber core, electric-quadruple and magnetic dipole moments may contribute towards second order nonlinearity under certain conditions. Thus, equation (2.51) may be rewritten as

$$P = \varepsilon_0 \chi_1 + \frac{3}{4}\chi_3 {E_o}^2 E_o \cos(\omega t - kz) + \frac{1}{4}\varepsilon_0 \chi_3 {E_o}^3 \cos 3(\omega t - kz) + \cdots. \quad (2.52)$$

The third order susceptibility is accountable for instigating non-linear effects of lowest order. It is responsible for FWM and non-linear refraction (phenomenon of intensity dependence of refractive index leading to SPM, XPM) [30] [29]. These non-linear effects are studied in detail in subsequent sections of this chapter.

In order to obtain non-linear wave equation for propagation of light inside the fiber, impact of linear and non-linear polarization is taken into account by [31] and Equation (2.53)-(2.59) are reproduced for better understanding of the concept. Thus, equation (2.5) may be rewritten as

$$\nabla^2 E = \frac{1}{c^2}\frac{\partial^2 E}{\partial t^2} + \mu_o \frac{\partial^2 P_L}{\partial t^2} + \mu_o \frac{\partial^2 P_{NL}}{\partial t^2} \quad (2.53)$$

Substituting the value of P_L and using the expression $= \sqrt{1+\chi_1}$, the expression may be rewritten as

$$\nabla^2 E - \frac{n^2}{c^2}\frac{\partial^2 E}{\partial t^2} = \mu_o \frac{\partial^2 P_{NL}}{\partial t^2} \quad (2.54)$$

For the field propagating along the z-direction represented by

$$E = \frac{1}{2}(F(r,\emptyset)A(z)e^{i(\beta_o z - \omega_o t)} + cc, \quad (2.55)$$

where cc means complex conjugate, A(z) is the longitudinal and F(r, ∅) the transverse part of field amplitude. The power of field may be obtained by integrating the intensity in transverse plane. Considering the symmetry of single mode waveguide, this yields

$$P = \frac{1}{2}\epsilon_o cn|A(z)|^2 2\pi \int |F(r,)|^2 r\, dr = B^2|A(z)|^2 \quad (2.56)$$

where , $B^2 = \pi\epsilon_o cn \int |F(r)|^2 r\, dr$ (2.57)

Substituting Equation (2.55) in (2.53) and solving, we obtain

$$\frac{\partial A}{\partial z} \approx i\left[\frac{3\omega}{8cn}\chi_3|F(r)|^2|A|^2A + A(\beta-\beta_o)\right] \quad (2.58)$$

Introducing a normalized amplitude U=BA(z) and multiplying both sides by $\int|F(r)|^2 r\, dr$, equation (2.58) becomes

$$\frac{\partial U}{\partial z} = i[U(\beta-\beta_o) + \gamma|U|^2U] \quad (2.59)$$

Here, γ is nonlinearity coefficient given by $\gamma = \frac{2\pi}{\lambda}\frac{n_2}{A_{eff}}$, A_{eff} is effective core area.

Solving equation (2.59) through Fourier analysis,

$$i\frac{\partial U}{\partial z} - \frac{1}{2}\beta_2\frac{\partial^2 U}{\partial z^2} + [\gamma|U|^2U]=0 \quad (2.60)$$

Equation (2.60) is non-linear Schrodinger equation describing the propagation of pulse inside the fiber considering the impact of linear as well as non-linear impairments.

2.2.1 Self Phase Modulation

Self Phase modulation (SPM) is the non-linear phenomena that influence the phase of propagating wave due to intensity dependent component of refractive index. The dependence of refractive index n of optical fiber on intensity is given by relation

$$n=n_o + n_2 I, \quad (2.61)$$

where, n_o-ordinary refractive index of material,

n_2-non-linear index coefficient also known as Kerr nonlinearity, given by

$$n_2=\frac{3}{8n_o}Re(\chi_3) \quad (2.62)$$

and I is optical intensity of signal and is equal to the optical power per unit effective area [32]. In single wavelength links, this converts optical power fluctuations in lightwave to spurious phase variations in the same wave.

The impact of SPM may be obtained from equation (2.60) by neglecting the linearity component as is presented by [31] and reproduced here. Equation (2.60) becomes

$$\frac{\partial U}{\partial z} = i[\gamma PU] \quad (2.63)$$

Here, $P=U^2$ is pulse input power. For a fiber of length L, the general solution of this equation for field amplitude is

$$U(L,\tau) = U(0,\tau)\exp\,(i\emptyset_{NL}(L,\tau)) \tag{2.64}$$

Where U(0, τ) is the pulse envelope and $\emptyset_{NL}(L,\tau) = \gamma P(\tau)L$ is the nonlinearity induced phase change. The electric field transmitted in the fiber is given by

$$E(L,t) = \frac{1}{2}[E(0,\tau)\ \exp\{\mathrm{i}[(\beta_0 + \gamma\mathrm{P})\mathrm{L} - \omega_0\mathrm{t}]\} + \mathrm{cc}] \tag{2.65}$$

It is evident from equation (2.65) that nonlinearity induced phase change $\emptyset = (\beta_0 + \gamma\mathrm{P})\mathrm{L} - \omega_0\mathrm{t}$ depends on the power of wave. This phenomenon of phase modulation of the wave owing to its power variations is called Self phase modulation. The parameter indicating the magnitude of non-linear effect for SPM is given by [30] as:

$$\gamma = \frac{2\pi}{\lambda}\frac{n_2}{A_{eff}} \tag{2.66}$$

Phase shift arising from SPM is given by $\Delta\phi = \gamma L_{eff}\frac{dP}{dt}$, (2.67)

$$L_{eff} = \frac{1-e^{-\alpha L}}{\alpha}, \tag{2.68}$$

Where, λ is free space wavelength, A_{eff} is the effective core area and L_{eff} is effective length.

α is attenuation and $\frac{dP}{dt}$ is derivative of optical pulse power. [30]

For an ultra short pulse with a Gaussian shape and constant phase, the optical intensity at time *t* is given by:

$$I(t) = I_o e^{-\left(\frac{t}{\tau}\right)^2} \tag{2.69}$$

where, I_0 is the peak intensity, and τ is half the pulse duration.

As the pulse propagates in the fiber, the intensity variations produce a time-varying refractive index given by:

$$\frac{dn(I)}{dt} = n_2\frac{dI}{dt} = n_2 I_o \frac{-2t}{\tau^2} e^{-\left(\frac{t}{\tau}\right)^2} \tag{2.70}$$

This variation in refractive index generates a shift in the instantaneous phase of the pulse given by:

$$\phi(t) = \omega_o t - kz = \omega_o t - \frac{2\pi}{\lambda_0} n(I)L \tag{2.71}$$

where ω_o and λ_o are the carrier frequency and wavelength of the pulse, and L is the distance the pulse has propagated. The resulting instantaneous frequency ω(*t*) is given by:

$$\omega(t) = \frac{d\phi(t)}{dt} = \omega_o - \frac{2\pi L}{\lambda_o}\frac{dn(I)}{dt} \tag{2.72}$$

Using equation (2.70),

$$\omega(t) = \omega_o + \frac{4\pi L\, n_2 I_o}{\lambda_o \tau^2} t e^{-\left(\frac{t}{\tau}\right)^2} \tag{2.73}$$

The shift in values of instantaneous frequency of pulse can be observed by plotting ω(t). For $t = \pm\tau/2$, the linear frequency shift is given by:

$$\omega(t) = \omega_o + \alpha t, \quad \text{where } \alpha = \frac{4\pi L n_2 I_o}{\lambda_o \tau^2} \tag{2.74}$$

In order to visualize the impact of SPM, intensity and frequency of pulse is plotted with respect to time and is shown in Figure 2.18.The frequencies shift responsible for broadening is due to SPM. Here, some new frequencies are generated responsible for broadening of frequency spectrum of the pulse. The front of the pulse is shifted to lower frequencies, the back to higher frequencies. In the centre of the pulse the frequency shift is approximately linear.

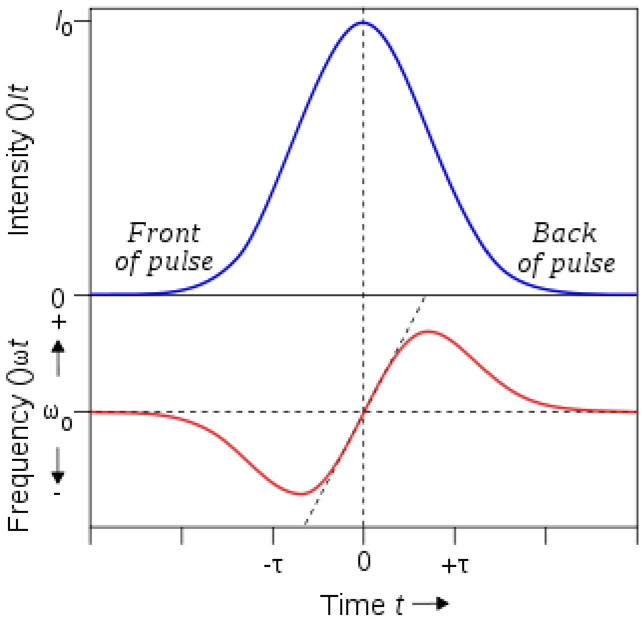

Figure 2.18: Frequency shift because of SPM

The overall effect of SPM is the broadening of optical spectrum, and is more pronounce in systems with high transmitted power. In order to study the impact of input power on the pulse broadening, the setup of Figure 2.7 is used with a variable power source. The values of input power of laser are varied ranging from 10-20 dBm and the corresponding phase shift across the output is studied. The optical spectrum for 10, 14, and 20 dBm are shown in Figure 2.19 to Figure 2.21 with input and output waveforms being superimposed. It is clear that upto 10dBm, effect of SPM is almost negligible. The input waveform is completely overlaid by the output spectrum. With the increase in magnitude of input power beyond 10dBm, the output pulse is shifted outwards and this broadening goes on increasing with increased power. The effect of pulse broadening is small for 12dBm power and goes on increasing when power is increase to 20 dBm. The overall spectrum broadening is summarized by superimposing all the spectrums obtained is shown in Figure 2.22. Inner most curve (in green) represent the lowest input power i.e. 10 dBm and outer most curve (in brown) represents 20 dBm power. The upper limit of power so as to decrease or nullify the impact of SPM may be obtained from equation (2.67). Typically, for attenuation coefficient 0.2 dB/km at 1550 nm wavelength and γ =22.35X10^{-3}, the input power should be kept below 19.6 mW.

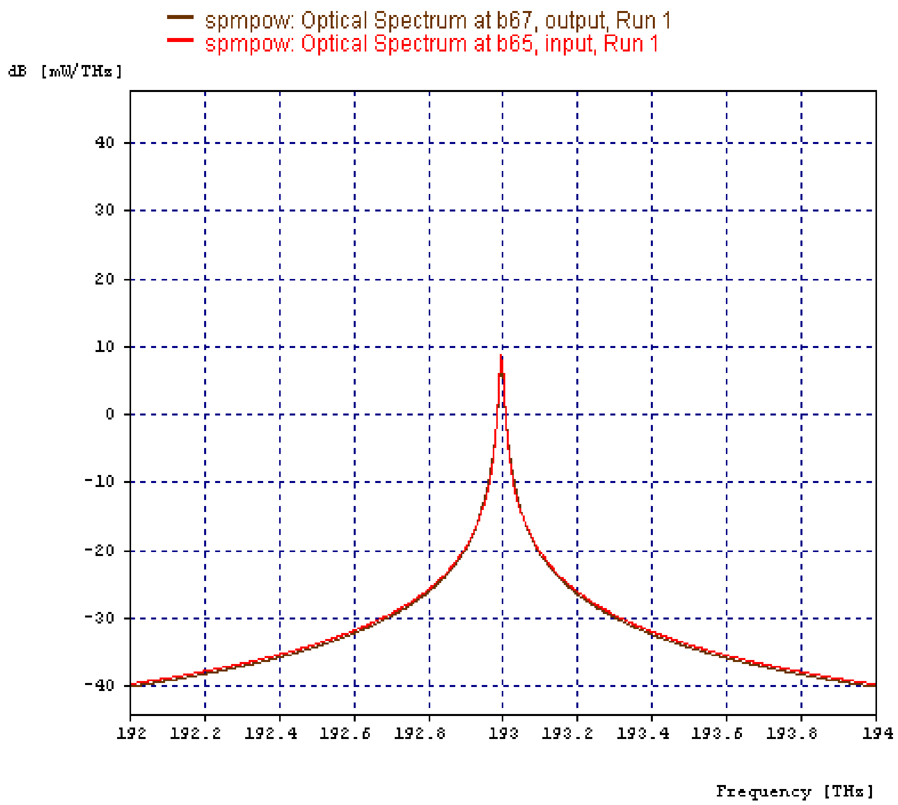

Figure 2.19: The input spectrum of system with input power 10 dBm superimposed over the spectrum obtained at output terminal.

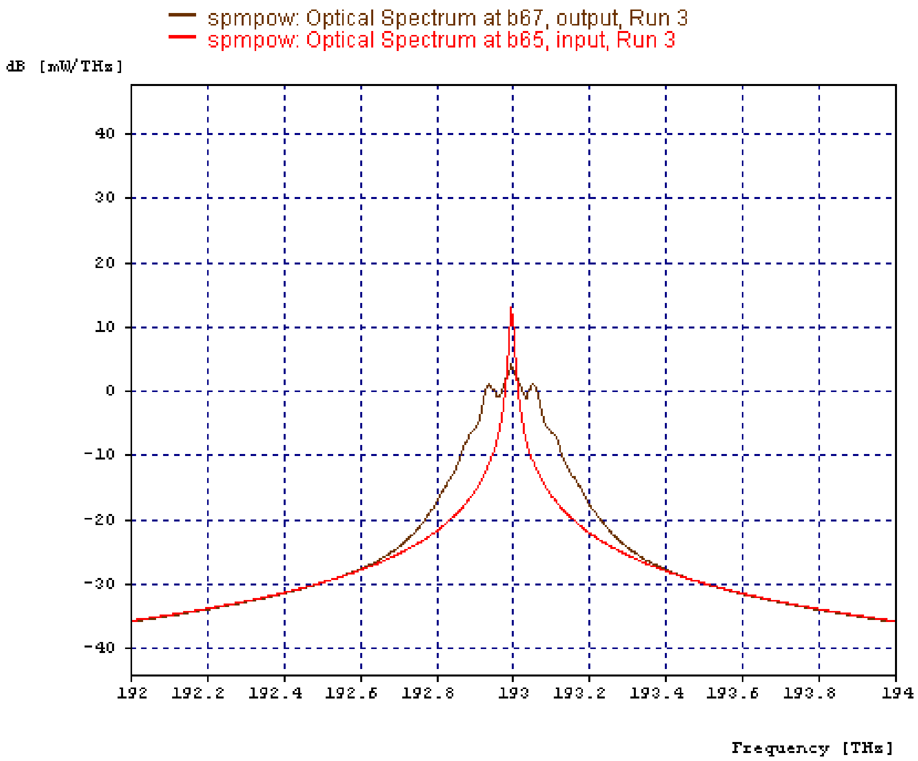

Figure 2.20: The input spectrum of system with input power 14 dBm superimposed over the spectrum obtained at output

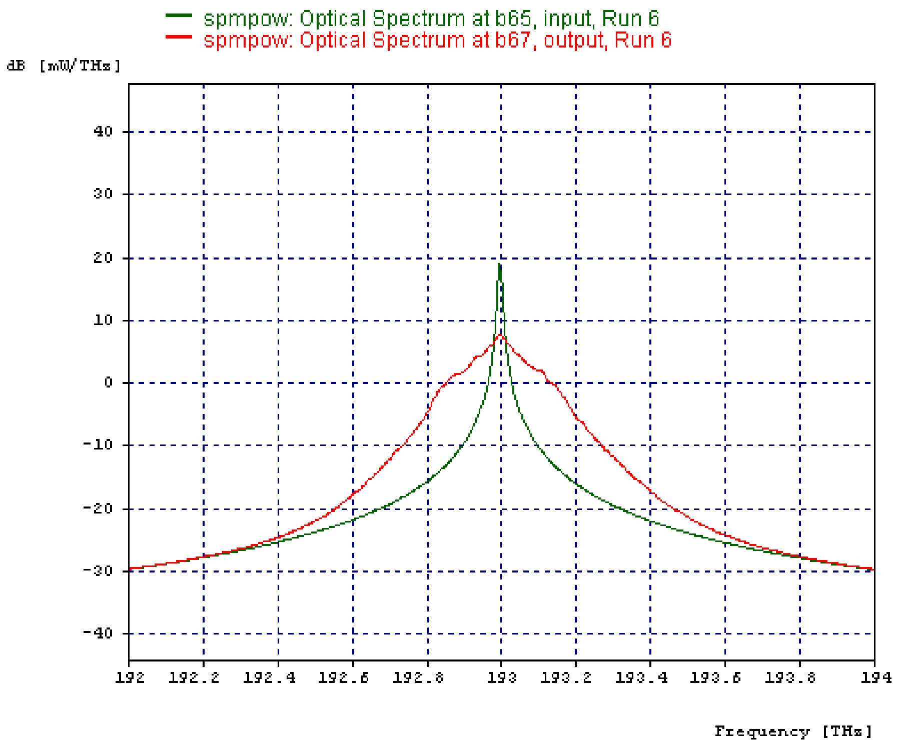

Figure 2.21: The input spectrum of system with input power 20 dBm superimposed over the spectrum obtained at output terminal

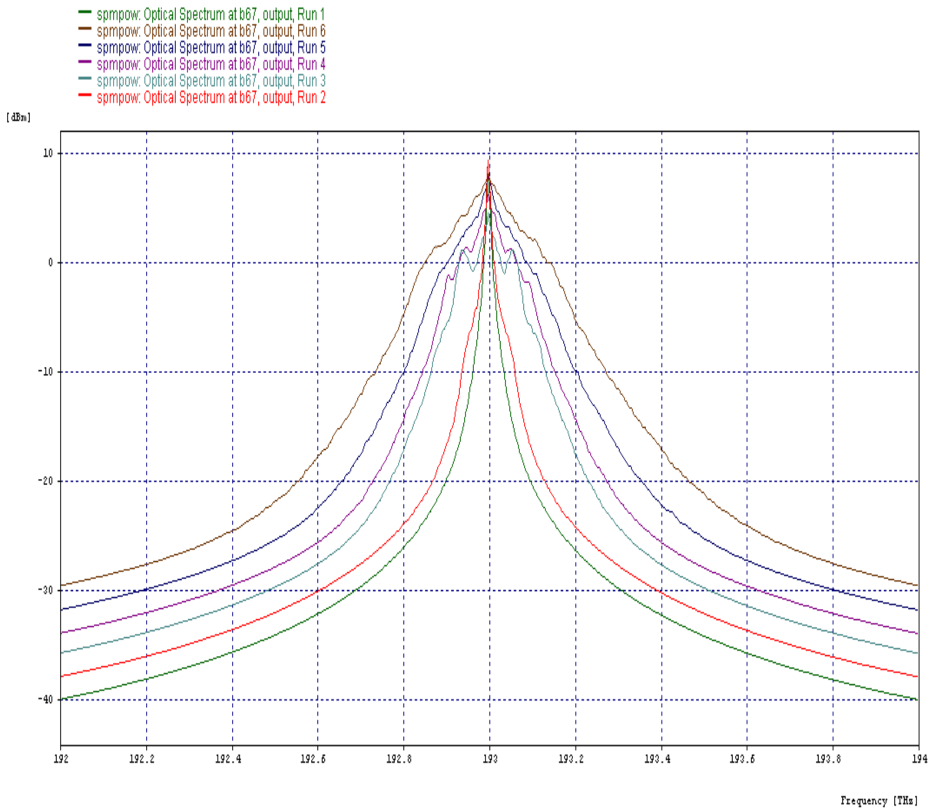

Figure 2.22: The spectrum of system with input power varying from 10 dBm to 20 dBm being superimposed

The various non-linear effects are weak and requies long length transmision for interaction and intensity variations. Also, the properties of fiber like dispersion pose counteracting effect on the degradation effect of SPM. The implementation of fibers with higher values of effective area may also help in counteracting this effect.

2.2.2 Cross Phase Modulation

The impact of XPM is analogous to SPM in principle, but originates due to the interaction of two light signals instead. It appears in WDM networks when refracive index nonlinearity converts optical intensity variations in a particular wavelength channel to phase variations in the adjacent channels. It must be noted that refractive index variations are influenced by optical intensity of its own as well as intensity variations in neighbouring waves. Thus, SPM is always present when XPM occurs. For two interacting wavelengths, the XPM induced frequency shift is given by [33] as:

$$\Delta\phi = \gamma L_{eff}\left(\frac{dP_i}{dt} + 2\sum_{i\neq j}\frac{dP_j}{dt}\right) \quad (2.75)$$

Here first term represents SPM contribution and second term trepresents XPM contribution in pulse broadening. To better understand the concept of XPM, [31] demonstrated the behavious of two different wavelengths prapagating analogously in the fiber. The mathematical expressions involved are reprodeced here for reference here in equations(2.76)-(2.85). Two optical fields propagating in the fiber can be written as

$$E(r,z,t) = \frac{1}{2}\left(F(r)\frac{U_j(z)}{B_j}e^{i(\beta_j z-\omega_j t)} + cc, j = 1,2 \qquad (2.76)$$

where F(r) gives the transversal distribution of the single mode supported by the fiber, $U_j(z)$ is the normalized slowly varying amplitude such that square of its absolute value is equal the power of wave with wave with frequency ω_j, B_j is given by equation (2.57) and β_j is propagation constant. The slowly varying amplitude of signals may be expressed as

$$\frac{\partial U_1}{\partial z} + \frac{1}{v_{g1}}\frac{\partial U_1}{\partial t} + i\frac{\beta_{21}}{2}\frac{\partial^2 U_1}{\partial t^2} = i\gamma_1[(|U_1|^2 + 2|U_2|^2)U_1 + U_1^2 U_2^* exp\{i(\Delta\beta z - \Delta\omega t)\}] \qquad (2.77)$$

$$\frac{\partial U_2}{\partial z} + \frac{1}{v_{g2}}\frac{\partial U_2}{\partial t} + i\frac{\beta_{22}}{2}\frac{\partial^2 U_2}{\partial t^2} = i\gamma_2[(|U_2|^2 + 2|U_1|^2)U_2 + U_2^2 U_1^* exp\{i(-\Delta\beta z + \Delta\omega t)\}] \qquad (2.78)$$

Here v_g is group velocity, β_{2j} is GVD coefficient, γ_j is non-linear effect parameter due to SPM. The last term in both the equations are due to FWM effect and are ignored at this stage, pulse duration is assumed to be long enough that linear terms may be neglected, power of wave $P_j=|U_j|^2$. the solution of equation (2.77) and (2.78) is

$$U_1(L) = U_1(0)\exp\{i\gamma_1(P_1 + 2P_2)L\} \qquad (2.79)$$

$$U_2(L) = U_2(0)\exp\{i\gamma_2(P_2 + 2P_1)L\} \qquad (2.80)$$

Thus, it is evident that the phase of signal is not only modified due to its own power (called as SPM), but also due to its neighbouring signal as well and is referred as XPM and the effect is twice as effective as SPM.

The electric field of wave with frequency ω_1 transmitted in the fiber may be written as

$$E_1(z,t) = \frac{1}{2}[E_1(0,t)\exp\{i[(\beta_1 + \gamma_1 P_1 + 2\gamma_1 P_2)z - \omega_1 t]\} + cc] \tag{2.81}$$

Similar equation for $E_2(z,t)$ may be written by changing the indices. The total refractive index of fiber as seen by the wave may be written as

$$n_{tot}=n_o+n_2I_1+2n_2I_2 \tag{2.82}$$

The phase of wave represented by equation (2.81) is

$$\Phi1= (\beta_1 + \gamma_1 P_1 + 2\gamma_1 P_2)z - \omega_1 t \tag{2.83}$$

The non-linear phase shift resulting from combination of SPM and XPM is

$$\emptyset_{1nl} = \gamma_1 (P_1 + 2P_2)L_{eff} \tag{2.84}$$

The XPM-induced frequency shift is

$$\Delta\omega_{1XPM} = -2\gamma_1 L_{eff} \frac{\partial P_2}{\partial t} \tag{2.85}$$

This means the part of signal at frequency ω_1 that is affected by leading edge of signal at ω_2 will be downshifted in frequency, whereas the part overlapping with the trialing edge will be shifted up in frequency. This determines spectral broadening of signal at ω_1, which is twice the spectral broadening by SPM.

In order to study the effect of XPM, a system shown in Figure 2.23 is used.

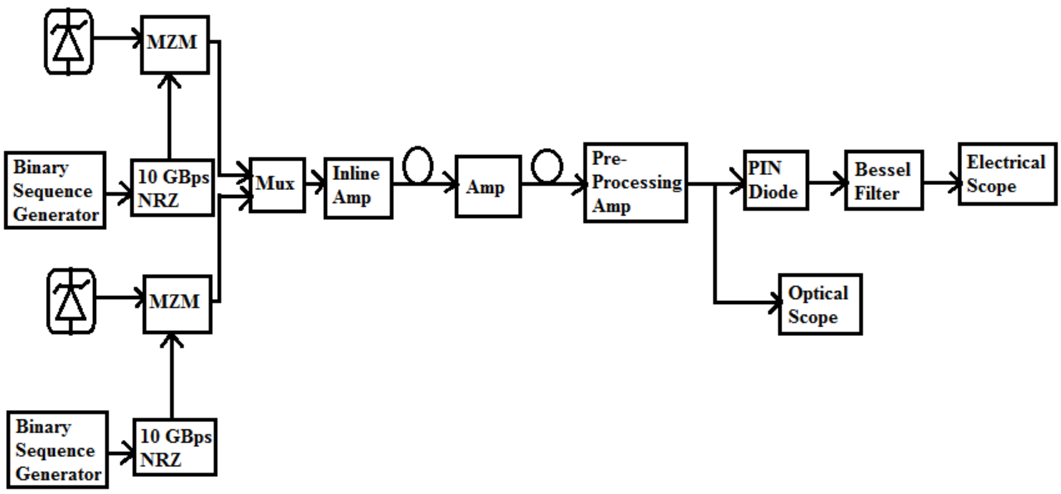

Figure 2.23: Two channel WDM network

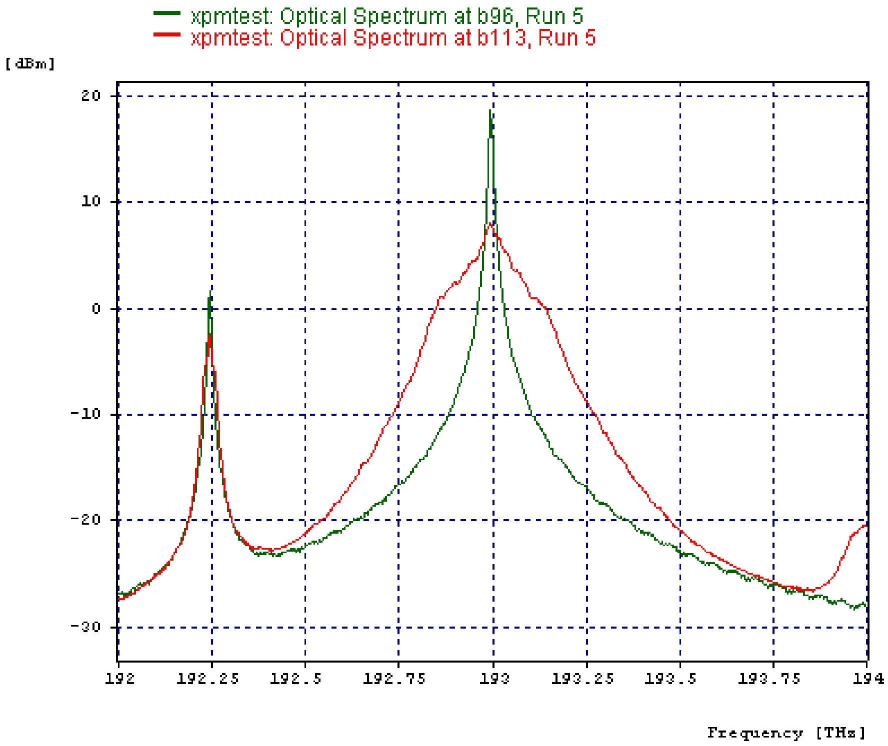

Figure 2.24: The input spectrum of system with probe power 0.08 mW superimposed over the spectrum obtained at output terminal

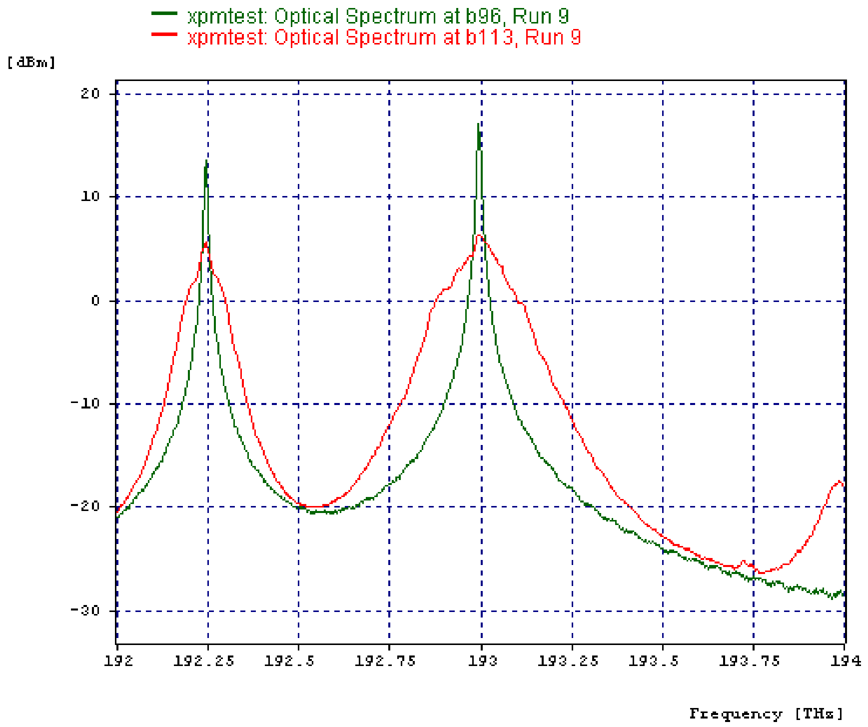

Figure 2.25: The input spectrum of system with probe power 1.8 mW superimposed over the spectrum obtained at output terminal

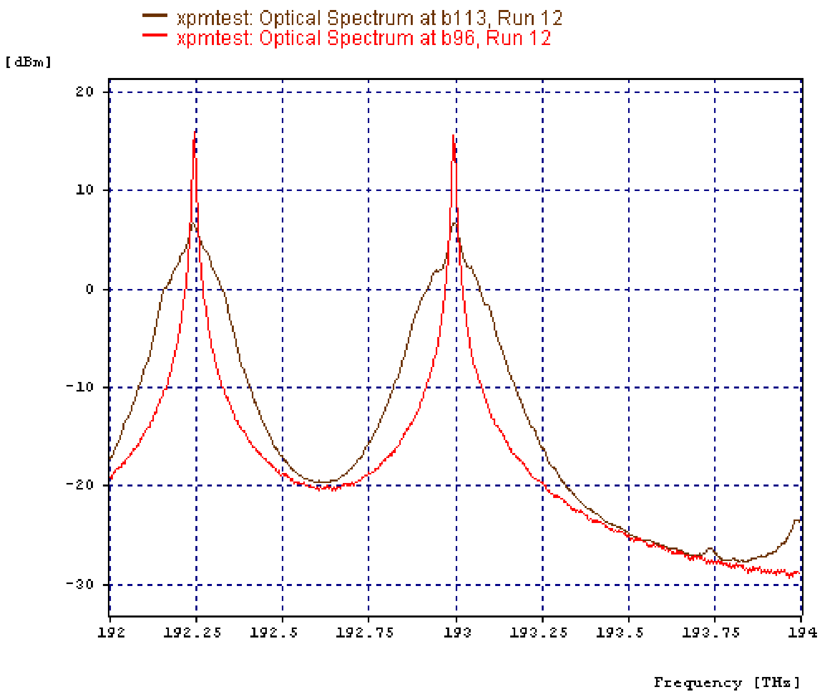

Figure 2.26: The input spectrum of system with probe power 4.4 mW superimposed over the spectrum obtained at output terminal

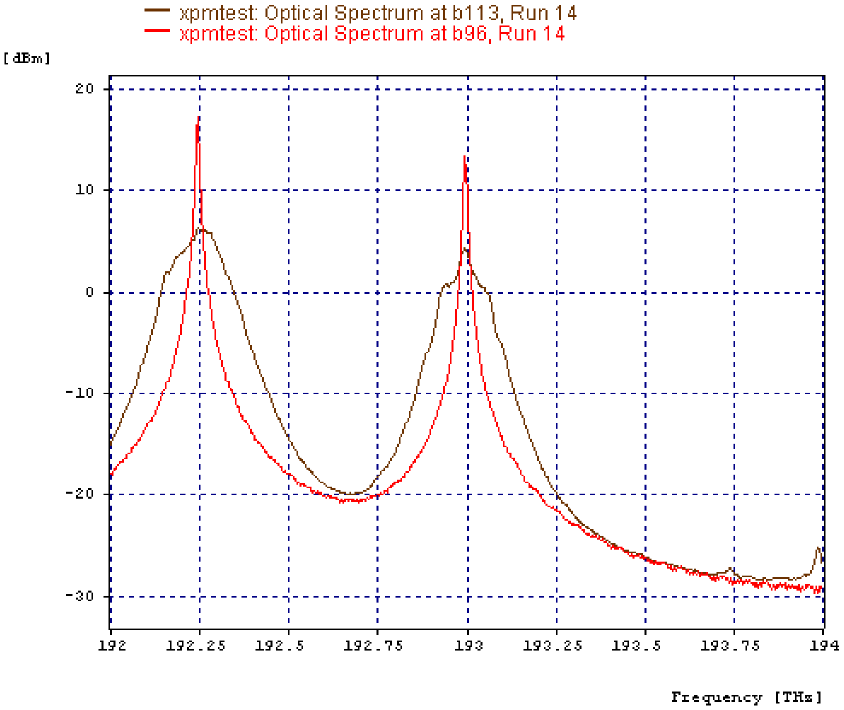

Figure 2.27: The input spectrum of system with probe power 10 mW superimposed over the spectrum obtained at output terminal

The source with higher power act as the pump, while the other one act as the probe signal. In order to visualize the effect of XPM, it is must that both signals must overlap in time and space. To study the impact of XPM effect due to interaction of light from two optical sources, the power of one source is varied from 0.08 to 10 mW. The optical spectrum obtained by superimposing the input over the output is shown in Figure 2.24 to Figure 2.27. As it was there in case of SPM, XPM introduces a non-linear phase shift reflected in the form of spectral broadening.

2.2.3 Four Wave Mixing

WDM networks utilize 1550 nm window and launch power of 1 mW per channel to transmit the data of high capacity over long distance with minimum repeater spacing. For such networks, optimum system performance is achieved with high input power and low dispersion properties of fiber. This result in generation of new frequencies due to phenomena called FWM. As per third order nonlinearity component, the channels positioned near zero dispersion point, carrying three signals of optical frequencies ν_i, ν_j and ν_k will observe the generation of fourth signal of frequency given by [1]

$$\nu_{ijk} = \nu_i + \nu_j - \nu_k \quad \text{with } i \neq j \tag{2.86}$$

This newly generated frequency introduces high crosstalk in the channel, especially when this frequency lies within the transmission window. The number of new frequencies that can be introduced due to FWM in the fiber carrying N wavelengths is given by [1]

$$M = \frac{N^2}{2}(N-1) \tag{2.87}$$

If the channels are equaly spaced, new waves will have the same frequency as input signals, which will also introduce crosstalk. The impact of FWM decrease with higher the group velocity difference between the signal waves and autogenerated waves and wider the channel spacing.

The power generated at the frequency ν_{ijk} is given by [1]

$$P_{ijk}(L) = \eta (xk)^2 P_i(0) P_j(0) P_k(0) e^{-\alpha L} \tag{2.88}$$

Where η is efficiency of FWM and is given by

$$\eta = \left(\frac{\alpha^2}{\alpha^2+\Delta k^2}\right)\left[1 + 4e^{-\alpha L}.\frac{\sin^2\left(\frac{\Delta kL}{2}\right)}{(1-e^{-\alpha L})^2}\right], \tag{2.89}$$

where Δk represents the phase mismatch. The phase mismatch between the signals increase with higher transmission lengths, high dispersion parameter and large difference in signal frequency resulting in decreased FWM efficiency. In terms of signal frequencies, phase mismatch may be expressed as

$$\Delta k = \frac{2\pi\lambda^2}{c}|f_i - f_k||f_j - f_k|.\left\{D + \frac{dD}{d\lambda}\frac{\lambda^2}{2c}(|f_i - f_k| + |f_j - f_k|)\right\} \tag{2.90}$$

where D is dispersion parameter and x is degeneracy factor, with value 3 or 6 for two wave mixing i.e. i=j or three wave mixing i.e. i≠j respectively.

Non-linear interaction constant, $k = \frac{32\pi^3\chi_{1111}}{n^2\lambda c}\left(\frac{L_{eff}}{A_{eff}}\right)$. (2.91)

χ_{1111} is third order non-linear susceptibility. [34]

The multiple orders of FWM waves generated when power of signal becomes high are shown in Figure 2.28. Here, P_1, P_2 are channel powers P_{11}, P_{12} represents first order FWM products, where notation P is used to donate the power of signal generated. P_{21}, P_{22} represents second order FWM, P_{31}, P_{32} is third order FWM signal. The first number of subscript represents the channel on which this component arises.

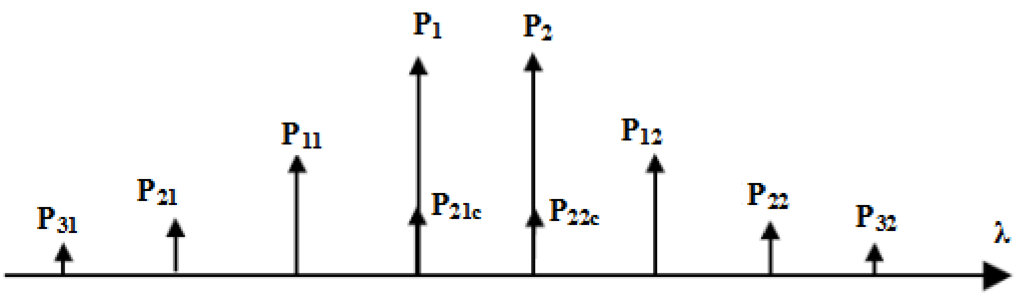

Figure 2.28: Multiple orders of FWM waves generated at high power of signal

The expressions for different FWM products as presented in [35] may be written as

$$P_{11} = \eta_{11}P_1^2P_2 \quad and\ P_{12} = \eta_{12}P_2^2P_1 \tag{2.92}$$

$$P_{21c} = \eta_{21c-1}\eta_{12}P_1P_2^4 + \eta_{21c-2}\eta_{11}P_1^3P_2^2 \tag{2.93}$$

$$P_{22c} = \eta_{22c-1}\eta_{11}P_1^4P_2 + \eta_{22c-2}\eta_{12}P_1^2P_2^3 \tag{2.94}$$

$$P_{21} = \eta_{21-1}\eta_{12}P_1^3P_2^2 + \eta_{21-2}\eta_{11}P_1^3P_2^2 \tag{2.95}$$

$$P_{22} = \eta_{22-1}\eta_{11}P_1^2P_2^3 + \eta_{22-2}\eta_{12}P_1^2P_2^3 \tag{2.96}$$

$$P_{31} = \eta_{31-1}(\eta_{22-1}\eta_{11} + \eta_{22-2}\eta_{12})P_1^4P_2^3 + \eta_{31-2}\eta_{11}P_1^4P_2^3 + \eta_{31-3}\eta_{11}\eta_{12}P_1^4P_2^3 + \eta_{31-4}(\eta_{21-1}\eta_{12} + \eta_{21-2}\eta_{11})P_1^4P_2^3 \tag{2.97}$$

$$P_{32} = \eta_{32-1}(\eta_{21-1}\eta_{12} + \eta_{21-2}\eta_{11})P_1^3P_2^4 + \eta_{32-2}\eta_{12}P_1^3P_2^4 + \eta_{32-3}\eta_{11}\eta_{12}P_1^3P_2^4 + \eta_{32-4}(\eta_{22-1}\eta_{11} + \eta_{22-2}\eta_{12})P_1^3P_2^4 \tag{2.98}$$

Here, η_{mn-k} is FWM efficiency, where m(m=1,2,3…) is order of mixing product and n (n=1,2,1c,2c) represents left or right FWM products, k is k^{th} primary FWM product that contributed to power P_{mn}.

The interaction of waves involving FWM may also be expressed using non-linear Schrodinger equation represented by equation (2.60). Considering the pulse duration large enough that linear terms may be neglected, equation (2.60) becomes

$$\frac{\partial u}{\partial z} = i\gamma|U|^2U \tag{2.99}$$

Let us assume that equation (2.99) is obtained by superposition of four waves given by equation

$$U = U_1e^{i(\beta_1 z+\omega_1 t)} + U_2e^{i(\beta_2 z+\omega_2 t)} + U_3e^{i(\beta_3 z+\omega_3 t)} + U_4e^{i(\beta_4 z+\omega_4 t)} \tag{2.100}$$

Using equation (2.99) and (2.100), the equation for normalized amplitude of U_1 is obtained as

$$\frac{\partial U_1}{\partial z} = i\gamma\left[\left(|U_1|^2 + 2\sum_{j\neq 1}|U_j|^2\right)U_1 + 2U_3U_4U_2^*e^{i\Delta Kz}\right] \tag{2.101}$$

The first term in the bracket corresponds to impact of SPM, second to impact of XPM, remaining represents the generation of new frequency components due to FWM. The similar equations may be obtained for other three normalized amplitudes of U_2, U_3, U_4 and is given as

$$\frac{\partial U_2}{\partial z} = i\gamma\left[\left(|U_2|^2 + 2\sum_{j\neq 2}|U_j|^2\right)U_2 + 2U_3U_4U_1^*e^{i\Delta Kz}\right] \tag{2.102}$$

$$\frac{\partial U_3}{\partial z} = i\gamma\left[\left(|U_3|^2 + 2\sum_{j\neq 3}|U_j|^2\right)U_3 + 2U_1U_2U_4^*e^{i\Delta Kz}\right] \tag{2.103}$$

$$\frac{\partial U_4}{\partial z} = i\gamma\left[\left(|U_4|^2 + 2\sum_{j\neq 4}|U_j|^2\right)U_4 + 2U_1U_2U_3^*e^{i\Delta Kz}\right] \tag{2.104}$$

The impact of FWM is more in the system with equal channel spacing as most of the new frequencies generated coincide with the original channel frequencies. The interference between the original and new generated waves depends upon the bit pattern and leads to significant fluctuations in the detected signal at the receiver. The impact of FWM on system behavior may be studied using two channel WDM network shown in Figure 2.23. In order to demonstrate the effect of FWM, CW lasers with central emission wavelength of 1553.12761559 nm, 1552.72540723 nm are used. The value of dispersion coefficient is set to 0.5 ps/nm/km. The signal being input to the fiber and corresponding output is shown in Figure 2.29. The extended number of peaks is due to FWM effect resulting in some new waveforms. With increased channel spacing, the interaction of waveforms is reduced thereby decreasing the impact of FWM. The optical spectrum for channel spacing of 0.07 THz and 0.075 THz is represented in Figure 2.30 and Figure 2.31.

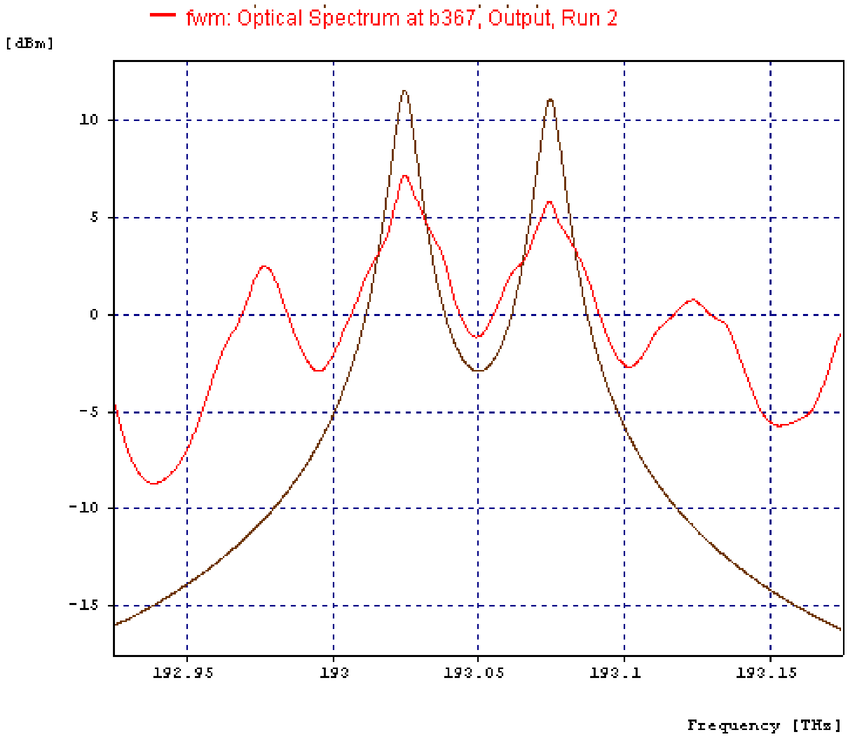

Figure 2.29: Input and output optical spectrum being superimposed for the system with input wavelength of 1553.128 nm and 1552.725 nm and D=0.5 ps/nm/km

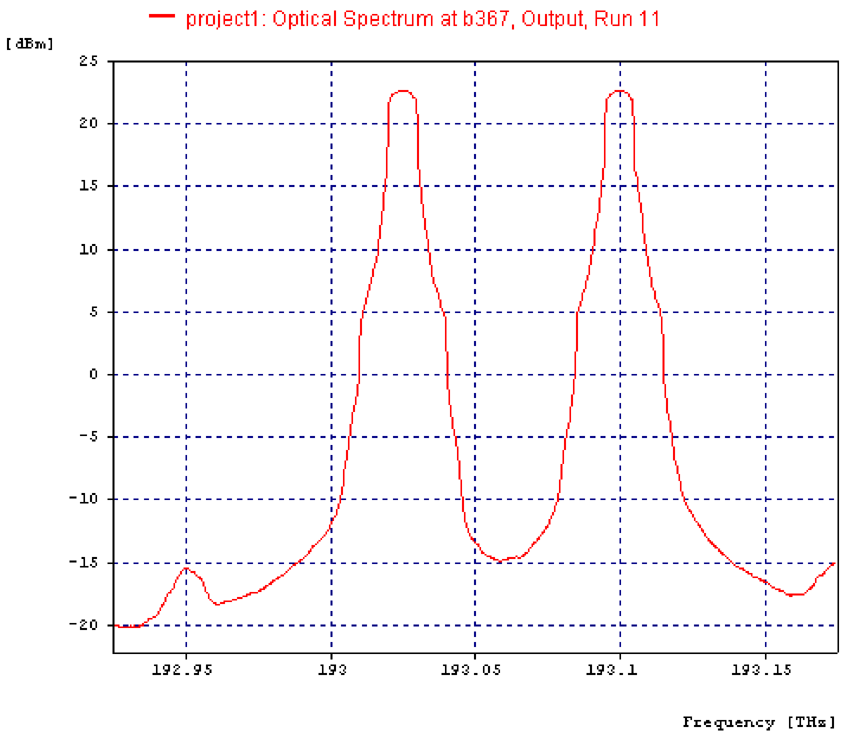

Figure 2.30: Output optical spectrum channel spacing of 0.07 THz

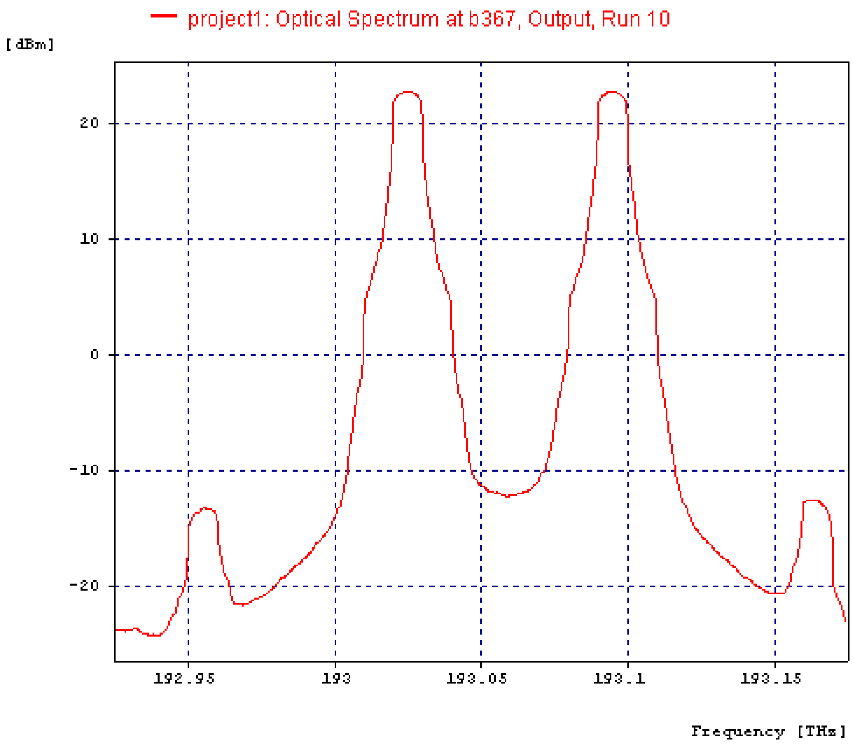

Figure 2.31: Output optical spectrum channel spacing of 0.075 THz

2.3 CHAPTER SUMMARY

In this chapter, the different physical layer impairments posing degradation effect on the signal quality has been identified. The effects are classified as linear and non-linear effects. The linear effects including dispersion, attenuation, ASE and non-linear effects including SPM, XPM, and FWM are discussed in detail. The mathematical model for each of them, including higher order impairments is discussed. Then the effect of impairments on optical spectrum and eye diagrams is demonstrated. The reason behind selecting optical spectrum and eye diagram is that in the present work, both of them will be utilized to quantify the effect of these impairments individually in subsequent chapters. It has been found that dispersion pose broadening of pulse in time domain which can be clearly seen through eye diagram analysis. The effect of higher order dispersion is studied. It has been found that even order dispersion parameters significantly influence the transmission quality while odd orders of dispersion poses negligible influence on signal transmission. The optical spectrum remains unaltered in presence of dispersion. Attenuation decreases the spectrum height and eye height, thus can be visualized from optical spectrum as well as eye diagram. The total power loss taking place inside the fiber can be easily estimated using attenuation coefficient and required regeneration may be planned accordingly. SPM and XPM pose broadening effect on spectrum without any effect on temporal distributions. The magnitude of signal power is among the parameters significantly influencing the broadening of spectrum. Higher is the power, more is the magnitude of broadening. It has been found that in order to neglect the impact of input power, its magnitude must be kept below 19.6 mW. Usually the power is increased above this so as to improve the system performance for long distance communication. FWM results in power transfer from one channel to generation of new waves which may lead to power depletion and interference. The new waves generated depend on the number of wavelengths travelling in the fiber and channel spacing. Since the different factors degrading the signal quality are identified and quantized, their influence on system performance will be studied in the next chapter. Also, influence of variations in system parameters like wavelength, length of fiber and interaction between different impairments will be discussed. The effect will then be utilized in routing applications and optimum utilization of physical resources.

Chapter 3

Optical performance monitoring

This chapter discusses the methodology, various issues and challenges involved in measurement of physical layer impairments. The system response for these impairments is studied and their influence on system BER and Q-value is presented

CHAPTER 3: OPTICAL PERFORMANCE MONITORING

The advancements in the field of optical communication system has resulted into its tremendous growth and wide implementation in day to day life. Advanced optical modulation formats with high spectral efficiency, advanced components like Reconfigureable Optical Add Drop Multiplexers (ROADMS), OXC, and large bandwidth requirements contributed significantly in existance of dynamic, flexible translucent and transparent networks [36]. The prime concerns of research in the field now focus on reducing the Capital Expenditure (CAPEX) and Operation Expenditure (OPEX). While designing a specified capacity network, CAPEX is almost fixed. Thus the focus must be on reducing OPEX by utilizing the available resources to full of its capacity. Even when all the components are functional, the quality of signal flowing may be degraded by PLIs existing in the fiber links. Thus, for optimum operation of network, the performance of all the components installed must be monitored regularly and suitable compensation techniques must be initiated as and when required [37]. The network monitoring must be done in accurate and repeatable manner and accurately reflected in routing tables so that traffic may be re-routed based on physical layer conditions. The monitoring of impairments is quite a challenging task due to their dependency on time, present state of network, signals flowing in adjoining channels and fibers. With increased data rate, complexity in networks increases, making the prediction of impairments difficult. Also, networks are vulnerable to non-catastrophic degradations where the power level of signal flowing is adequate, but detection is hindered by pulse spreading, addition of new frequencies etc. Moreover, PLIs may interact with each other to degrade the signal or pose the cancellation effect on each other thereby making it difficult to predict and manage them accurately.

The focus of present research is to monitor the non-catastrophic impairments like dispersion, attenuation, ASE, XPM, SPM and FWM. The fundamental principle of these impairments and their mathematical models are already discussed in previous chapter. The different techniques used to monitor them may be classified as digital and analog and are shown in Figure 3.1 [36]. Digital techniques focus on digital bits being transferred through the fiber while analog techniques analyse the signals at the output to extract the information about network stage, the identification, location and measurement of different impairments being present. Digital monitoring is mainly employed for measurement of BER so as to access the overall state of the network. Analog monitoring involves polarization domain, time domain and frequency domain analysis. Polarization domain analysis involves extracting the information regarding the network state by studying the variations in polarization of signals being launched into the fiber. The technique finds its implementation in measuring noise [38] [39] [40] and polarized mode dispersion [41] [42] [43] through polarization nulling or by studying degree of polarization. The main drawback of this technique is that it can be used only for coherent sources. Time domain analysis studies the variation in signal magnitude with time so as to quantify different impairments present. The techniques may or may not require the extraction of clock signals for generating various plots. Accordingly they are classified as synchronous monitoring techniques (using eye diagram plots, synchronous histogram plot) and asynchronous sampling techniques (delay tap sample plot, constellation diagrams) [44] [45] [46] [47] [48] [49] [50] [51] [52] [53] [54] [55] [56] [57] [58] [59] [60] [61] [62]. These plots are used to extract the information regarding individual impairments present. Among the different type of time domain analysis methods, eye diagram generation is most popular as it qualitatively reflects the effect of almost all impairments. Another popular approach is Q-factor monitoring owing to its direct relation between Q-factor and BER. Frequency domain analysis involves optical and RF spectrum analysis. The optical spectrum analysis may be obtained through optical filter implementation or homodyne detection involving tunable lasers. The RF spectral measurements monitoring techniques involves monitoring clock tone, pilot tone and RF tone inherently present in various frequencies or modulation format. It can effectively measure CD, PMD, OSNR and wavelength [63] [64] [65] [66] [67] [68] [69]. Although they are transparent to modulation format and data rate, but introduce interference in signal resulting in increased BER.

Among the different techniques, BER and Q-value analysis is employed to access the overall quality of the network in the present work. BER is used as it provides information about overall state of the network. The major limitation of this technique is that it is not so effective method to diagnose the cause of degradation, as the individual impairments cannot be isolated.

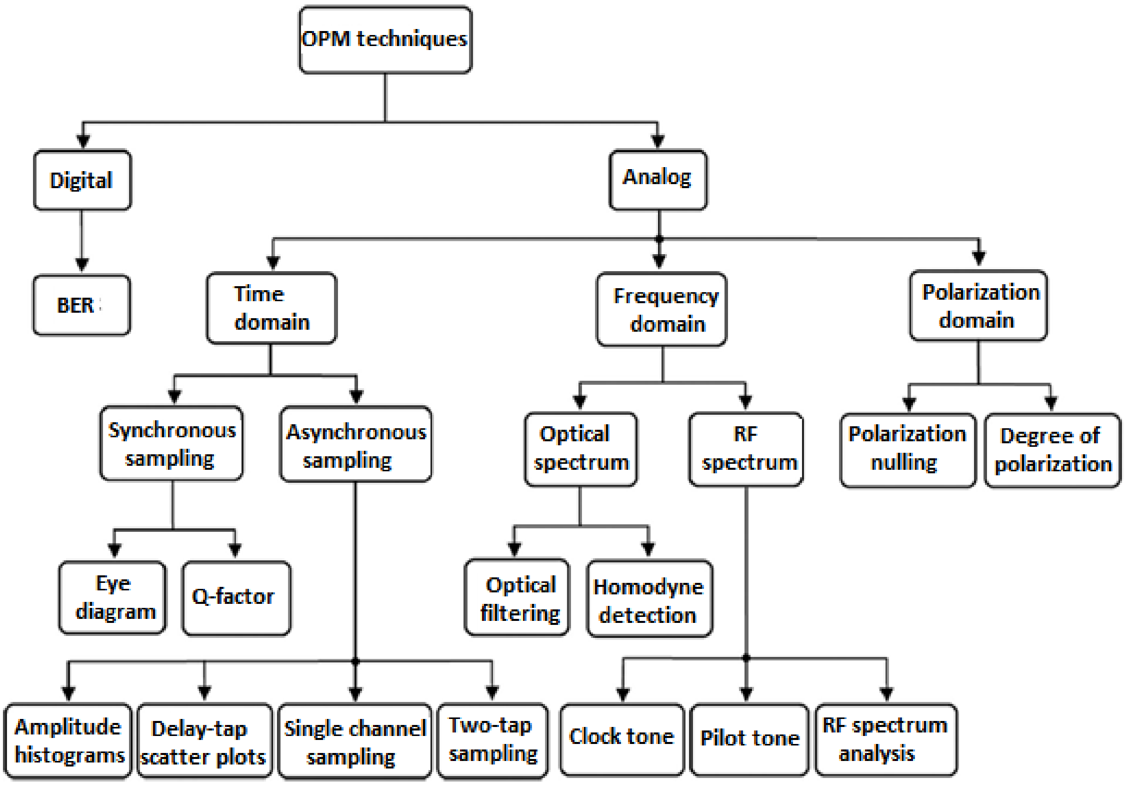

Figure 3.1: Optical performance monitoring technique

The individual impairments are diagnosed through eye diagrams and optical spectrum. In order to study the magnitude of power flowing in optical fiber, optical spectrum is studied. The power flowing can give the good estimation of OSNR, attenuation loss, wavelength drifts, non-linear impairments being present. The limitation of optical spectrum is that the effect of dispersion cannot be studied as it does not influence the optical spectrum. In order to measure these effects, eye diagram analysis is carried out. In this chapter, first section discuss the impact of varying system parameters specially wavelength on system behavior, interaction between various linear and non-linear impairments, effect of individual impairments on BER and Q-factor. The second section discusses the quality estimation technique used by present RWA for updating the Q-matrix.

3.1 IMPACT OF PHYSICAL PARAMETERS ON SYSTEM BEHAVIOUR

To study the effect of different physical layer impairments on system performance, a simple source to destination node link as shown in Figure 2.7 is considered. Continuous Wave (CW) Lorentzian laser is used as the source of optical signal. 10 Gbps Non Return to Zero (NRZ) signal is modulated using dual arm MZM. Standard single mode fiber (implementing recommendation ITU-T G.652 or TIA 492CAAA / OS1) of 100 Km length is used to transmit the signal. Following bit sequence is used to generate the required digital signal:

1	0	0	0	1	0	1	0	0	1	1	0	1
1	1	0	1	0	1	0	1	1	0	0	1	0
0	1	1	0	1	0	1	0	0	1	1	0	1
0	0	0	0	0	1	0	1	0	0	0	1	0
1	0	0	0	0	0	1	0	1	1	1	0	1
1	1	1	1	1	1	0	1	0	0	0	1	0

At the receiver end, PIN diode is used for O-E conversion. The electrical output is filtered using fourth order Bessel filter and the output is used to generate eye diagrams. In order to obtain optical spectrum of signal, the optical scope is placed before receiver. The optical spectrum and eye diagrams so obtained are used to calculate quantified parameters like BER, Q-value, delay, eye closure and opening using the various post-processing techniques. The optical spectrum is obtained at the receiver end using optical scope and analyzed to calculate power at the receiving end. For calculating different impairments, the corresponding conditions are arranged by varying the source power, the parameters of fiber or the properties of amplifier, receiver etc. The different results obtained for various impairments are illustrated in the subsequent segments of this chapter.

The value of BER is calculated using Gaussian approximation at optimum and mean threshold values. The Probability Density Function (PDF) is calculated for minimum and maximum detected bit across the threshold value. The probability density function calculated for minimum (zero level) and maximum (one level) is given by [68] [69]:

$$P_o(V_{th}) = \int_{V_{th}}^{\infty} p(y|0)\,dy \;= \frac{1}{\sqrt{2\pi\,\sigma_0^2}}\exp\left(-\frac{(u-\mu_2)^2}{2\sigma_0^2}\right) \tag{3.1}$$

$$P_1(V_{th}) = \int_{-\infty}^{V_{th}} p(y|1)\, dy \;\; = \frac{1}{\sqrt{2\pi\sigma_0^2}} \exp\left(-\frac{(u-\mu_1)^2}{2\sigma_0^2}\right)$$

(3.2)

where σ^2 is variance of noise, μ_1 and μ_2 is mean of V^+ and V^- respectively.

In order to reduce the average probability of error or BER, the optimal decision threshold value is selected instead of mean threshold value (is mean of maximum and minimum V) and is given by

Optimal Threshold $V = \frac{\mu_1 + \mu_2}{2}$ (3.3)

And the total BER is given by

$P_e = (P_o + P_1)/2$ (3.4)

Q-value is obtained by $\text{BER} = \frac{1}{2}\text{erfc}(\frac{Q}{\sqrt{2}})$

(3.5)

3.1.1 Effect of varying system parameters on Dispersion

In WDM networks, different wavelengths may be propagating inside the fiber for signal transfer. In the system with wavelength convertors being present at each node, it is possible that a signal may be using different wavelengths while it propagates from source to destination node. This may be due to pre-occupancy of currently used wavelength as the signal passes through intermediate nodes. The change in wavelength may affect the quality of signal propagating inside the fiber due to change in behavior of different physical layer impairments. Thus, study of effect of changing wavelengths on the system behavior is mandatory. In order to simulate the effect, Figure 2.7 is used where the wavelength of source with wavelengths 1310, 1490 and 1550 nm is used. For each wavelength, the value of dispersion coefficient is varied and the system response is observed through eye diagrams. To isolate the effect from other impairments, the non-linear properties of fiber are turned off. The value of attenuation coefficient is set to 0 and dispersion slope is set to 0.07 ps/nm^2/km. Figure 3.2 to Figure 3.4 shows eye diagrams obtained for 1310 nm wavelength with dispersion coefficient being varied from 2 ps/nm/km to 25 ps/nm/km.

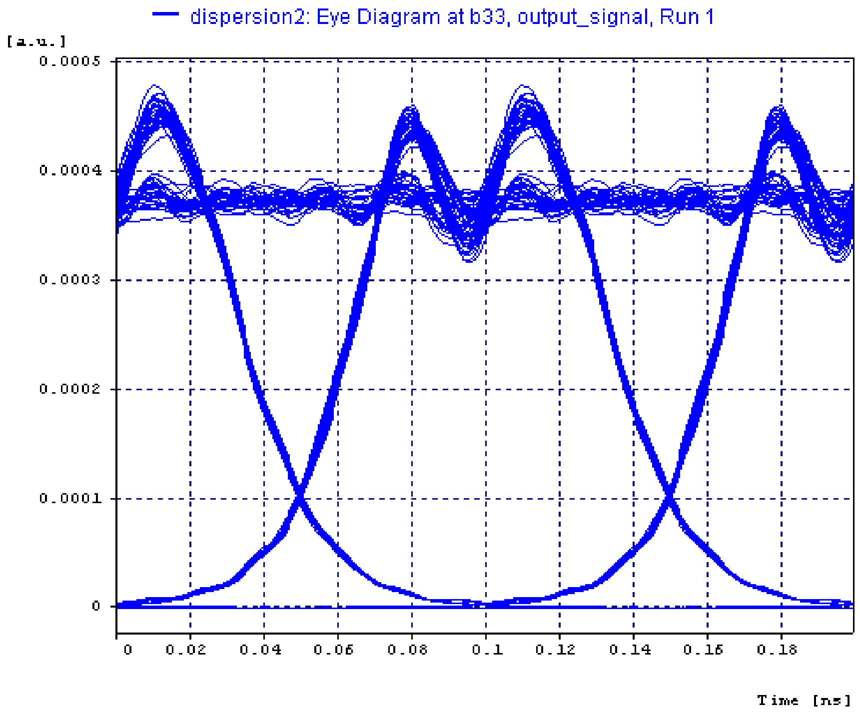

Figure 3.2: Eye diagram for wavelength of 1310 nm with D=2.8019 ps/nm/km

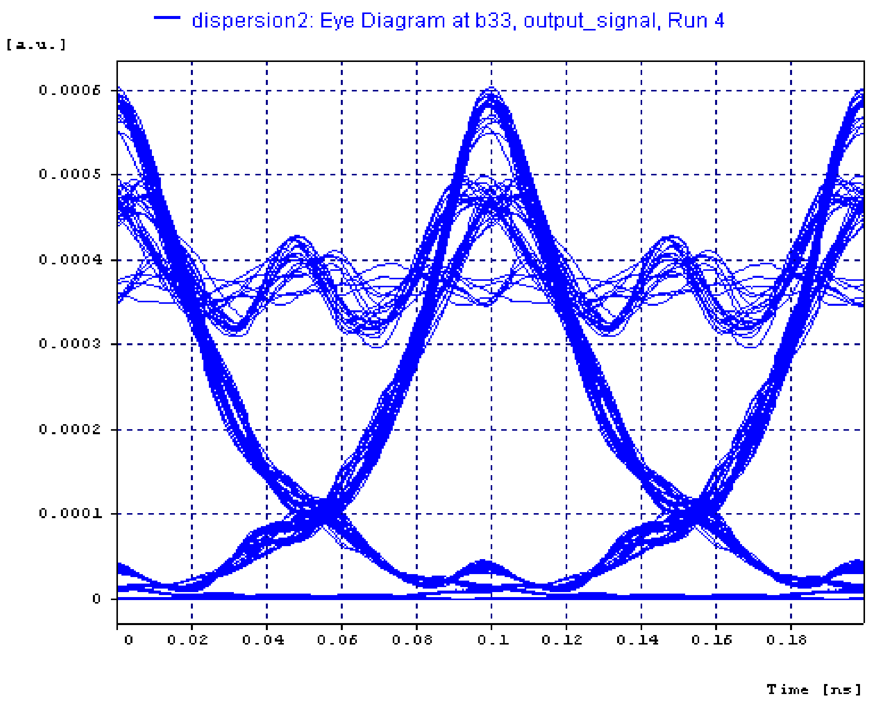

Figure 3.3: Eye diagram for 1310 nm with D=7.0047 ps/nm/km

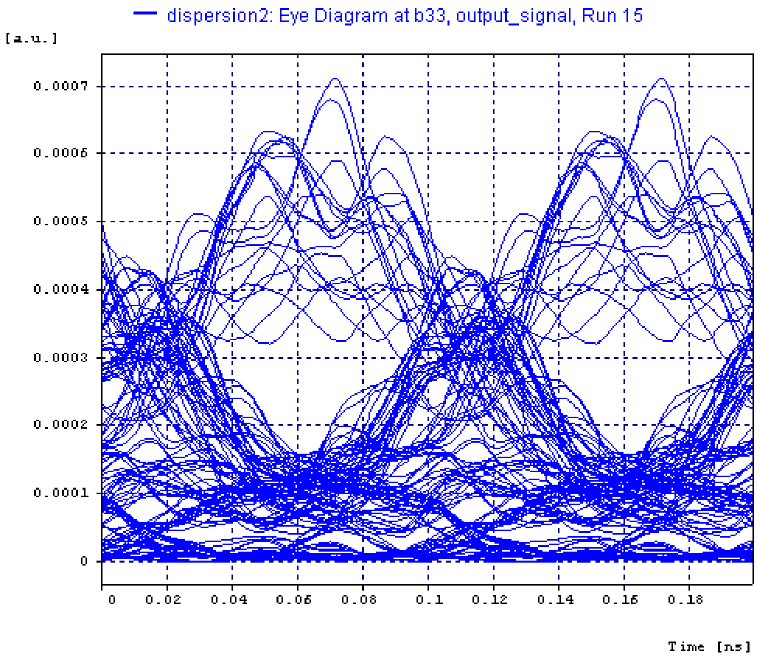

Figure 3.4: Eye diagram for 1310 nm with D=25.2170 ps/nm/km

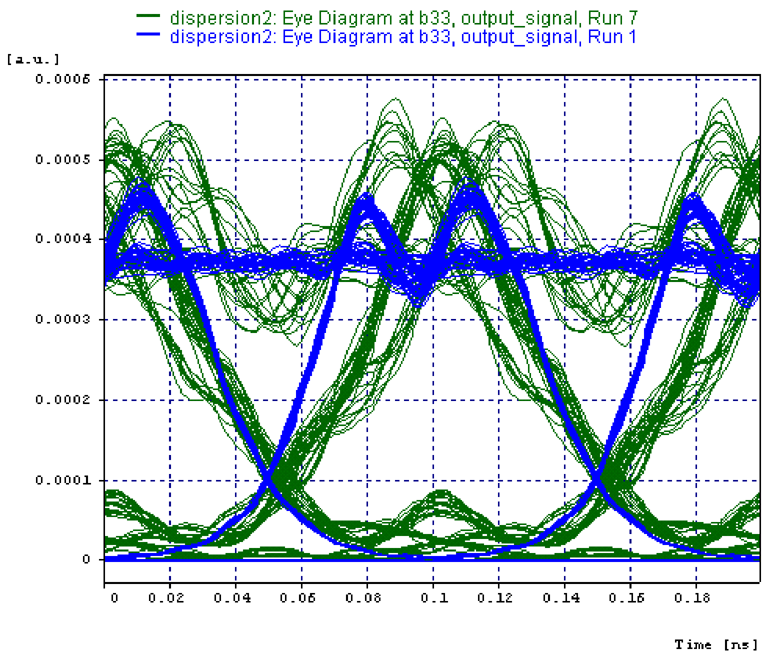

Figure 3.5: Superimposed eye diagram of D= 2.8019 and 11.2076 ps/nm/km for 1310 nm

It is quite evident that with increase in dispersion, the distortions in eye increases. For D=2.8019, the eye width and height is maximum and decrease as dispersion coefficient approaches its maximum value. Typical values of different parameters quantifying the state of eye diagram include eye closure 0.4 dB, eye opening 36E-03 and jitter 10.66 ps for dispersion coefficient of 2.8019 ps/nm/km. Q-value corresponding to the signal being transmitted is 28.5 dB while BER is 1E-40. When value of D is increased to 7 ps/nm/km, the value of eye closure becomes 0.64 dB, eye opening 0.3186E-3, jitter becomes 16.18 ps, Q-value 22.6 dB, BER 0.99E-40. Till this stage, the value of BER and Q-factor are much higher than above the threshold limits of the system. But as the value of dispersion coefficient reaches D=25.2 ps/nm/km, the different eye diagram parameters shoot towards their upper limit. Eye closure is 9.04 dB, eye opening is 0.25E-3 and jitter of 21 ps is obtained. Q-value corresponding to the signal being transmitted is 7.3 dB while BER 0.107E-1. The quality of signal is degraded such that further rise in value of dispersion will increase the BER and decrease the Q-value below 6 dB, thereby making system vulnerable to breakdown or resulting in link failure. In order to visualize the degradation taking place, the eye diagram of lower and higher D values is superimposed as shown in Figure 3.5. Blue colour eye diagram corresponds to D=2.8019 ps/nm/km while the green colour eye diagram corresponds to D=11.2076 ps/nm/km. The waveforms peaking above the upper line (+1 level of eye diagram) are because of presence of CD and is much higher in the later case. The precise formation of eye transforms to distorted eye owing to increased jitter with increase in dispersion value.

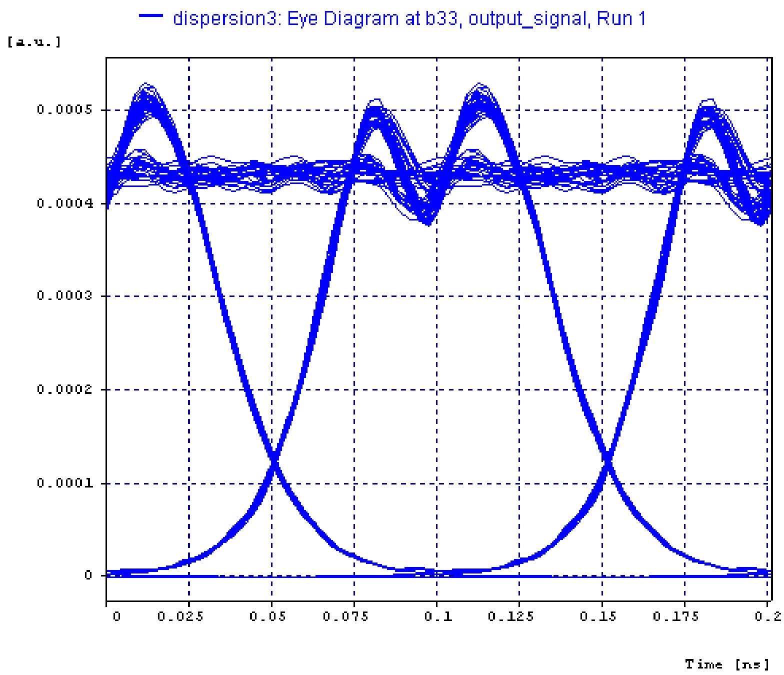

Figure 3.6: Eye diagram for 1490 nm with D=2.1658 ps/nm/km

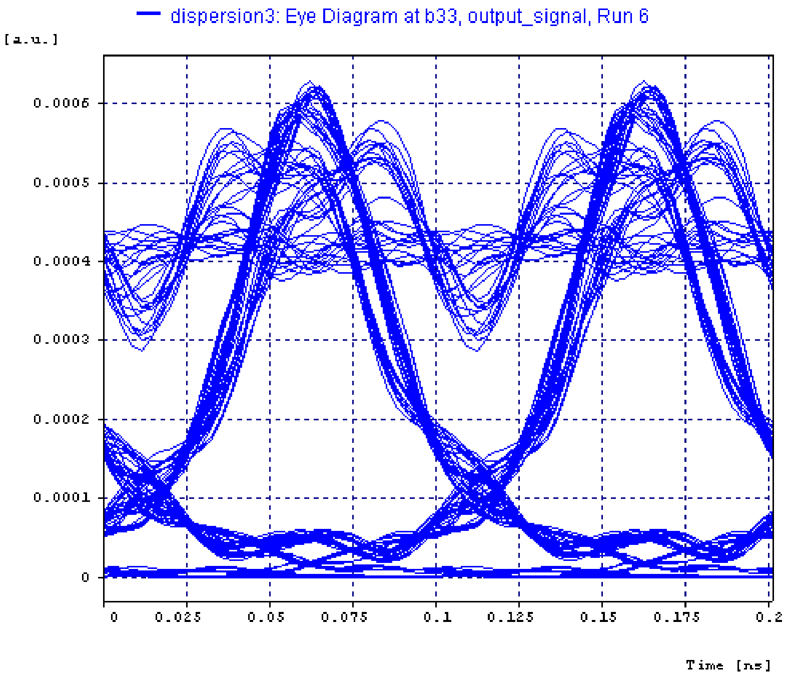

Figure 3.7: Eye diagram for 1490 nm with D=7.5804 ps/nm/km

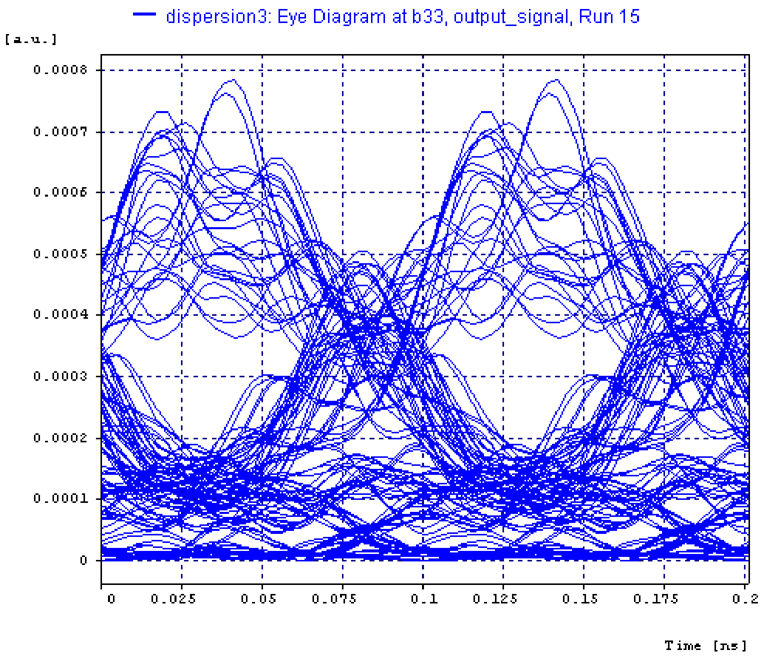

Figure 3.8: Eye diagram for 1490 nm with D=19.4923 ps/nm/km

Now, the wavelength of source is changed to 1490nm to study the difference in behavior of dispersion on system performance. The value of D is varied from 2ps/nm/km to 25 ps/nm/km. Eye diagrams obtained for selective values i.e.2.1658, 7.5804, 19.4923 ps/nm/km are represented in Figure 3.6 to Figure 3.8.

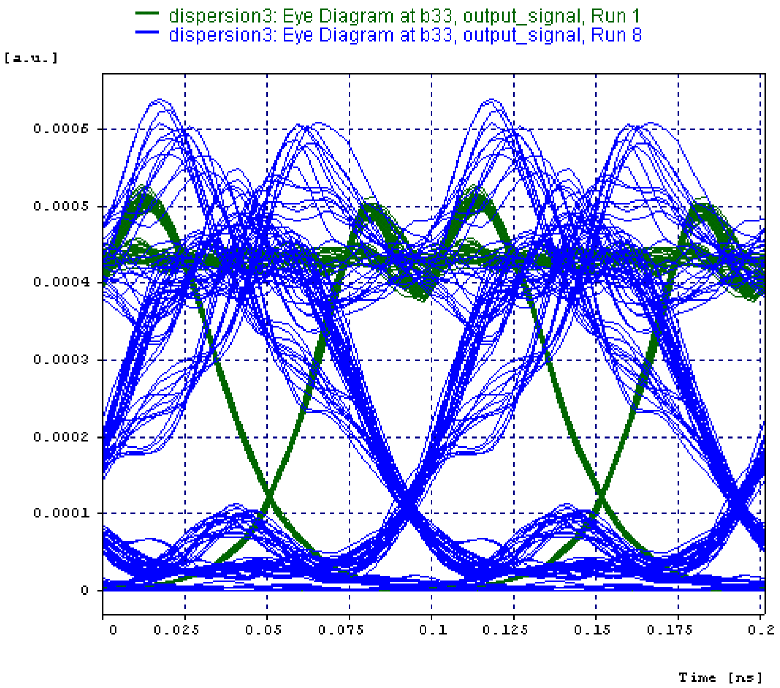

Figure 3.9: Superimposed eye diagram of D=2.1658 and 10.8291 ps/nm/km for 1490 nm

The variations in the patterns of eye formation are similar to that for 1310 nm source, i.e. with increase in dispersion, the distortions in eye diagram increase with the increase in dispersion. The typical values of system parameter are summarized. For dispersion coefficient of 2.1658 ps/nm/km, eye closure is 0.271 dB, eye opening is 0.4306E-03 and jitter of 17.259 ps is obtained. Q-value corresponding to the signal being transmitted is 30.59 dB while BER is 1E-40. When value of D is increased to 7.58 ps/nm/km, the value of eye closure becomes 1.35 dB, eye opening 0.3386E-03, jitter becomes 17.5567 ps, Q-value16.31 dB, BER 0.7125E-10. Eye closure is 8.034 dB, eye opening is 0.449E-04 and jitter of 23.175 ps is obtained. Q-value corresponding to the signal being transmitted is 7.51 dB while BER 0.8789E-2. In order to demonstrate the overall impact, the eye diagram of D=2.1658 (green color eye diagram) and 10.8291 (blue color eye diagram) are superimposed and shown in Figure 3.9. The increased jitter, increased closing and reduced eye opening effects can easily be seen. In the next case, the wavelength of source is changed to 1550 nm and the corresponding eye diagrams obtained are shown in Figure 3.10 to Figure 3.13.

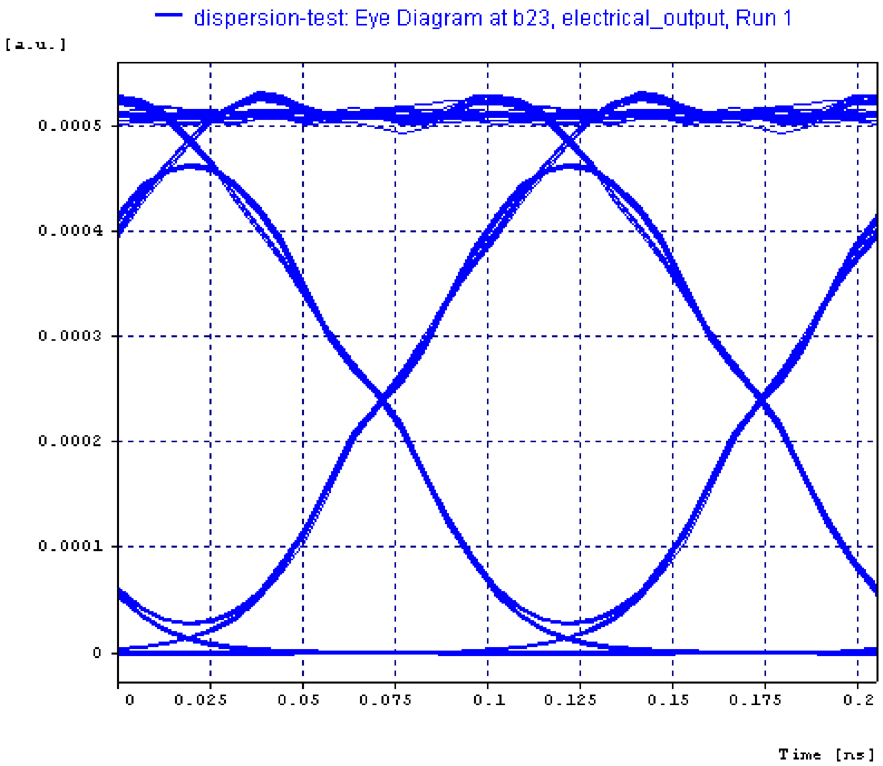

Figure 3.10: Eye diagram for 1550 nm with D=2.0014 ps/nm/km

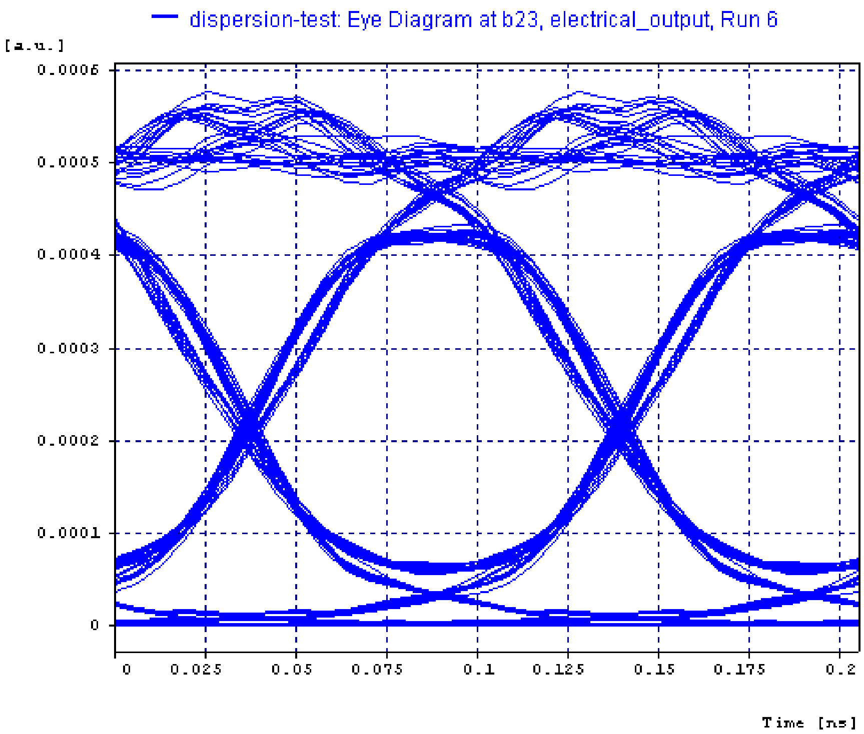

Figure 3.11: Eye diagram for 1550 nm with D=7.0048 ps/nm/km

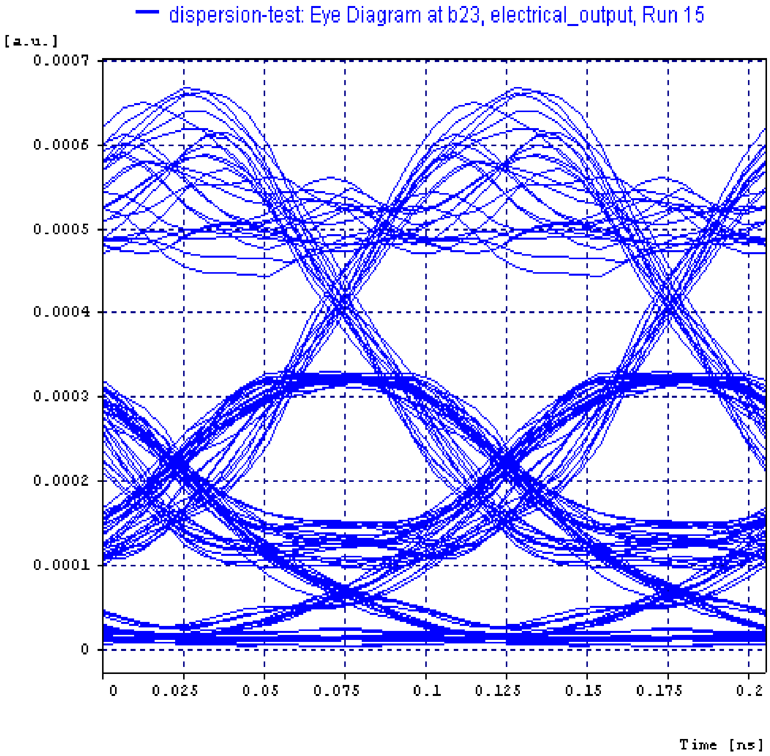

Figure 3.12: Eye diagram for 1550 nm with D=18.0125 ps/nm/km

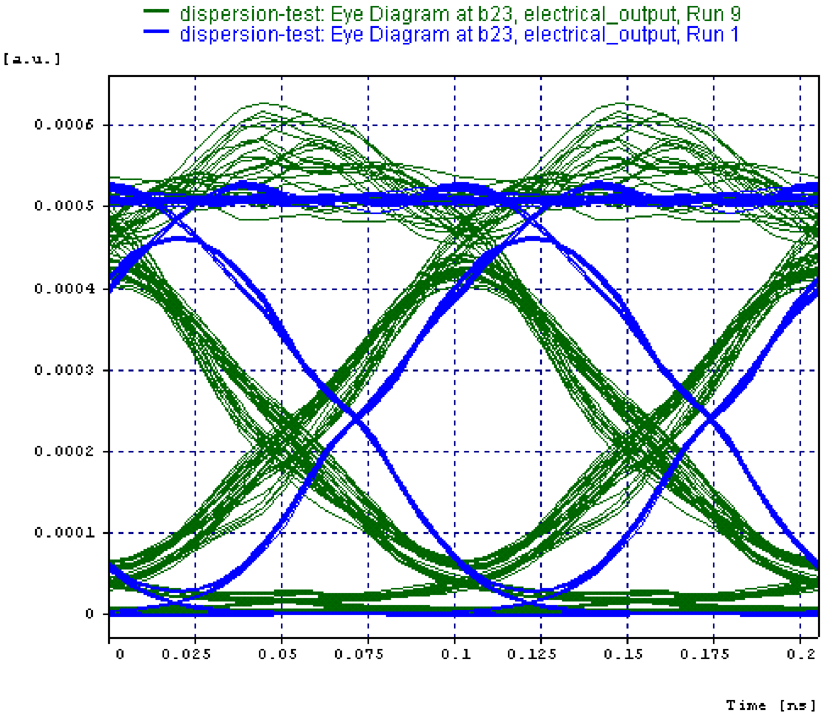

Figure 3.13: Superimposed eye diagram of D=11.0076 and 2.0014 ps/nm/km for 1550 nm

The eye diagrams obtained are having minimum jitter and distortions. For dispersion parameter 2.0014 ps/nm/km, the eye opening is 0.46e-3, closure is 0.35 dB, jitter 15.8 ps, Q value 23 dB, BER 1E-40. Dispersion parameter 7.0048 ps/nm/km resulted in eye opening of 0.21E-03, eye closure 0.887, jitter 22.18 ps, Q-value 17 dB, BER 0.5E-13 while dispersion parameter 18.0125 ps/nm/km has eye opening of 0.31E-02, eye closure 3.18, jitter 23.7 ps, Q-value 8 dB, BER 0.3E-2. The eye diagram for dispersion parameter 11.0076 ps/nm/km (shown in green) is superimposed over dispersion parameter 2.0014 ps/nm/km (shown in blue) to demonstrate the variation in eye patterns with increased dispersion.

The overall range of these quantifying parameters including eye closure, delay introduced, BER and Q-value are summarized. As the eye opening and closure are counteracting phenomena i.e. increase in eye opening will decrease the closure and vice versa, the eye closure is used to study this variation and is shown in Figure 3.14.

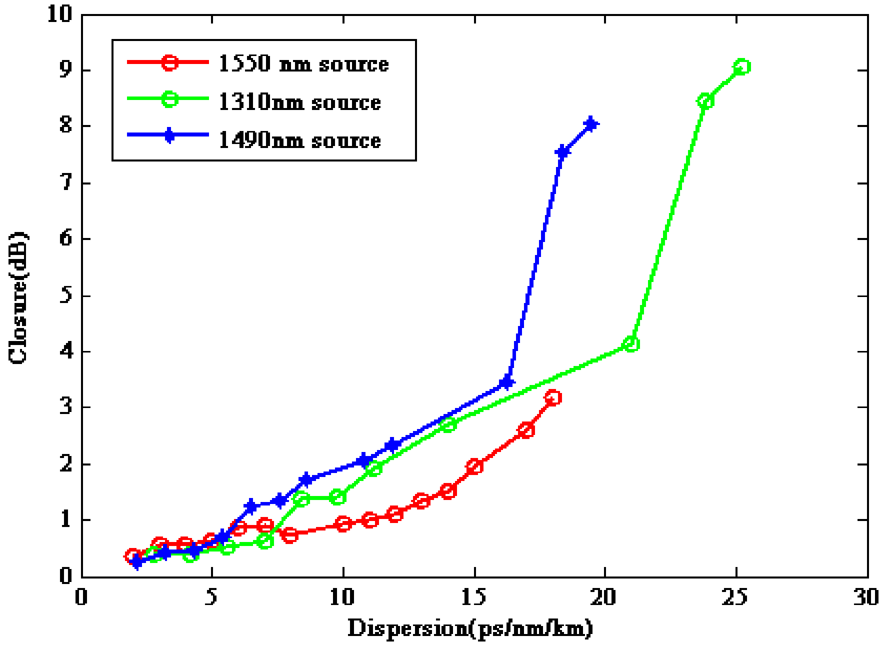

Figure 3.14: Eye closure for different values of D for 1550, 1310, 1490 nm source

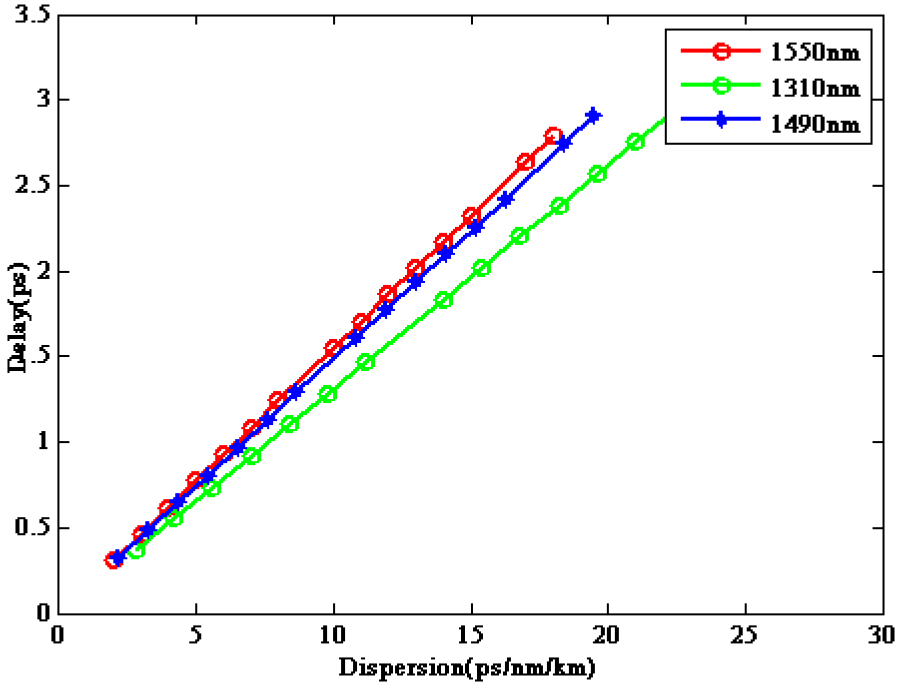

Figure 3.15: Delay at output for different values of D for 1550, 1310, 1490 nm source

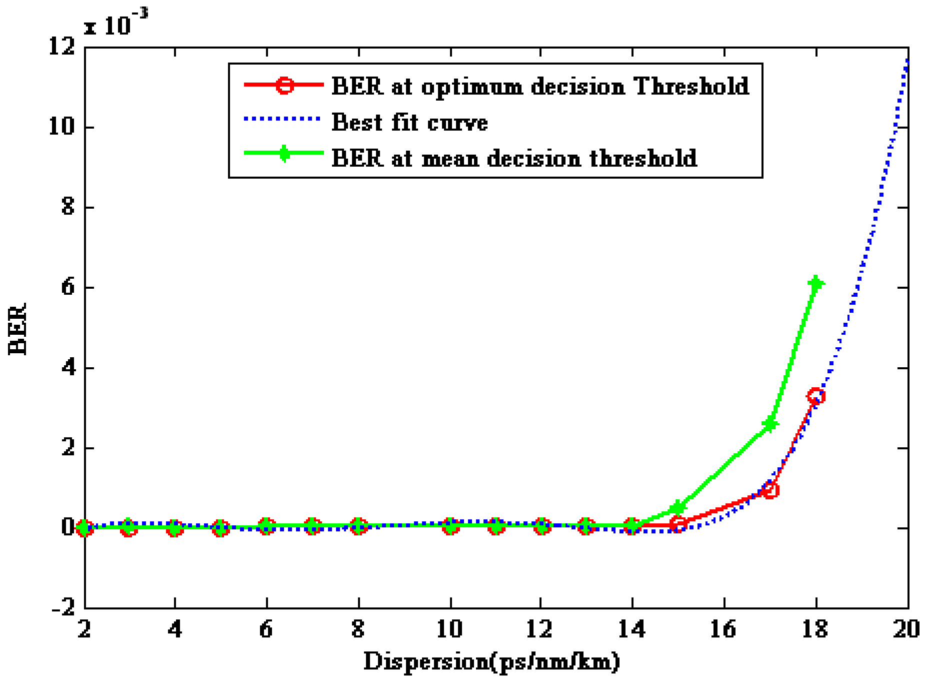

Figure 3.16: BER for 1550 nm source at optimum and mean decision threshold

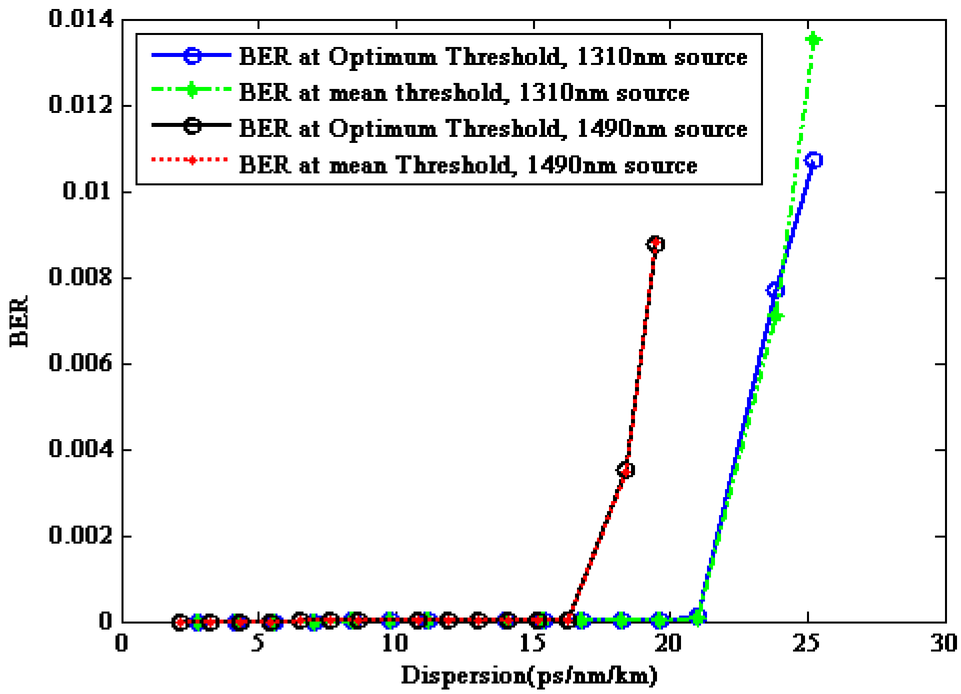

Figure 3.17: BER for 1310 and 1490 nm source at optimum and mean decision threshold

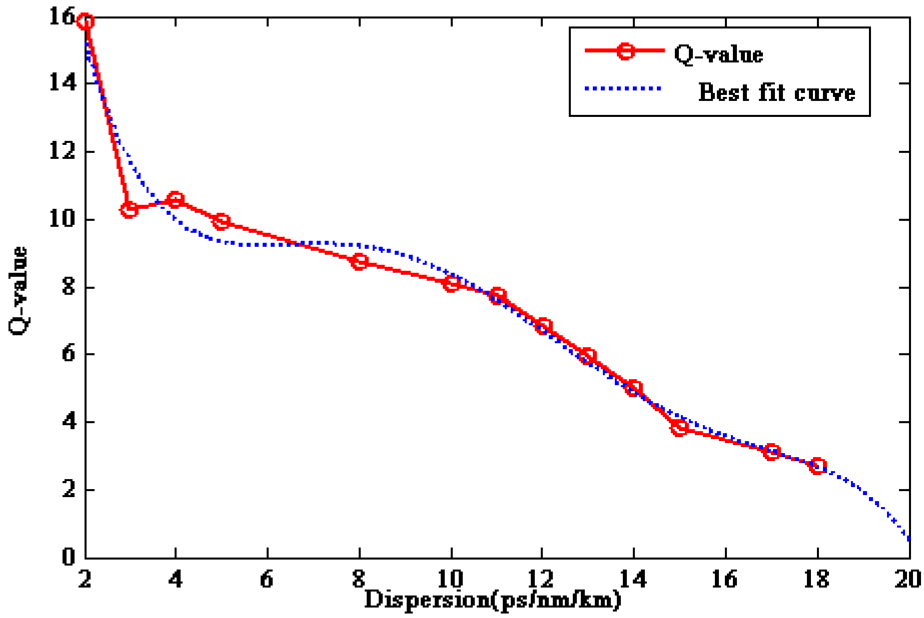

Figure 3.18: Q-value for 1550 nm source

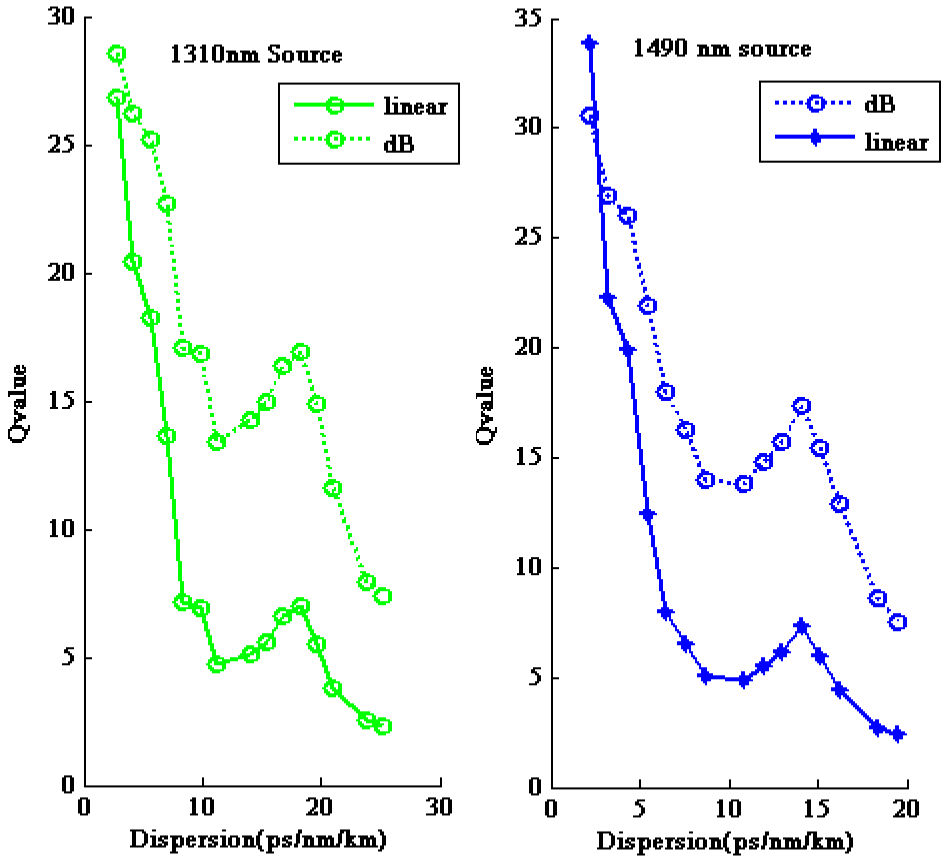

Figure 3.19: Q-value for 1310 and 1490 nm source

The maximum range of variation of eye closure is obtained for 1310nm wavelength i.e. between 0.4 to 9 dB, while minimum for 1550 nm (0.33 – 3 dB). The fact is supported by various eye diagrams obtained. The difference in magnitude of delay introduced by different wavelengths is very small as shown in Figure 3.15. This is the reason for implementing any of these wavelengths for WDM communication. Further, impact of BER, Q-value for varying dispersion is shown in Figure 3.16 to Figure 3.19 for different wavelength sources. The value of BER abruptly increase as the dispersion coefficient increase 14, 15 and 20 ps/nm/km value in case of 1510, 1490 and 1310 nm wavelengths respectively. As the BER and Q-factor are directly related by equation, the increase in BER is reflected in diagram of Q-value. The curves obtained for BER and Q-value are analysed and corresponding mathematical model is obtained by curve fitting so as to have an analytical model of effect of system performance and may be used in route finding algorithms to calculate the cost function representing the effect of impairment on system performance if required. Considering the trends in system response for various wavelengths, the various equations representing the best fit curve for BER and Q value are calculated using curve fitting techniques. The equations for best fit curve for 1550nm wavelength as calculated is

BER:

$$y = 1.1e\text{-}007x^5 - 4.8e\text{-}006x^4 + 7.7e\text{-}005x^3 - 0.00056x^2 + 0.0018x - 0.0019 \quad (3.6)$$

Q-value

$$y = -0.0002x^5 + 0.012x^4 - 0.26x^3 + 2.7x^2 - 13x + 32 \quad (3.7)$$

3.1.2 Effect of varying system parameters on Attenuation

As WDM networks employ different wavelength sources it is essential to study the response of optical souces for attenuation effect. So the source selection of different wavelengths is done for system represented in Figure 2.7 and the power delivered across the load is measured.The attenuation coefficient for different wavelengths is represented in Figure 3.20.

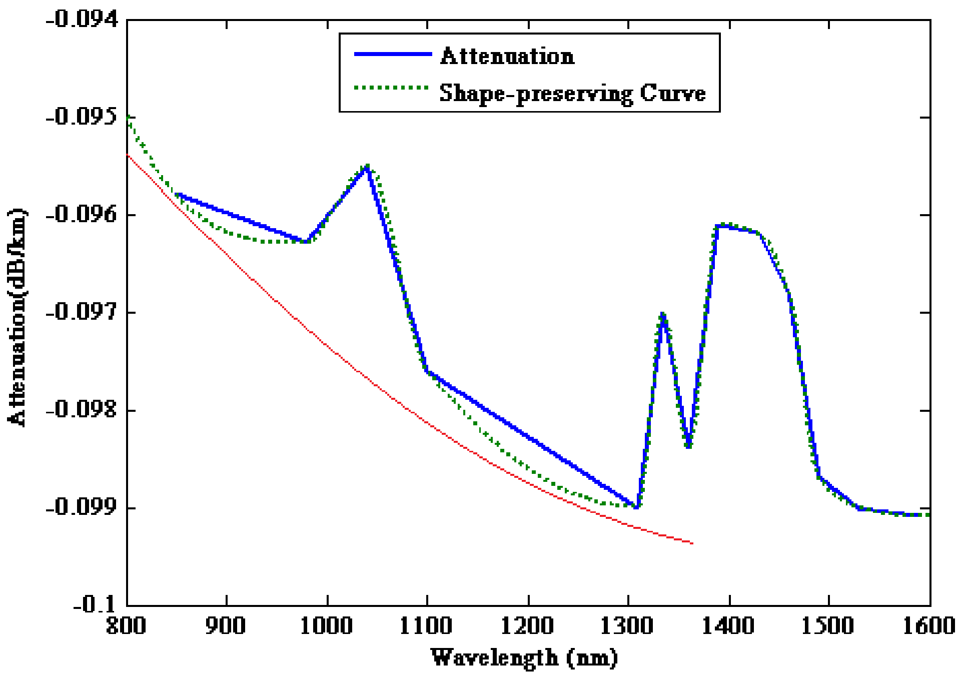

Figure 3.20: Attenuation coefficient for different wavelength sources

In the graph, the peaks obtained are due to absorption losses arising from atomic defects in material of fiber, absorption by basic constituent and impurity atoms present in fiber. Atomic defects include missing molecules, high density clusters of atom groups in fiber. The losses caused by them increase tremendoulsy on exposure to radiative environments as radiations further damage the internal structure of material. The impurity atoms leading to absorption (also called extrinsic absorption) include presence of OH ions, transition metal ions such as iron, copper, chromium etc causing loss ranging from 0 to 4 dB/km. The absorption by basic constituents of fiber materials (intrinsic absortion) results from electronic absorption bands in ultra violet regions and atomic vibration bands in near infra red regions. The red line indicates the losses taking place due to Rayleigh scaterring effect. The scatering may arise from variations in material density, compositional fluctuations, structural inhomogeneties or manufacturing defects. Since it has inverse propotional relationship with respect to wavelength, it decreases dramatically with increased wavelength.

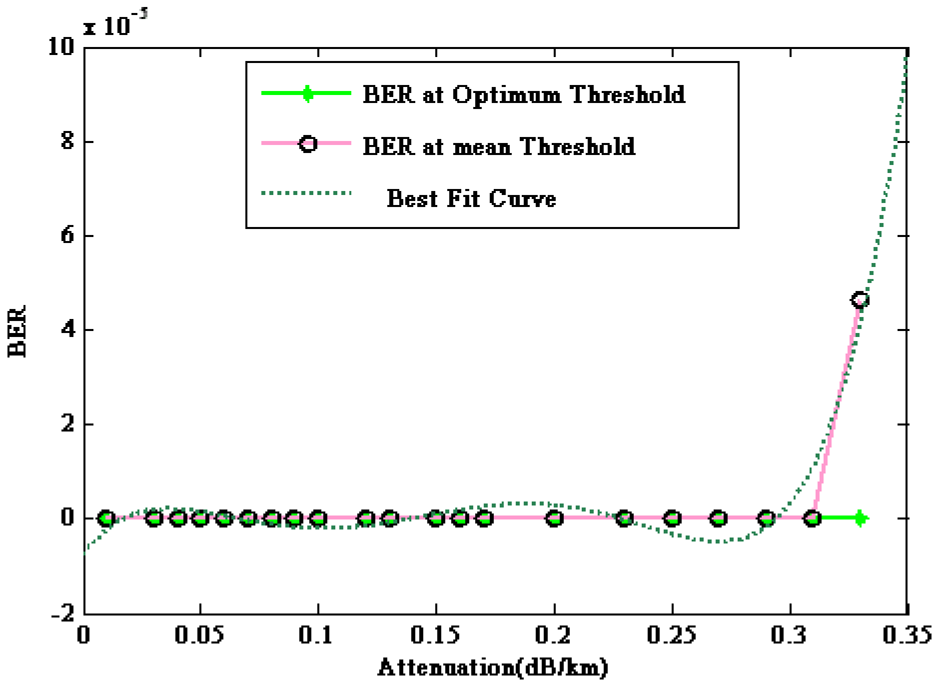

Figure 3.21: BER at optimum and mean threshold for different attenuation coefficients

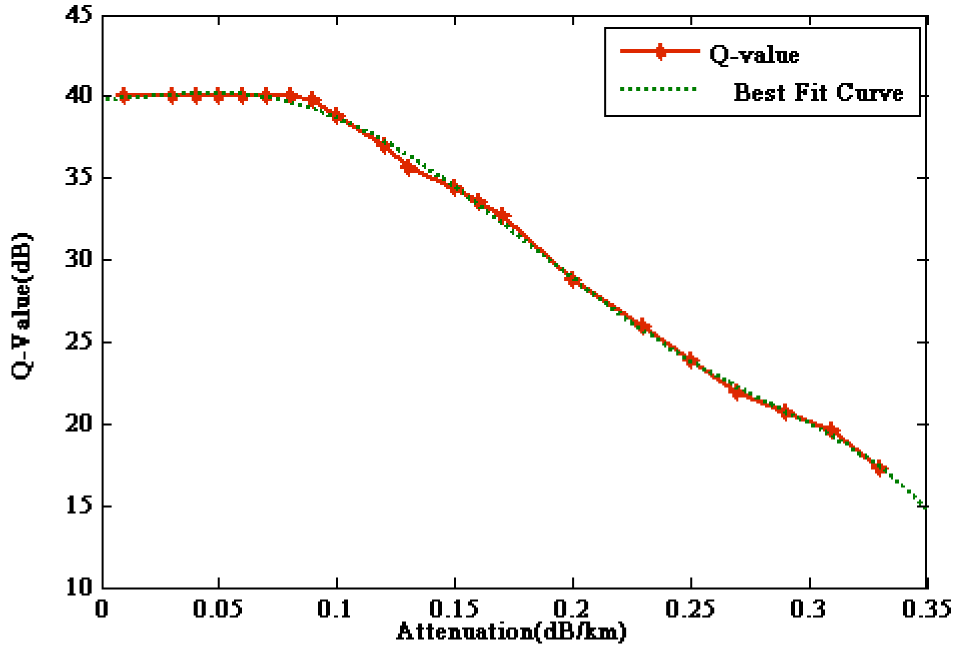

Figure 3.22: Q-value for different attenuation coefficients

The variation of BER and Q-factor with attenuation is presented in Figure 3.21 and Figure 3.22 respectively. The curves obtained are analyzed and corresponding mathematical model is obtained by curve fitting. Fifth order equation is calculated representing trends of BER and Q-value curve are:

$$\text{BER-------}y = 0.72x^5 - 0.54x^4 + 0.14x^3 - 0.016x^2 + 0.00067x - 7.5e\text{-}006 \quad (3.8)$$

$$\text{Q-value-----}y = - 49000x^5 + 40000x^4 - 10000x^3 + 560x^2 - 0.28x + 40 \quad (3.9)$$

The mathematical model equations obtained represent variation trends of BER, Q-value with varying attenuation, which has been verified by different wavelength sources and network conditions. Thus, in nearby future, these equations may successfully be used for representing circuit behavior for various attenuation coefficients. The total power that may be transferred to the receiver may be estimated which will further support the network designer in regenerator placement and utilization issues. Also, it finds an important application to calculate cost function of RWA problems in PLI aware networks and predict quality of transmission for satisfying service level agreements by service providers.

3.1.3 Effect of system parameters on Phase Modulation (due to SPM and XPM)

Phase modulation is the non-linear phenomena in which phase of the pulse is modulated either due to influence of high power of the same signal, or due to influence of adjoining wavelengths travelling in the same fiber. The basics equations involved with generation of SPM and XPM, effect of channel power and the adjoining channel power has already been discussed. In order to have the impact of XPM, a system shown to Figure 2.23 with two transmitters is implemented. Initially, impact of SPM is studied with varying wavelength of source one in absence of second transmitter. It has been found that with increase in wavelength, the impact of non-linearity component is reduced. The reason for the same is inverse dependence of γ with free space wavelength. The fact can be visualized in Figure 3.23, where, the non-linear effect is decreasing linearly with increase in wavelength.

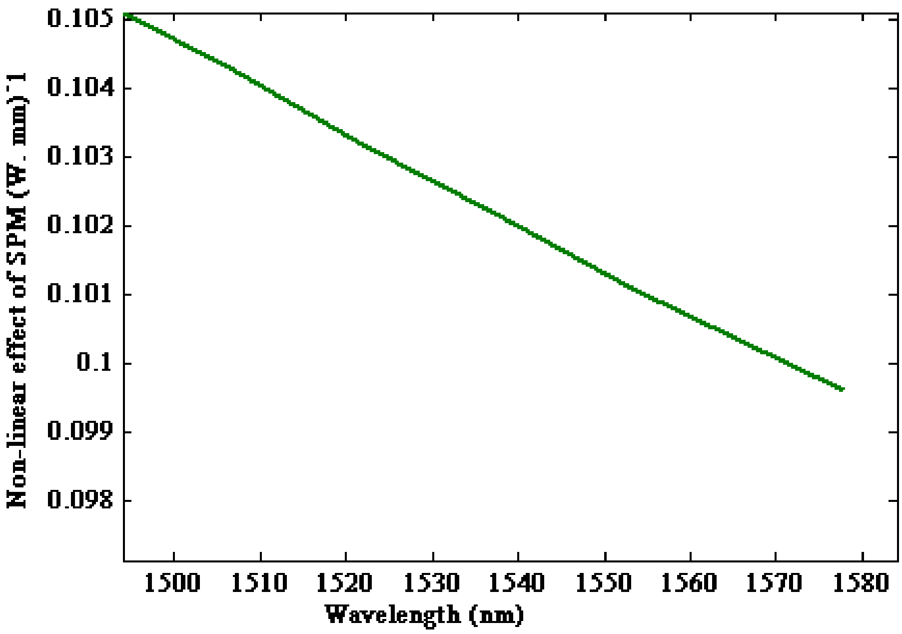

Figure 3.23: Non-linear effect of SPM with varying wavelengths

The impact of this non linear coefficient on phase of propagating signal is studied. The phase variation of output signal is measured for increased wavelength of source. Although the non-linear effect of SPM is measured to be decreasing with increased wavelength, but the phase shift is increasing. The reason behind this may be long interaction length of fiber available with varying refractive index of fiber. The variation of phase shift with wavelength is shown in Figure 3.24.

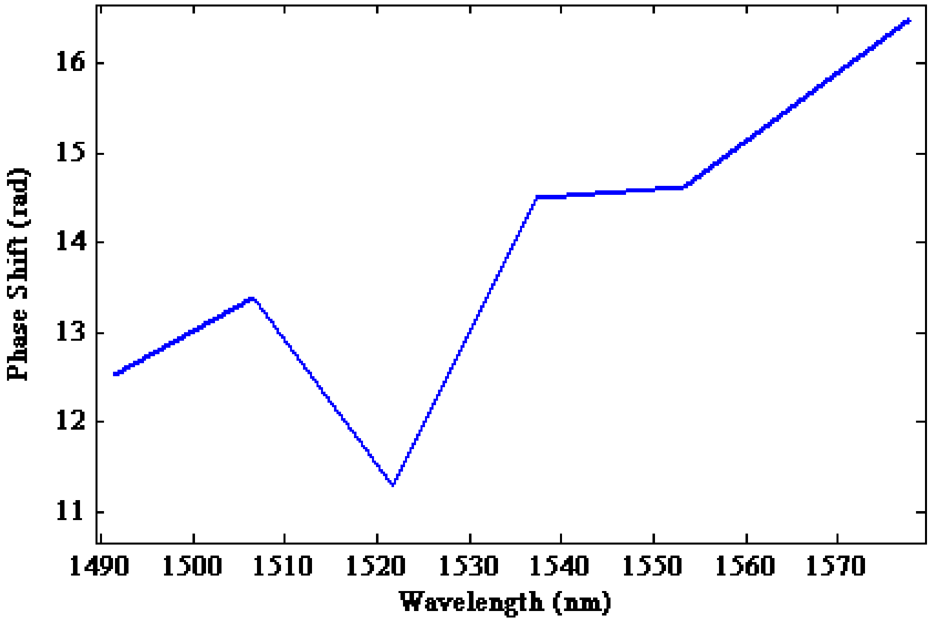

Figure 3.24: Phase shift due to non-linear effect of SPM with varying w wavelength

In optical communication systems, the presence of multiple impairments also influences the overall system performance due to interaction between them. Normally, the linear impairments pose counter acting effect on non-linear impairments thereby reducing their overall impact on the system performance. On one hand, it is advantageous as it reduces the impact of degradations taking place in the system, on the other side they adversely impact the process of compensation as the impairments cannot be accurately measured. The impact of phase shift nonlinearity is reduced due to counteracting effect posed by dispersion. To study the impact of dispersion on phase shift, the value of D is vaired from -14 ps/nm/km to 14 ps/nm/km and the variations in optical spectrum obtained for different inputs are studied. The spectrum obtained for -4 and 0.4 ps/nm/km is shown in Figure 3.25 and Figure 3.26 respectively.

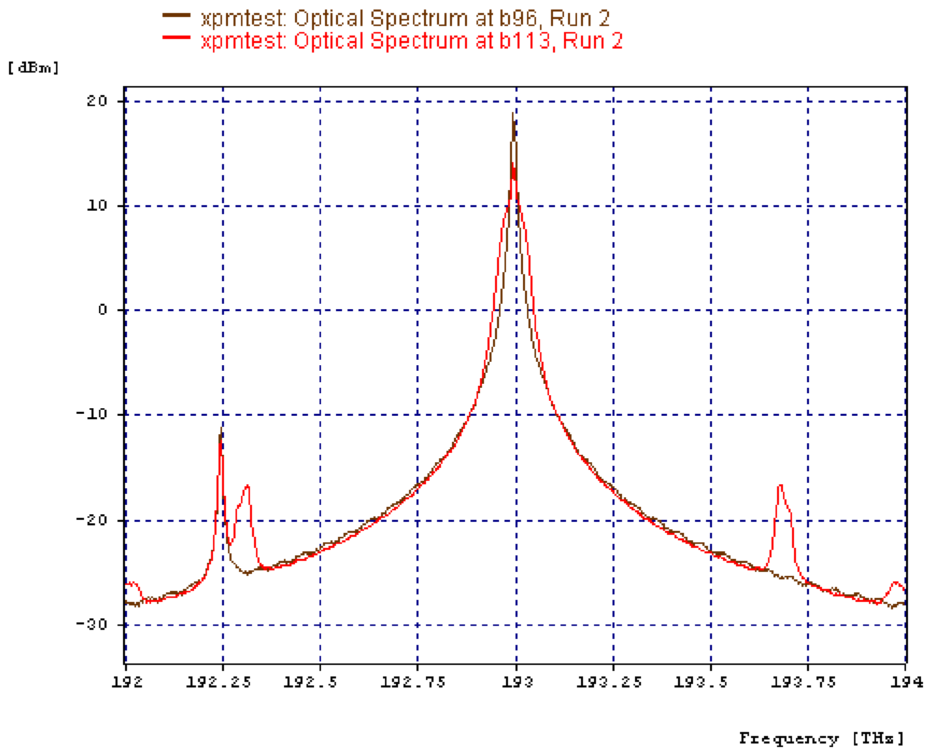

Figure 3.25: Impact of XPM on optical spectrum constant pump power of 0.004 mW and D=-4 ps/nm/km

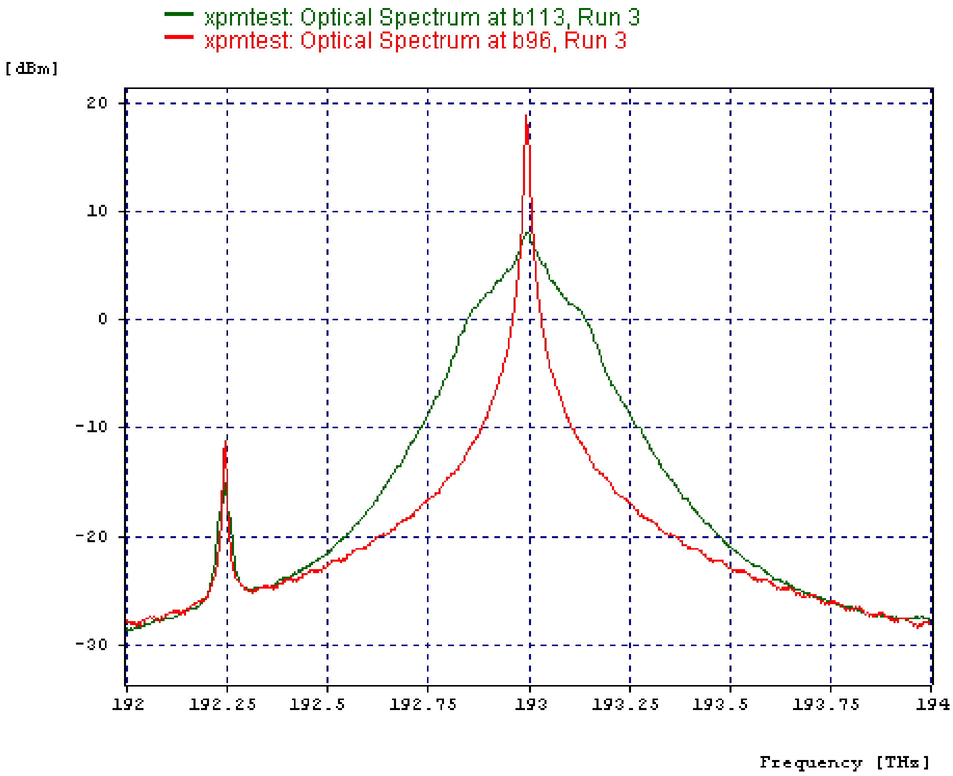

Figure 3.26: Impact of XPM on optical spectrum constant pump power of 0.004 mW and D=0.4 ps/nm/km

The value of phase shift increase as the dispersion coefficient tends to zero. This is due to the fact that dispersion offers cancellation effect on SPM and XPM and decrease in dispersion reduces the counteracting effect, thereby increasing the phase shift. Further decrease in phase shift may be obtained by reducing the power of input signal. The threshold condition for nullifying the effect of phase modulation has already been discussed.

As the distance of propagation of light wave is large in long haul backbone networks, the common approach adopted by today's network is to raise the power at the input so as to balance the impact of power loss caused by scattering and attenuation. The increased power introduces nonlinearity components into the fiber link, making it mandatory to study their impact on system behavior through BER and Q-value. Figure 3.27 and Figure 3.28 presents the effect of power input on BER in the presence of SPM only and combined impact of XPM and SPM respectively.

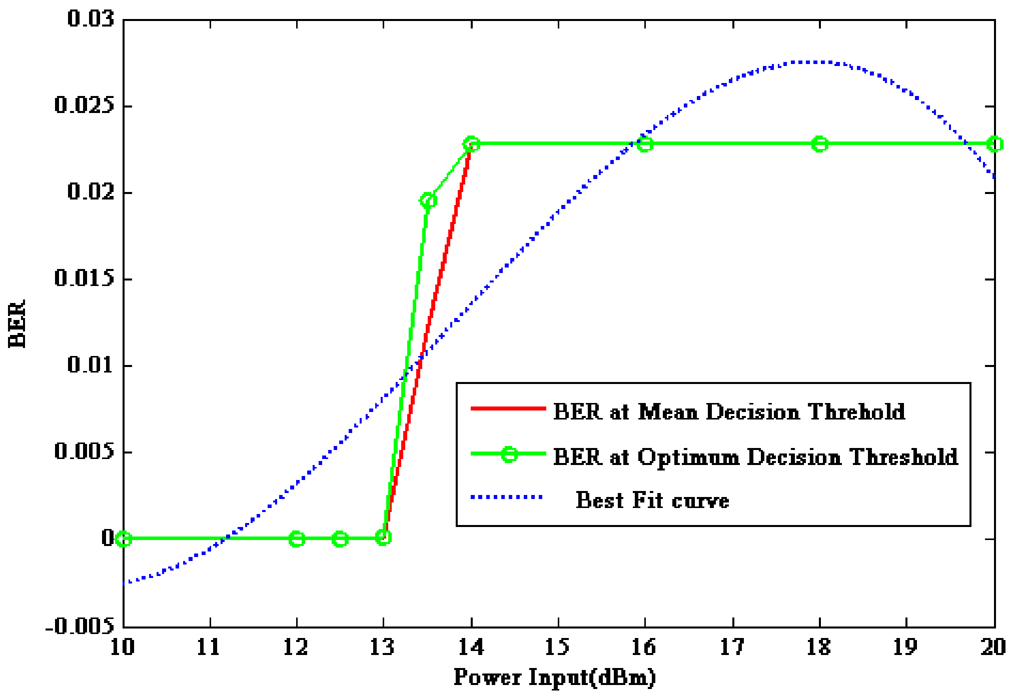

Figure 3.27: Impact of input power on BER due to SPM only

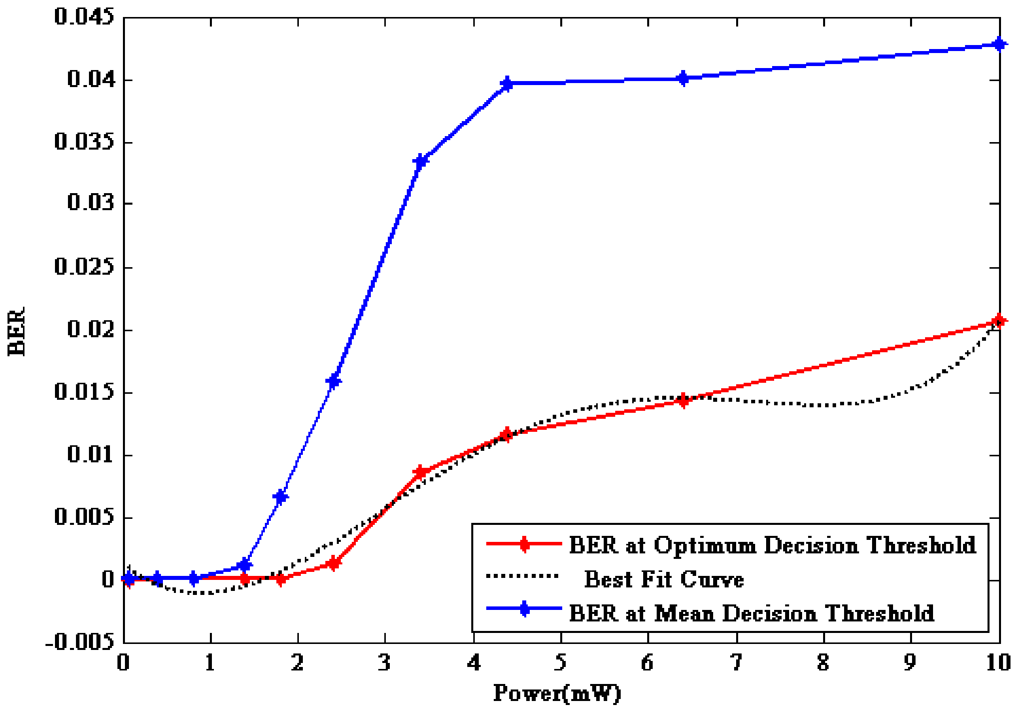

Figure 3.28: Impact of input power on BER due to combine effect of SPM and XPM

The best fit curve obtained for SPM only is represented by equation

$$y = -0.00011x^3 + 0.0044x^2 - 0.055x + 0.22 \quad (3.10)$$

While that of the system having SPM in presence of XPM is

$$y = 3.3e\text{-}005x^4 - 0.00066x^3 + 0.0041x^2 - 0.0059x + 0.0013 \quad (3.11)$$

In the presence of SPM, the value of BER increase drastically as the power of input source increase 13 dBm i.e. 19.8 mW and becomes above the unacceptable as power reaches 14 dBm. It must be noted that the threshold value obtained in presence of SPM is almost equal to threshold value obtained by analytical calculations (19.6 mW). In presence of both SPM and XPM, the value of BER starts increasing from 2 mW (3 dBm). The BER crosses its threshold value at 3 mW or 4.77 dBm and 10 mW or 10 dBm when measured at mean and optimum decision threshold respectively.

The corresponding variation in Q-value may be seen with increased power levels. The Q-value curve for system with SPM only is shown in Figure 3.29 and in presence of both SPM and XPM is shown in Figure 3.30.

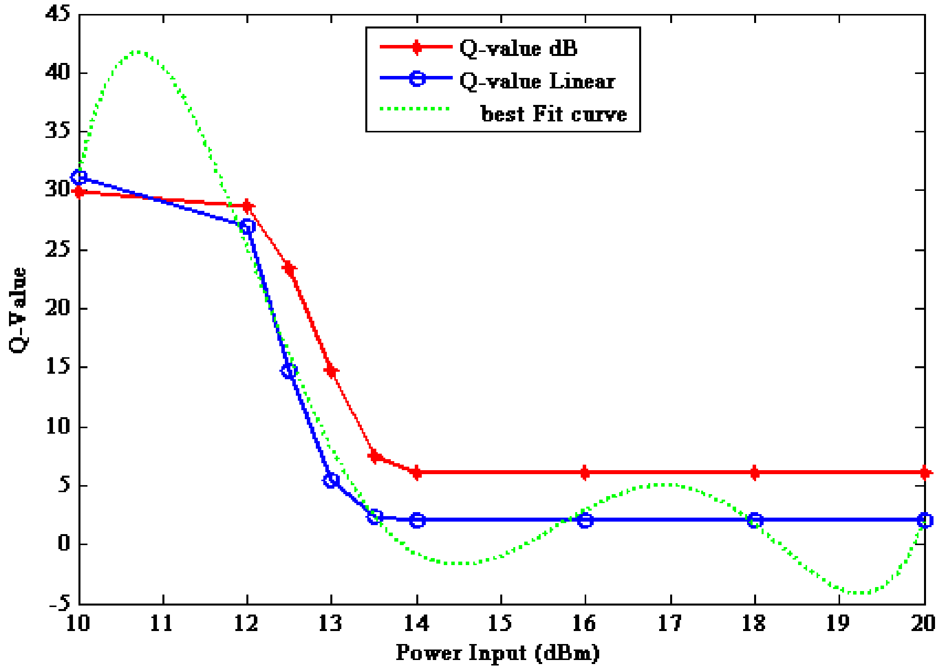

Figure 3.29: Impact of input power on Q-value in presence of SPM only

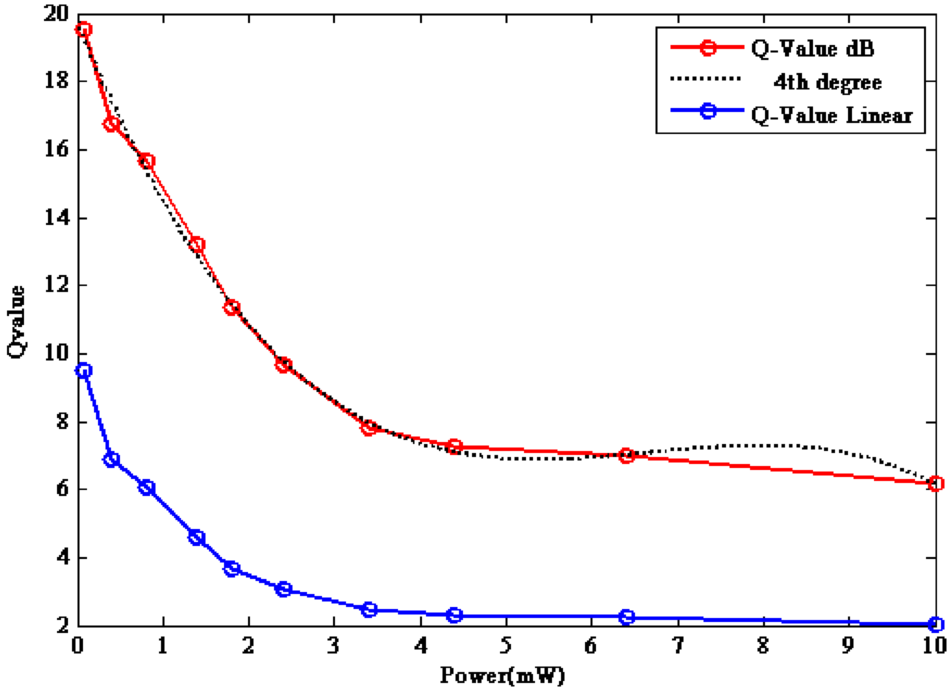

Figure 3.30: Impact of input power on Q-value in presence of SPM and XPM

The best fit curve for Q value considering effect of SPM only implements the following equation

$$y = 0.033x^5 - 2.5x^4 + 76x^3 - 1.1e{+}003x^2 + 8.2e{+}003x - 2.4e{+}004 \qquad (3.12)$$

The equation representing best fit curve for Q-value considering effect of XPM and SPM is

$$y = 0.0001x^4 - 0.05x^3 + 0.97x^2 - 6.2x + 20 \qquad (3.13)$$

The trends of variation are similar to that of BER curve. The Q-value decreases with increased power and became unacceptable below 13 dBm power in presence of SPM only and by 10dBm in presence of both SPM and XPM.

3.1.4 Effect of system parameters on Four Wave Mixing

Another dominating effect degrading the signal quality includes FWM, where interaction of different waves results in mixing of new frequencies which travel along the signal. These new frequencies deplete the power of original signal and influence the data travelling in the fiber.

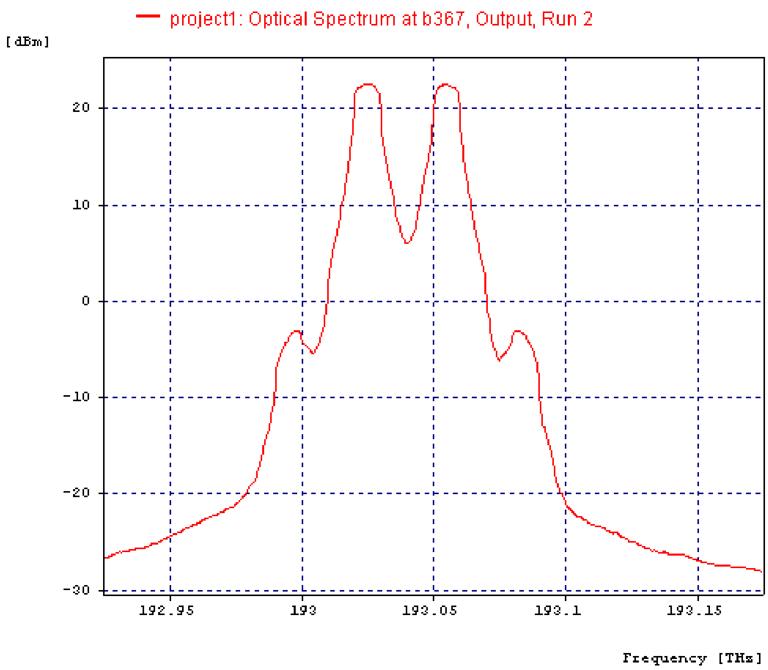

Figure 3.31: Optical spectrum for two channel WDM network with 30GHz channel spacing

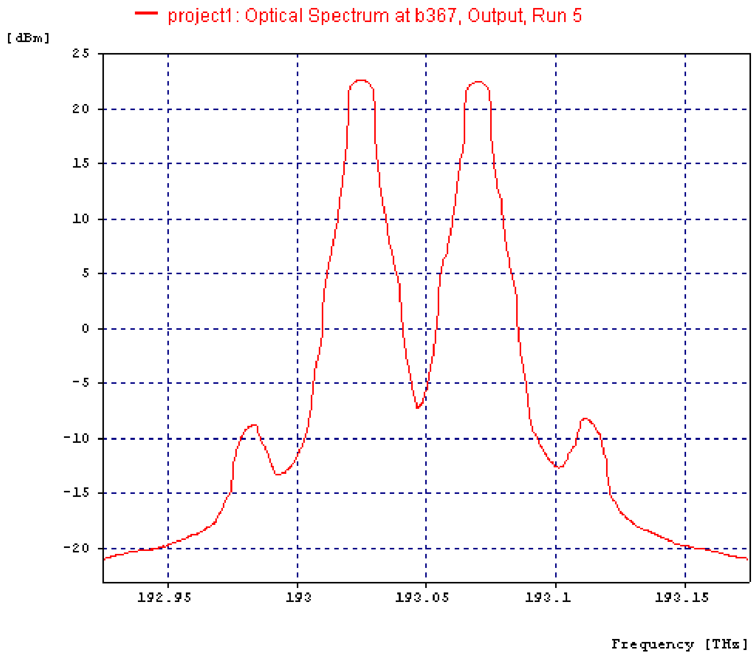

Figure 3.32: Optical spectrum for two channel WDM network with 45 GHz channel spacing

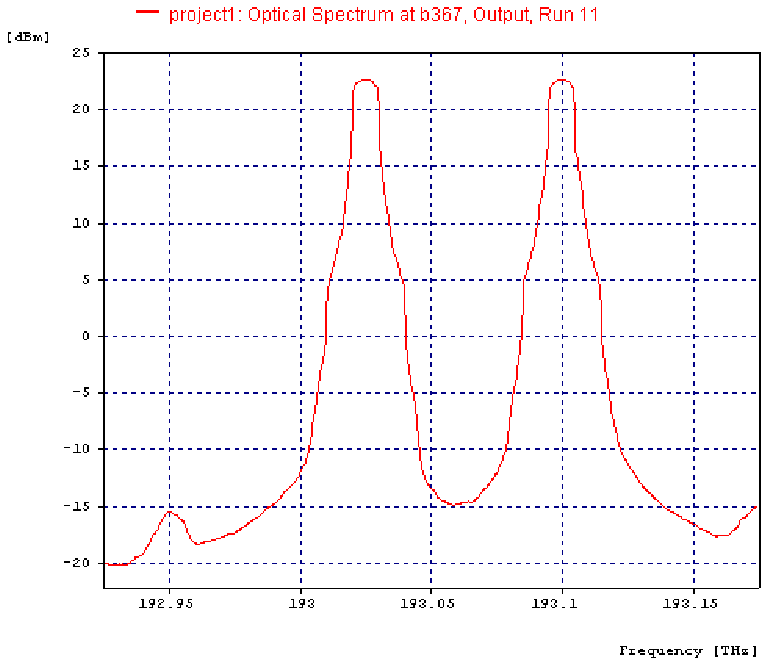

Figure 3.33: Optical spectrum for two channel WDM network with 60 GHz channel spacing

The parameters influencing the FWM effect include channel spacing, power flowing in the channel and dispersion effect prevailing in optical fiber. To study the impact of channel spacing, the system represented in Figure 2.23 is used where the central emission frequencies of laser source are varied by frequency Δf channel spacing (varying between ranges 30 to 70 GHz). The optical spectrum obtained for 30 GHz, 45 GHz, 60 GHz and 75 GHz are presented in Figure 3.31 to Figure 3.34.

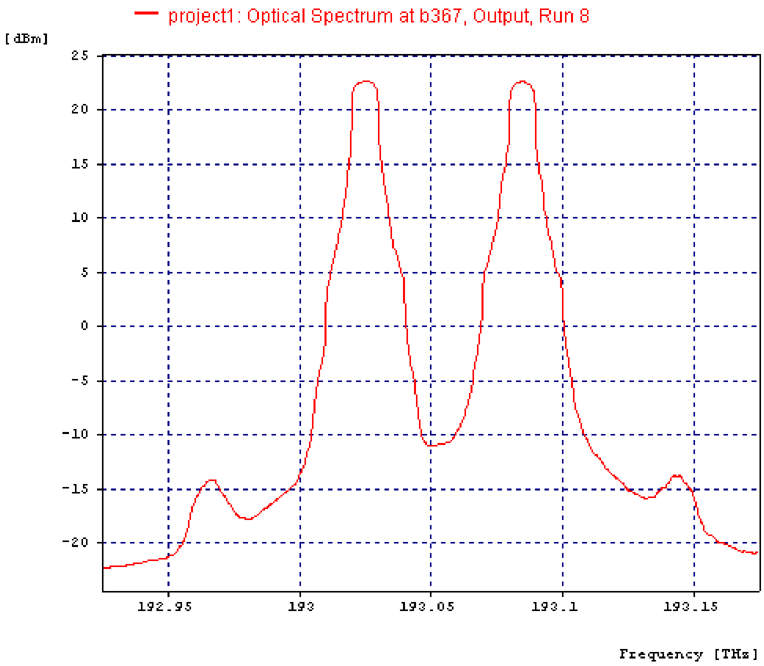

Figure 3.34: Optical spectrum for two channel WDM network with 75 GHz channel spacing

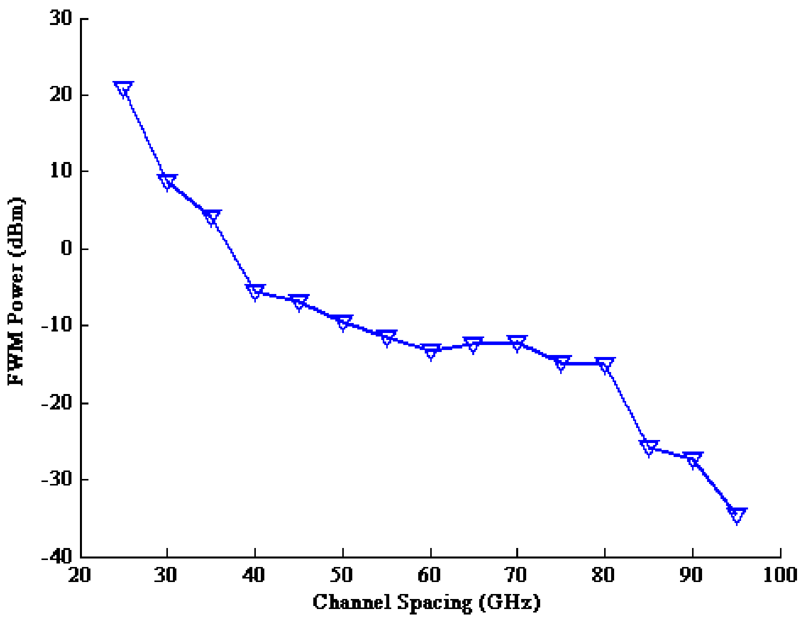

Figure 3.35: Relation between channel spacing and generated FWM power

It has been observed that decreased channel spacing increase the magnitude of FWM. The magnitude of waveforms for 30 GHz spacing is maximum and closer to the frequencies of source. While the channel spacing reach up to 75GHz, the magnitude of FWM is reduced to one-forth its initial value. The overall impact is summarized in Figure 3.35.

Another technique to minimize the impact of FWM is to increase the distance travelled by wave. The impact of decrease in distance with varies valued of dispersion coefficient is shown in Figure 3.36.

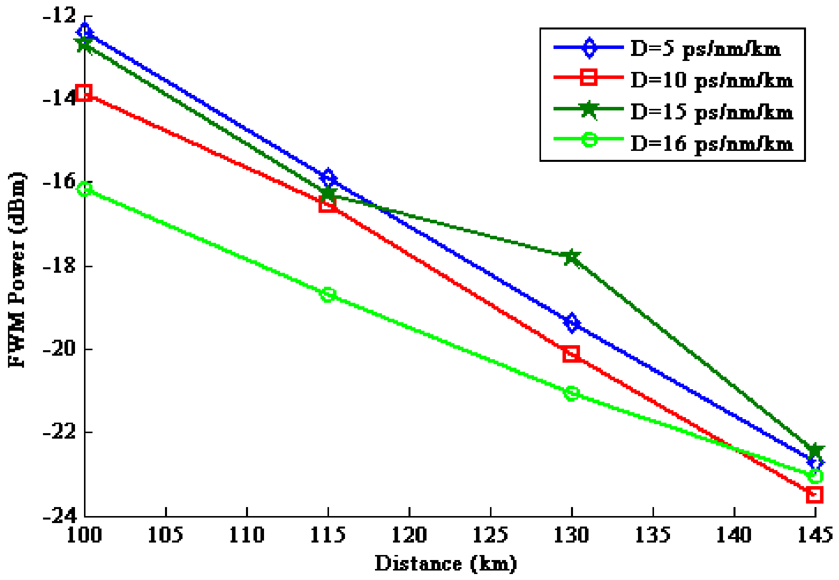

Figure 3.36: Variations in generated FWM power with distance

It can be observed that increased value of D decrease the FWM power being generated. This is because the linear impairments especially dispersion has counteracting impact on non-linear impairments. The impact of dispersion on generation of side waveforms can be clearly seen from spectrum diagrams. The value of dispersion coefficient is varied from -1 ps/nm/km to 10 ps/nm/km. The input power of source is kept constant and the amplifier with constant power gain configuration is used to visualize the impact of dispersion. The optical spectrum for dispersion coefficient value -1 ps/nm/km, 0.4 ps/nm/km, 3 ps/nm/km and 8 ps/nm/km is presented in Figure 3.37 to Figure 3.40 respectively. Here, the green color waveform represents input waveform, while red color waveform represents output waveform. The magnitude of sidebands and pulse broadening so obtained is maximum for fiber with zero dispersion coefficient value. The impact of wave mixing is decreased with increase in value of dispersion.

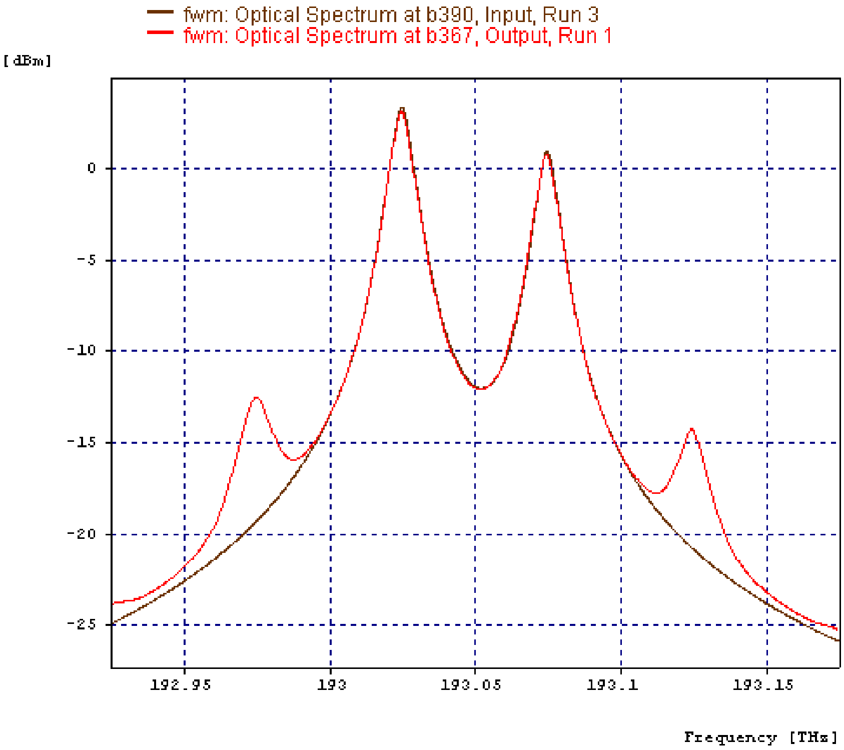

Figure 3.37: Optical spectrum for two channel WDM network with D=-1 ps/nm/km

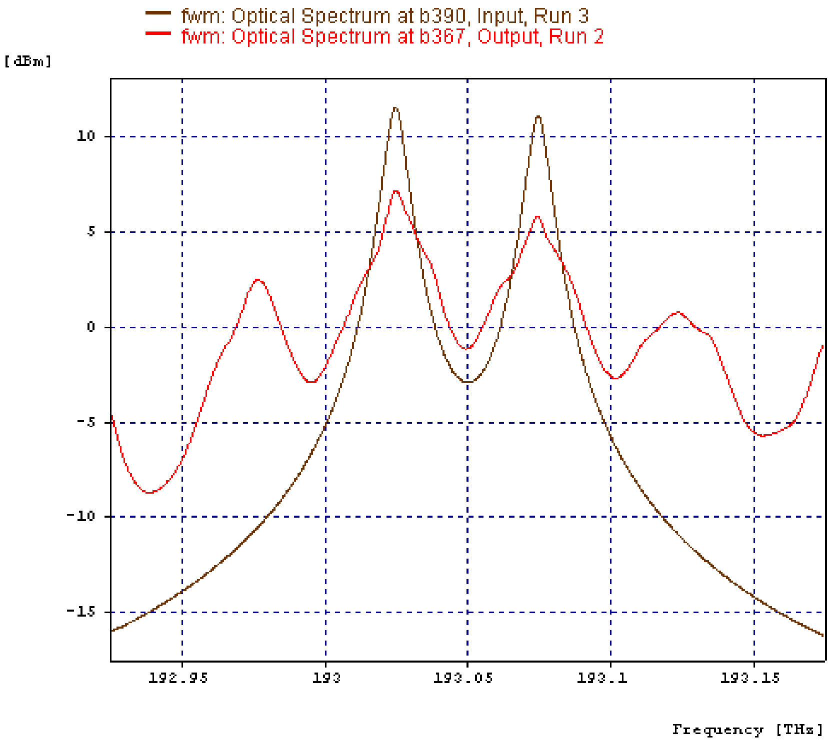

Figure 3.38: Optical spectrum for two channel WDM network with D=0.4 ps/nm/km

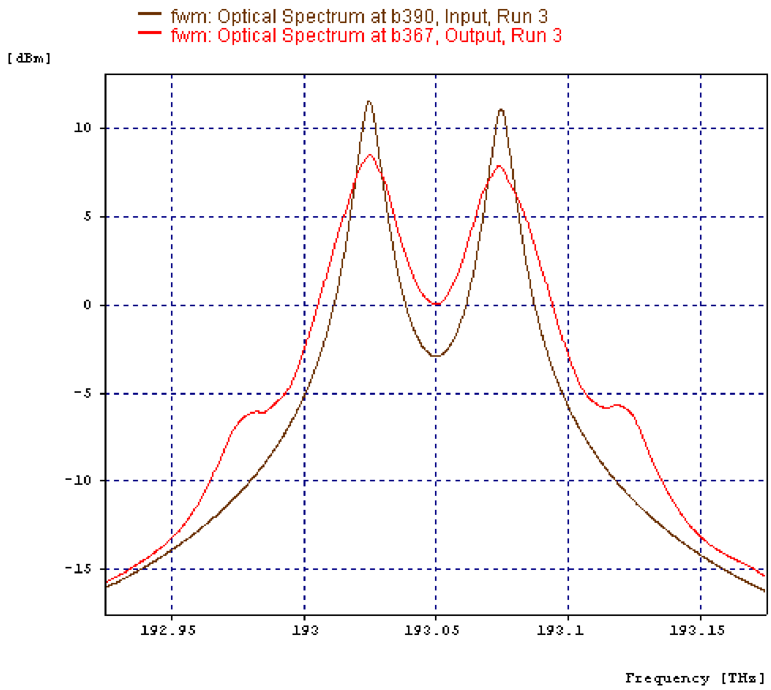

Figure 3.39: Optical spectrum for two channel WDM network with D=3 ps/nm/km

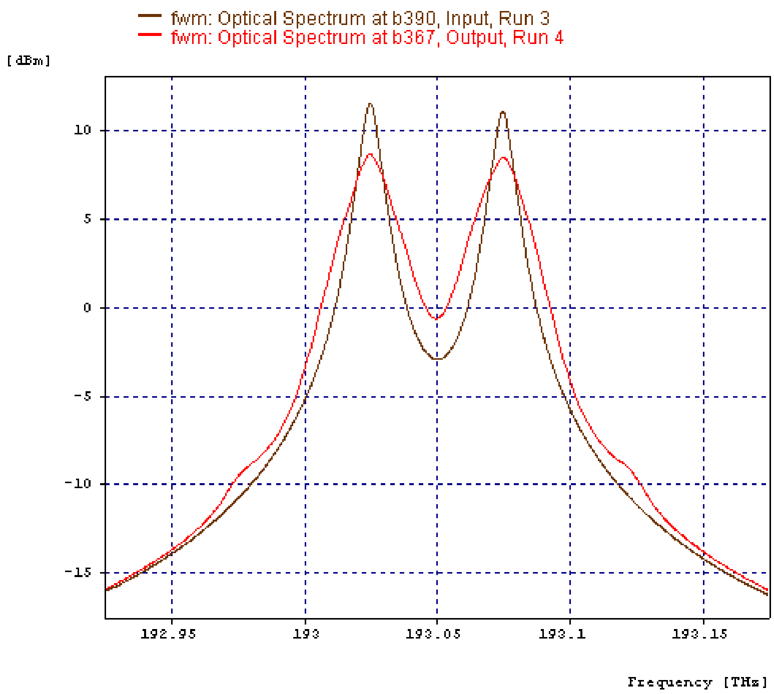

Figure 3.40: Optical spectrum for two channel WDM network with D= 8ps/nm/km

The variation in FWM power with increase in dispersion is summarized in Figure 3.41 for different channel spacing so as to inter relate the three parameters. It can be see that incresed channel spacing has lower FWM power and for same spacing, the value of FWM will be maximum for zero dispersion and will decrease linearly for each increase in value of D.

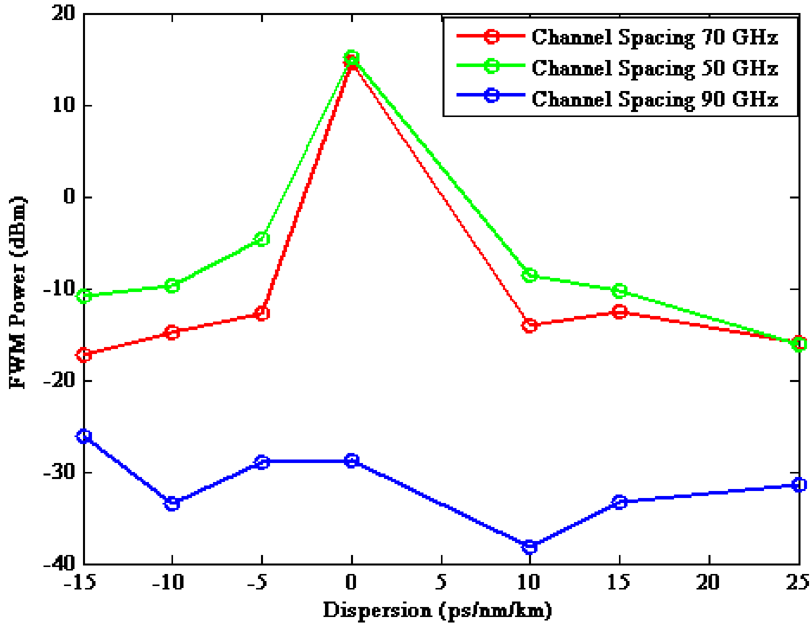

Figure 3.41: Effect of D in FWM power generated for different channel spacing

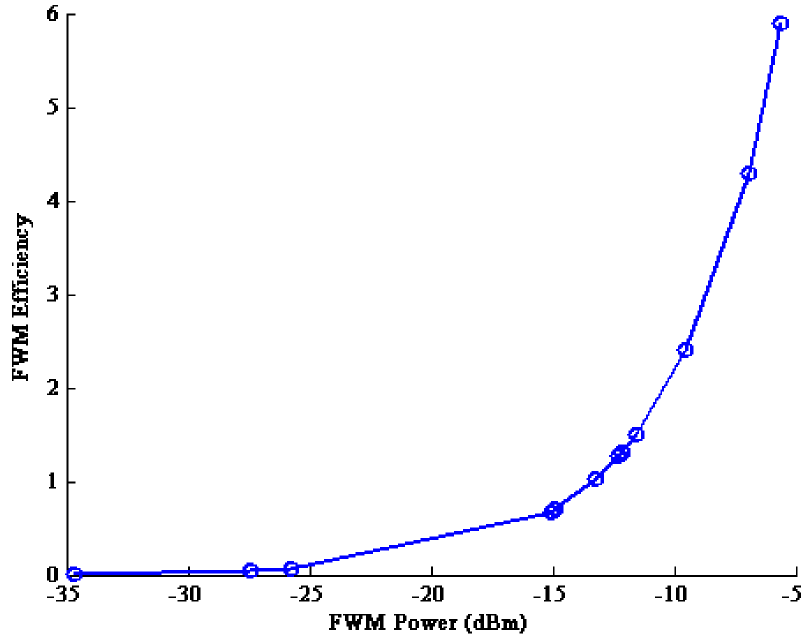

Figure 3.42: Relation between FWM power and efficiency

The relation between FWM power and FWM efficiency is represented in Figure 3.42. With increase in FWM power, the FWM efficiency increases and helps in generating wide range of new frequency waves. The effect of FWM on system behavior can be studied in the form of BER and Q-value analysis. The BER curve for varying FWM power levels is shown in Figure 3.43. The increased power levels will increase FWM efficiency and the probability of new wave generation which will degrade the system response and increase the BER value. The increase in BER will decrease the Q-value following the similar trend and shown in Figure 3.44. The curves obtained are processed to obtain best fit curve and the equation representing the best fit curve is as follows:

Curve fitting BER

$$y = 1.1x^3 - 1.1x^2 + 0.3x - 0.0014 \quad (3.14)$$

Q-value equation

$$y = - 2.1e{+}003x^3 + 1.1e{+}003x^2 - 1.7e{+}002x + 9.7 \quad (3.15)$$

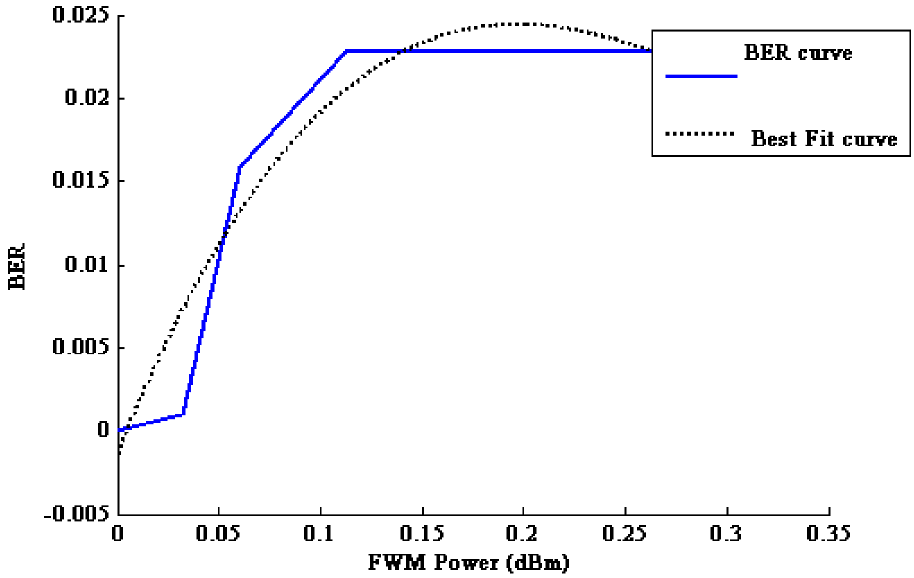

Figure 3.43: BER for FWM power generated

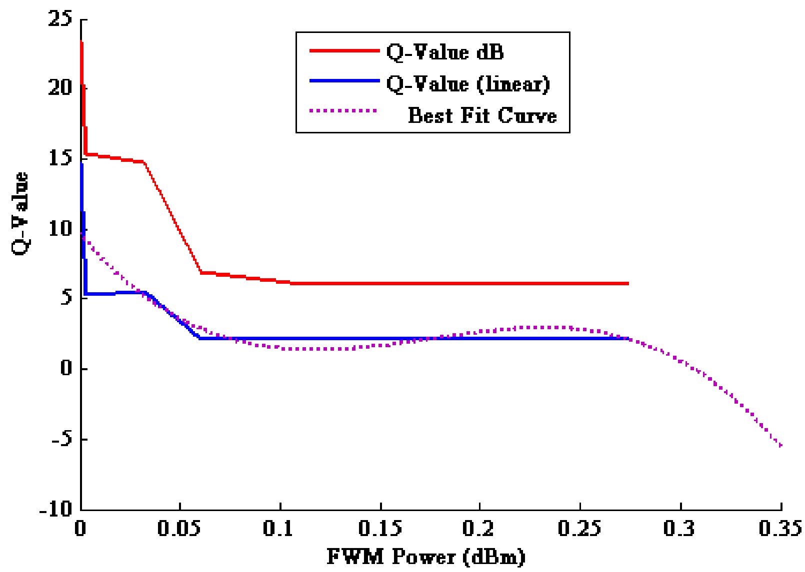

Figure 3.44: Q-value for FWM power generated

Thus, the relation between the system performance and presence of individual physical layer impairments is discussed in this section. The complexity in the system arises due to presence of multiple impairments which makes designing quality estimator a challenging task. In the next section, methodology adopted to generate quality matrix representing quality of link in presence of multiple impairments will be discussed.

3.2 QUALITY OF LINK MATRIX CALCULATION

The precise calculation of estimation of quality of link is an essential requirement for sucessful implementation of RWA in any network. This is due to the fact that quality estimation is the decisiding factor for selecting one path from number of available options and a wrong decision may result in huge data loss. The major challenge in quality estimation is imposed by presence of multiple impairments in the link interacting to increase or decrease the overall impact thereby making it diffcult to accurately monitor the individual impairments and start their compensating devices. Thus, quality estimation technique must be combination of analytical models and interpolation of measurements being taken for robust and efficient operation and should be fast enough for assisting RWA process without intoducing any delay in link set up. The different physical layer impairments that may pose degradation effect are already discussed in the previous sections. In this section, the methodology used to monitor the quality of link and generation of Q-matrix will be discussed. This Q-matrix will be further utilized by presented routing algorithm as one of the constraints for path set-up.

In the present routing algorithm, the prime requirement of quality estimation is to give the status of overall quality of link without going into the details of the cause of degraded quality. Accordingly, the measurement of either BER or Q-value accurately will serve the purpose.

During path setup between a set of source to destination node, a signal may have to transverse through a number of nodes. It is assumed that monitoring scopes are installed at every nodes (including electrical and optical scopes). The statergy used for regenerater placement will be discussed in subequent chapters. The signal is being measured for quality of link being used and Q-matrix is being updated accordingly. The schematic of number of components used by a lightwave while transversing from source to destination node are represented in Figure 3.45.

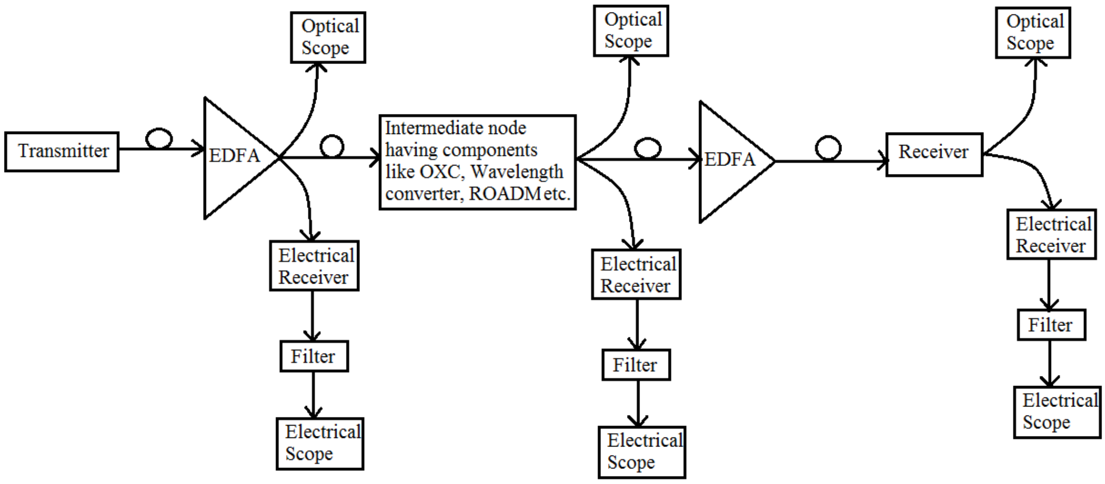

Figure 3.45: Different network components transverse by lightwave during the path setup

The transmitter at each node consists of CW Lorentzian laser, binary sequence generator, electrical generator, MZM modulator. CW Lorentzian laser with specified central emmission frequency/wavelength and power, having output state of polarization aligned with geometric x-axis and Full Width Half Maximium (FWHM) of 10 MHz is used as the source. The data source consistes of a binary squence generator with specified sequence of bits to be transmitted. The data rate of 10 Gbps is used for the present work, although may be varied easily through this component.

The sequence of bits transmitted, modulator used, technical specification of fiber are already discussed in the beginning of this chapter. The scope of both the types electrical and optical are used. The optical scope consists of optical spectrum analyzer implementing the method of modified periodograms for spectrum generation is used. The optical spectrum is used to visulaize the presence of non-linear effects and measure the power flowing in the system. To use the electrical scope, the optical signal being tapped is converted into electrical signal using the set-up sumilar to reciever (consisting of PIN photodiode and filters) and is used to generate the eye diagram and vertical histogram. Eye diagram is used to visualize the current status of the signal and to measure the impact of dispersion, while the vertical histogram plotted on eye diagram is used to calculate the mean and standard deviation values for Q-value calculation. The signal will be tranversing through intermediate nodes before it reaches its destination node. It is assumed that unless specified, no regeneration process is taking place and signal transverses the particular node by using all-optical componenents like OXC, wavelength convertors etc, whichever is required. At the intermediate node, the signal is being tapped for monitoring the staus of the link.

The Q-value of signal being flowing into the circuit can be easily calculated from eye diagram as

$$Q = \frac{\mu_1 - \mu_0}{\sigma_1 + \sigma_0} \tag{3.16}$$

Where μ_i, σ_i are mean and standard deviations at mark i=0 and i=1 level distributions respectively as shown in Figure 3.46.

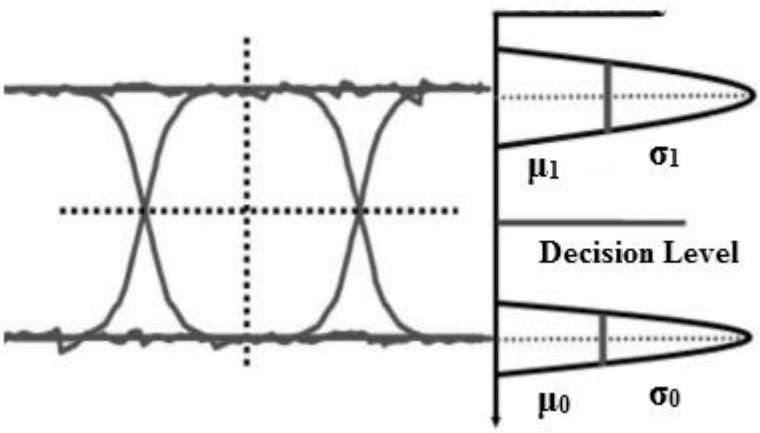

Figure 3.46: Eye diagram and corresponding histogram to calculate standard deviations an mean values

BER and Q-value are related by expression

$$\mathrm{BER} = \frac{1}{2}\mathrm{erfc}\left(\frac{Q}{\sqrt{2}}\right) \tag{3.17}$$

In the present work, the BER is measured directly using OPTSIM and used in Q-matrix of routing algorithm. Q-value is also measured to ensure the signal satifying the threshold conditions as per SLAs. Figure 3.47 and Figure 3.48 shows different Q-values and corresponding BER of a link supporting 16 and 32 wavelengths for different fiber lengths. The Q-value for signal propaging in the fiber link decreases with increased length of fiber due to higher accumulation of impairments in the fiber. The corresponding value of BER is increased. This is the reason making uniform placement of regenerators a neccesasity in obtical fiber links. The quality of link is also influenced by the number of wavelengths travelling in the fiber and the effect is demostrated in Figure 3.49 and Figure 3.50, here the Q-value and corresponding BER is studied for a channel supporting wavelengths ranging from 4 to 64.

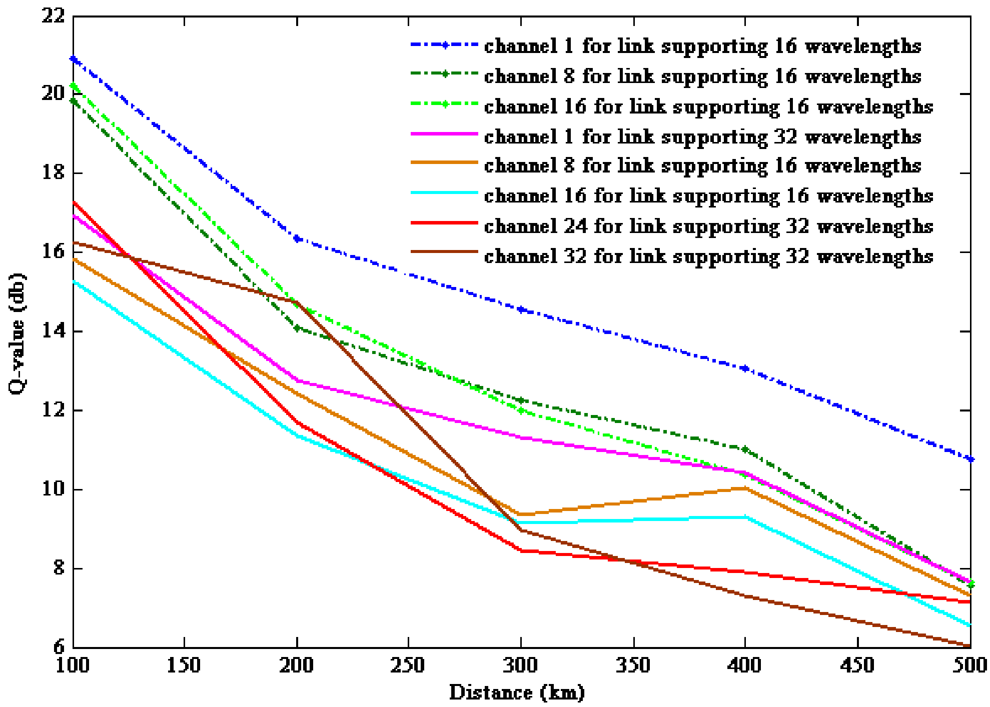

Figure 3.47: Q-value for fiber link supporting 16 and 32 wavelengths with distance

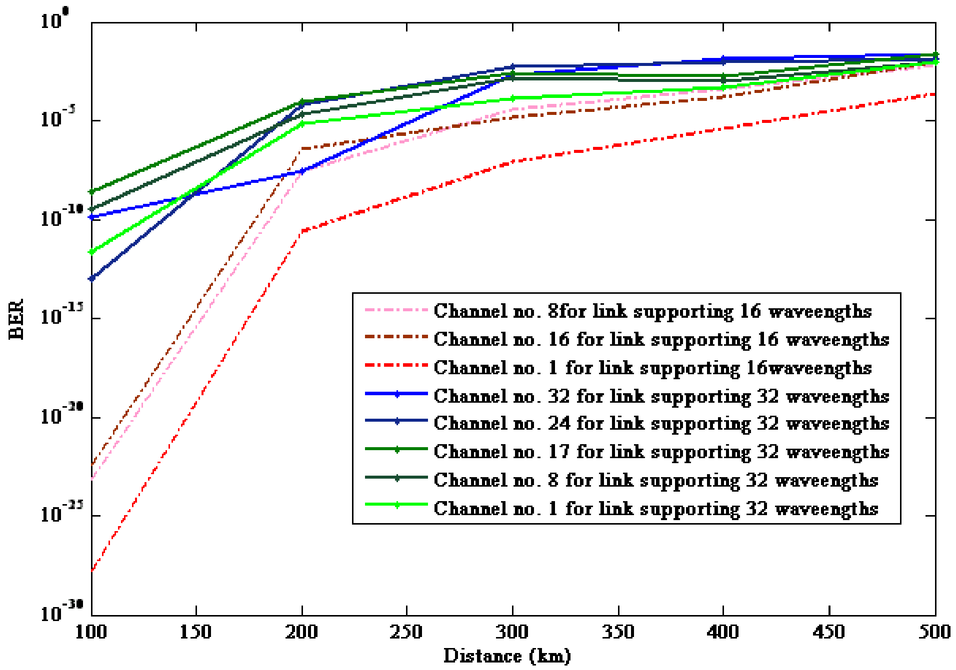

Figure 3.48: BER for fiber link supporting 16 and 32 wavelengths with distance

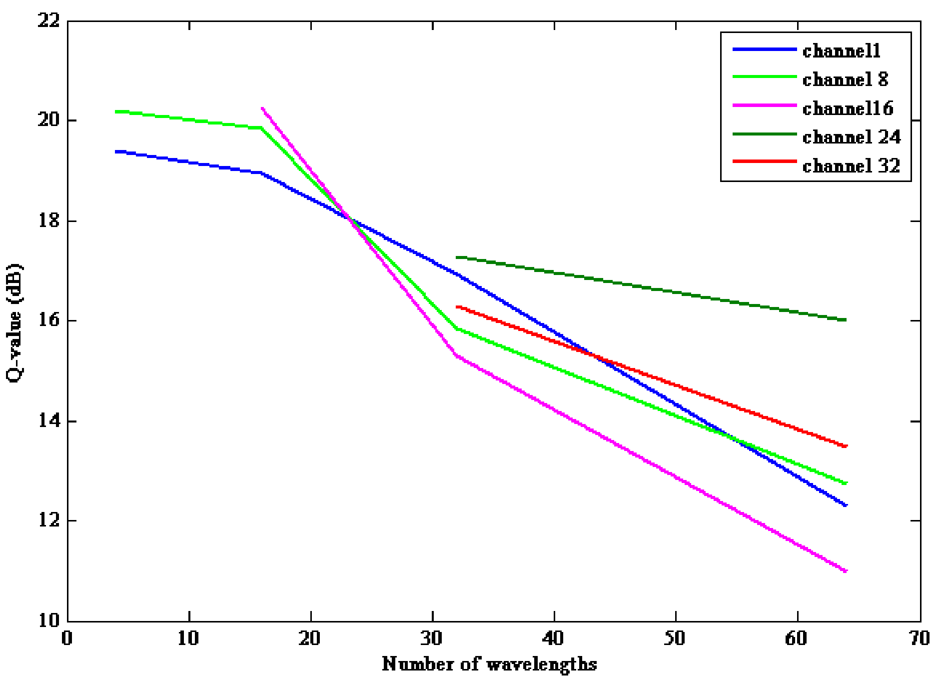

Figure 3.49: Q-value for 100 Km fiber link for various wavelengths travelling in fiber

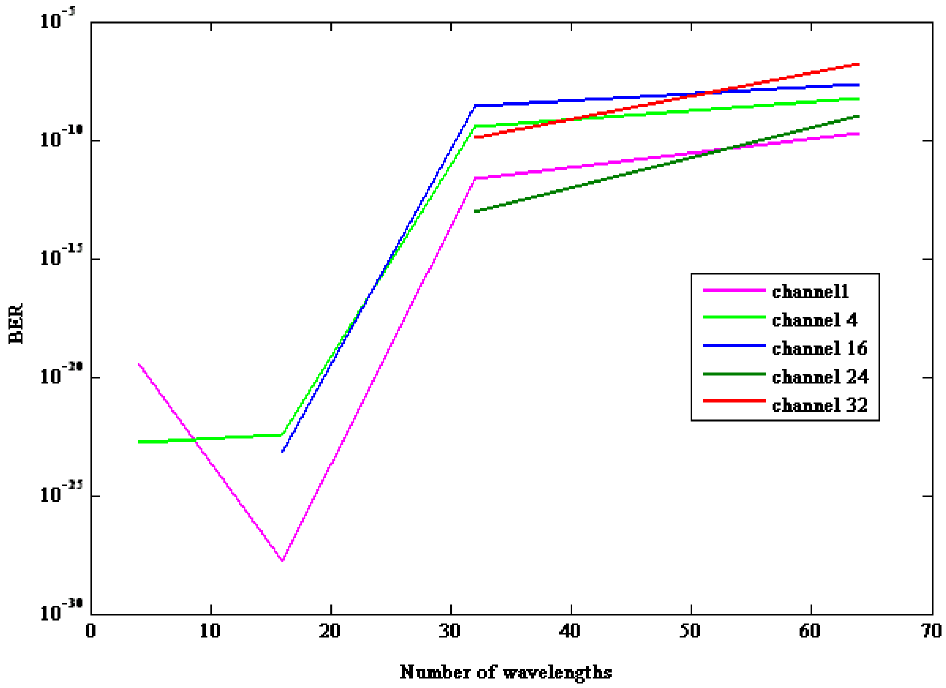

Figure 3.50: BER for 100 Km fiber link for various wavelengths travelling in fiber

In order to calculate the impairments being present, the magnitude of GVD is calculated by measuring delay across the output signal and then implementing equation (2.33) to (2.44). The amount of attenuation may be calculated using equation (2.44), (2.45). Once the wavelength in operation is known, magnitude of non linear effect of SPM is calcutated using equation (2.55), XPM using equation (2.64), FWM using equation (2.67), (2.68). The implementation of these equations for measurement of impairments have already been discused in previous section of this chapter. Although these individual impairments are not used directly in RWA, but may play a cruicial role in initiating the compensation techniques for maintaining the quality of link.

3.3 CHAPTER SUMMARY

In this chapter, need for performance monitoring, the variation in system behavior in the presence of different physical layer impairments and Q-matrix estimation for present routing algorithm is studied. The different monitoring techniques existing to date include digital and analog (further classified as time domain, frequency domain, polarization domain). As the prime focus of present research is on transparent monitoring for dynamically reconfigurable networks, the digital monitoring through BER is selected for updating the Q-matrix. The individual impairments are monitored using eye diagram analysis (time domain monitoring) and optical spectrum analysis (frequency domain monitoring). Both time and frequency domain monitoring need to be implemented as some of the linear impairments are not reflected in frequency domain graph (e.g. dispersion) while the others are more dominating in frequency domain only. Using the combination of both will result in monitoring of all linear and non-linear impairments. The system used for monitoring the different impairments, methodology to calculate BER, Q-value is presented. The system behavior for varying parameters especially wavelength is studied followed by impact of individual impairment on BER and Q-value. The curve fitting is done so as to obtain the equation representing the BER and Q-value curves. The equations so obtained may be utilized for estimating the system behavior in case the direct estimation cannot be achieved. The subsequent section discusses the monitoring technique for Q-estimation used in present routing algorithm. The nodes and the network components used by light wave whenever a link between specified source to destination node is achieved is discussed. The quality estimation is a significant building block of path set-up process presented in this research, so the efficient calculations must be done, with regularly updating the link quality in the specified matrix so as to achieve the optimum results.

Chapter 4

Impairment aware routing

This chapter discusses the routing algorithm designed, its implementation on various standard networks and comparison with the different algorithms already existing in literature

CHAPTER 4: IMPAIRMENT AWARE ROUTING

Routing in WDM networks involves lightpath setup between specified source and destination nodes through wavelength channels and is referred as Routing and Wavelength Assignment (RWA). Most of the heuristics proposed so far for addressing RWA issues assume physical layer to be ideal one. As stated in previous chapters, the lack of O-E conversion in today's networks make the signals prone to degradation factors of physical layer. These factors degrade the signal quality making the decisions of RWA unacceptable for practical implementation in accordance with SLAs, although they seem to be viable solution by the heuristics. The research community is working on finding the optimal solutions to RWA considering the role of physical layer on transmission either by considering impairments as one of the constraints to route calculations, known as Impairment Constraint Based Routing (ICBR), or by setting some threshold for quality factor of link and calculating route considering the links satisfying the minimum threshold, known as Physical Layer Impairment Aware Routing (PLIAR). The different ICBR and PLIAR algorithms reported so far by eminent researchers are broadly categorized depending upon:

a. The processing unit of network: It may be centralized or distributed one.
b. The approach used in RWA: There are two different methods according to which a route can be calculated. First one called integrated RWA performs routing and wavelength assignment in one go while second method known as Two Step RWA which treats RWA as subset of two problems namely path calculation and wavelength assignment.
c. Quantifying parameters used to predict the network state. They may be BER, Q-factor, OSNR or combination of any of them. They estimate the quality of link thereby predicting the feasibility of lightpath as per SLA requirements.
d. The physical layer impairments considered for estimating quality of transmission play a major role as non-linear impairments are network state dependent and vary dynamically. Also, counteracting effect of dispersion and non-linear impairments may improve the quality of link and must be taken into account for.

e. Method used to measure PLIs is equally important. The PLIs may either be considered as a priori through analytical models existing in literature or may be monitored regularly using real time monitors.

Some of the dominant research work reported so far in literature is presented before discussing the designed algorithm. The impact of polarized mode dispersion on network design is discussed in [70] using hill-climbing search algorithm. In [71], static RWA for transparent optical networks with focus on OSNR improvement is discussed. In order to include the impact of physical layer, penalty of amplified spontaneous emission noise, and XPM are considered. A series of Monte-Carlo simulations are used to calculate noise variance and implemented in greedy algorithms based on First Fit, Minimum Hop, best-OSNR value and two metaheuristic algorithms namely Simulated Annealing and Tabu Search. Among these, condition of minimum OSNR is satisfied in most of cases by best OSNR and always by Simulated Annealing.

The aggregate power flowing in lightpath is a crucial factor for proper operation of components like amplifiers involved in its set up. It must be maintained unto certain threshold value for optimum gain of amplifier. RWA considering threshold power constraints, maximum power of a link, maximum small signal gain of EDFA is demonstrated in [72]. A Mixed Integer Non-linear program is proposed aiming at maximum lightpath established by maintaining three power constraints. In the two phase solution reported, ILP formed using fixed set of routes without power constraints and Smallest Gain First and Genetic Algorithm are implemented for assigning different power levels to source nodes. It is found that though smallest Gain first algorithm is less time consuming, but Genetic Algorithm performs well for broad range of network parameters.

Impairment Aware Best Path and First Fit algorithms are proposed in [73] considering the impact of PMD and OSNR only. In the proposed algorithms, route is calculated first using shortest path algorithm and then wavelength is assigned using first fit or best fit approach. After performing RWA, PLI for selected route is calculated to verify whether it satisfies the threshold requirements or not. It has been found that on 220 Erlangs load, best path algorithm improves the blocking probability of network by 14.9% while first fit algorithm 34.4%. The data rates of 10, 20 and 40 Gbps were considered implementing distributed Raman Amplifiers and EDFAs.

The effect of ASE noise accumulation, PMD and XPM on OSNR is considered in [74] for RWA algorithms based on First-Fit Minimum Hop, First-Fit Least-Congested and Best OSNR for wavelength assignment. Minimum Hop algorithm considers shortest path calculated while the Least-Congested considers the available paths dynamically arranged in accordance with offered wavelengths. Best OSNR algorithm finds route and wavelength simultaneously. The dynamically configurable transparent optical networks are considered.

Another approach for PLIAR implements PLIs during path computation and then verifies the feasibility of lightpath as represented in [75]. Link cost functions are calculated analytically using the variation of Q-factor along the lightpath and are implemented in route calculations through k-shortest path algorithm. The minimum cost lightpath is selected if Q-value is above the stated threshold value. The further extension to this RWA is demonstrated by considering the effect of CD, PMD, ASE, crosstalk in [76] for design of metropolitan networks. Noise figure, span length, bit rate are considered to evaluate blocking probability of the network. PLI aware architecture implementing GMPLS protocol is discussed in [77]. Centralized and distributed ICBR is proposed for dynamic establishment of lightpath in transparent optical networks.

Offline monitoring of PLI (both Linear and non-linear) for 10 Gbps NRZ-OOK modulated WDM network using centralized approach is presented in [78]. The effect of impairments like ASE, PMD, XPM, FWM and SRS on Q-factor is studied through analytical methods already reported in literature. Variations in Q-factor are used to calculate the link metric and are used for authentication of path feasibility using Standard Shortest Available Transparent Path Algorithm. The blocking probability of network is studied for different inputs to the algorithm. The prime variations include Algorithm with no PLI constraints, shortest transparent path with physical layer constraints (SATP-IA), wavelength dependency constraints (SAPT-WD) considering all available wavelengths to have maximum Q-value and minimum Q-value satisfying threshold value.

The effect of ASE and dispersion is considered in [79] and [80] implementing distributed network approach. In [79] the degradation parameters are discussed for Automatically Switched Optical Networks (ASON). The link metrics is computed through Q-factor variations w.r.t. eye closure penalty of paths. OSPF protocol is then modified to calculate maximum Q-factor paths and paths requiring regeneration to meet the optimum values. In [80] ICBR algorithm is proposed, addressing two issues namely the amount of information sharing required between the network elements and RWA complexity. The optimum behavior of system is achieved with mean provisioning errors existing between 0-6.5% with crest values below 12.5% even in highly degraded scenario.

Similar works have been reported in [81] [82] [83] [84] [85] [86] [87] considering centralized optical network configuration, except [84] which demonstrate both centralized and distributed networks for PLIAR. [81] consider impact of ASE, crosstalk, FWM and XPM to calculate Q-factor of link path which is further used as link factor for path computation. RWA proposed is basically a three step process, where information regarding network state and Q-factor calculation is done in preprocessing stage and route is calculated using joint optimization technique for shortest path. For the calculated routes, feasibility constraint is checked. [82] consider FWM, XPM and OSNR for analytical modeling of physical layer in form of Q-factor. Path and wavelength selection is done with focus on least congestion and best performance of optical layer respectively. The system performance is further enhanced in [83] by including path length, channel noise and path congestion as cost metrics for routing algorithm.

The effect of BER along with Q-factor considering its mathematical dependence on OSNR is used as link cost function in [84]. The effect of ASE, PMD, CD and SPM is considered. GMPLS based routing protocol OSPF-TE and signaling protocol RSVP-TE is used for path calculation and inclusion of effect of physical layer impairments. Path Computation Element (PCE) based approach is used for centralized optical network. Impact of ASE, crosstalk and OSNR penalty caused by non-linear degradation factors is used to calculate Q-factor and BER in [86] [87]. GMPLS standards are assumed for information sharing and routing purposes. Former present two adaptive routing based algorithms while the later one present four heuristics for BER and blocking probability calculation.

Another approach to reduce the quality constraints in networks as proposed by [85] is implementation of adjustable power management sources instead of fixed source management. It has been found that the expected quality of service can be successfully achieved with using much lower average power source. It has been found that decreased power flowing in the lightpath results in decreased effect of non-linearity thereby optimizing the system performance. The same BER may successfully be achieved by using much lower power sources. As a result, deteriorating effect of fiber non-linearities is considerably reduced, leading to much enhanced network performance.

Most of the studies are based on assumption that the PLIs are of static nature therefore may be estimated analytically. But impairments like crosstalk, SPM, XPM, FWM depends upon the network state. Their values may vary by bare minimum variations in properties of signal being transmitted in channel e.g. power, bit rate or by the state of signal flowing in adjacent channels. In dynamically reconfigurable networks, there is a need to monitor them online and broadcast the information into the control plane through centralized or distributed architectures. In the reports demonstrating online monitoring of PLIs, only one or two impairments are considered. For accurate estimation of optical reach in links, it is necessary that not only all the impairments (both linear and non-linear) must be monitored, but the impact of mutual interaction of specific impairment must also be considered during RWA.

The different parameters adversely influencing the signal quality are identified in the previous chapters and their impact on signal quality has been quantified. Although monitoring of these parameters may be done at impairment level known as Optical Impairment Monitor (OIM) or aggregate level known as OPM [88]. In the former technique, each tunable component should communicate its state e.g. power, noise etc to control plane while in later one, monitors are placed at each node and the effect of different degradations is identified. The aggregate monitoring offers advantages like its implementation for individual channel monitoring, fault localization, component alarms and compensation techniques, future physical and control layer extensions over the traditional component monitoring technique. So, in the present work, performance monitoring is done using OPMs at different nodes and link performance indicator is calculated and used in route calculation.

It has been assumed that present network is homogeneous and single granularity network. The maximum number of wavelengths that can be supported by a link is identical and all wavelengths are capable of carrying same bit rate. The routing algorithm must be sensitive to inter domain transitions in the network, granularities present, physical layer constraints and must effectively communicate them through either peer to peer exchange or through global information sharing which can collectively be represented in the form of cost functions. In accordance with IETF standards, with minor extensions, PCE may be implemented supporting GMPLS architecture for route calculation. PCE performs the task of PLI aware route calculation using Traffic Engineering Database (TED) and can be effectively used for intra, inter domain and inter layer applications. [88].Although multiple PCEs can be implemented (distributed network approach), in the present work, centralized PCE is used and on the basis of this element, route calculation is performed. All the information regarding network topology, routes and wavelength occupancy is shared globally through centralized processing.

Wavelength assignment may be done by three strategies: i) the wavelength assigned at source node is maintained throughout the path, ii) wavelengths are assigned at each node being transverse by the signal i.e. may be changed at all intermediate nodes, iii) wavelengths may be changed at some of nodes because limited number of convertors are made available [88]. In the present work, first strategy is adopted so as to reduce the computational complexity. The wavelength assigned by the source is maintained throughout the network unless initially requested.

In this chapter, the above said issues of impairment aware routing are investigated and an effort has been put in to design an algorithm which can be efficiently applied for routing of WDM networks despite of physical layer constraints. The prime focus of the research work is to efficiently implement the algorithm satisfying various service level agreements and path protections despite of certain impairment and wavelength constrains. In the present work, the connection demand arises through traffic matrix, where all the unanswered calls waiting for path set-up are queued as per their class w.r.t. their time of arrival. A connection call consists of four labels-s, d, w, c. Here, s is source node, d-destination node, w number of wavelengths requested between source and destination, c class. The networks with wavelength continuity constraint have w =0 otherwise, its value is 1 and must be specified for the connections requiring more than one wavelengths for higher data rate. The algorithm supports four classes of users namely Premium (c=1), Gold (c=2), Silver (c=3) and Bronze (c=4). The threshold values of acceptable BER, Q-factor for different classes are already specified in Table 1.2. The performance of proposed algorithm is evaluated through blocking probability criteria and is tested and validated for certain set of path set up demands. The major contributions and applications of the algorithm are then summarized.

4.1 ELEMENTRY UNITS OF PROPOSED ALGORITHM

The basic building blocks of the algorithm proposed are:

4.1.1 The Network Model

In order to design the algorithm, a nine node network model as shown in Figure 4.1 is assumed. The network comprises of 9 nodes and 30 links. The path length between each node pair, if connected, is specified in Table 4.1 and link length distribution is shown in Figure 4.2.

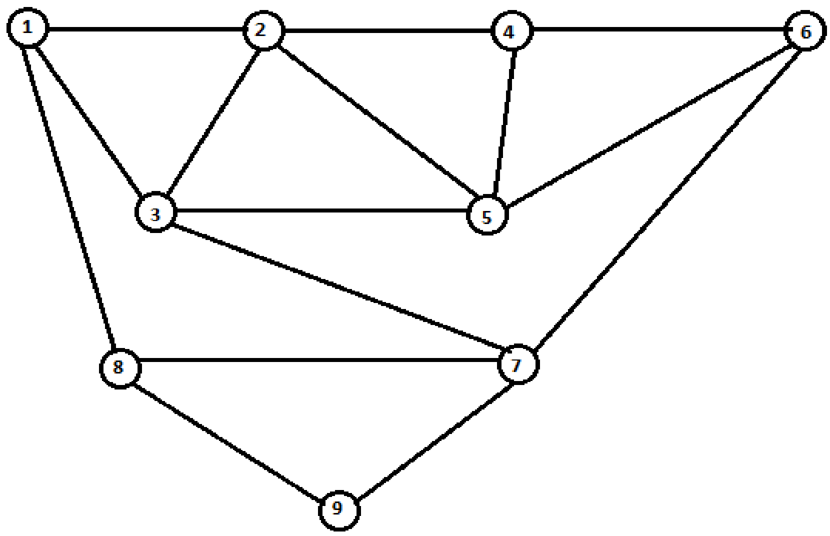

Figure 4.1: Sample 9 node network

Table 4.1: Path length considered for 9 node network

Node No	1	2	3	4	5	6	7	8	9
1	-	80	30	-	-	-	-	70	-
2	80	-	90	50	20	-	-	-	-
3	30	90	-	-	10	-	30	-	-
4	-	50	-	-	90	70	-	-	-
5	-	20	10	90	-	100	-	-	-
6	-	-	-	70	100	-	10	-	-
7	-	-	30	-	-	10	-	10	20
8	70	-	-	-	-	-	10	-	30
9	-	-	-	-	-	-	-	20	30

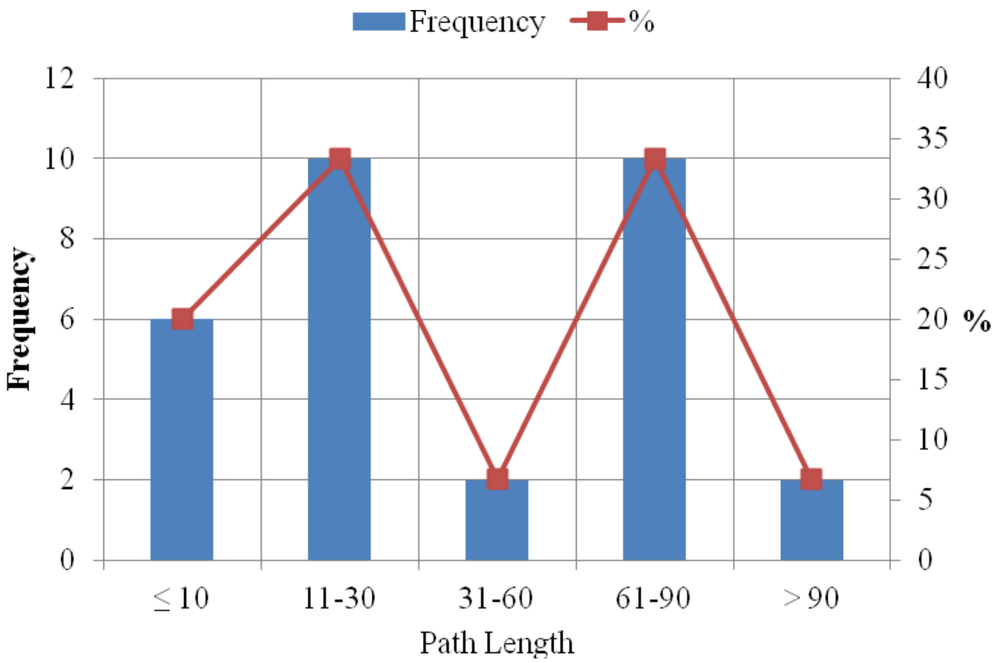

Figure 4.2: Link length distribution of 9 node network

In this network each node is made capable enough to accept or transmit the signal to/from any of the adjacent nodes, add a signal to fiber link by acting as a source node and drop a signal from link, whenever it has to act as a destination node.

Also, each link is capable enough to support all wavelengths of C and L-band. To facilitate the same, wavelength convertor switches are present at each node.

To abstract the signal flowing in the link for further processing, the spectrum analyzers, optical and electrical scopes are placed at each node. The provisioning of network is such that any signal may undergo OEO conversions or may pass through a node in all-optical domain as per the requirement of connection set-up. The optimization of implementation of regenerators and OEO conversions will be discussed in detail in chapter 5. The detailed description of optical components used including optical sources, modulators, modulation formats, bit rates, receivers, filters etc is already discussed in chapter 3. The composition of every node is represented shown in Figure 4.3.

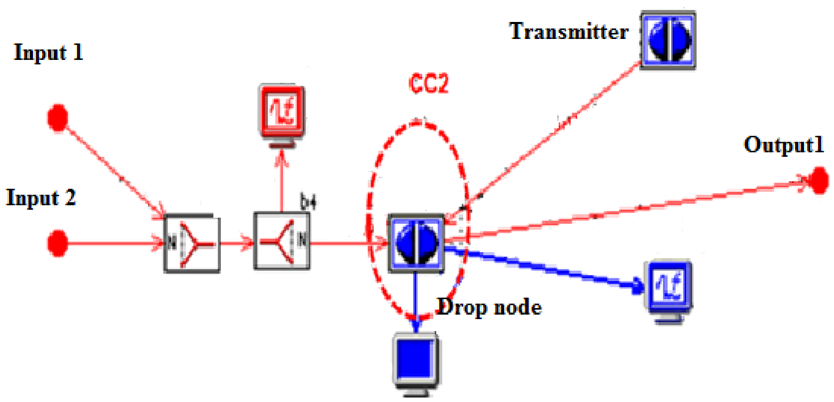

Figure 4.3: Composition of each node

The input to any node may be classified under two heads namely, new signal being generated through a transmitter when the node act as source node for a new connection request or signal being passed through from any adjacent node when it is acting as intermediate or destination node. The new signal is added using compound component trans1 and output is dropped to receiver by drop_node2. The signal is bypassed to another linked node through connecting point output and received through point input. A number of monitoring devices including spectrum analyzer, electrical scopes are connected to analyze the state of signal flowing in the network.

The composition of compound component CC2 is shown in Figure 4.4, where signal is received through input connection, filtered using bandpass and notch filters and supplied back to network through output connection point. Any signal may be added or dropped using compound components transmitter (Figure 4.5) and receiver (Figure 4.6).

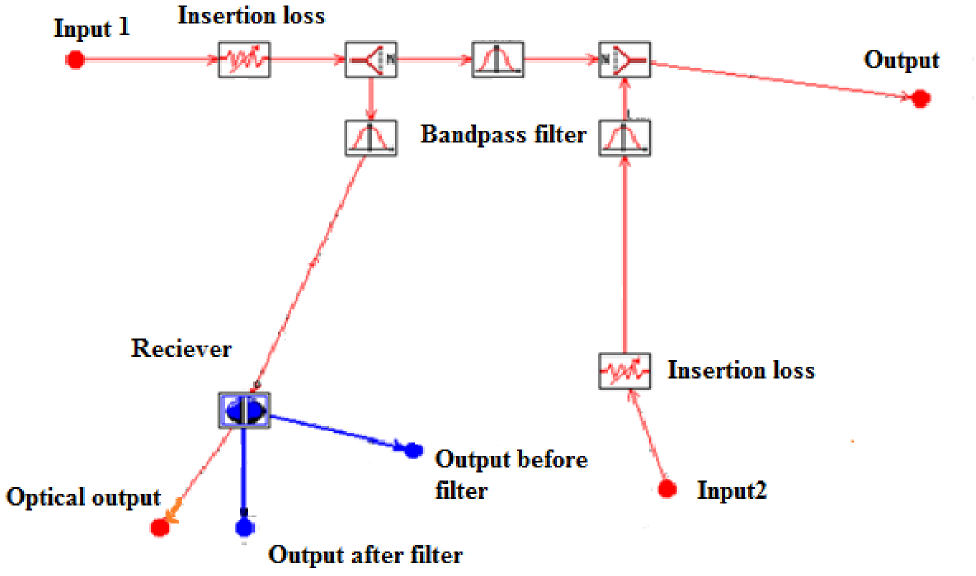

Figure 4.4: Composition of CC2

The transmitter consists of CW Lorentzian laser source, binary sequence generator, electrical signal generator and dual arm MZM. In the whole network, standard single mode fiber implementing recommendation ITU-T G.652 or TIA 492CAAA / OS1 is used. The receiver consists of PIN photodiode, bandpass filters and scopes. The detailed description of these components has already been discussed in chapter 2 and 3.

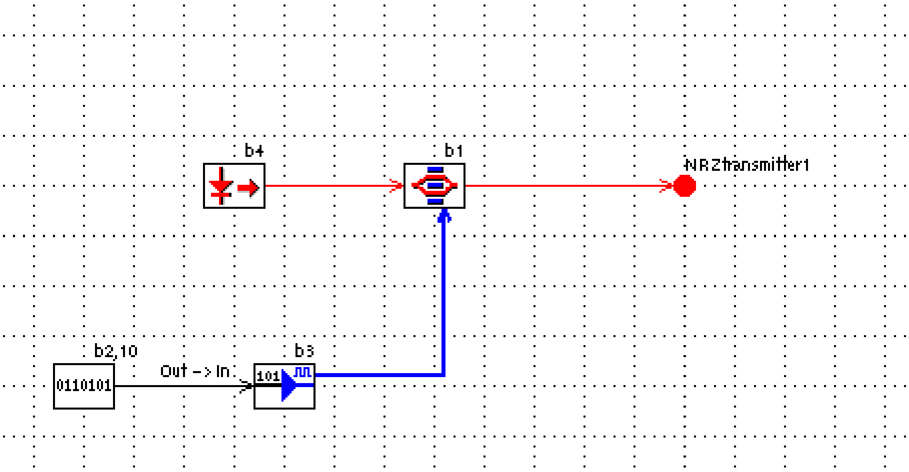

Figure 4.5: Transmitter

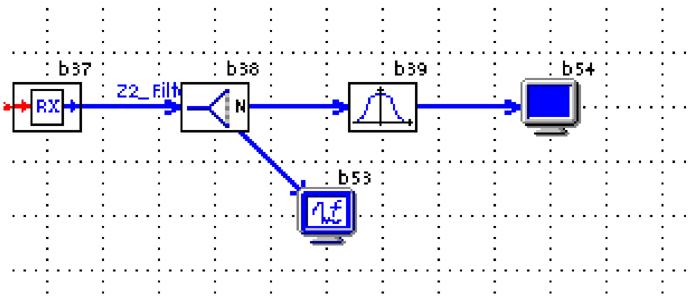

Figure 4.6: Receiver

4.1.2 Pre-Processing Module

The sequence in which the call requests will be entertained by route calculating module is decided by the pre-processing module. Every call request is represented by vector X(s,d,w,c), where s is source node, d is destination node, c is class of path request, w is wavelength constraint of call request. The value of c=1 corresponds to premium class, c=2 is gold, c=3 is silver and c=4 is bronze class. This class is used to decide the optimum threshold values of quality matrix for path set up. Following are the sequence of steps executed by preprocessing unit whenever a call request is received:

a) Firstly, it identifies the class of request. Although the signals are queued as per their time of arrival, but the higher priority class may supersede over the lower priority class. Among the different classes defined, premium class has the highest priority while bronze class has lowest priority. The reason behind allowing superseding over the lower priority class is to consider the SLAs promised to different class. Premium class has minimum wait time for connection set up while bronze class has the maximum time. If the request is not entertained within the specified wait period, it is automatically dropped from the queue. For two or more requests of same class, arrival time will be considered for queuing up the call request.

b) The wavelength requirements of the request are then identified. If no wavelength continuity constraint is there on the network, any of the wavelengths may be assigned to connection request at any node. But in the presence of wavelength continuity constraint, it must be ensured that specific wavelength must be accessible for the connection set up. The pre-processing module ensures the availability of wavelength from wavelength utilization matrix and if not available, call is dropped at this point only.

In case, two connection requests of same class arrives at the same time, the preference is given to request with minimum constraints i.e. call with no wavelength continuity or with no protection required will be given preference.

4.1.3 Optical Performance Monitoring Module

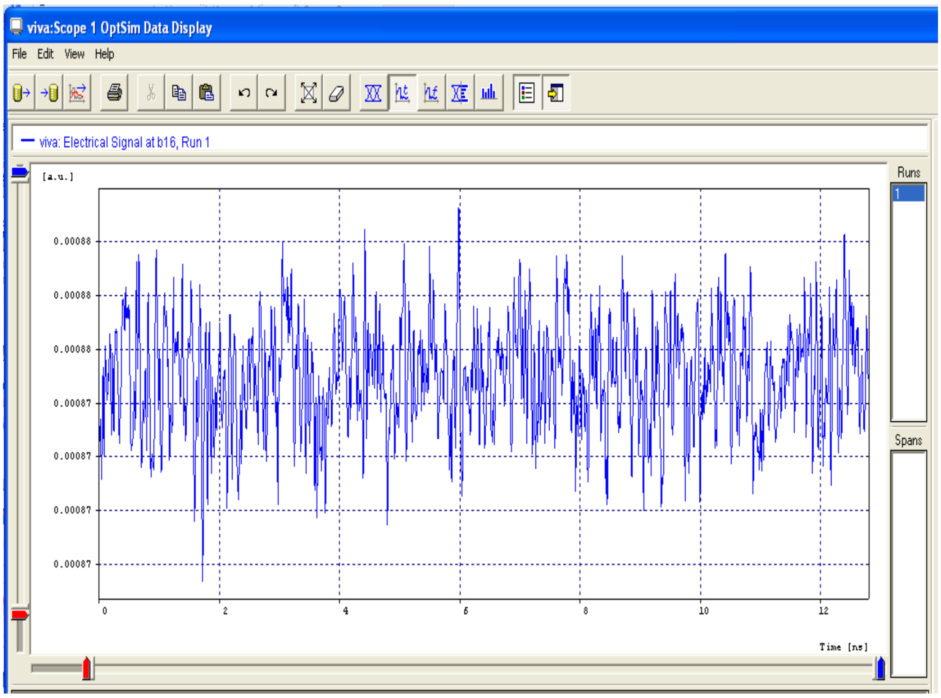

Figure 4.7: The electrical signal retrieved at node 4 being transmitted from node1

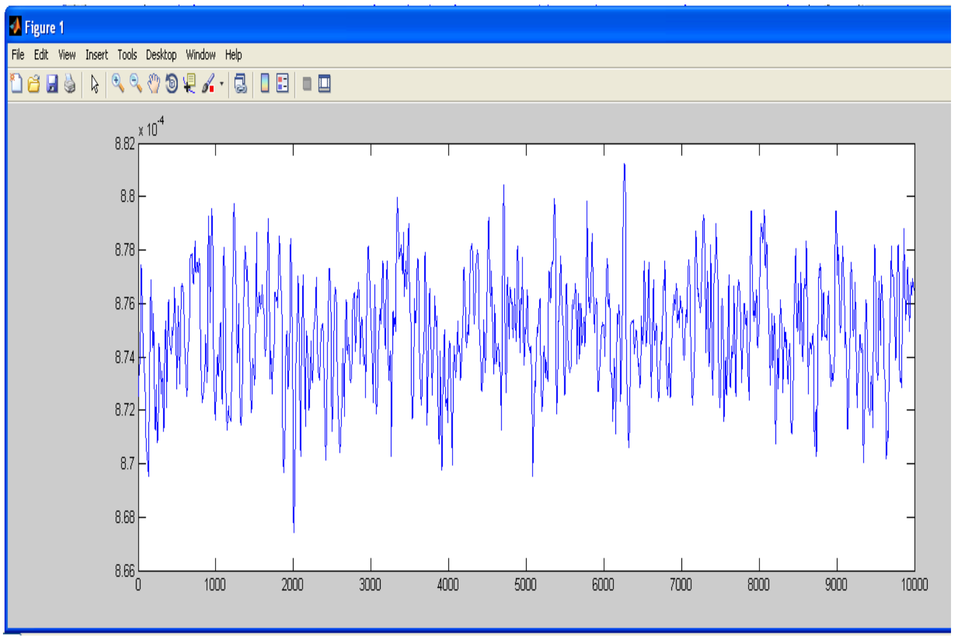

Figure 4.8: The signal exported and reproduced in MATLAB.

To monitor the quality of link, monitoring module is designed and installed at each node. The signal is analyzed for different impairments present, the Q-factor and BER of link and is saved in Q-matrix and is further used by routing algorithm. The performance monitoring module is used to analyze the quality of links and update the status in Quality matrix. The monitoring module is discussed in detail in chapter 3. The module is designed using OPTSIM, while the network path computations are done in MATLAB. In order to demonstrate the efficient transfer of signal at the output to MATLAB for implementation in calculating different performance parameters, a test signal at the output in OPTSIM being exported and then retrieved in MATLAB is shown in Figure 4.7 and Figure 4.8 respectively.

4.1.4 Candidate Selector Module

This is the main processing unit where all the constraints and available resources are considered and an optimum route is selected for the connection request. The information regarding utilized resources like links, wavelengths, nodes etc is updated in their corresponding matrices and used for next call set up. The working of this module is reflected through flowchart (Figure 4.9) and detailed description of methodology for path set up will be discussed in subsequent sections.

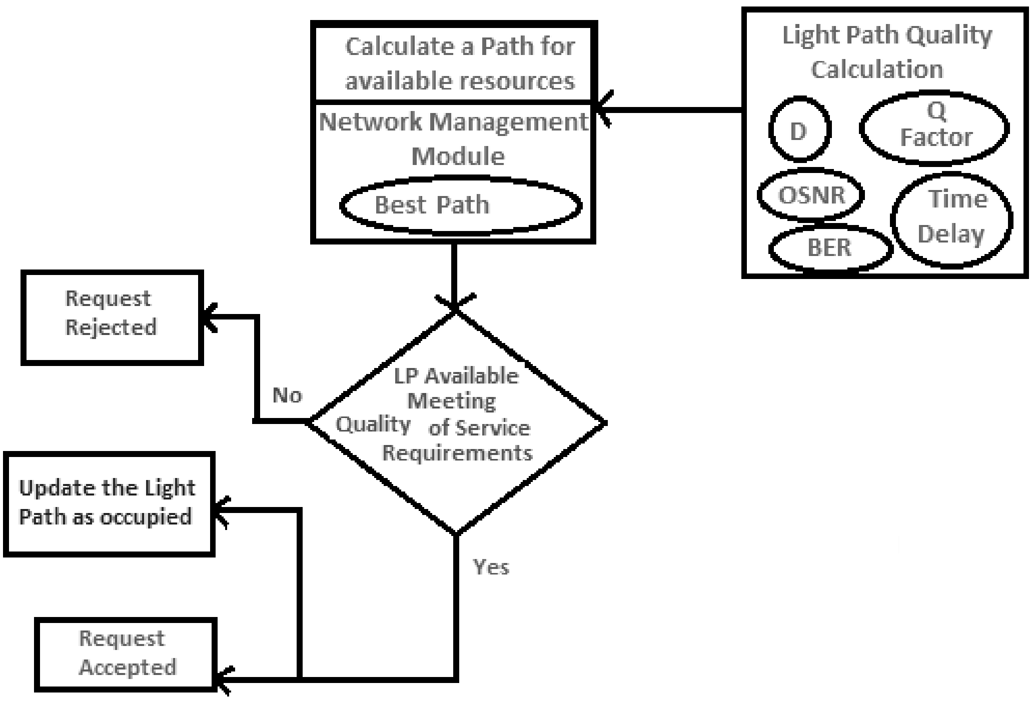

Figure 4.9: Flow chart of route computing algorithm

4.2 PARAMETERS USED FOR ROUTE COMPUTATION

The parameters like variables, notations and matrices used in the subsequent sections and implemented by routing algorithm are summed up in the Table 4.2. Note that capital letters are used to represent the matrix of the parameter while small alphabets are the values for matrix. For example N is the matrix representing the nodes of network while n is when we are referring to some specific node say node 3 i.e. n=3.

Table 4.2: Parameters used in algorithm

S. No.	**Var. Name**	**Variable Dimension**	**Remarks**
1.	n		Number of nodes.
2.	N	1 x n matrix ={1,2,3…n},where n is total no of nodes.	Set representing number of nodes
3.	(i, j,a,b) Є N	Variables	To represent node numbers
4.	L	1 x l matrix={1,2,3,…l}	Set of links available
5.	H	1 x w	Representing different number of

		matrix={1,2,3,…W}	wavelengths supported by network
6.	W	1 x L matrix	Representing the number of wavelengths supported by each link.
7.	$x_{i,j}$		Path length between node i,j. $x_{i,j}$=0 if i=j and $x_{i,j}=\infty$ if nodes are not connected.
8.	P(m,n)	m x n path length matrix	$x_{i,j-}$ Є P
9.	S	source node	To be selected by user
10.	D	destination node	To be selected by user
11.	Q(m,n)	m x n Quality matrix	$x_{i,j-}$ Є Q represents quality of path between node i,j as calculated from Performance monitor.
12.	A(m,n)	m x n Occupied paths matrix	For $x_{i,j-}$ Є A, $x_{i,j}$=0 if path between node i,j is already occupied and $x_{i,j}$=1 if it is not.
13.	c	Variable	Priority of connection request based on class of end user requesting path set up. c=1 if high priority (Premium class),c =2 medium priority (Gold Class), c=3 further low priority (Silver Class); c=4(Bronze class), =5 if no class is satisfied.
14.	B	15 x 30 matrix	Matrix representing different possible paths between node s & d. $b_{i,j}$ represents sequence of nodes a signal will travel to reach from s to d. e.g. s=1, d=5 if $b_{1,j}$=[1 3 2 5] means 1st path calculated to reach node 5 is through node 1 to 3 to 2 to 5.
15.	D	m x 1 edge Vector	Vector representing length of path calculated by B. e.g. $d_{1,1}$=length of path represented by $b_{1,j}$.
16.	E	m x 1 Quality Matrix w.r.t C matrix	Vector representing quality of path calculated by B. e.g. $e_{1,1}$=quality of path represented by $b_{1,j}$
17.	F	m x n matrix	Wavelength channels being occupied. $f_{i,,j}$

			represents the utilization status of j^{th} available wavelength of i^{th} link. =0 if wavelength is not utilized, =1 if it is being utilized for path set up.
18.	G1	1 x 8 matrix	Final path selected as first fit, satisfying the minimum E.
19.	G2	1 x 8 matrix	Final path selected as best fit, satisfying the maximum E.
20.	G3	1 x 8 matrix	Final path selected as shortest path, satisfying the minimum E.

4.3 ALGORITHM

The designed algorithm implements sequential approach for path computation. In order to determine the route for given path request, a virtual network topology is formed. The network is defined by graph G= (N, L), with each link supporting wavelengths from a set of H wavelengths and each link has $w_{1,j}$ Є H wavelengths. The network topology is represented by directed vector graph, where each node is replicated W times to represent the network behavior for different wavelengths of each node. Here, each node replication is represented by n(1), n(2),….,n(w). The link l_{ij} Є L connects node i and j, then nodes $n_i(w)$ and $n_j(w)$ are connected by links $l_{ij}(w)$ and $l_{ji}(w)$ for all w Є H. The layered vector graph is represented in Figure 4.10.

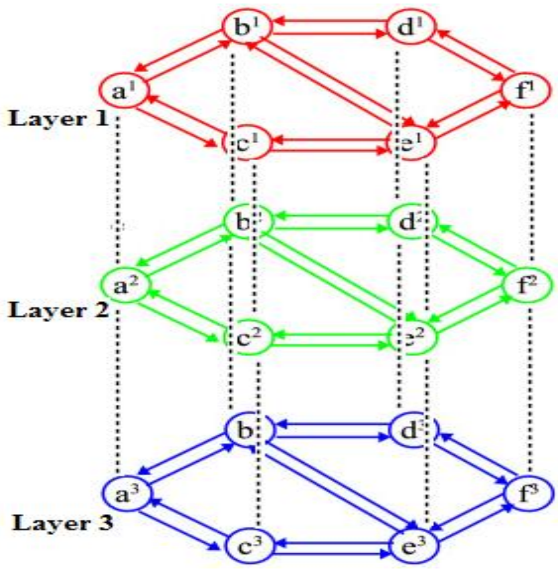

Figure 4.10: Network layered graph

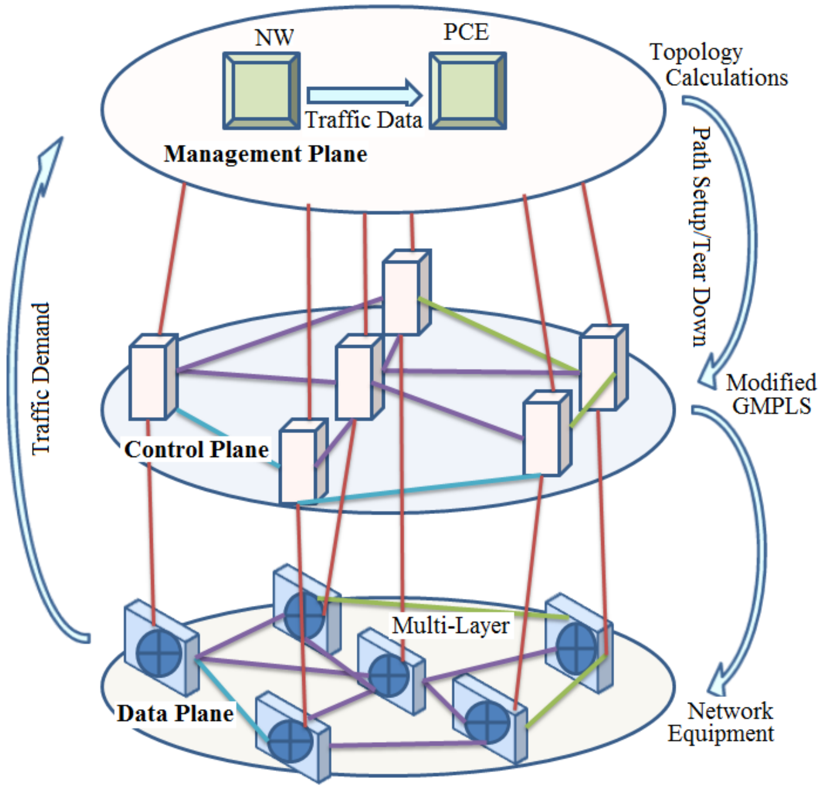

Figure 4.11: GMPLS control plane

The control plane is basically GMPLS plane and the network behavior may be studied as integration of data plane, control plane and management plane as shown in Figure 4.11. The data plane is basically the physical layer where all the components are present and parameters representing the system behavior are extracted and sent to control plane. The control plane in addition to management plane implements RSVP-TE and OSPF-TE as routing and signaling protocols for path computation. The working of algorithm is presented in flow chart shown in Figure 4.12.

For the nine node network as shown in Figure 4.1, the values of different variables used by the algorithm are as follows:

n= Number of nodes of network=9

N= [1 2 3 4 5 6 7 8 9]

l=Number of links available=14.

Path length vector P is

0	80	30	∞	∞	∞	∞	70	∞
80	0	90	50	20	∞	∞	∞	∞
30	90	0	∞	10	∞	30	∞	∞
∞	50	∞	0	90	70	∞	∞	∞
∞	20	10	90	0	100	∞	∞	∞
∞	∞	∞	70	10	0	10	∞	∞
∞	∞	30	∞	∞	10	0	10	20
70	∞	∞	∞	∞	∞	10	0	30
∞	∞	∞	∞	∞	∞	20	30	0

The values of links where no physical links are present is set to infinity. Moreover, node is not provisioned to make a call on itself, so its respective link length is shown as 0.

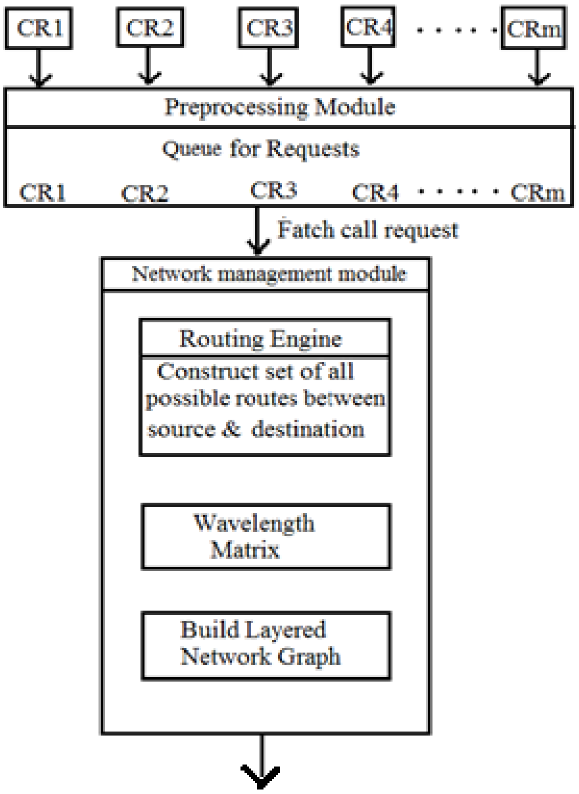

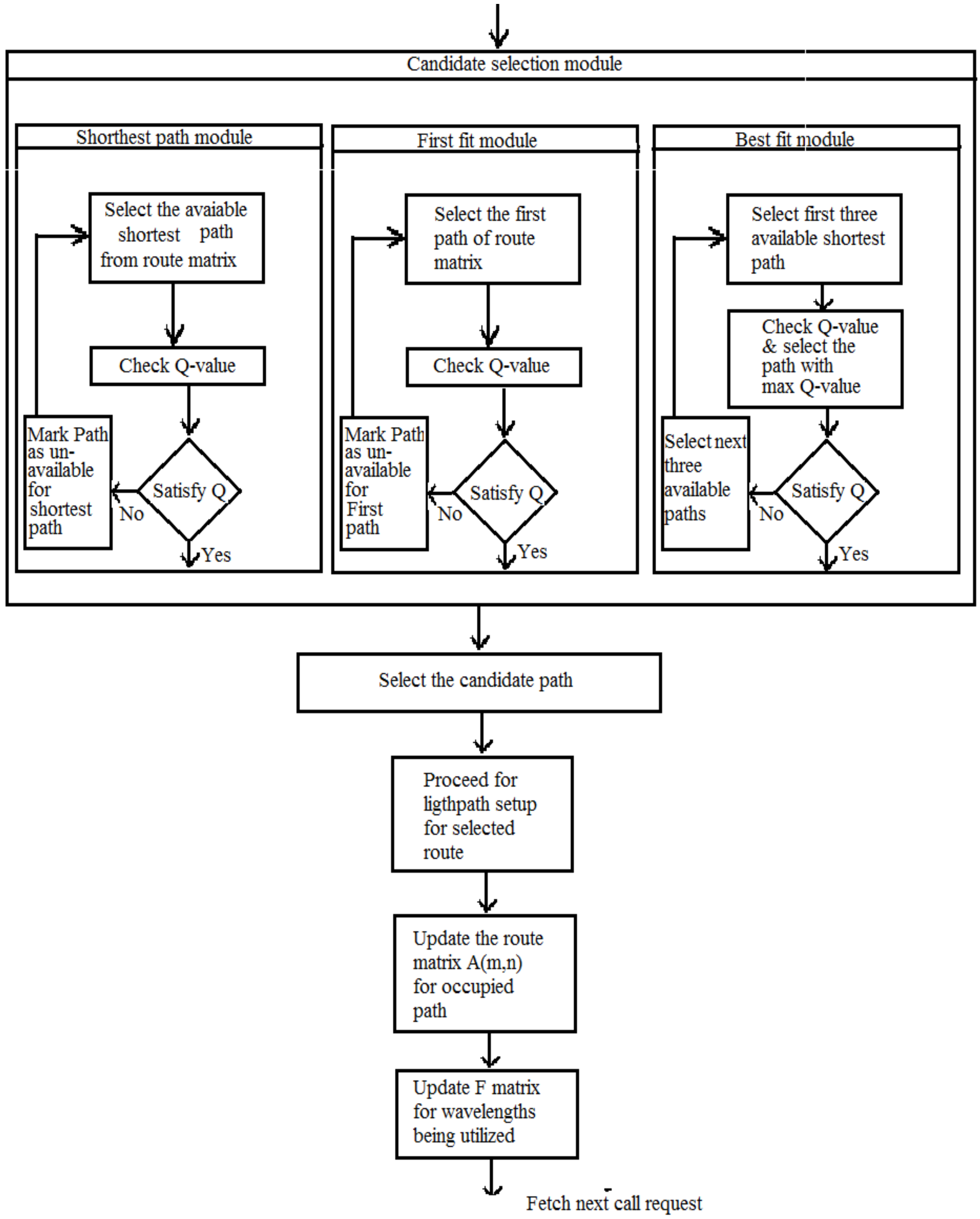

Figure 4.12: Flow chart of algorithm designed

For the path request between node s, d let us say between node 2 to 6, all the possible combinations of existing paths are calculated and saved in matrix B. The value of matrix B is

2	1	3	5	4	6	0	0	0
2	1	3	5	6	0	0	0	0
2	1	3	7	6	0	0	0	0
2	1	8	7	3	5	4	6	0
2	1	8	7	3	5	6	0	0
2	1	8	7	6	0	0	0	0
2	1	8	9	7	3	5	4	6
2	1	8	9	7	3	5	6	0
2	1	8	9	7	6	0	0	0
2	3	1	8	7	6	0	0	0
2	3	1	8	9	7	6	0	0
2	3	5	4	6	0	0	0	0
2	3	5	6	0	0	0	0	0
2	3	7	6	0	0	0	0	0
2	4	5	3	1	8	7	6	0
2	4	5	3	1	8	9	7	6
2	4	5	3	7	6	0	0	0
2	4	5	6	0	0	0	0	0
2	4	6	0	0	0	0	0	0
2	5	3	1	8	7	6	0	0
2	5	3	1	8	9	7	6	0
2	5	3	7	6	0	0	0	0
2	5	4	6	0	0	0	0	0
2	5	6	0	0	0	0	0	0

The values of matrix D are summarized below. The highlighted values show the total path length that need to be covered (in Kms) to establish the connection between node 2 and 6 for already calculated path.

0	80	110	120	210	280	0	0	0
0	80	110	120	220	0	0	0	0
0	80	110	140	150	0	0	0	0
0	80	150	160	190	200	290	360	0
0	80	150	160	190	200	300	0	0
0	80	150	160	170	0	0	0	0

0	80	150	180	200	230	240	330	400
0	80	150	180	200	230	240	340	0
0	80	150	180	200	210	0	0	0
0	90	120	190	200	210	0	0	0
0	90	120	190	220	240	250	0	0
0	90	100	190	260	0	0	0	0
0	90	100	200	0	0	0	0	0
0	90	120	130	0	0	0	0	0
0	50	140	150	180	250	260	270	0
0	50	140	150	180	250	280	300	310
0	50	140	150	180	190	0	0	0
0	50	140	240	0	0	0	0	0
0	50	120	0	0	0	0	0	0
0	20	30	60	130	140	150	0	0
0	20	30	60	130	160	180	190	0
0	20	30	60	70	0	0	0	0
0	20	110	180	0	0	0	0	0
0	20	120	0	0	0	0	0	0

Now, the link selector module will have to select the correct path from this matrix based on different constraints and update the resource utilization matrix A accordingly. Three different variations for path selection are designed namely First Fit (FF), Best Fit (BF) and Shortest Path (SP). The FF will check the paths detected by matrix B in the sequential manner i.e. first path represented by row one 2-1-3-5-4-6 will be checked for all the constraints and if it fulfill all the constraints, will be established for end user. If it does not satisfy all the criteria, next available path 2-1-3-5-6 will be checked for all the constraints. The process will continue till a suitable route is found else the request will be aborted. SP will check the shortest path first 2-5-3-7-6. In case of multiple paths satisfying BF or SP parameters, a path will be selected for further processing based on following criteria in the sequential order:

1. Minimum number of nodes it will be transacting for path set up.
2. High quality for SP algorithm and short path length in case of BF algorithm.
3. Minimum constraints e.g. for wavelength utilization.
4. Path having least traffic load.

For example, in SP criteria, if (2-5-3-7-6) does not meet the other constraints, the algorithm will analyze next available shortest path. Now, two paths (2-5-6) and (2-4-6) are having same path length. The algorithm will check the number of nodes involved, which is again same unfortunately. Both paths have one intermediate node. Now it will check Q matrix and will set up the path having high value. If there is tie again, next the constraints will be checked and process will go on till a suitable path is found.

BF algorithm will take 3- shortest path approach to find the route between the given destination and node pair. In the above example, it will consider 2-5-3-7-6, 2-5-6, 2-4-6 and select the one with maximum quality signal. If none of the paths meet the minimum quality threshold requirements, pair of next three will be selected and optimum lightpath will be searched. In case of tie between two paths criteria of path selection will be same as that of shortest path algorithm.

Once the path to be processed further is selected, it will consider matrix A to check the preoccupied paths, matrix F for availability of wavelengths. Although the wavelength continuity constraint and availability of desired wavelength for transmission is already checked by pre-processing module, then even it is rechecked and the paths not meeting the requirements are deleted. Wavelength assignment is done on the basis of first come and first serve. The candidate path selected is saved in matrix G and lightpath setup process is initiated. The information regarding the utilization of path and wavelengths is updated in vector A and F.

4.4 PERFORMANCE EVALUATION OF ALGORITHM DESIGNED

To evaluate the performance of designed algorithm, a number of simulations were performed. The behavior of the algorithm with different operating conditions, physical layer properties, wavelength constraints, protections required and user specific demands is studied for testing the algorithm. In order to validate the results obtained, the system response is compared with Internet2 and European Optical Network (EON) topology.

The nine node network with average node degree 1.556 is implemented first for testing of algorithm. The distribution of link length is shown in Figure 4.2. Almost

1000 connections are served for each test run where, network load of 50 Erlangs is modeled. The average number of demands between each node pair is represented by $D/_{N(N-1)}$, where N is number of nodes. In the present network, average number of demands per node pair is 6.944. The average call rate for the network is assumed to be 6 per second. The call rate on each node be represented by matrix $\lambda_i = \{ \lambda_1, \lambda_2, \lambda_3 \ldots\ldots, \lambda_9 \}$. In order to calculate the arrival of call requesting a particular node pair as source and destination node, arrival of call at each node pair is calculated using Poisons process. According to Poisons process, probability of non-arrival of call at some node for that particular minute is $e^{-\lambda t}$.

Using Taylor series expansion, this probability = $1 - \lambda t + \frac{\lambda^2}{2} t^2 \ldots \ldots$

The value of t selected is small enough that second and higher order of t results in almost negligible values. The function representing the sum of second and higher order terms is given by g(t) will be such that $\lim_{t \to 0} \frac{g(t)}{t} = 0$

Thus, probability of zero arrival=$1-\lambda t+g(t)$

Probability of one arrival= $e^{-\lambda t}. \lambda t= \lambda t(1 - \lambda t + \frac{\lambda^2}{2} t^2 \ldots \ldots) = \lambda t+g(t)$

Probability of two arrival=g(t)

While selecting a source-destination node pair for path computation, a special care is taken that every node must be selected atleast once as source for better approximation of results. The parameter used as performance indicator is blocking rate which is defined as the ratio of number of blocked lightpath requests over the total number of requested lightpath. Figure 4.13 shows the blocking rate of network with varying number of wavelengths for FF, BF and SP algorithm. It has been found that the blocking probability decreases with increase in number of wavelength channels. In the diagram, dotted line represents the output of FF, BF and SP algorithms without considering effect of PLIs while the solid line represents the response of all the three links consider the quality of path being used. It can be seen that as the effect of PLIs came into picture, the blocking rate increase. This is due to rejection of paths due to non-satisfaction quality being offered to signal transverse through it.

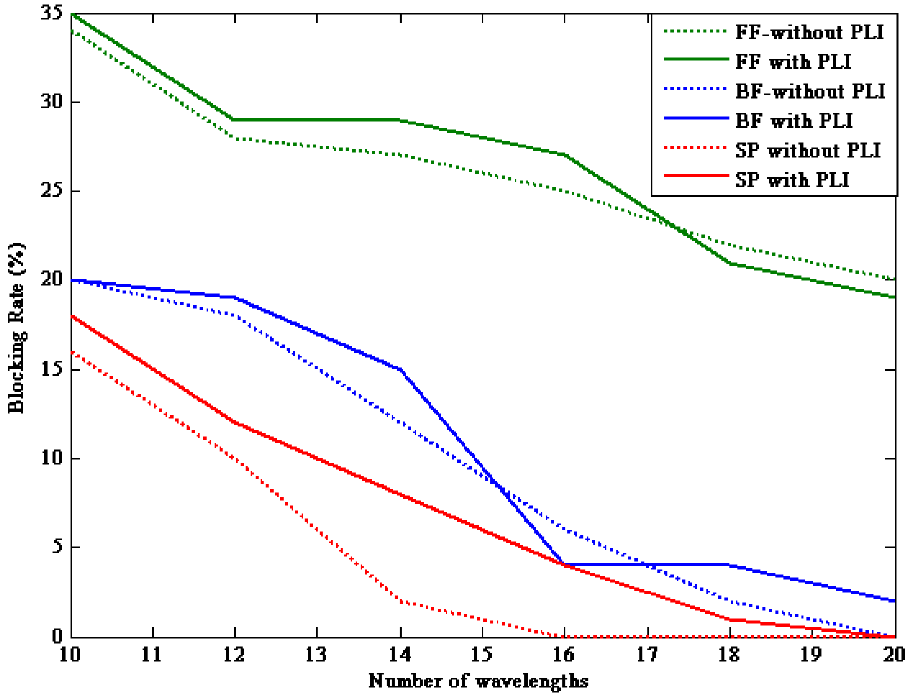

Figure 4.13: Blocking rate curve for nine node network using FF, BF and SP algorithm

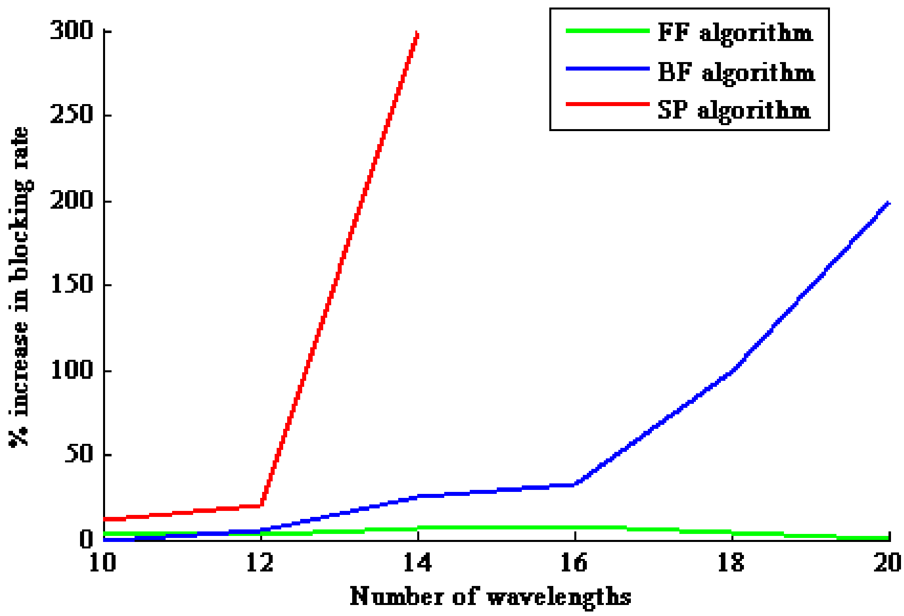

Figure 4.14: Percentage increase in blocking rate by considering impact of PLI in RWA

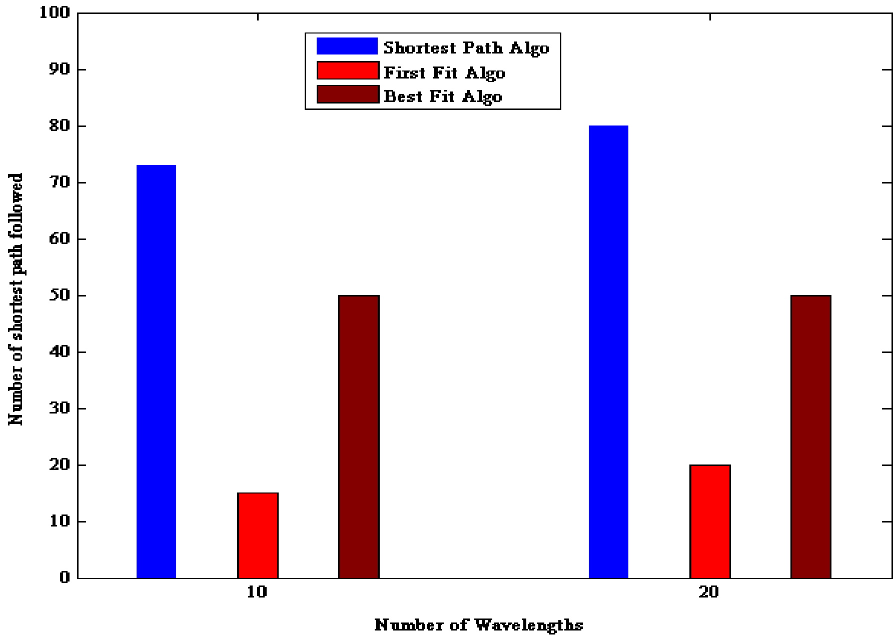

Figure 4.15: Number of shortest paths followed

For the case not considering the quality of link for signal transmission, these calls will be set up at some node, but will not successfully received at destination nodes as most of them will be dropped in between or are degraded at the end and cannot be recovered. It is better to block the call at entrance node only so as to make the other links of the path free for further use. This will not only help in successful completion of call, but also decrease the call drop rate. The percentage increase in blocking rate due to presence of impairments as compared to the case when no PLIs are considered is shown in Figure 4.14.

Among the three algorithms, the performance of SP is better than other algorithms. Reason behind this is FF algorithm finds the route beginning from node 1 till the last. This approach will tend to divert the traffic more towards node 1 and least towards node 9, resulting in network congestion. Moreover, the increased load will tend to increase the data flowing in the optical fiber. This results in inter-channel interferences especially because of non-linear impairments, thereby preventing significant improvement in probability of call acceptance. Thus, the blocking probability does not decrease much. While in case of SP algorithm, the connections are uniformly distributed in the whole network, thereby avoiding the network congestion. Most of the blockings taking place is due to non-satisfactory quality matrix. The number of SP followed is shown in Figure 4.15. The average number of shortest paths calculated by this algorithm further support this statement. For all the number of wavelengths, the percentage of shortest paths followed varies between 70-85 %. The shortest paths followed means least number of physical resources utilized, minimum transmission impairments and least effect on signal already flowing in the network. Ideally, this percentage should be 100% for SP, but is limited by non-availability of wavelengths in network at heavy demand scenario.

Although the performance of BF algorithm is adequate enough for the practical implementation, but performance is little inferior than SP algorithm. This is because best path selects path from the lot of 3 shortest paths which is not optimum utilization of available paths. The number of available paths for selection decrease with increased load on the network, degrading the performance of algorithm.

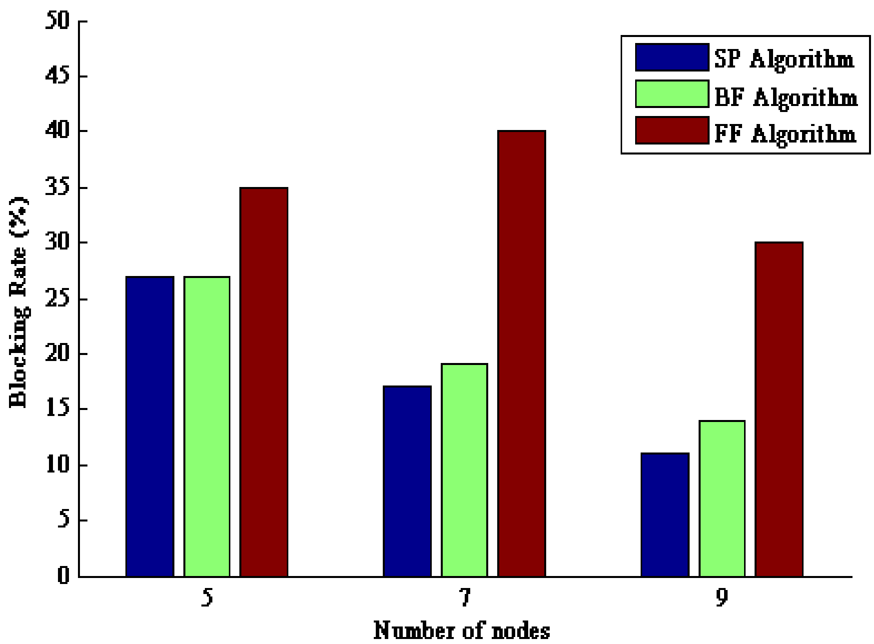

Figure 4.16: Blocking probability of a network with varying number of nodes

In the present work, the numbers of blocking taking place do vary with number of nodes available for routing purpose. In order to study the impact, the numbers of nodes involved are varied from 5 to 9. For these cases, all the other nodes (for 5, other 4 nodes) are assumed to be inactive and no signal can traverse through it. The blocking probability of system obtained is shown in Figure 4.16. It must be noted that the traffic matrix is kept as same while increasing the number of nodes. The blocking probability of the network is decreased as introduction of new nodes resulted in new paths available for same path request.

To validate the designed algorithms, the algorithm is implemented over Internet2 network and EON (European Optical Network) and the response obtained is analysed. The parameters for both the networks are obtained from [89]. The topology for Internet2 and EON network is presented in Figure 4.17 and Figure 4.18 respectively. Internet2 network is a 9 node network with 26 links and average node degree of 2.89. EON network is 18 node network with 66 unidirectional links and average node degree of 3.67. It must be noted that for EON network, only the highlighted portion of the network is considered for validation of results. The link lengths for both the networks are summed up in Table 4.3 and Table 4.4.

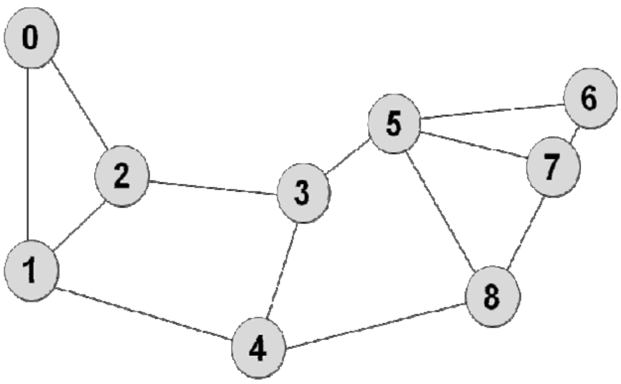

Figure 4.17: Internet 2 Network topology

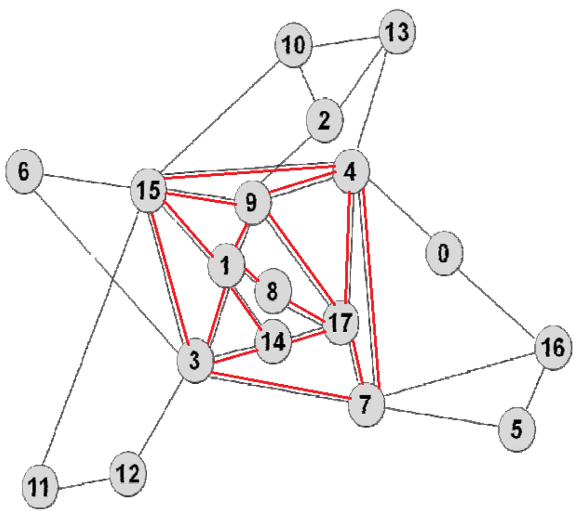

Figure 4.18: EON network topology

Table 4.3: Link length for Internet2

	0	1	2	3	4	5	6	7	8
0		1342	913	-	-	-	-	-	-
1	1342		1303	1330	1705	-	-	-	-
2	913	1303		-	-	-	-	-	-
3	-	1330	-		818	690	-	-	-
4	-	1705	-	818		-	-	-	1385
5	-	-	-	690	-		1400	905	1045
6	-	-	-	-	-	1400		278	-
7	-	-	-	-	-	905	278		700
8	-	-	-	-	1385	1045	-	700	

Table 4.4: Link length for EON

	1	3	4	7	8	9	14	15	17
1		261.2	-	-	115.8	205	488.7	380	-
3	261.2		-	1102	-	-	302.9	484	-
4	-	-		735.1	-	680	-	934.3	379
7	-	1102	735.1		-	-	-	-	1200
8	115.8	-	-	-		-	-	-	371.2
9	205	-	680	-	-		-	401	714.5
14	488.7	302.9	-	-	-	-		-	530.4
15	380	484	934.3	-	-	401	-		-
17	-	-	379	1200	371.2	714.5	530.4	-	

The link length distribution for both the networks is shown in Figure 4.19. The curves obtained for blocking rate with varied number of wavelengths using FF, BF, SP algorithm are presented in Figure 4.20 and Figure 4.22. The results obtained are compared with that obtained by [89] which are reproduced for the reference purpose in Figure 4.21 and Figure 4.23.

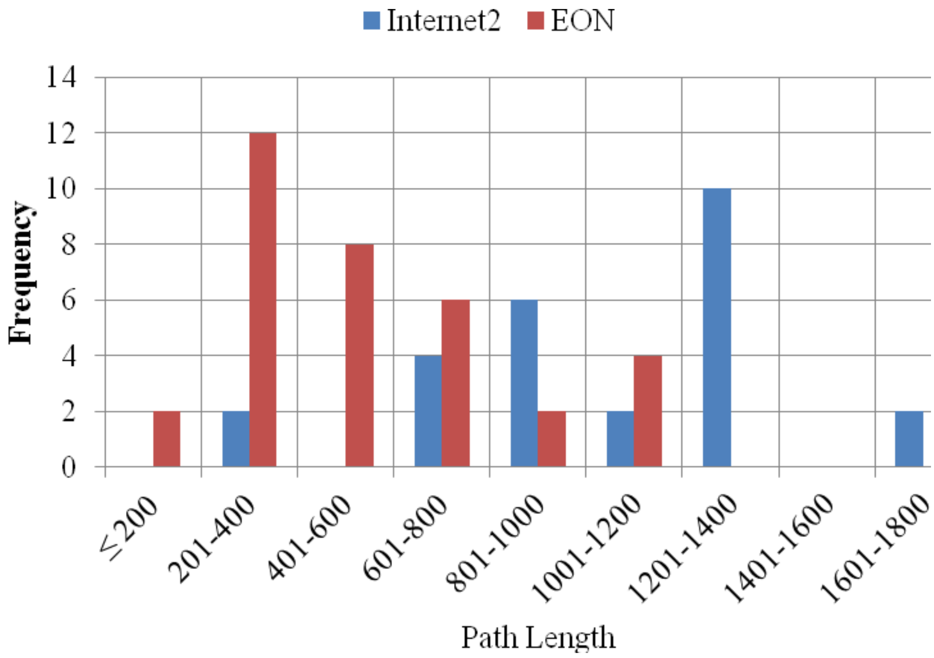

Figure 4.19: Link length distribution for Internet2 and EON

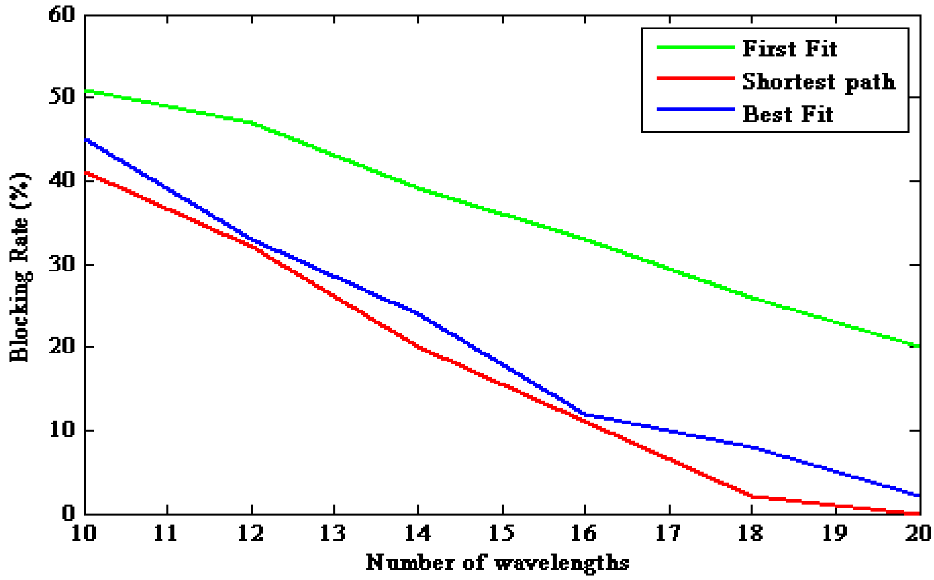

Figure 4.20: Blocking rate of Internet2 network with varying wavelengths using FF, BF, SP algorithms

The author proposed two algorithms for offline impairment aware routing using Q-tool. This Q-tool calculates Q-value and BER of the system and implements the same for RWA purposes. The RWA algorithm heuristically mingles a set of Binary Integer Liner Programming (BILP) that allows a global search of solutions space. In this algorithm phase-I is a preprocessing space which calculates a set of PLIA valid pairs and degradation matrix.

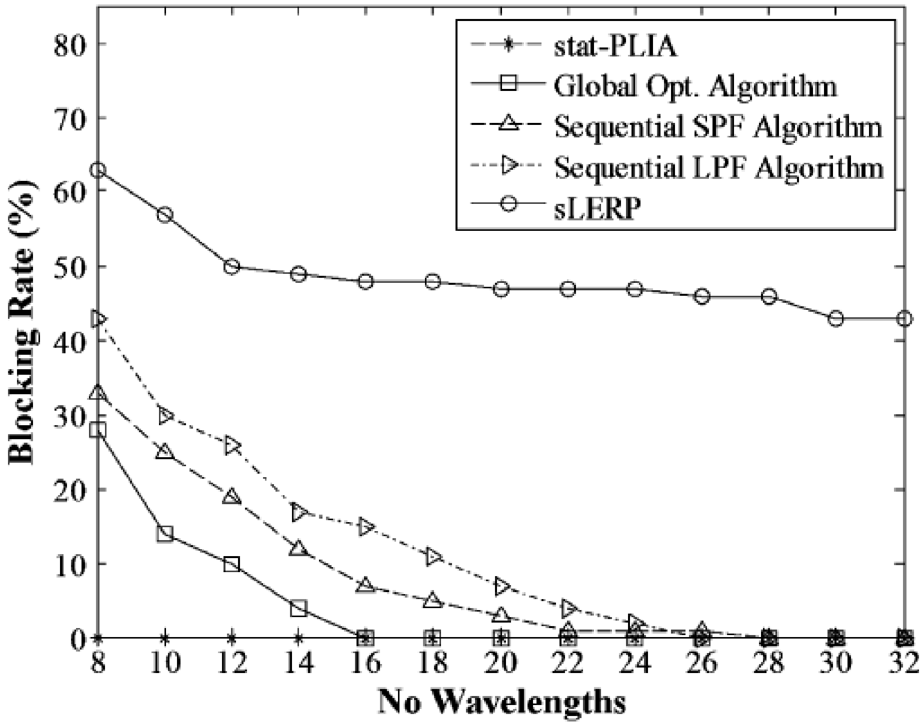

Figure 4.21: Blocking rate of Internet2 network with varying number of wavelengths

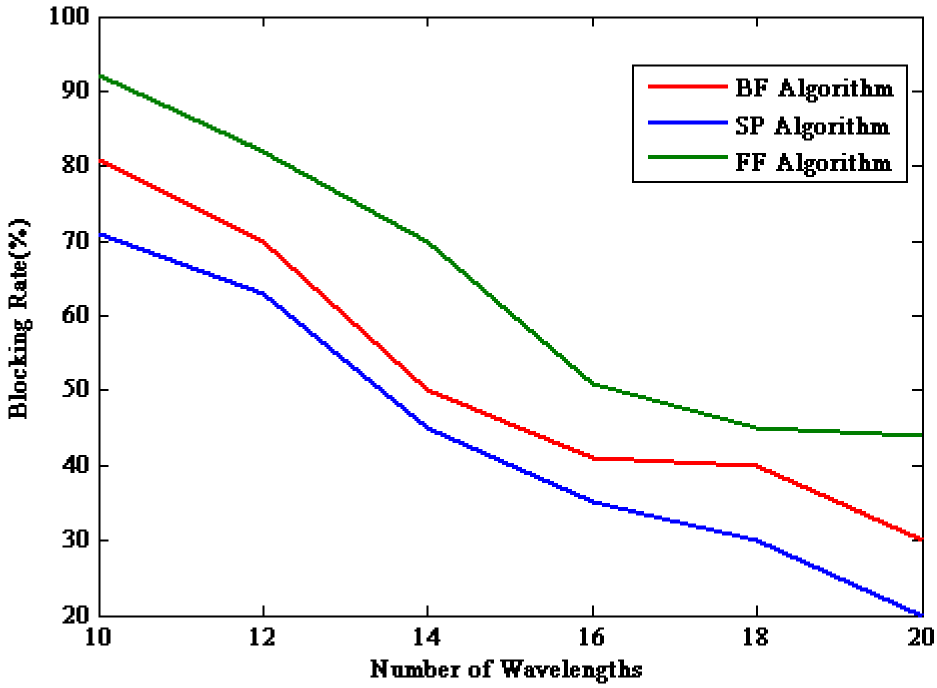

Figure 4.22: Blocking rate obtained with varying wavelengths using FF, BF, SP algorithms for EON

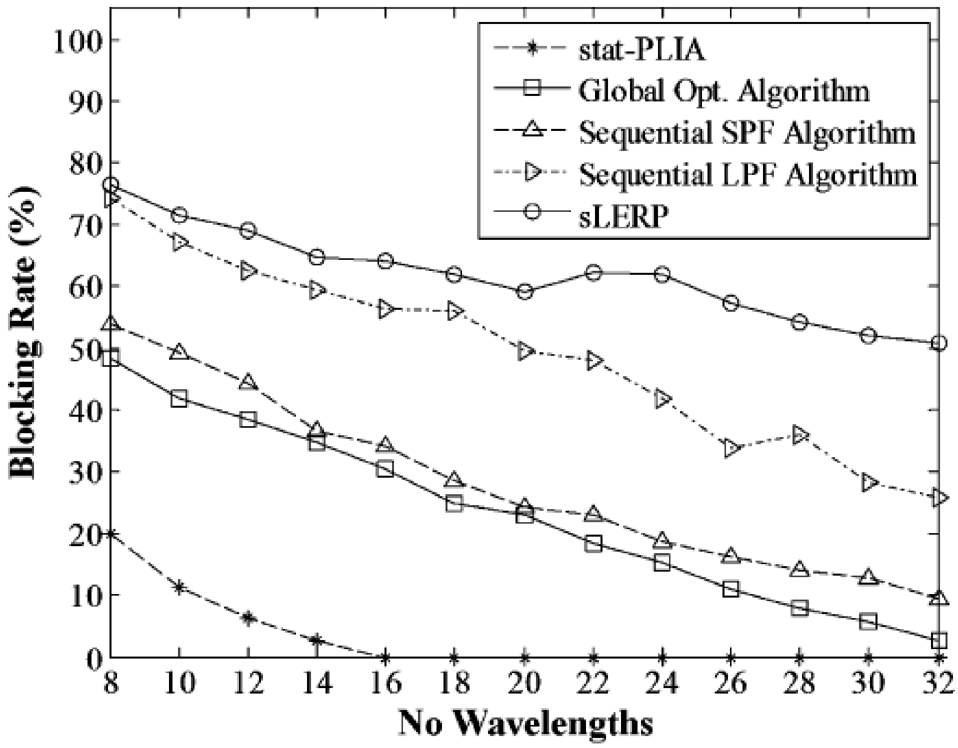

Figure 4.23: Blocking rate of EON network with varying number of wavelengths

Both calculations do not depend on traffic demand but network topology. Phase-II searches for feasible solutions carrying highest number of lightpaths preventing any wavelength conflict. The effects of dynamic PLI constraints are not considered in this phase. Phase-III and IV emphasize on improvement of Q-value of feasible lightpaths. Organization of demands is done either by ascending or descending order strategies. Ascending order selects nodes with minimum demands and shortest path first while descending order prefers maximum utilized paths first. The list so formed is processed in sequential manner for each node pair. If a route and wavelength exists for the lightpath demand without influencing all the previously established lightpaths, connection is setup, otherwise it is blocked. The results obtained are compared with Simplified Lightpath Establishment and Regenerator Placement (sLERP) algorithm, skipping its regeneration phase. The curve stat-PLIA algorithm considers static impairments to calculate the blocking rate.

The results obtained by presented algorithm are compared. It has been found that the response of presented algorithm is better than sLERPS due to less blocking rate being offered and comparable with SPF and LPF algorithm. All the algorithms (BF, FF and SP) outperform than LPF as LPF consider longest path first. The increased path length will increase the impairment level of Q-matrix, thereby increasing the blocking probability of network. Moreover a signal which transverse more distance in the network will influence more number of already established lightpaths, resulting in call drops. The number of paths acting as potential candidates for lightpath setup through routing matrix plays an important role. The SPF algorithms use 10-shortest path search for lightpath set up, while the designed algorithm has no limit on number of potential paths for lightpath setup. This help in finding more optimum paths for specified connection request. Moreover, the performance of network changes with the network topology, number of nodes involved. The algorithm is implemented on a portion of EON network (only 9 nodes), while referred author used 15 nodes. The blocking probability for EON is high because the presented algorithm uses few nodes of EON (9 out of 15) so the number of available paths between source to destination is less, making it difficult to find path for high traffic load. The increased number of nodes might have increased the blocking rate of the network. The reason for difference in behavior of FF, BF and SP is same as already stated. The performance of SP is most reliable than all other algorithms.

4.5 CHAPTER SUMMARY

Thus, an algorithm for PLIAR is discussed in this chapter. It employs multiple physical layer constraint environments with focus on providing best service quality for lightpath setup. Three different variations are presented implementing the first calculated path, shortest path, and the best among the shortest paths in sets of three. In order to test the performance a nine node network is used. The blocking rates are studied considering pure RWA problem and by inculcating impact of PLIs. The percentage increase in blocking rate due to impairments is compared with that without considering the effect of PLIs and the factor responsible and advantages of including impairments are laid out. Although optimum results are obtained by all the three algorithms, but the performance shortest path is best to find path between specified source and destination node. In order to validate the results, the algorithm is implemented over EON and Internet2 networks. The response of the presented algorithm is evaluated and analyzed with respect to sequential SPF and Sequential LPF algorithm. It has been found that the algorithm outperforms both of them in terms of blocking rate of the network for varied available wavelengths.

Chapter 5

Regenerator position strategy

This chapter discusses the different strategies of regenerator placement in translucent or transparent network. The effect of these techniques on routing algorithms of chapter 4 is presented

CHAPTER 5: REGENERATOR POSITION STRATEGY

The present optical networks are moving towards transparent networks with minimal O-E-O conversions resulting in accumulated impairments at the destination end. As demonstrated in previous chapters, these impairments decrease the performance of networks by obstructing the path setup and signal transfer process. To improve the system performance it is mandatory to improve the quality of link for signal transfer. The optimum placement of regenerators is one of the solutions for the same, where signal regeneration may takes place at certain pre-specified nodes. While selecting the nodes for regenerator placement, equilibrium between CAPEX (capital expenditure) and OPEX (operational expenditure) must be maintained for best system performance.

The existing strategies for regenerator placement are broadly classified as sparse regenerator placement and generation of transparent islands. [90] The sparse placement involves uniform distribution of regenerators in the network deliberately so that maximum regeneration of signals takes place thereby improving the system behavior. The concept of transparent islands involves generating the sections where there are specified regions have no signal regeneration taking place inside the boundary as explained in chapter 1. The sparse placement of regenerators seems to be a more economical solution since it distributes the regenerators throughout the network and probability of signal successfully reaching at destination node is more as it helps the signal maintaining its quality requirements. The nodes where regenerator must be placed may be calculated either by using an approximation algorithm [91] [92] [93] [94] or a heuristic algorithm [95] [96] [97] [98] [99] [100] [101] where the incremental traffic [102] [103] [104] and static traffic scenario [105] [106] [107] [108] [109] are considered. In the present work, sparse placement of regenerators is considered for dynamic traffic scenario. Three different algorithms are presented using information of network topology, history of traffic flow in the network and presence of PLIs. The advantage of presented algorithms includes the simplicity in implementation and better network performance for the load distribution used during the optimization process. The nine node network presented in Figure 4.1 is considered. The network has topology G = (N, L) with problem of placing X regenerators at every selected node so that it can facilitate regeneration and wavelength conversion all the feasible lightpaths as possible. The three different strategies are presented for regenerator placement.

5.1 ALGORITHM FOR REGENERATOR PLACEMENT

5.1.1 Maximum Utilized Node First

In the dynamic reconfigurable optical networks, the connection requests arrive in the random manner and cannot be known in advance. In such scenarios, the problem of regenerator placement may be addressed through knowledge of network topology, arrangement and utilization of nodes. The first approach presented is to place the regenerator at most utilized nodes. Among two different nodes, the node which is transverse maximum time for all the possible call requests between different source to destinations will be considered as most utilized.

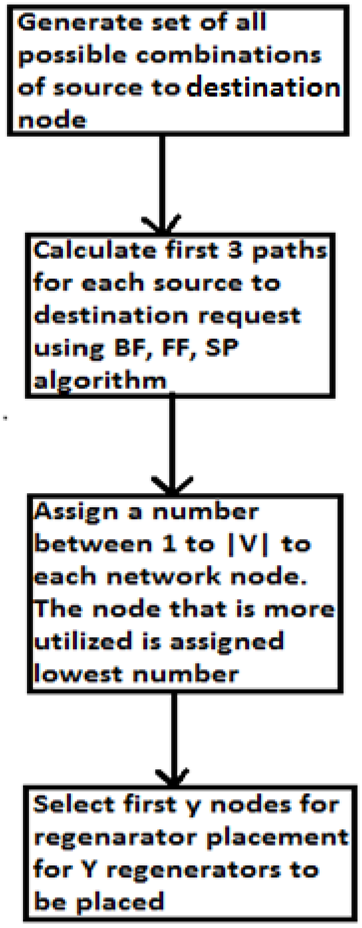

Figure 5.1: Flow chart for maximum node utilization strategy of regenerator placement

In order to calculate the nodes most utilized, a traffic matrix with all the possible combinations of source to destination route are generated. The three algorithms proposed in previous chapter are used to calculate the first three possible routes for each source to destination request. A unique number initialized by zero is assigned to each node and is incremented by 1 each time node is utilized. The nodes used maximum time is identified as the most utilized node has larger number. Depending on the number of regenerators to be utilized, the nodes are selected as per decreasing order. For example, if 40% of the presented 9 node network is to be equipped with regenerators, nodes with number 1 to 4 will be provided with regenerators. The working of this algorithm is shown as flow chart in Figure 5.1.

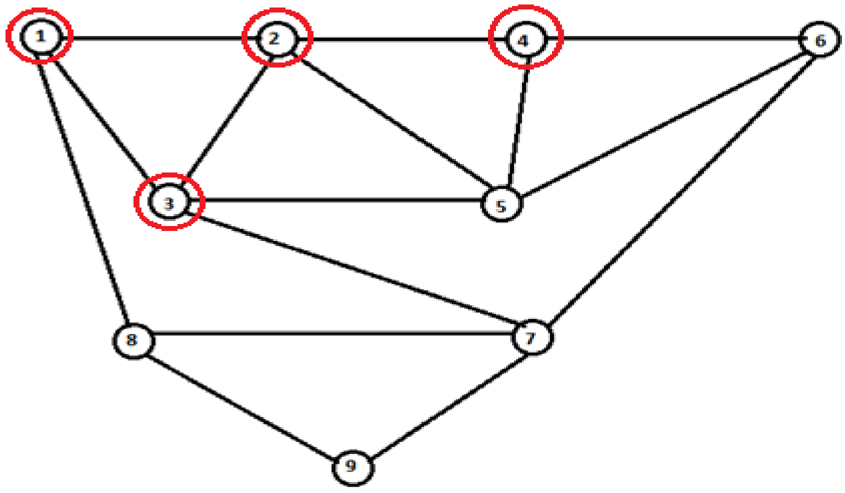

Figure 5.2: Nodes with regenerator placed by implementing FF algorithm on the network using maximum node utilization strategy

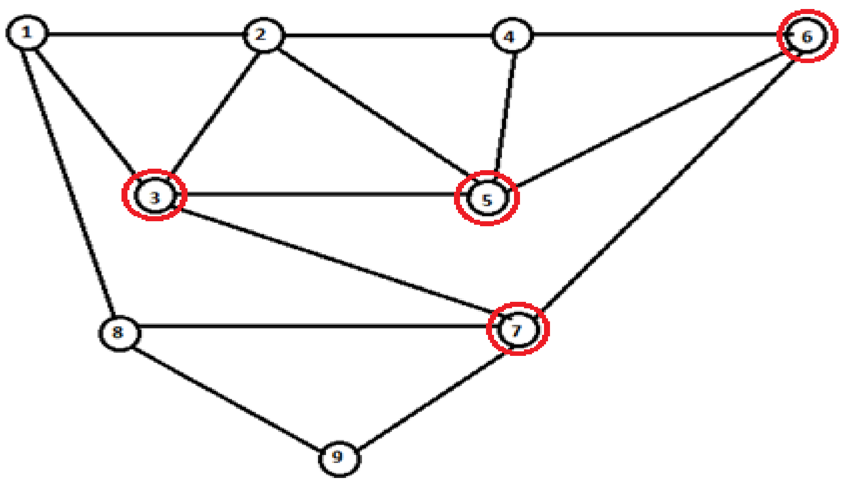

Figure 5.3: Nodes with regenerator placed by implementing SP algorithm on the network using maximum node utilization strategy

Among the three routing algorithms SP and FF will calculate the different routes for given request as the basic principle of operation of both is different. The shortest path will have maximum signals transverse through shortest hops while FF will have maximum utilization of nodes with lowest number. BF and FF will generate the same utilization as the quality of link is assumed to be above threshold before any signal is being practically sent over it. The two different possible network configurations for FF and SP path are shown in Figure 5.2 and Figure 5.3 where highlighted nodes are regeneration capable.

5.1.2 Traffic Based Regenerator Placement

Once the network has been designed, depending upon the past usage of traffic, the trends to be followed in the nearby future can be easily predicted. It is quite possible that future traffic may or may not follow the same pattern, but pre-estimation is often done so as to design and plan any network. Another approach presented implements the traffic prediction so as to estimate the most utilized nodes of the network. The working of algorithm is shown in Figure 5.4.

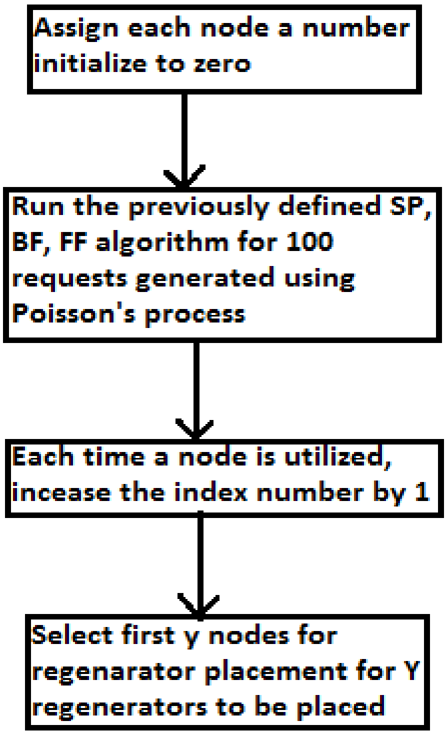

Figure 5.4: Flow chart for traffic based regenerator placement strategy

In this algorithm, traffic prediction is done using poisons process described in chapter 5, where total 100 requests are generated. Each node is assigned a unique number initialized to zero. While path selection, each time a node is selected, this number is incremented by 1. For regenerator placement, the nodes are selected as per decreasing order of unique number. The different configurations of the network obtained for 40% nodes capable of regeneration are presented in the Figure 5.5 and Figure 5.6.

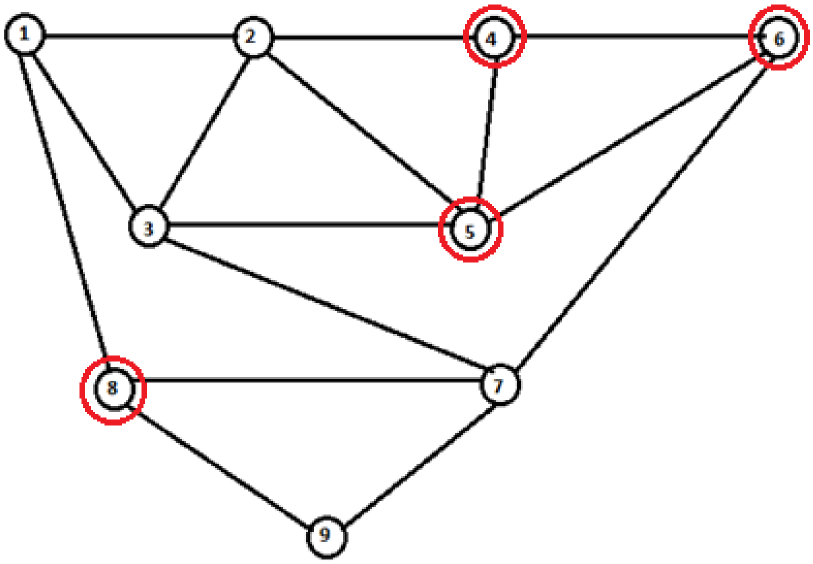

Figure 5.5: Nodes with regenerator placed by implementing SP algorithm on the network using Traffic load estimation strategy

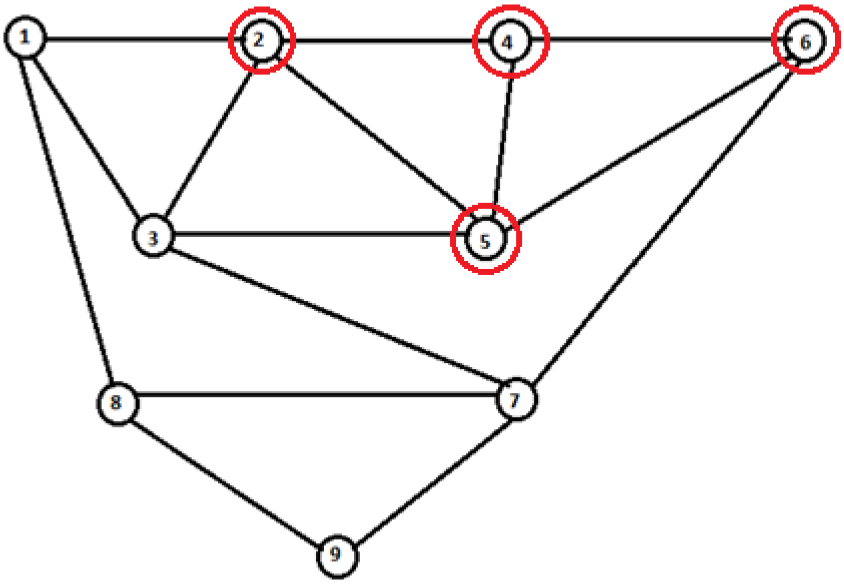

Figure 5.6: Nodes with regenerator placed by implementing FF algorithm on the network using Traffic load estimation strategy

5.1.3 Physical Layer Constraint Based Regenerator Placement

The algorithm proposed in section 2 considers the pre-estimated traffic for calculating the node requiring regeneration. To improve the blocking rate of the network, the number of connections blocked because of decreased link quality owing to presence of PLIs are considered. This will help in selecting the nodes where the quality of transmission is degrading and requires the regeneration of signal to restore threshold values of transmission. In this case, a number will be assigned to each node, and initialized to 0. For selecting the number of nodes for regenerator placement, FF and SP algorithms are executed for 500 connection requests. The number of connections has been increased as the blocking of connection due to unsatisfactory quality is less than the blocking due to unavailable paths. Whenever connection call is discarded because of reduced quality of a particular link, the number corresponding to the nodes involved is incremented by 1. The working of algorithm is demonstrated in Figure 5.7. During regenerator placement, the nodes are selected as decreasing order of number assigned. The network configuration obtained for 40% nodes capable of regeneration is shown in Figure 5.8 and Figure 5.9.

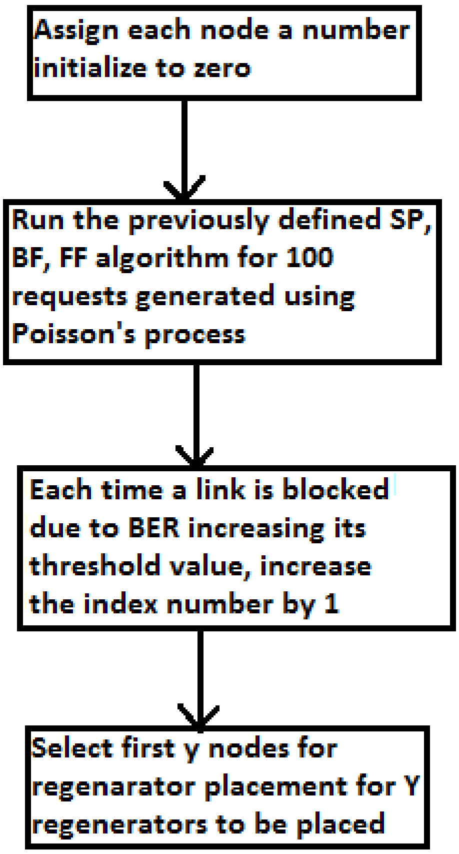

Figure 5.7: Flow chart for PLI based constraints regenerator placement

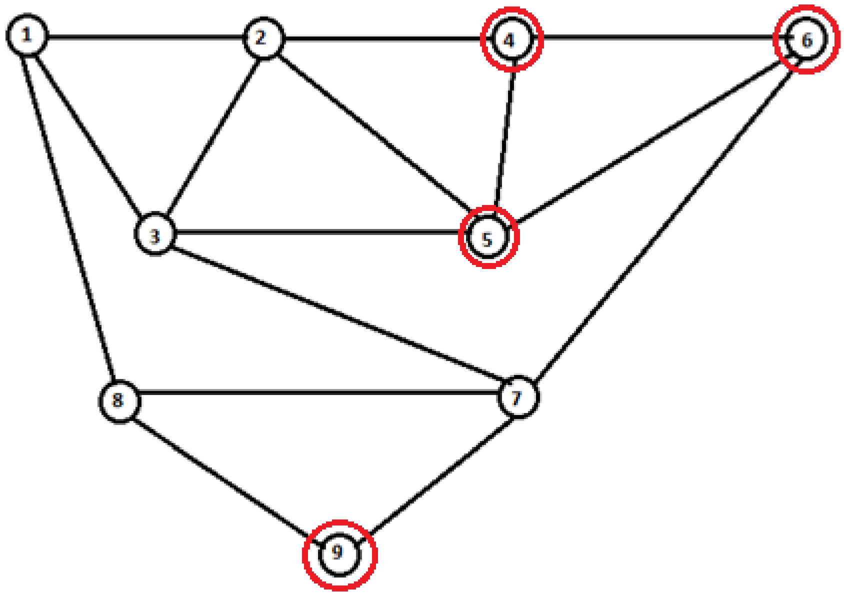

Figure 5.8: Nodes with regenerator placed by implementing SP algorithm on the PLI constraint based strategy

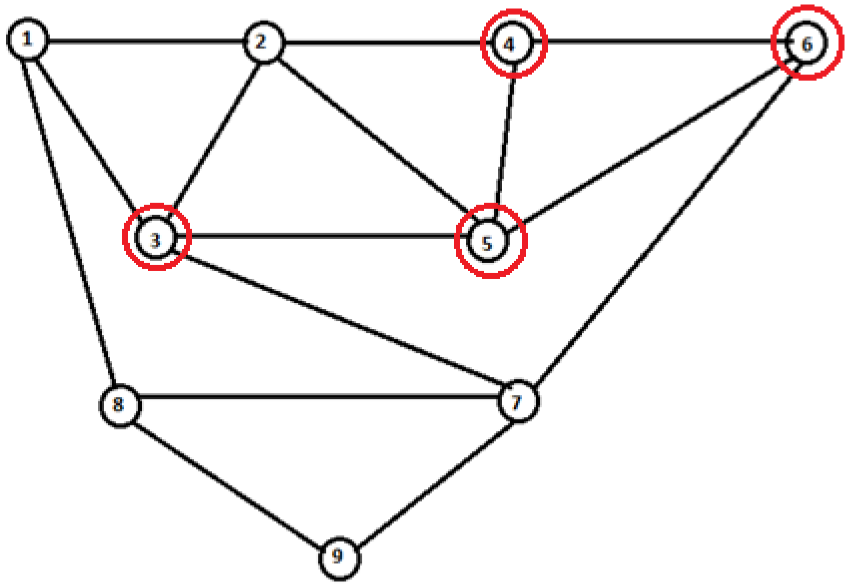

Figure 5.9: Nodes with regenerator placed by implementing FF algorithm on the network PLI constraint based strategy

5.2 PERFORMANCE EVALUATION OF ALGORITHMS

In order to study the system response for all the algorithms presented, the basic algorithms of SP, FF and BF are implemented on networks obtained by placement strategies based on node utilization, traffic history and presence of physical layer impairments. The Figure 5.10 represents the behavior of network when SP algorithm is implemented on nine node network. Three different cases of regenerator placement are considered i.e. when no regenerator is placed at all, when 40% of the available nodes are equipped with regeneration capability and when all the nodes have regeneration capability. The blocking rate of all the three cases is studied for a link supporting maximum of 15 wavelengths.

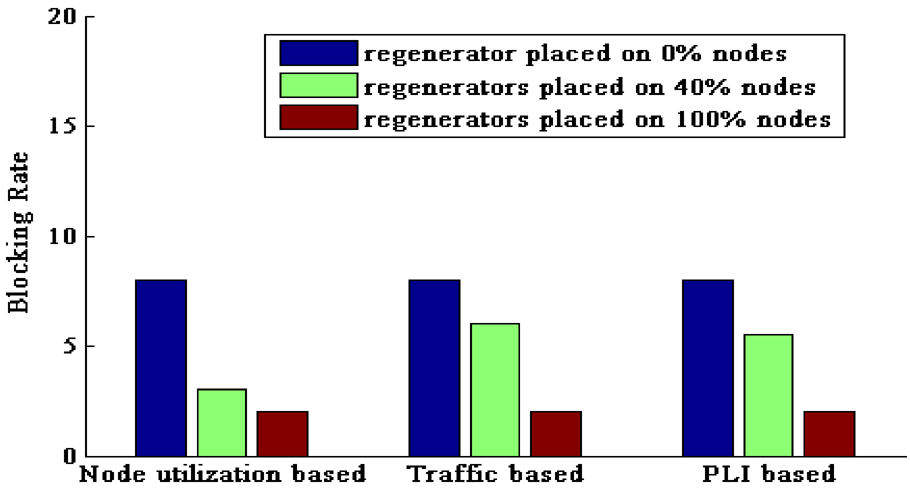

Figure 5.10: Behavior of nine node network with application of SP algorithm

As the number of nodes equipped with regeneration facility is increased, the blocking rate is decreased. The reason for this is the regeneration capability improves the signal quality and prevents the signal degradation to threshold levels. But as the number of regenerators is increased, i.e. for 100% nodes equipped with regenerators, still some calls are blocked. This is mainly due to unavailability of physical resources.

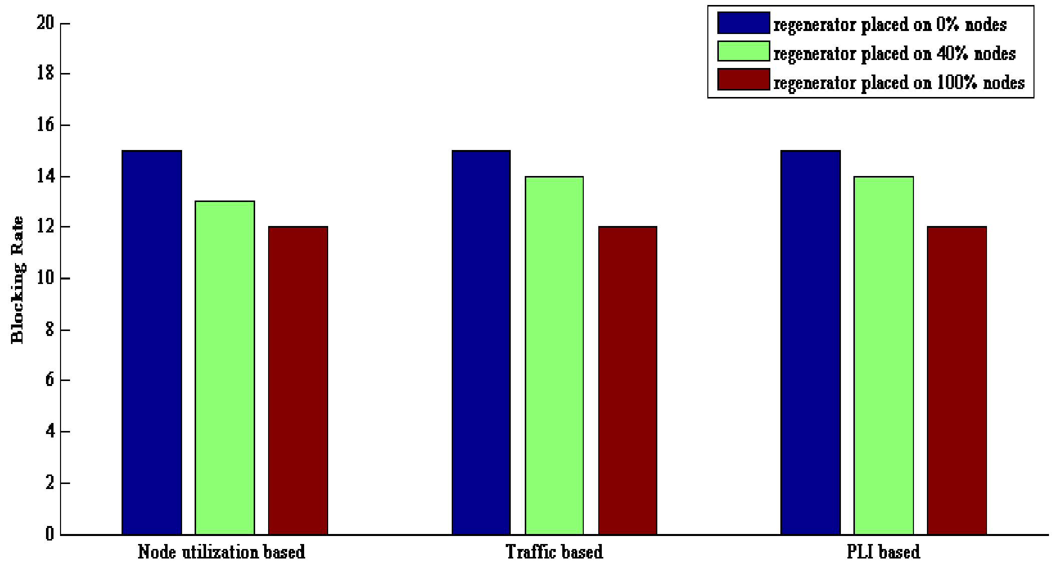

Figure 5.11: Behavior of nine node network with application of BF algorithm

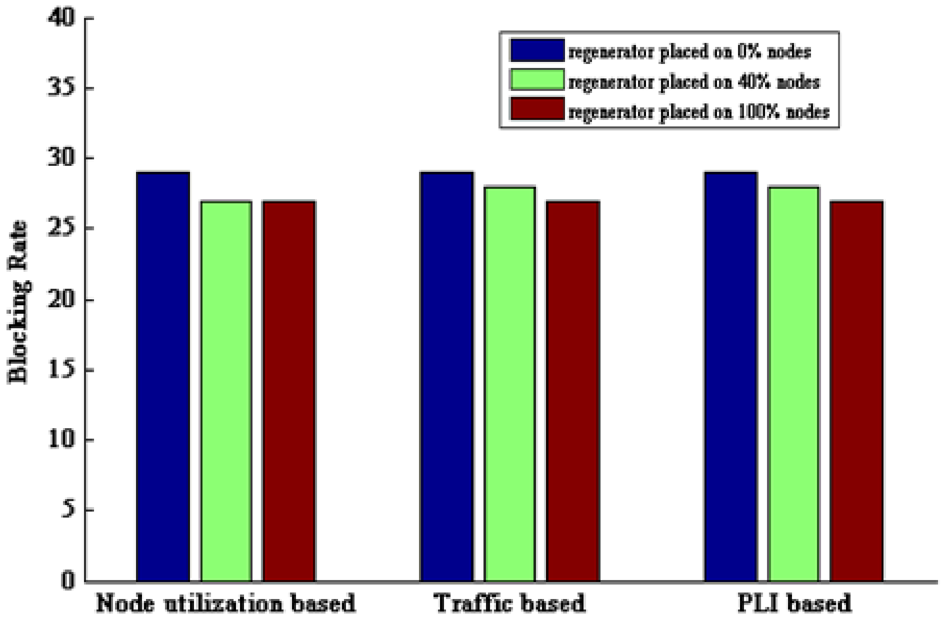

Figure 5.12: Behavior of nine node network with application of FF algorithm

Figure 5.11 and Figure 5.12 shows the blocking rate when BF and FF algorithms are implemented on the presented regenerator strategies. The blocking rate is decreased with increased number of regeneration capability.

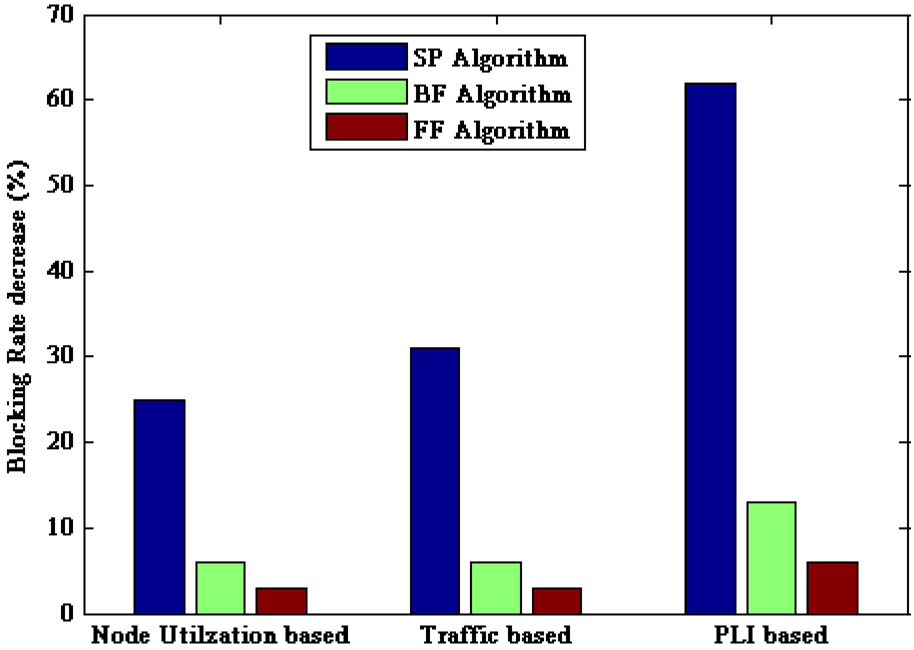

Figure 5.13: Blocking rate comparison of SP, BF and FF algorithms

For these systems having 15 wavelengths travelling over each link, the blocking probability is already high as compared to SP algorithms due to unavailability of resources. That is why the presence of regenerators does not affect the system performance much. Among the three placement strategies presented, the percent decrease in blocking probability for regenerators placed at 40% of nodes using the SP, BF and FF algorithms is presented in Figure 5.13. Among the different routing algorithms SP algorithm responds best to all the three regenerator based strategies. Among the different regenerator based strategies, PLI based regenerator placement has maximum effect on reducing the blocking rate of the network.

The performance of regenerator placement algorithms is compared with the results represented by [107], which are reproduced here for the reference in **Figure 14**.14. The author implemented different routing algorithms on a 28 node network in presence of amplifier noise with dedicated values of OSNR. The set of source and destination nodes is randomly selected and path computation is done using Exact Impairment-Aware Routing Algorithm (based on basic Dijkstra Algorithm)(referred as A-1 in the subsequent sections), Tunable Impairment-Aware Routing Algorithm (heuristic based, referred as A-2), Loop Avoidance Heuristic based algorithm (referred as A-3 in the subsequent section), k-shortest path algorithm(A-4, A-5, A-6, A-7 are used in context with k=1,5,10, 100 respectively). The regenerator nodes are randomly chosen. The author used success ratio and average time used to find the suitable route as the performance parameters. In order to compare the present work, the output representing the acceptance ratio is considered. The success ratio is the ratio of feasible paths meeting the system requirements to total number of requests and is related to blocking rate as (1- Blocking Rate)*100 %.

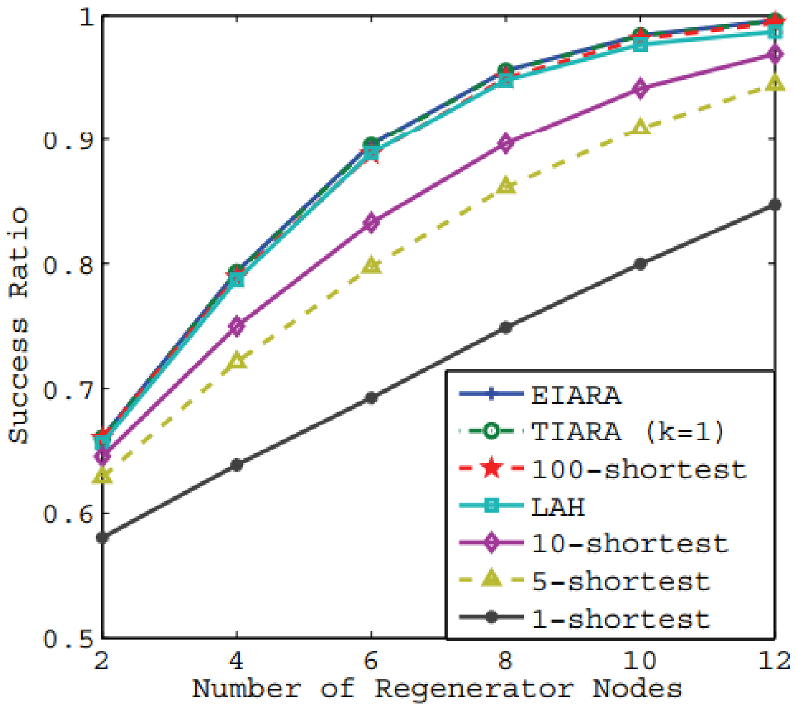

Figure 14.14: Success rate of a 28 node network for different number of regenerator nodes

Since the present work considers three different scenarios of regenerator placement only (at 0 % nodes, 40% nodes and 100% nodes), the case where 40% nodes are regeneration capable may be compared. As per the given diagram, blocking rate may be obtained approximately as 20 %, 10%, 6%, 3%, 2%, 2%, 2% for A-4, A-5, A-6, A-3, A-1, A-2, A-7 respectively. Among the different routing algorithms of present work, the performance of FF algorithm in all the different combinations (node utilization, traffic based, PLI based regenerator placement) is worst as is higher than A-1 toA-7 algorithms. For best fit routing algorithm, the performance is better than A-1 and A-2, but less than A-3 to 7. The performance of SP is better than A-4, A-5, A-6 for all the three strategies of regenerator placements. Although the performance of traffic based and PLI based regenerator algorithm is not equivalent to A-1 to -3, A-7, but performance of node utilization based is comparable. Still, the performance of A-1, A-2 and A-7 lies on the higher side of performance matrix and this might be due to numerous assumptions and network states considered by the author. The foremost reason is that referred work does not put any limitation on the maximum number of wavelengths but assume that there are wavelengths so that wavelength continuity constraint is relaxed, while the present work consider maximum of 15 wavelengths being transferred through the fiber. The number of impairments considered also influences the signal quality and overall call acceptance probability. The referred work considers only one impairment i.e. ASE, while the present work consider all impairments. The network considered in the referred work has higher number of nodes while present network considers nine nodes only. Thus, for increased number of nodes, with each link supporting higher number of wavelengths, the present work might have achieved performance indicators much better.

5.3 CHAPTER SUMMARY

In this chapter, the methodology of improving signal quality is discussed through regenerator placement the network. The sparse placement is considered owing to its simplicity in implementation and optimization. Three different strategies namely, maximum utilized node first, traffic based regenerator placement and physical layer constraint based regenerator placement are presented. The performance of these strategies is calculated by SP, BF and FF algorithms already presented on nine node network with 40% node being considered to be regeneration capable. It has been found that among the different strategies presented, PLI constraint based regenerator placement has the best performance using SP algorithm. This is due to the fact that the cause of network blocking due to decreased quality is directly dealt with using this approach. Hence, technique can be effectively implemented for improving the network performance in presence of different PLIs.

Chapter 6

Conclusion and future scope

CHAPTER 6: CONCLUSION AND FUTURE SCOPE

The present research focused on study of different physical layer impairments and their impact on route calculation for connection calls between specified source and destination nodes. The process of connection set up is often referred to as RWA and is a crucial step in planning any network. Various heuristic and meta-heuristic algorithms are present to date to solve RWA problem. Most of them consider fiber to be ideal black box, where the physical layer does not at all influence the signal flowing into it. Practically, the signal flowing depends on construction, physical properties of fiber, environmental conditions, the quantity and quality of co-propagation signals. The scenario is further complicated by absence of O-E-O conversion in the present day translucent or transparent optical networks. Moreover, these impairments are additives in nature and tend to increase as the distance transverse by the signal inside fiber is increased. All these factors acted as driving force to influence the necessity to consider the impact of physical layer on network performance.

Another factor that fueled the requirement is huge data traffic being carried by optical networks where link failure may lead to a critical situation for service providers. The present work focused on development of novel algorithm for routing in optical networks taking in to account the presence of impairments in the link. In order to improve the performance of network, techniques for regeneration placement are also discussed.

The different parameters influencing the system quality are indentified as linear and non linear degradation factors. The classification is based on intensity dependent nature of these factors. Linear impairment discussed in this research included dispersion (DGD, PMD) and attenuation while non-linear included SPM, XPM and FWM. Using Maxwell's equation, the mathematical model is derived for electromagnetic interaction taking place in the fiber as the lightwave propagates along the length of fiber and impact is demonstrated using OPTISM. The parameters like wavelength, power are considered to study their influence on system performance. The interaction between linear and non-linear impairments is also considered.

In order to transfer the influence of signal to route finding algorithm, effect of each impairment as well as accumulation effect of all impairments on BER and Q-value is calculated. The mathematical model for higher order impairments is also presented. Eye diagram and optical spectrum analysis is used to calculate the impact of individual impairments on BER and Q-value. It has been found that with increased distance of propagation the value of BER increase and the corresponding q-value decreases. The physical state of network also influences the quality of signal being transferred. The factors like high power of the signals, simultaneous propagation of more number of wavelengths into the fiber, channel spacing adversely affect the quality of signal. The impact of these factors on BER and Q-value is demonstrated. The value of quality matrix is used in routing algorithm to act as a constraint for path selection.

Although there exists two approaches to address impairment aware routing namely ICBR and PLIAR, PLIAR is implemented in the present work. The system developed consists of monitoring module, pre processing module, path selection module for its operation. Three different algorithms namely, shortest path algorithm, best fit algorithm, first fit algorithm are presented for route calculation. SP selects the path where signal transverse through minimum hops, FF transverse through node with lowest number first, while BF acts in steps as k-SP algorithm, k=3, and selects the path with maximum quality. A nine node network with thirty links and average node degree 1.556 is used to test the routing algorithm design. It supports four classes of users namely premium, gold, silver and bronze and maximum up to thirty wavelengths across each link. The monitoring module is designed using OPTISM while the network path computations are done in MATLAB. In order to validate the results, the algorithm is tested on Internet2 and EON networks and the results obtained are compared with already existing algorithm.

The response of algorithms for 10-20 wavelengths travelling simultaneously in the fiber is studied in the form of blocking probability. The results are compared with the scenario when no impairments are present at all. For instance, among the different cases presented, when 14 wavelengths were propagating within the fiber of nine node network, blocking probability of SP algorithm raise from 2% to 8% with the consideration of PLIs. Similarly, for BF algorithm, blocking probability increase from 12 to 15 % while for FF algorithm, it changes from 27 to 29%. With increased number of co-propagating wavelengths, blocking probability further increases. Although more number of calls is blocked by inculcating the PLIs but this will help improve the network performance by maintaining the transmission quality and decreasing the call drop rate.

Among the different algorithms presented, the performance of SP is best as the blocking rate for it is minimum as compare with other algorithms. The variation in the network through number of nodes is studied. The network configuration includes 5, 7 and 9 node network. It has been found that with increase number of nodes, if the traffic matrix remains the same, the performance of network is improved.

The optimum regenerator placement is viewed as key method to increase the network performance and three methods namely node utilization, traffic based and PLI based regenerator are presented. The performance of all the three algorithms is studied for three cases viz when no regenerator is placed at all, when 40 % nodes are equipped with regeneration capability and when 100% nodes are regeneration capable. The blocking rate for link supporting 15 wavelengths is presented. The PLI based algorithm outperforms than all other strategies using SP route calculation techniques. For 40 % nodes having regenerator placement strategy, the decrease in blocking rate using SP algorithm ranges from 25% to 62%, BF from 6% to 13 % while that of FF from 3% to 6%. Hence among the different algorithms proposed, SP algorithm for route calculation and PLI based regenerator placement are best for practical implementation.

RECOMMENDATIONS AND FUTURE SCOPE

The present work demonstrated the routing algorithm for a 9-node network allowing maximum of 30 wavelengths over a fiber link. Considering the various pros and cons of the present work, following issues are identified that can be addressed in future works:

1. It is recommended that the same algorithm may be worked upon a more complex network (increased number of nodes) and allowing more wavelengths to pass through link for estimation and evaluations. As the number of links and permissible wavelengths will increase the computational complexity will increase and may affect the blocking rate of the network. The

time required for computation of feasible paths and path selection may also be another crucial factor to consider.

2. Although the algorithm is unanimously applicable for different modulation formats and higher bit rates, the work may be extended for advanced modulation formats and higher bit rates.
3. Also, the present work only considers class based requests between source and destination node. The impact of protection, back path storage and link re-storage may also be considered.
4. The multiple granularity networks with varying data rates, varying modulation formats may be another interesting topic for future implementation.
5. The different control plane extensions, multilayer architectures with different functionalities may be explored as well.
6. Another growing concern over the last years is the energy consumption in the links and network elements and may be introduced as a constrained in routing algorithm.

References

REFERENCES

[1] G. Keiser, Optical Fiber Communication, 4 ed., Tata McGraw Hill Ltd, 2008.

[2] T. Y. Chai, T. H. Cheng, G. Shen, S. K. Bose and C. Lu, "Design and performanec of optical cross connect architectures with convertor sharing," *Optical Networks Magazine*, pp. 73-84, July 2001.

[3] M. Ilyas and H. T. Mouftah, The handbook of Optical Communication Networks, CRC Press.

[4] I. Tomkos, B. Mukherjee, S. K. Korotky, R. S. Tucker and L. Lunardi, "The evolution of Optical Networking," in *Proceedings of the IEEE*, 2012.

[5] M. W. Chbat and H. J. Schmidtke, "Falling boundries from metro to ULH optical transport equipment," in *Proceedings of Optical Fiber Communication/National Fiber Optic Enginnering Conference (OFC/NFOEC'07)* , Anaheim, CA, Mar 2007.

[6] G. Ellinas, J. A. Walker, S. Chaudhuri, L. Lin, E. Goldstein and K. Bala, "Network Control And Management Challenges In Opaque Networks Utilizing Transparent Optical Switches," *IEEE Communications Magazine*, pp. S17-S24, Feb 2004.

[7] G. Rizzelli, G. Maier, R. Longo and A. Pattavina, "Comparison of Opaque and Translucent WDM Networks with Different Regenerator-Placement Strategies under Static and Dynamic Traffic," in *GTTI Annual Meeting*, Brescia, Italy, June 2010.

[8] Jean and Zhenshen Zhang, "Opaque and Transparent Networking," *Optical Networks Magazine*, pp. 3-7, 2003.

[9] G. Shen and R. S. Tucker, "Translucent Optical Networks: The Way Forward," *IEEE Communications Magazine*, pp. 48-54, Feb 2007.

[10] Fujitsu Network Communications Inc., "The Emerging Optical Control Plane," Texas, Dec2014.

[11] H. M. Foisel, "ASON-GMPLS Control Planes Overview," in *Conference on Converged and Optical Networks*, Brussels, September 2008.

[12] G. Li, J. Yates, D. Wang and C. Kalmanek, "Control plane design for reliable optical networks," *IEEE Communications Magazine,* vol. 40, no. 2, pp. 90-96,

2002 Feb 2002.

[13] H. Liu, D. Pendarakis, N. Komaee and D. Saha, "GMPLS-Based Control Plane for Optical Networks: Early Implementation Experience," in *Proc. SPIE , Optical Transmission Systems and Equipment for WDM Networking*, July 2002.

[14] W. Fawaz, B. Daheb, O. Audouin, B. Berde, M. Vigoureux, M. Du-Pond and G. Pujolle, "Service Level Agreement and Provisioning in Optical Networks," *IEEE Communications Magazine,* pp. 36-43, Jan 2004.

[15] G. Agrawal, Fiber-Optic Communication Systems, US: John Wiley $ Sons, Inc., 2010.

[16] L. N. Binh, Advanced Digital Communication, CRC Press, 2015.

[17] L. Nelson and R. M. Jopson, "Introduction to polarized mode dispersion in optical Systems," in *Polarized Mode Dispersion*, Springer, 2004, pp. 1-35.

[18] I. Shake, H. Takara and S. Kawanishi, "Simple Measurement of Eye Diagram and BER Using High-Speed Asynchronous Sampling," *Journal of Lightwave Technology,* vol. 22, no. 5, pp. 1296-1301, 2004.

[19] J. Hult, R. S. Watt and C. F. Kaminski, "Dispersion Measurement in Optical Fibers Using Supercontinuum Pulses," *Journal of Lightwave Technology,* vol. 25, no. 3, pp. 820-824, 2007.

[20] H. Chi and J. Yao, "Fiber chromatic dispersion measurement based on wavelength-to-time mapping using a femtosecond pulse laser and an optical comb filter," *Journal of Optics Communications,* vol. 280, no. 2, pp. 337-342, 2007.

[21] N. G. B. a. S. Wagner, "Novel time-of-flight fiber dispersion measurement technique using supercontinuum light sources and acousto-optical tunable filters," *Journal of Applied Optics,* vol. 54, no. 21, pp. 6406-6409, 2015.

[22] J. Cheng, M. E. V. Pedersen, K. Wang, C. Xu, L. Grüner-Nielsen and D. Jakobsen, "Time-domain multimode dispersion measurement in a higher-order-mode fiber," *Optics Letters,* vol. 37, no. 3, pp. 347-349, 2012.

[23] C. Quan, M. Thakur and C. J. Tay, "Lau Phase interferometry with vibrating objects," *Optik- Intenational Journal for Light and Electron optics,* vol. 117, no. 1, pp. 9-14, 2006.

[24] L. Qian, B. Qi, W. S. Mohammed, M. A. Galle and F. Ye, "Measuring chromatic dispersion using single-arm interferometers: from millimeters to

kilometers," in *SPIE 7072, Optics and Photonics for Information Processing I*, September 2008.

[25] K. A. Lathief, "Attenuation Measurement in Optical Fiber Communication," *Journal of Research Studies in Science, Engineering and Technology,* vol. 1, no. 4, pp. 62-67, 2014.

[26] M. K. Barnoski and S. M. Jensen, "Fiber waveguides: a novel technique for investigating attenuation characteristics," *SPIE milestone series* , vol. 165, no. 1, pp. 93-96, 2001.

[27] K. Inada, "A new graphical method relating to optical fiber attenuatio," *Optics Communications,* vol. 19, no. 3, pp. 437-439.

[28] T. Horiguchi and M. Tateda, "Optical-fiber-attenuation investigation using stimulated Brillouin scattering between a pulse and a continuous wave," *Optics letters,* vol. 14, no. 8, pp. 408-410.

[29] S. P. Singh and N. Singh, "Nonlinear Effets in optical Fibers: Origin, Management and Applications," *Progress in Electromagnetics Research (PIER),* vol. 73, no. 1, pp. 249-275, 2007.

[30] G. P. Agrawal, Nonlinear Fiber Optics, New York: Academic Press, 2001.

[31] M. F. S.Ferreira, NONLINEAR EFFECTS IN optical fibers, Wiley ans Sons, Inc., 2011.

[32] S. O. Kasap, Principles of electronic materials and devices, New York: McGraw-Hill, 2006.

[33] J. Toulouse, "Optical nonliniearities in fibers: review, recent examples and system applications," *Journal of Lightwave Technology,* vol. 23, no. 11, pp. 3625-3641, 2005.

[34] M. W. Maeda, W. B. Sessa, W. I. Way, A. Yi-Yan, L. Curtis, R. Spicer and R. Laming, "The effect of Four Wave Mixing in Fibers on Optical Frequency Division Multiplexed Systems," *Journal of Lightwave Technology,* vol. 8, no. 9, pp. 1402-1408, 1990.

[35] S. Song, "Higher -order four wave mixing and its effect in WDM systems.," *Optical Communications,* vol. 7, no. 4, pp. 166-171, 2000.

[36] Z. Dong, F. N. Khan, Q. Sui, K. Zhong, C. Lu and A. P. T. Lau, "Optical Performance Monitoring: A Review of Current and Future Technologies," *Journal of Lightwave Technology,* vol. 34, no. 2, pp. 525-543, 2016.

[37] D. Kilper, R. Bach, D. Blumenthal, D. Einstein, T. Landolsi, L. Ostar, M. Preiss and A. Willner, "Optical performance monitoring," *Journal of Lightwave Technology* , vol. 22, no. 1, pp. 294-304, 2004.

[38] J. H. Lee, H. Y. Choi, S. K. Shin and Y. C. Chung, "A review of the polarization-nulling technique for monitoring optical-signal-to-noise ratio in dynamic WDM networks," *Journal of Lightwave Technology,* vol. 24, no. 11, p. 4162–4171, 2006.

[39] Q. Sui, A. P. T. Lau and C. Lu, "OSNR Monitoring in the presenceof first-order PMD using polarization diversity and DSP," *Journal of Lightwave Technology,* vol. 28, no. 15, p. 2105–2114, 2010.

[40] M. Cheung, L. Chen and C. Chan, "PMD-insensitive OSNR monitoring based on polarization-nulling with off-center narrow-band filtering," *Journal of Photonics Technology Letters,* vol. 16, no. 11, p. 2562–2564, 2004.

[41] N. Kikuchi, "Analysis of signal degree of polarization degradation used as control signal for optical polarization mode dispersion compensation," *Journal of Lightwave Technology,* vol. 19, no. 4, p. 480–486, 2004.

[42] J. Yang, M. R. Chitgarha, L. Zhang, J. Wang, L. Paraschis and A. Willner, "Optical monitoring of PMD accumulation on a Pol-MUX phase-modulated signal using degree-of-polarization measurements," *Optics Letters,* vol. 36, no. 16, p. 3215–3217, 2011.

[43] Y. Wang, S. Hu, L. Yan, J. Yang and A. E. Willner, "Chromatic dispersion and polarization mode dispersion monitoring for multi-level intensity and phase modulation systems," *Optics Express,* vol. 15, no. 21, p. 14038–14043, 2007.

[44] I. Shake, H. Takara and S. Kawanishi, "Technology for flexibly monitoring optical signal quality in transparent optical communications," *Journal of Optical Networking,* vol. 6, no. 11, p. 1229–1235, 2007.

[45] Z. Li, C. Lu, Y. Wang and G. Li, "In-service signal quality monitoring and multi-impairment discrimination based on asynchronous amplitude histogram evaluation for NRZ-DPSK systems," *Photonics Technology Letters,* vol. 17, no. 9, p. 1998–2000, 2005.

[46] Z. Li and G. Li, "Chromatic dispersion and polarization-mode dispersion monitoring for RZDPSK signals based on asynchronous amplitude histogram evaluation," *Journal of Lightwave Technology,* vol. 24, no. 7, p. 2859–2866, 2006.

[47] B. Kozicki, O. Takuya and T. Hidehiko, "Optical performance monitoring of phase-modulated signals using asynchronous amplitude histogram analysis," *Journal of Lightwave technology,* vol. 26, no. 10, p. 1353–1361, 2008.

[48] R. S. Luıs, A. Teixeira and P. Monteiro, "Optical signal-to-noise ratio estimation using reference asynchronous histograms," *Journal of Lightwave Technology,* vol. 27, no. 6, pp. 731-743, 2009.

[49] T. S. R. Shen, K. Meng, A. P. T. Lau and Z. Y. Dong, "Optical performance monitoring using artificial neural network trained with asynchronous amplitude histograms," *Photonics Technology Letters,* vol. 22, no. 22, p. 1665–1667, 2010.

[50] S. D. Dods and T. B. Anderson, "Optical performance monitoring technique using delay tap asynchronous waveform sampling," in *Optical Fiber Communication Conference, paper-OThP5*, USA, 2006.

[51] Z. Li, Z. Jian, L. Cheng, Y. Yang, C. Lu, A. P. T. Lau, C. Yu, H. Y. Tam and P. K. A.Wai, "Signed CD monitoring of 100 Gbit/s CS-RZ-DQPSK signal by evaluating the asymmetry ratio of delay-tap sampling," *Optics Express,* vol. 18, no. 3, p. 3149–3157, 2010.

[52] F. N. Khan, A. P. T. Lau, Z. Li, C. Lu and P. K. A.Wai, "Statistical analysis of optical signal-to-noise ratio monitoring using delay-tap sampling," *Photonics Technology Letters* , vol. 22, no. 3, p. 149–151, 2010.

[53] F. N. Khan, A. P. T. Lau, Z. Li, C. Lu and P. K. A. Wai, " OSNR monitoring for RZ-DQPSK systems using half-symbol delay-tap sampling technique," *Photonics Technology Letters,* vol. 22, no. 11, p. 823–825, 2010.

[54] H. Y. Choi, Y. Takushima and Y. C. Chung, "Optical performance monitoring technique using asynchronous amplitude and phase histograms," *Optics Express* , vol. 17, no. 26, p. 23953–23958, 2009.

[55] M. C.Tan, F. N. Khan, W.H.Al-Arashi, Y.Zhou and A. P.T.Lau, "Simultaneous optical performance monitoring and modulation format/bit-rate identification using principal component analysis," *Journal of Optical Communications and Networking,* vol. 6, no. 5, p. 441–448, 2014.

[56] X.Wu, J. Jargon, C.M.Wang, L. Paraschis and A. E.Willner, "Experimental comparison of performance monitoring using neural networks trained with parameters derived from delay-tap plots and eye diagrams," in *Optical Fiber Communication Conference, Paper-JThA17*, San Diego, USA, 2010.

[57] T. B. Anderson, A. Kowalczyk, K. Clarke, S. D. Dods, D. Hewitt and J. Li, "Multi impairment monitoring for optical networks," *Journal of Lightwave Technology* , vol. 27, no. 16, p. 3729–3736, 2009.

[58] A. P. T. Lau, Z. Li, F. N. Khan, C. Lu and P. K. A. Wai, "Analysis of signed chromatic dispersion monitoring by waveform asymmetry for differentially-coherent phase-modulated systems," *Optics Express,* vol. 19, no. 5, pp. 4147-4156, 2011.

[59] K. C. Jong, H. W. Tsao and S. L. Lee, "Q-factor monitoring of optical signal-to-noise ratio degradation in optical DPSK transmission," *Electronics Letters,* vol. 44, no. 12, p. 761–762, 2008 .

[60] F. N. Khan, A. P. T. Lau, C. Lu and P. K. A.Wai, " Chromatic dispersion monitoring formultiple modulation formats and data rates using sideband optical filtering and asynchronous amplitude sampling technique," *Optics Express,* vol. 19, no. 2, p. 1007–1015, 2011.

[61] Y. Yu, B. Zhang and C. Yu, "Optical signal to noise ratio monitoring using single channel sampling technique," *Optics Express,* vol. 22, no. 6, p. 6874–6880, 2014.

[62] H. Singh and B. Behera, "New approach to optical modelling, performance analysis and evaluation," *Optical Engineering,* vol. 30, no. 9, pp. 1347-1354, 2005.

[63] Y. K. Lize, L. Christen, J. Yang, P. Saghari, S. Nuccio, A. E. Willner and R. Kashyap, "Independent and simultaneous monitoring of chromatic and polarization-mode dispersion in OOK and DPSK transmission," *Photonics Technology Letters* , vol. 19, no. 1, p. 3–5, 2007.

[64] Y. Wang, S. Hu, L. Yan, J. Yang and A. E. Willner, " Chromatic dispersion and polarization mode dispersion monitoring for multi-level intensity and phase modulation systems," *Optics Express,* vol. 15, no. 21, p. 14038–14043, 2007.

[65] A. Liu, G. J. Pendock and R. S. Tucker, "Improved chromatic dispersion monitoring using single RF monitoring tone," *Optics Express,* vol. 14, no. 11, p. 4611–4616, 2006.

[66] H. C. Ji, K. J. Park, J. H. Lee, H. S. Chung, E. S. Son, K. H. Han, S. Jun and Y. C. Chung, "Optical performance monitoring based on pilot tones for WDM network applications," *Journal of Optical Networking,* vol. 4, no. 7, p. 510–533, 2004.

[67] J. Zhao, A. P. T. Lau, K. K. Qureshi, Z. Li, C. Lu and H. Y. Tam, "Chromatic dispersion monitoring for DPSK systems using RF powerspectrum," *Journal of Lightwave Technology*, vol. 27, no. 24, p. 5704–5709, 2009.

[68] S. Berber, "An automated method for BER characteristics measurement," *IEEE Transactions on Instrumentation and Measurement*, vol. 53, no. 2, pp. 575-580, 2004.

[69] X. Zhang, Z. Qu, G. Zhang and G. Yang, "Applicability of Gaussian Noise Approximation for Optically Pre-Amplified DPSK Receivers with Balanced Detection," 2004. [Online]. Available: https://arxiv.org/ftp/physics/papers/0410/0410029.pdf. [Accessed 2015].

[70] M. Ali and L. Tancevski, "Impact of Polarization Mode Dispersion on the Design of Wavelength Routed Networks," *IEEE Photonics Technology Letters,* vol. 14, no. 5, pp. 720-722, May 2002.

[71] B. Gloria, C. Vittorio and M. Marco, "Considering Transmission Impairments in RWA Problem:Greedy and Metaheuristic solutions," in *Optical Fiber Communication Conference and Exposition and The National Fiber Optic Engineers Conference*, 2007.

[72] M. Ali, B. Ramamurthy and J. S. Deogun, "Routing and wavelength assignment with power considerations in optical networks," *Computer Networks,* vol. 32, no. 5, pp. 539-555, 2000.

[73] Y. G. Huang, J. P. Heritage and B. Mukherjee, "Connection Provisioning With Transmission Impairment Consideration in Optical WDM Networks With High-Speed Channels," *Journal of Lightwave Technology,* vol. 23, no. 3, pp. 982-993, March 2005.

[74] R. Cardillo, V. Curri and M. Mellia, "Considering Transmission Impairments in Wavelength Routed Networks," in *Optical Network Design and Modeling* , Milan, Italy, 2005.

[75] P. Kulkarni, A. Tzanakaki, C. M. Machuka and I. Tomkos, "Benefits of Q-factor based Routing in WDM Metro Networks," in *European Conference on Optical Communication*, 2005.

[76] l. Tomkos, D. Vogiatzis, C. Mas, l. Zacharopoulos and A. Tzanakaki, "Performance Engineering of Metropolitan Area Optical Networks through Impairment Constraint Routing," *IEEE Optical Communications August 2004,* pp. 540-547, August 2004.

[77] R. Martínez, C. Pinart, J. Comellas and G. Junyent, "On-line ICBR in a transparent GMPLS network: a reality check," in *Proc. V Workshop on G/MPLS networks (WGN5)*, Spain, 2006.

[78] S. Duhovnikov, D. A. Schupke, G. Lehmann, T. Fischer and F. Rambach, "Dynamic RWA for All Optical Networks Using Linear Constraints for Optical Path Feasibility Assessment," in *European Conference on Optical Communication*, France, 2006.

[79] J. C. Li, K. Hinton, S. D. Dods and P. M. Farrell, "Enabling ASON Routing via Novel Signal Quality Metrics," in *IEEE Conference on Optical Fiber Communication*, 2006.

[80] C. Pinart and H. Harai, "On using optical-layer link information parameters in distributed impairment constraint-based routing," in *IEEE - Conference on Optical Fiber Communication*, 2006.

[81] I. Tomkos, S. Sygletos, A. Tzanakaki and G. Markidis, "Impairment Constraint Based Routing in Mesh Optical Networks," in *Optical Fiber Communication*, 2007.

[82] C. Politi, V. Anagnostopoulos, C. Matrakidis and A. Stavdas, "Physical Layer impairment Aware Routing Algorithms based on Analytically Calculated Q-Factor," in *IEEE Optical Fiber Communication Conference* , 2006.

[83] C. Politi, C. Matrakidis, A. Stavdas, V. Anagnostopoulos and M. Gunkel, "Cross Layer Routing in Transparent Optical Networks," in *IEEE conference on Optical Fiber Communication*, 2007.

[84] P. Castoldi, F. Cugini, L. Valcarenghi, N. Sambo, E. L. Rouzic, M. J. Poirrier, N. Andriolli, F. Paolucci and A. Giorgetti, "Centralized vs Distributed Approaches for Encompassing Physical Impairments in Transparent Optical Networks," in *ONDM* , Greece, 2007.

[85] T. Deng and S. Subramaniam, "Source Power Management in Transparent Wavelength Routed Mesh Networks," in *IEEE International Conference on Communications*, 2004.

[86] T. Deng and S. Subramaniam, "Adaptive QoS Routing in Dynamic Wavelength-Routed Optical Networks," in *IEEE Conference on Broadband Networks*, 2005.

[87] Y. Pointurier, M. Brandt-Pearce, T. Deng and S. Subramaniam, "Fair QoS-Aware Adaptive Routing and Wavelength Assignment in All-Optical

Networks," in *IEEE conference on Communications*, 2006.

[88] C. V. Saradhi and S. Subramaniam, "Physical layer impairment aware routing (PLIAR) in WDM optical networks: issues and challenges," *IEEE Communications Surveys & Tutorials*, vol. 11, no. 4, pp. 109-130, 2009.

[89] P. Pavon-Marino, S. Azodolmolky, R. Aparicio-Pardo, B. Garcia-Manrubia, Y. Pointurier, M. Angelou, J. Sole-Pareta, J. Garcia-Haro and I. Tomkos, "Offline Impairment Aware RWA Algorithms forCross-Layer Planning of Optical Networks," *Journal of Lightwave Technolgy*, vol. 27, no. 12, pp. 1763-1775, 2009.

[90] D. A. R. Chaves, H. A. Pereira and C. B.-F. a. J. F. M. Filho, "Novel strategies for sparse regenerator placement in translucent optical networks," *Photonics Network Communication*, vol. 24, pp. 237-251, 2012.

[91] M. Flammini, M.-S. A., G. Monaco and M. L. Z. S., "On the complexity of the regenerator placement problem in optical networks," *IEEE transactions on Networking*, vol. 19, no. 2, pp. 498-5111, 2011.

[92] N. Sambo, N. Andriolli, A. Giorgetti, P. Castoldi and G. Bottari, "Multiple path based regenerator placement algorithm in translucent optical network," in *11th International Conference on Transparent Optical Networks*, July 2009, pp 1-4.

[93] K. Manousakis, P. Kokkinos, K. Christodoulopoulos and E. Varvarigos, "Joint online routing, wavelength assignment and regenerator allocation in translucent optical networks," *Journal of Lightwave Technology*, vol. 28, no. 8, pp. 1152-1163, 2010.

[94] Y. Ye, T. Y. Chai, T. H. Cheng and C. Lu, "Dynamic routing and wavelength assignment algorithms in wavelength division multiplexed translucent optical network," *Comput. Commun.*, vol. 29, no. 15, pp. 2975-2984, 2006.

[95] Y. Ye, T. Cheng and C. Lu, "Novel algorithm for upgrading of translucent optical networks," *Optical Express*, vol. 11, no. 23, pp. 3022-3033, 2003.

[96] Y. Peng, W. Hu, W. Sun, X. Wang and Y. Jin, "Impairment constraint multicasting in translucent WDM networks: architecture, network design and multicasting routing," *Photonic Network Communication*, vol. 13, no. 1, pp. 93-102, 2007.

[97] X. Yang and B. Ramamurthy, "Sparse regeneration in a translucent WDM optical network," in *Proceedings of SPIE-The International Society of Optical Engineeering*, Jan 2001 pp 61-70.

[98] X. Yang and B. Ramamurthy, "Sparse regeneration in translucent wavelength routed optical networks: architecture, network design and wavelength routing," *Photonic Network Communication*, vol. 10, no. 1, pp. 39-53, 2005.

[99] N. Sambo, N. Andriolli, A. Giorgetti, L. Valcarenghi, F. Cugini and P. Castoldi, "Accounting for shared regenerators in GMPLS-controlled translucent optical networks," *Journal of Lightwave Technology*, vol. 27, no. 19, pp. 4338-4347, 2009.

[100] D. A. R. Chaves, C. Ayres, R. Carvalho, H. Pereira, C. Bastos-Filho and J. Martins-Filho, "Multiobjective sparse regeneration placement algorithm in optical networks considering network performance and capex," in *12th International Conference on Transparent Optical Networks*, July 2010, pp 1-4.

[101] D. A. R. Chaves, C. Ayres, R. Carvalho, H. Pereira, C. Bastos-Filho and J. Martins-Filho, "Sparse regeneration placement for translucent optical networks using multiobjective evolutionary algorithm considering quality of service in capital cost," in *SBMO/IEEE MTT-S International Microwave and Optoelectronics Conference*, Nov 2009, 417-422.

[102] S. Pachnicke, T. Paschenda and P. Krummrich, "Assessment of a constraint-based routing algorithm for translucent 10 Gbps DWDM networks considering fober nonlinearities," *Journal of Optical Networking*, vol. 7, no. 4, pp. 365-377, 2008.

[103] M. Youssef, S. A. Zahr and M. Gagnaire, "Traffic-driven Vs. topology-driven strategies for regeneration sites placement," in *IEEE International Conference on Communications*, MAy 2010, pp 1-6.

[104] M. Youssef, S. A. Zahr and M. Gagnaire, "Cross optimization for RWA and regenerator placement in translucent WDM networks," in *14th Conference on Optical Network Design and Modeling*, Feb 2010, pp 1-6.

[105] M. Flammini, A. Marchetti-Spaccamela, G. Monaco, L. Moscardelli and S. Zakas, "On the complexity of the regenerator placement in optical networks," *IEEE/ACM Trans. Netw.*, vol. 19, no. 2, pp. 498-511, 2011.

[106] S. Chen, I. Ljubic and S. Raghavan, "The regenerator location problem," *Networks*, vol. 55, no. 3, pp. 205-220, 2010.

[107] F. Kuipers, A. Beshir, A. Orda and P. V. Mieghem, "Impairment aware path selection and regenerator placement in translucent optical networks," in *18th IEEE International Conference on Network Protocols*, Oct 2010, pp 11-20.

[108] S. Rumley, C. Gaumier and R. Szymanek, "Multiobjective optimization of regenerator placement using constraint programming," in *International Conference on Optical Network Design and Modeling*, Feb 2011, pp 1-6.

[109] M. Youssef, S. A. Zahr and M. Gagnaire, "Translucent network design from a capex/opex perspective," *Photonic Network Communication,* vol. 22, pp. 85-97, 2011.